UNIVERSITAT POLITÈCNICA
DE CATALUNYA

Ph.D. Thesis

Contribution to Wireless Access Optimization and Dynamic Enhancement of WCDMA Networks

Author: Mario García Lozano

Advisor: Dr. Silvia Ruiz Boqué

Radio Communication Research Group
Department of Signal Theory and Communications
Universitat Politècnica de Catalunya

Barcelona, July 2008

Abstract

The deployment of 3rd and 3.5th Generation (3G/3.5G) cellular networks challenges traditional radio planning and optimization strategies. Unlike Frequency Division Multiple Access (FDMA) based 2nd Generation (2G) systems, coverage and capacity are tightly coupled and must be treated as a whole. Besides new and more sophisticated Radio Resource Management (RRM) algorithms are present along with a more flexible conception of the network with many interdependent parameters, whose joint adjustment is not trivial. A new radio planning paradigm appears in which the network is optimized by means of complex algorithms both in a static and a dynamic way.

This Ph.D. thesis provides a contribution to the access network optimization of 3G/3.5G systems. Several issues to improve radio planning have been investigated and new methods, guidelines and strategies of analysis have been proposed with the final objective of enhancing the network performance. Dynamic mechanisms being in the blurred line between radio planning and RRM are also devised and studied.

The first part of this dissertation deals with the configuration of Base Stations (BSs). The impact of pilot powers, downtilt of antennas and interactions thereof with soft handover (SHO) parameters are investigated. Effects beyond well-known facts are outlined and new planning guidelines are derived. Given the results, an Automatic Planning strategy is proposed to automate the configuration of these parameters and to find a combination such as traffic is effectively equalized among cells and a higher capacity is achieved. The technique is based on the Simulated Annealing metaheuristic and is able to improve the global performance of the network, represented by a cost function containing information on the load factor and subject to constraints on coverage, degradation of the Quality of Service (QoS) and Downlink (DL) power consumption. The importance of Uplink (UL) requirements, usually missed by existent proposals, has been also included and analytically addressed.

Reconfiguring BSs is not the only means to modify cell shapes, in this sense the study is extended by introducing repeaters, which allow generating distributed coverage areas. This is the context of the second part of the thesis. New effects, not present in FDMA based 2G systems, imply that the radio planning process becomes more complex. Most existent works dealing with repeaters in Wideband

Code Division Multiple Access (WCDMA) networks ignore these effects or claim their irrelevance in that particular study-case. That is why the research work was focused in modeling them, quantifying their impact and deriving radio planning guidelines to enhance the final performance of the radio access network. The new expression for the feasibility condition has been analytically obtained showing a tradeoff between capacity and coverage. This has been analyzed both theoretically and by means of simulations. The adjustment of several parameters with a significant impact is also discussed to derive practical rules of thumb. Variation on the coverage of the donor cell before and after installing repeaters is modeled as well. Subsequently, it is proposed a new methodology to analyze WCDMA networks with repeaters deployment, considering realistically path delays and the behavior of Rake receivers. This allows an enhanced analysis with respect to traditional approaches which, under certain circumstances, tend to provide erroneously optimistic metrics.

The final part of the dissertation goes one step further in Automatic Planning and two dynamic mechanisms are proposed and validated so that the network can react and self tune in front of changes in traffic conditions. The first one, based on previous conclusions, aims at detecting if one of the links has capacity problems and if so, favors it to delay congestion control actions. Finally, High Speed Downlink Packet Access (HSDPA) technology is introduced and, after analyzing the resources to be shared with a previous release of the Universal Mobile Telecommunications System (UMTS), it is concluded that an automatic tuning system that dynamically manages the Orthogonal Variable Spreading Factor (OVSF) code tree is desired. A mechanism aiming at maximizing cell throughput while guaranteeing blocking and dropping criteria is proposed and validated.

Resumen

El despliegue de las redes celulares 3G/3.5G plantea un reto a las estrategias de planificación y optimización radio tradicionales. A diferencia de los sistemas 2G basados en FDMA, cobertura y capacidad están estrechamente ligadas y deben ser tratadas conjuntamente. Además, están presentes nuevos y más sofisticados algoritmos de RRM así como una concepción de la red más flexible, con múltiples parámetros cuyo ajuste conjunto no es trivial. Un nuevo paradigma de planificación radio aparece y la red se optimiza mediante complejos algoritmos ya sea estática o dinámicamente.

Esta tesis doctoral supone una contribución a la optimización de las redes de acceso radio en sistemas 3G/3.5G. Varios aspectos susceptibles de mejorar la planificación han sido investigados y nuevos métodos, directrices y estrategias de análisis se proponen con el objetivo final de mejorar el rendimiento de las redes. También se han diseñado y estudiado mecanismos dinámicos que se encuentran en la frontera difusa entre la planificación y la RRM.

La primera parte de la tesis trata la configuración de las estaciones base. El impacto de las potencias piloto, inclinación de antenas y sus interacciones con los parámetros de SHO son investigados. Se hace énfasis en los efectos que van más allá de los conocidos y se derivan nuevas guías de planificación. A partir de los resultados, se propone una estrategia para su Planificación Automática. El objetivo final es encontrar una combinación de configuraciones tal que el tráfico sea ecualizado de manera efectiva entre las celdas y conseguir una capacidad superior del sistema. La técnica se basa en la metaheurística *Simulated Annealing* y es capaz de mejorar el rendimiento global de la red, representado por una función de coste que contiene información sobre el factor de carga y sujeta a condiciones de cobertura, degradación de la calidad de servicio y consumo de potencia en el DL. La importancia de los requisitos que impone el UL, a menudo olvidados en propuestas anteriores, también se ha incluido y estudiado analíticamente.

La reconfiguración de las bases no es el único medio para modificar las áreas de cobertura de las celdas, en este sentido el estudio se amplía mediante la introducción de repetidores, que permiten la generación de celdas distribuidas. La planificación radio con repetidores es más compleja debido a la aparición de nuevos efectos que no estaban presentes en las redes clásicas 2G basadas en FDMA. La mayoría de los trabajos que tratan con repetidores tienden a ignorarlos o afirman que no son

relevantes en su caso de estudio. Por ello, la investigación se centró en el modelado y cuantificación de su impacto así como en derivar directrices de planificación. Se ha obtenido analíticamente la nueva expresión que define la condición de viabilidad así como las regiones de admisión. Se concluye que existe un compromiso entre capacidad y cobertura que ha sido analizado tanto teóricamente como mediante simulación. Ciertos parámetros que presentan un mayor impacto en este compromiso han sido estudiados y se han derivado reglas prácticas para su ajuste. La variación de cobertura en la celda padre antes y después de la instalación de sus repetidores también ha sido modelada. Posteriormente, se propone una nueva metodología para analizar las redes WCDMA con el despliegue de repetidores, teniendo en cuenta de manera realista los retardos de propagación y el comportamiento del receptor Rake. Esto permite un análisis superior con respecto a los enfoques tradicionales que, en determinadas circunstancias, tienden a ofrecer cifras erróneamente optimistas.

La última parte de la tesis da un paso más en la Planificación Automática y se proponen y validan dos mecanismos dinámicos que permiten a la red reaccionar y auto-optimizarse frente a cambios en las condiciones del tráfico. El primero, basado en conclusiones de la primera parte, persigue detectar si uno de los enlaces presenta problemas de capacidad y, en caso afirmativo, favorecerlo para retrasar los mecanismos de control de congestión. Por último, se introduce la tecnología HSDPA y, después de analizar los recursos que deben ser compartidos con las versiones anteriores de UMTS, se concluye que es deseable un sistema para la gestión dinámica del árbol de códigos OVSF. Se propone y valida un mecanismo que maximiza el *throughput* de las celdas, garantizando al mismo tiempo criterios de bloqueo y *dropping*.

Resum

El desplegament de les xarxes cel·lulars 3G/3.5G planteja un repte a les estratègies de planificació i optimització ràdio tradicionals. A diferència dels sistemes 2G basats en FDMA, cobertura i capacitat estan estretament lligades i han de ser tractades conjuntament. A més, estan presents nous i més sofisticats algorismes de gestió de recursos ràdio (RRM) així com una concepció de la xarxa més flexible, amb múltiples paràmetres l'ajustament conjunt dels quals no és trivial. Un nou paradigma de planificació ràdio apareix i la xarxa s'optimitza mitjançant complexos algorismes ja sigui estàtica o dinàmicament.

Aquesta tesi doctoral suposa una contribució a l'optimització de les xarxes d'accés ràdio en sistemes 3G/3.5G. Diversos aspectes susceptibles de millorar la planificació han estat investigats i nous mètodes, directrius i estratègies d'anàlisi es proposen amb l'objectiu final de millorar el rendiment de les xarxes. També s'han dissenyat i estudiat mecanismes dinàmics que es troben en la frontera difusa entre la planificació i la RRM.

La primera part de la tesi tracta la configuració de les estacions base. L'impacte de les potències pilot, inclinació d'antenes i les seves interaccions amb els paràmetres de SHO són investigats. Es fa èmfasis en els efectes més enllà dels ja coneguts i es deriven regles per al seu ajust. A partir dels resultats, es proposa una estratègia per a la seva Planificació Automàtica. L'objectiu final és trobar una combinació de configuracions tal que el tràfic sigui equalitzat de manera efectiva entre les cel·les i aconseguir una capacitat superior del sistema. La tècnica es basa en la meta-heurística *Simulated Annealing* i és capaç de millorar el rendiment global de la xarxa, representat per una funció de cost que conté informació sobre el factor de càrrega, subjecta a altres condicions de cobertura, degradació de la qualitat de servei i consum de potència en el DL. La importància dels requisits que imposa el UL, sovint oblidats en propostes existents, també s'ha inclòs i estudiat analíticament.

La reconfiguració de les bases no és l'únic mecanisme per a modificar les àrees de cobertura de les cel·les, en aquest sentit l'estudi s'amplia mitjançant la introducció de repetidors, que permeten la generació de cel·les distribuïdes. En aquest cas la planificació és més complexa a causa de l'aparició de nous efectes que no es donaven en les xarxes clàssiques 2G basades en FDMA. La majoria dels treballs que tracten amb repetidors tendeixen a ignorar-los. Per això, la investigació es va centrar en el modelatge i quantificació del seu impacte així com a derivar directrius de planifi-

cació. S'ha obtingut analíticament la nova expressió que defineix la regió d'admissió i es conclou que existeix un compromís entre capacitat i cobertura, analitzat tant teòricament com mitjançant simulació. Certs paràmetres presenten un impacte significatiu, aquests han estat estudiats i s'han obtingut regles pràctiques per al seu ajust. La variació de cobertura en la cel·la pare abans i després de la instal·lació de repetidors també ha estat modelada. Posteriorment, es proposa una nova metodologia per a analitzar aquests desplegaments, tenint en compte de manera realista els retards de propagació i el comportament del receptor Rake. Això permet una anàlisi superior pel que fa a enfocaments tradicionals que, en determinades circumstàncies, tendeixen a oferir xifres erròniament optimistes.

L'última part de la tesi dóna un pas més en la Planificació Automàtica i es proposen i validen dos mecanismes dinàmics que permeten a la xarxa reaccionar i auto-optimitzar-se enfront de canvis en les condicions de tràfic. El primer, basat en conclusions anteriors, persegueix detectar si un dels enllaços presenta problemes de capacitat i, en cas afirmatiu, afavorir-lo per a retardar els mecanismes de control de congestió. Finalment, s'afegeix a l'estudi la tecnologia HSDPA i, després d'analitzar els recursos que han de ser compartits amb les versions anteriors de UMTS, es conclou que és desitjable un sistema per a la gestió dinàmica de l'arbre de codis OVSF. Es proposa i valida un mecanisme que maximitza el *throughput* de les cel·les, garantint al mateix temps criteris de bloqueig i *dropping*.

Contents

Acronyms

1G	First Generation
1xRTT	One Time Radio Transmission Technology
2G	Second Generation
3G	Third Generation
3GPP	Third Generation Partnership Project
AC	Admission Control
AGC	Automatic Gain Control
AP	Access Point
ARQ	Automatic Repeat Request
AS	Active Set
ATS	Automatic Tuning System
B3G	Beyond Third Generation
BER	Bit Error Rate
BLER	BLock Error Rate
BS	Base Station
CAPEX	CAPital EXpenditure
cdf	Cumulative Distribution Function
CDMA	Code Division Multiple Access
CIO	Cell Individual Offset
CIR	Carrier-to-Interference-Ratio
CINR	Carrier-to-Interference-plus-Noise-Ratio
CPICH	Common PIlot CHannel
CQI	Channel Quality Indicator
CS	Circuit Switched
DCH	Dedicated CHannel
DL	DownLink

DPCH	Dedicated Physical CHannel
DSCH	Downlink Shared CHannel
EDGE	Enhanced Data Rates for GSM Evolution
EV-DO Rev B	Evolution-Data Optimized Revision B
FACH	Forward Access CHannel
FDD	Frequency Division Duplex
FDMA	Frequency Division Multiple Access
GA	Genetic Algorithm
GERAN	GSM EDGE Radio Access Network
GPS	Global Positioning System
GSM	Global System for Mobile Communications
H-ARQ	Hybrid Automatic Repeat Request
HSDPA	High Speed Downlink Packet Access
HS-DPCCH	High Speed Dedicated Physical Control CHannel
HSPA	High Speed Packet Access
HS-PDSCH	High Speed Physical Downlink Shared CHannel
HS-SCCH	High Speed Shared Control CHannel
HSUPA	High Speed Uplink Packet Access
IF	Intermediate Frequency
IMS	IP Multimedia Subsystems
KPI	Key Performance Indicator
LOS	Line Of Sight
LS	Local Search
LTE	Long Term Evolution
LUT	Look-Up-Table
MAC	Medium Access Control
OFDMA	Orthogonal Frequency Division Multiple Access
OPEX	OPerational EXpenditure
OVSF	Orthogonal Variable Spreading Factor
P-CPICH	Primary Common Pilot Channel
pdf	Probability Density Function
PF	Proportional Fair
QAM	Quadrature Amplitude Modulation
QoS	Quality of Service

QPSK	Quadrature Phase Shift Keying
RAB	Radio Access Bearer
RACH	Random Access CHannel
RF	Radio Frequency
RNC	Radio Network Controller
RoF	Radio Over Fiber
RR	Round Robin
RRM	Radio Resource Management
RSCP	Received Signal Code Power
RSSI	Received Signal Strength Indicator
SC-FDMA	Single Carrier Frequency Division Multiple Access
SCCPCH	Secondary Common Control Physical CHannel
SCM	SubCarrier Multiplexing
SF	Spreading Factor
SHO	Soft HandOver
SIR	Signal-to-Interference-Ratio
SINR	Signal-to-Interference-plus-Noise-Ratio
SSINR	Signal-to-Signal-plus-Interference-plus-Noise-Ratio
TDD	Time Division Duplex
TDMA	Time Division Multiple Access
TF	Transport Format
TS	Tabu Search
UE	User Equipment
UL	UpLink
UMTS	Universal Mobile Telecommunications System
UTRAN	UMTS Terrestrial Radio Access Network
WCDMA	Wideband Code Division Multiple Access
WLAN	Wireless Local Area Network

List of Tables

List of Figures

Chapter 1

Introduction

1.1 Background and Motivation

The demand for data services in wireless environments is currently growing faster than ever. In this sense, Universal Mobile Telecommunications System (UMTS) with High Speed Packet Access (HSPA) technology and its continuous evolution to Beyond Third Generation (B3G) is becoming the primary mobile-broadband solution. Together with the outstanding success of the Global System for Mobile Communications (GSM), both systems are establishing a worldwide dominance.

Several important factors are boosting the adoption of enhanced wireless data services. These include increased user awareness, phones becoming "smart" with enhanced data capabilities, computers with integrated Third Generation (3G) technology and a continuously growing range of applications, including standard networking applications and those designed for wireless systems, as it is analyzed in [Ris07]. All this covered by the main factor: improved network capability and coverage.

In this context of evolution and growth, it is essential that operators deploy spectrally efficient networks with superior performance to meet customer requirements in terms of capacity, coverage and Quality of Service (QoS). Network planning becomes a key factor to achieve these objectives while minimizing capital and operational expenditures (CAPEX and OPEX). Especially because data applications are bound to demand significantly more network resources than traditional voice services.

Radio network planning has not remained constant along time and has evolved with the development of access technologies and the requirements set by those [LWN06]. First mobile communications systems (or generation zero) where characterized by high power Base Stations (BSs) located in elevated sites, with omnidirectional antennas and extensive coverage areas (50–70 km). These systems used analogical channels for both signalling and traffic. Their capacity was low and they

were mainly planned to provide coverage. With First Generation (1G) systems, the cellular concept was introduced based on frequency reuse policies which permitted a higher capacity. But it was with the evolution of Second Generation (2G) systems, that capacity became a first order issue. Cell radius were reduced, also did frequency reuse distances and trisectorial layouts were deployed to minimize interferences and increase capacity. Radio link budgets were also recalculated to reconsider the initial assumption about most users being vehicular. Propagation models did also evolve to better predict losses in microcellular environments and the theoretical hexagonal network layout was relegated to preliminary estimations and studies.

Not only assumptions on propagation conditions, type of transmitters, antennas, etc. had to be modified, radio planning also progressed towards a more sophisticated process in which simulations and mathematical models became crucial. For instance, as the GSM system evolved, site deployment became so dense that, even though frequency hoping was implemented, investigations on algorithms to solve the frequency allocation problem were necessary. In this context, metaheuristic techniques played an important role. With the deployment of UMTS, the situation has become more complex and simulation is now even more present. In Wideband Code Division Multiple Access (WCDMA) based systems, isolation among cells is paramount because of a frequency reuse factor of 1 and the resulting mutual interference among nearby cells. Furthermore, in GSM systems, coverage and capacity concepts could be treated in a relatively independent manner, but with the deployment of UMTS networks, the situation is more complicated. Coverage and capacity are tightly coupled and must be treated as a whole. The use of new and more sophisticated Radio Resource Management (RRM) algorithms along with a more flexible conception of the network imply that planning engineering has to deal with much more interdependent parameters, whose joint adjustment is not trivial. A new radio planning paradigm appears in which the network is optimized by means of complex algorithms both in a static and a dynamic way.

This Ph.D. dissertation provides a contribution to the radio network optimization of 3G/3.5G networks. Several issues to improve radio network planning have been investigated and new methods, guidelines and strategies of analysis have been proposed with the final objective of enhancing the wireless access network performance. Dynamic mechanisms being in the blurred line between radio planning and RRM are also investigated. The specific aspects that have been covered concerning this general objective are detailed in the following section.

1.2 Scope of the Thesis and Structure

The main objective of this Ph.D. dissertation is the design of new and advanced radio network planning techniques so that wireless access performance is optimized in the context of mature 3G/3.5G networks. New methods, guidelines and strategies of analysis have been proposed with the final objective of improving the radio access network performance. For this purpose, challenges an open issues were derived by studying existent literature. The methodology followed during the research has been

a combination of mathematical studies and simulations.

The document is organized in 9 chapters plus 3 appendixes. After this introduction, 7 chapters comprise the core of the dissertation and are closed by the conclusions and a description of possible future lines of research. Chapters can be grouped in 3 parts, each one focusing in different though interrelated strategies to optimize the wireless access network of WCDMA based systems, mainly the UMTS Terrestrial Radio Access Network (UTRAN). Unless the contrary is explicitly stated, it is assumed the Frequency Division Duplex (FDD) mode.

The first part of the dissertation, comprised by chapters 2, 3 and 4, addresses the problem of configuring BSs[1], in particular those parameters with an important impact on capacity and coverage footprint. Capacity maximization goes hand in hand with careful cell size dimensioning to equalize traffic correctly among cells and an *Automatic Planning* strategy based on metaheuristics is proposed to jointly optimize the target cells. Reconfiguring BSs is not the only means to modify cell shapes, in this sense the study is extended by introducing repeaters, which allow generating distributed cells. This is the context of the second part of the thesis composed of chapters 5 and 6. A novel analytical study is conducted on the particularities of WCDMA networks including repeaters and thus distributed load and coverage. From this study planning guidelines are derived and a new approach for the analysis of these systems is proposed, overcoming shortcomings of traditional ones. The final part of the dissertation goes one step further in *Automatic Planning* and two dynamic mechanisms are investigated so that the network can react and self tune in front of changes in traffic conditions.

The reading of these different parts may not be sequential, but certain dependence among chapters should be respected for a full understanding. These possible sequences of reading are gathered at Figure 1.1.

A summary of each chapter and their main research contributions are indicated next. Publications derived from these results are listed in the following section.

Chapter 2 explains the challenges to optimize WCDMA networks through radio planning. Comparisons among previous contributions are done to detect challenges and potential improvements to be developed in parts 1 and 3. Because of its own particularities, the state-of-the-art for part 2 is reviewed in Chapters 5 and 6. Thus, initially, Chapter 2 extendedly revises approaches dealing with the design of *Automatic Planning* algorithms and with a particular insight in the use of metaheuristics. Comments on key parameters are also given along with works dealing with their optimization. Next, the chapter focuses on *Dynamic Planning* strategies and *Self Tuning* of RRM parameters. Again, a survey on the state-of-the-art is provided and open issues are detected.

Chapter 3 addresses the problem of adjusting two of the parameters with a more significant impact on the network performance. The power assigned to the primary

[1]Along the document, the UMTS nomenclature User Equipment (UE) has been used to denote terminals. Regarding the Node-B, if sectorial layouts are used, it has not a univocal relation with cells. For that reason the denomination Base Station (BS) has been preferred to denote the transceivers that compose a single sector or cell.

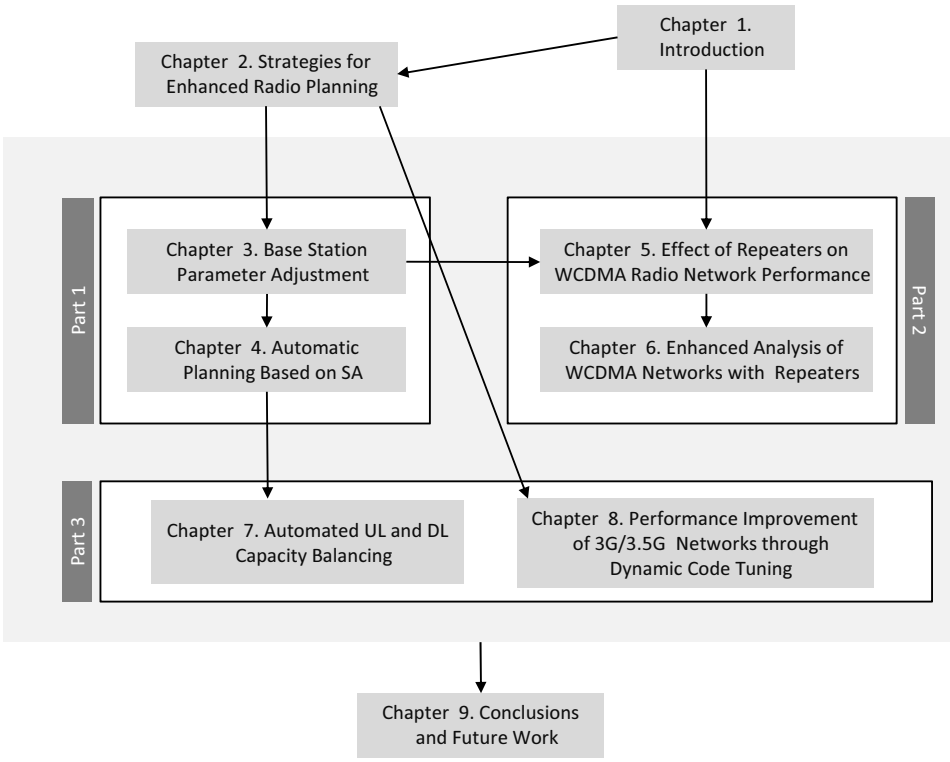

Figure 1.1: Dependence among chapters.

Common Pilot Channel (henceforth "CPICH" or "pilot channel") and tilt of antennas. Their impact on the system performance and interactions with other planning and RRM parameters is investigated. Detailed results, beyond well known effects, have been obtained in different scenarios. These results allow deriving guidelines for an enhanced radio planning and to design effective *Automatic Planning* algorithms considering these parameters.

Given the results, Chapter 4 proposes a novel *Automatic Planning* algorithm based on the Simulated Annealing metaheuristic so that both CPICH and downtilt angles are optimally adjusted and the network performance is improved. The problem optimizes all target cells jointly and not in a standard cell by cell manner. Uplink (UL) requirements are fully considered, since previous chapter showed that UEs transfer to alleviate the load of one cell is not always feasible. Results show the convergence of the algorithm towards better configurations. Traffic is correctly equalized among the cells and interference levels are reduced, eventually capacity is increased.

Repeaters are a cost effective option to extend coverage and achieve load balancing by creating distributed cells. This is the context of Chapter 5, which aims at characterizing several particular effects when deploying these devices in WCDMA networks and that are usually missed by existent literature. In this sense, one of the novelties of the chapter is deriving the new analytic expression of the feasibility condition for the UL in a multiservice environment with a general heterogeneous layout. In particular, a compact closed expression for the admission region is presented, suitable for a system where the users belong to an arbitrary number of different service classes. A tradeoff between capacity and coverage arises and it has been analyzed both theoretically and by means of simulations. Different parameters are shown to have a major impact and their adjustment is discussed to derive practical rules of thumb to operators. The chapter also generalizes the expression that relates the coverage of the *donor* cell before and after installing repeaters.

Simplifications when analyzing and optimizing radio access networks with repeaters are explained in Chapter 6. In this framework, it is derived a novel methodology to evaluate up- and downlink (DL) so that transmission powers and other RRM parameters can be calculated without simplifications. In particular, the real different path delays, taking into account the repeaters presence and the finite nature of the time window of Rake receivers are considered. This allows an enhanced analysis with respect to traditional approaches from a system level viewpoint. Results show more reliable and accurate predictions on network performance. Not taking into account these effects implies erroneously optimistic metrics. Indeed, some of the most relevant parameters in network performance evaluation are clearly affected.

Results from the first part, showed opposite effects in UL and DL under certain circumstances. In addition, because of variations in traffic patterns, the network may evolve from UL to DL limited situations and viceversa. However, many optimization strategies are focused in one single link, assuming that it is always the limiting one. Given this, Chapter 7 concentrates on the design of an *Automatic Tuning System* (ATS) to detect whether UL or DL is limiting capacity and favor it by means of

certain reconfigurations. This implies a new extra margin that permits delaying congestion control mechanisms and a more balanced capacity between both links. In particular, because of the opposing behavior of Soft Handover (SHO) parameters, their dynamic modification is revealed as a feasible option to achieve this objective. Along the chapter, a three block based auto-tuning architecture is described to adapt parameters to variations in the set of used services (subsequently called *service mix*) and overcome capacity problems. These blocks have been designed and tested, showing an effective adaptation to changes in traffic patterns. Significant capacity gains are obtained when the ATS is running. The approach is able to stabilize the network and avoid (or delay) congestion. Three different monitoring cases have been tested and validated the feasibility of the approach.

Finally, High Speed Downlink Packet Access (HSDPA) technology is introduced in the study in Chapter 8. After analyzing the resources to be shared by both technologies, the final objective is set to design an algorithm that maximizes the cell throughput while guaranteeing blocking and dropping criteria. In particular, it is proposed a mechanism to dynamically tune the number of codes to allocate for HSDPA when it coexists with UMTS. The optimum code reservation is dependent on traffic patterns and mobile geographical locations. Thus, the allocation is tightly coupled with the reported Channel Quality Indicators (CQIs). Results reveal that the proposal succeeds and an optimum number of codes is allocated for each technology. The cell throughput is increased while minimizing both blocking and dropping probabilities below specific thresholds.

All chapters are contextualized in the flowchart in Figure 1.2, which summarizes the standard radio planning process in UMTS networks (the reader is referred to [LWN06; NDA06; CBG+06] for basic theory on UMTS radio planning). Each bubble indicates the phase of the analysis in which the research contributions are useful.

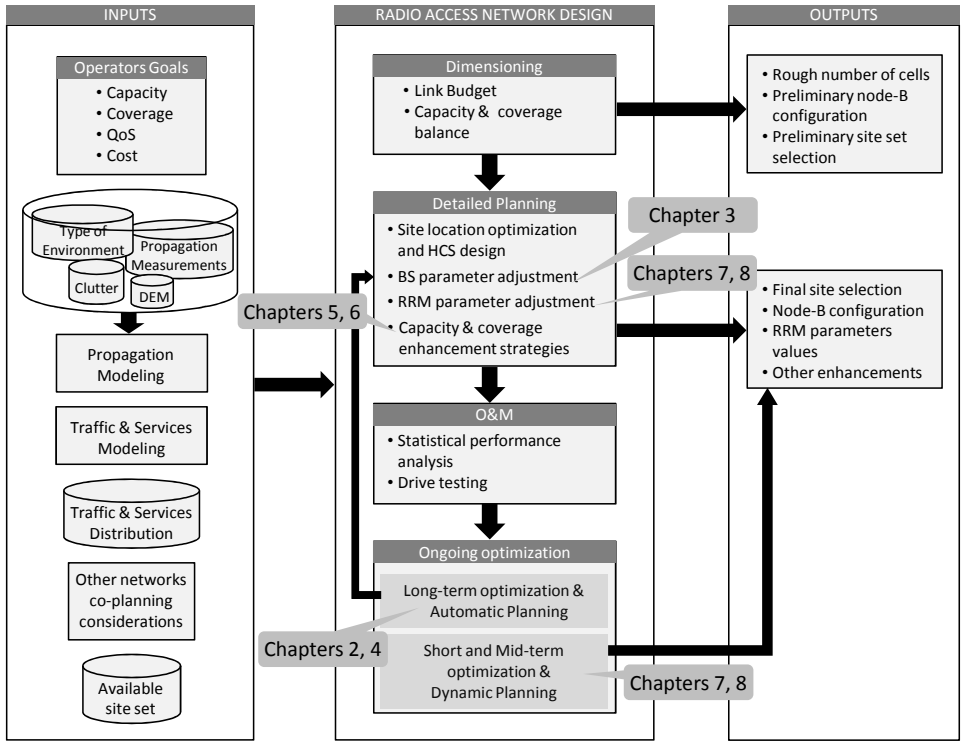

Figure 1.2: Radio network planning process and relationship with chapters.

1.3 Research Contributions

The different novelties of this Ph.D. dissertation have been published in several research contributions, whose details are indicated for each chapter in the following. During the development of this Ph.D. thesis, several contributions to the European COST Actions 273 and 2100 were done and these are also indicated.

The total number of publications is 1 book section, 4 journal papers, 8 conference papers and 8 contributions to COST Actions.

Chapter 3

1 book section. 2 conference papers. 2 COST 273 contributions.

- [Ce06] L.M. Correia (ed.), *Mobile Broadband Multimedia Networks. Techniques Models and Tools for 4G*, 1st ed. London, UK: Elsevier (Academic Press), 2006. Section entitled: *Base Station Parameter Configuration.*
- [GLR04] M. García-Lozano, and S. Ruiz, "Effects of Downtilting on RRM Parameters," in *Proc. of IEEE International Symposium on Personal, Indoor and Mobile Radio Communications (PIMRC 2004)*, Barcelona (Spain), Sep. 5–8, 2004.
- [GLRHO04] M. García-Lozano, S. Ruiz, R. Higuero, and J.J. Olmos "UMTS Network Optimisation: Impact of Donwtilted Antennas," COST 273, Athens (Greece), Tech. Rep. available as TD(04)033, Jan. 26–28, 2004.
- [GLRS+03] M. García-Lozano, S. Ruiz, O. Sallent, F. Adelantado, R. Agustí, M.A. Díaz-Guerra, J. Montero, E. Gago, J.L. Miranda, and F. Castejón "Analysing UTRA-FDD Pilot Power and Active Set Configuration in a Real Urban Scenario," in *Proc. of IEEE International Symposium on Personal, Indoor and Mobile Radio Communications (PIMRC 2003)*, Beijing (China), Sep. 7–10, 2003.
- [RSA+03] S. Ruiz, O. Sallent, R. Agustí, M. García-Lozano, F. Adelantado, M.A. Díaz-Guerra, J. Montero, E. Gago, J.L. Miranda "3G Planning by Using 2G Measurements," COST 273, Barcelona (Spain), Tech. Rep. available as TD(03)073, Jan. 15–17, 2003.

The author participated in the MORANS (Mobile Radio Access Network Reference Scenarios) [VB03; VBC+04] initiative. This activity was framed within the COST 273 Action and aimed at providing common system simulation environments so that research results and proposals from different researchers are comparable. In this context, several results derived from this chapter were also simulated and rechecked in the MORANS realistic scenario of Turin. These results can be found in 2 COST 273 contributions:

- [GLR05] M. García-Lozano, and S. Ruiz, "Effects of Donwtilt on the MORANS Real World Scenario of Turin," COST 273, Lisbon (Portugal), Tech. Rep. available as TD(05)111, Sep. 10–11, 2005.

- [GLFR05] M. García-Lozano, P. Falavigna, and S. Ruiz, "Detailed UL/DL Analysis of MORANS Torino Scenario under Different Traffic Behaviour," COST 273, Bologna (Italy), Tech. Rep. available as TD(05)022, Jan. 19–21, 2005.

Chapter 4

1 journal paper. 2 conference papers. 1 COST 273 contribution.

- [GLRO04a] M. García-Lozano, S. Ruiz, and J.J. Olmos, "Optimum Cell Balancing for UMTS Inhomogeneous Traffic Distribution," in *Proc. of International Symposium on Wireless Personal Multimedia Communications (WPMC 2004)*, Padova (Italy), Sep. 12–15, 2004.
- [GLRO04b] M. García-Lozano, S. Ruiz, and J.J. Olmos, "UMTS Optimum Cell Load Balancing for Inhomogeneous Traffic Patterns," in *Proc. of IEEE Vehicular Technology Conference Fall (VTC 2004 Fall)*, Los Angeles (USA), Sep. 26–29, 2004.
- [GLRO03b] M. García-Lozano, S. Ruiz, and J.J. Olmos, "CPICH Powers Optimization by means of Simulated Annealing in an UTRA-FDD environment," *IEE Electronic Letters*, vol. 39, no. 23, pp. 1676–1677, Nov. 2003.
- [GLRO03a] M. García-Lozano, S. Ruiz, and J.J. Olmos, "CPICH Powers Optimization by means of Simulated Annealing," COST 273, Paris (France), Tech. Rep. available as TD(03)103, May 21–23, 2003.

Chapter 5

2 journal papers. 1 conference paper. 1 COST 273 contribution.

- [GLACR07] M. García-Lozano, L. Alonso, F. Casadevall, and S. Ruiz,"Capacity and Coverage Tradeoff in WCDMA Environments with Repeaters Deployment," *Wireless Personal Communications Journal*, vol. 40, no. 2, pp. 329–342, Feb. 2007.
- [GLACR05a] M. García-Lozano, L. Alonso, F. Casadevall, and S. Ruiz,"Capacity and Coverage Tradeoff in WCDMA Environments with Repeaters Deployment," in *Proc. of International Symposium on Wireless Personal Multimedia Communications (WPMC 2005)*, Aalborg (Denmark), Sep. 18–22, 2005.
- [GLACR05b] M. García-Lozano, L. Alonso, F. Casadevall, and S. Ruiz,"Impact of Repeaters Deployment on UMTS Admission Control," COST 273, Lisbon (Portugal), Tech. Rep. available as TD(05)117, Sep. 10–11, 2005.
- [AGLC05] L. Alonso, M. García-Lozano, and F. Casadevall, "Feasibility Condition for the Uplink of a CDMA Multiservice Mobile Communications System with Repeaters", *IEEE Communications Letters*, vol. 9, no. 5, pp. 408–410, May 2005.

Chapter 6

1 journal paper. 1 conference paper.

- [GLAC+07] M. García-Lozano, L. Alonso, F. Casadevall, S. Ruiz, and L.M. Correia,"Enhanced Analysis of WCDMA Networks with Repeaters Deployment," *IEEE Transactions on Wireless Communications*, vol. 6, no. 9, pp. 3429–3439, Sep. 2007.
- [GLAC+06] M. García-Lozano, L. Alonso, F. Casadevall, S. Ruiz, and L.M. Correia, "On the Impact of Repeaters Deployment on WCDMA Networks Planning," in *Proc. of IEEE Vehicular Technology Conference Fall (VTC 2006 Spring)*, Melbourne (Australia), May 7–10, 2006.

Chapter 7

1 conference paper. 1 COST 2100 contribution.

- [GLSPR+07] M. García-Lozano, O. Sallent, J. Pérez-Romero, S. Ruiz, A. Gomez, and P.M. d'Orey, "Automated Up- and Downlink Capacity Balancing in WCDMA Networks," in *Proc. of IEEE Vehicular Technology Conference Fall (VTC 2007 Fall)*, Baltimore (USA), Sep. 30/Oct. 1, 2007.
- [GLRALOC07] M. García-Lozano, S. Ruiz, A. Andújar-Linares, and N. Oller-Camaute, "Automatic Tuning of Soft Handover Parameters in UMTS Networks," COST 2100, Duisbrug (Germany), Tech. Rep. available as TD(07)344, Sep. 10–12, 2007.

Chapter 8

1 conference paper. 1 COST 2100 contribution.

- [GLSPRR08] M. García-Lozano, O. Sallent, J. Pérez-Romero, and S. Ruiz,"Performance Improvement of HSDPA/UMTS Networks through Dynamic Code Tuning," in *Proc. of IEEE International Symposium on Personal, Indoor and Mobile Radio Communications (PIMRC 2008)*, Cannes (France), Sep. 15–18, 2008.
- [GLR08] M. García-Lozano, S. Ruiz, "Study on the Automated Tuning of HSDPA Code Allocation," COST 2100, Wroclaw (Poland), Tech. Rep. available as TD(08)410, Feb. 06–08, 2008.

Chapter 2

Strategies for Enhanced Radio Planning

2.1 Introduction

In the previous chapter it was briefly summarized how radio network planning has evolved along with access technologies and the requirements set by those. In the case of UMTS systems, new features appear and change how the problem must be addressed. In the first place, the close relationship between capacity and coverage implies that both must be studied as a whole and not sequentially, as it used to be in Frequency Division Multiple Access (FDMA) based 2G networks. Indeed, effective coverage areas are inversely proportional to traffic load and the term *cell breathing* has been coined to describe the effect. Secondly, with the use of WCDMA and the implementation of new and very tunable RRM strategies, UMTS networks introduce an increased level of flexibility. A great deal of adjustable parameters allow operators to completely design its network to meet service level agreements. Even though this flexibility can be initially seen as an advantage, this is at the cost of a more complex planning. Operators are able to manage all aspects of the radio network, but several of those parameters simultaneously influence the system performance, they show interdependencies and a joint adjustment is not trivial.

Usually, vendors provide a set of default configurations, however these cannot be optimal for the particularities of operation of each cell. Therefore operators shall optimize them as one of the tasks of the planning process. Human made cell by cell modifications with the help of statistics from the Operation and Maintenance (O&M) subsystem is a usual practice. But achieving the combination of parameters that jointly maximize the network performance requires a more complex analysis. Since efficient network planning is of outmost importance, optimization techniques are mandatory to plan 3G/3.5G networks. These strategies aim at providing automatic optimization mechanisms that simplify the task and reduce time and costs.

They are included in what is called *Automatic Planning* or *Automatic Optimization*, being the first denomination preferred in this dissertation.

Given this, the chapter is organized in two sections. The first one gives an insight view on *Automatic Planning* strategies. This is done along two subsections, one devoted to the use of metaheuristics in radio network planning and the second one dealing with the parameters with a major impact on the outcome of the planning process itself. A review of the state of the art is done and existent challenges are explained. The second main section is focused on dynamic strategies and again the state of the art is revised in two differentiated points. The first one deals with the concept of *Dynamic Planning* and the second one with *Automatic Tuning* of RRM parameters. Open issues and challenges are indicated for both cases.

2.2 Automatic Planning Strategies

2.2.1 Introduction

In *Automatic Planning*, human analysis is fully assisted by new mechanized strategies. This is an efficient way to keep track of the optimum plan as the network grows and evolves along time. *Automatic Planning* permits adapting the radio plan to long-term, seasonal changes. Opposite to *Dynamic Planning*, it refers to eminently static mechanisms that aim at obtaining an enhanced network configuration considering its average behavior.

Resolution methods are basically oriented to the optimization of a cost function F_{cost} that gathers the operator's requirements and expresses the global value of a certain radio planning solution S. For that purpose several goals are defined and quantified by different sub-functions f_{cost}. The final function to be optimized is usually a linear combination of those. Since different sub-functions are expressed in different units, a previous normalization is needed to ensure that the sum of values is meaningful. In addition, by changing the weight coefficients (ω_i), the importance of each indicator can be stressed or reduced according to each particular case:

$$F_{cost}(S) = \sum_i \omega_i f_{cost,i}(S) \tag{2.1}$$

For example, a widely used function is the one that relates dropping and blocking. In this case, the final cost is defined as the weighted sum of their probabilities (P_{block} and P_{drop} respectively), in which dropping is usually adjusted with a higher weight coefficient value since dropping an existing user is perceived as more detrimental than blocking a new one.

$$F_{cost}(S) = P_{block}(S) + \omega P_{drop}(S), \omega > 1 \tag{2.2}$$

A second approach is to solve the different sub-objectives by optimizing the

different sub-functions sequentially. However, this indirectly leads to favoring some functions over others. Of course, a bad choice in the relative weights that define F_{cost} can also lead to inappropriate favoring or penalizing different sub-functions.

Another widely used approach is defining and optimizing a simpler cost function but subject to several constraints derived from the other sub-objectives. Continuing with the previous example, a possibility would be:

$$\begin{aligned} \text{Minimize} \quad & P_{block}(S) \\ \text{Subject to} \quad & P_{drop}(S) < 0.02 \end{aligned} \tag{2.3}$$

Regarding sub-functions most are mainly defined according to coverage and capacity related criteria, but eventually economic aspects must be considered as well. Some examples are given next:

- Percentage of target area that is appropriately covered. This indicator can be defined in a service by service basis because requirements and Radio Access Bearers (RABs) are different, and so coverage areas differ as well. Furthermore, coverage must be guaranteed in three fronts:

  1. **Pilot coverage** indicates those areas in which the UE is able to detect an appropriate level of the broadcast pilot channel. Further details on this are given in Section 3.2.
  2. **UL coverage**, which is determined by the UE maximum available power. Although link budget calculus aim at balancing UE capabilities with DL and pilot coverage, each cell shows its own particularities in terms of traffic and propagation and unbalance situations can appear.
  3. Similar effects can be described for **DL coverage**, considering that operators limit the maximum power that can be devoted to one single link connection and also that the BS is limited in power. Further information and analysis on coverage variations with capacity and general cell breathing for both UL and DL can be found in [TYC05].

- The percentage of target area susceptible of suffering pilot pollution is also a coverage related parameter. This effect is observed in areas where UEs do not have enough RAKE fingers for processing all the received pilot signals. This excess of pilot signals does not contribute to improve coverage, on the contrary it can seriously contribute to degrade the received Signal-to-Interference-Ratio (SIR) due to increased interference.

- The percentage of areas in SHO is also an important metric to evaluate, so that smooth transitions among cells are guaranteed.

- Regarding capacity, traffic in UMTS Release 99 (Rel'99) systems is usually quantified in terms of number of users. Each user is assigned a Dedicated Channel (DCH). In this sense, maximum capacity can be defined as the situation when a certain percentage of UEs cannot be served with the required

E_b/N_0. This magnitude should be evaluated for both UL and DL since degradation might occur in different links of different connections.

- Another indicator directly derived from the previous one is the percentage of users consuming more than a certain percentage of its maximum power (in the UL or DL). This measurement permits detecting pre-congestion situations and can be obtained for the whole system or in a cell by cell basis. In this second case, a useful indicator is the number of cells with a certain percentage of users reaching the corresponding threshold.

- In HSDPA systems, since all user traffic is carried through a DL shared channel, a different dimensioning approach is necessary. In particular the throughput arises as the important dimensioning indicator, for instance the average and peak throughput per user and per cell should be measured.

Due to the soft capacity feature of WCDMA networks, maximizing capacity requires careful load balancing among cells. That is why, network performance is very sensitive to parameters such as the pilot powers, antennas configuration (tilt and azimuth angles, beamwidth, use of null filling mechanisms, etc) and variables that feed to the SHO or the Admission Control (AC) algorithm, among others. All these parameters influence the network in a non-linear manner and finding their optimum combination is a problem of complex resolution.

In this sense, two different approaches exist in the literature to find the optimal combination of planning parameters. First, researchers from the operations research field are frequently focussed on strategies involving mathematical programming. The problem is modeled in terms of (usually) linear equations and thus simplifications or focus on specific aspects are required, some smart examples can be found in [SY04; SVY07] and in several contributions from the MOMENTUM research project, which is an Information Society Technologies (IST) Project from the *5h Framework Program of the European Community*, see for example [EFF+03]. Because of non-linearities and dependencies among parameters, this approach is difficult to be applied when all variables in the system are taken into account. Actually, the problem can be considered a combinatorial optimization one with a very high number of solutions. That is why most of electrical engineers and scientists from computer science tend to make use of metaheuristics, which is also the approach chosen in this thesis.

2.2.2 Use of Metaheuristics in Automatic Planning

Along the previous section it was explained that radio planning optimization can be posed as a combinatorial optimization problem. Indeed combinatorial optimization aims at finding the set of parameters that maximizes (or minimizes) an arbitrary cost function, in this case defined by the radio planning engineer. This type of problems are present in many fields of knowledge and heuristic methods have been widely used in the past to tackle them. With the development of *Complexity Theory*,

Table 2.1: Timeline of most important metaheuristics.

1975	Genetic Algorithms
1983	Simulated Annealing
1986	Tabu Search
1991	Ant Colony Algorithm
1995	Greedy Randomized Adaptive
1995	Particle Swarm Optimization
1997	Cross Entropy Method
2001	Harmony Search
2007	Firefly Algorithm

it was demonstrated that most of these combinatorial problems were in fact NP-complete and so they required time which is exponential in the problem size. Given this, finding efficient and exact procedures to obtain the optimum solution was eliminated as a possibility.

In this sense, the most popular resolution approach was the Local Search (LS), which can be roughly summarized as an iterative search procedure that, starting from an initial feasible solution S, progressively improves it with a series of modifications. In particular, the set of new solutions that can be generated from the current one is the solution neighborhood $N(S)$ and all the possible solutions conform the solutions space. The search terminates when it encounters a solution that cannot be improved with any modification. Thus, with almost every likelihood the algorithm will not reach the best possible solution and will get trapped in a local minimum.

In 1983, Kirkpatrick, Gelatt and Vecchi described in [KGV83] a new heuristic approach called Simulated Annealing (SA) with the outstanding feature that converged to the optimal solution of a combinatorial problem, although infinite computing time was required. Nevertheless, the appearance of SA showed that other ways to tackle combinatorial optimization problems were possible and it boosted the interest of the research community. SA is based on an analogy with a physical phenomenon and in the following years many other new approaches appeared also inspired by nature. Genetic Algorithms (GAs), which were previous to SA were also recuperated. All these methods are now collectively known as metaheuristics and Table 2.1 shows the timeline of the most important ones.

Metaheuristics also require a procedure to generate a new combination (or solution, state...), usually derived from the current one. This is usually a probabilistic procedure that *mutates* the present solution. In most of them, it is interesting to note that moves in the space of solutions can be both *uphill* or *downhill* and that means accepting solutions with a worst cost at particular moments of the search. In fact, this is one of the main differences with respect to LS since it is intended to avoid getting trapped in local minima. This is graphically depicted by Figure 2.1.

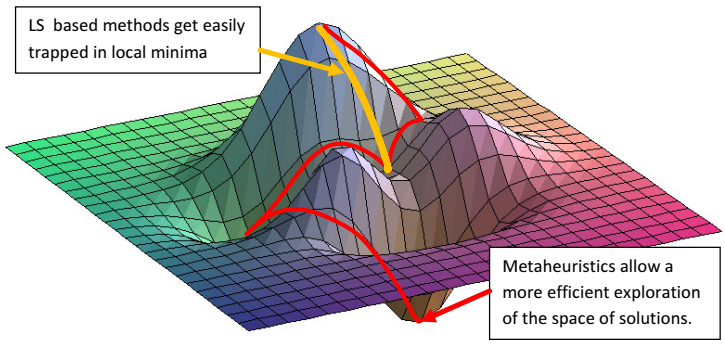

Figure 2.1: Comparison of behavior between LS and metaheuristics.

More sophisticated metaheuristics maintain and evaluate more than one solution, and mutation can be generated from the combination of more than one from this pool of possibilities, other algorithms also keep track of previous solutions to avoid closed loops, etc. Along next sections, the main strategies are revised along with its applications in radio planning optimization.

Simulated Annealing

As previously mentioned, SA is one of the algorithms that enjoys more popularity in the resolution of combinatorial optimization problems. The name and inspiration comes from the cooling process of a liquid and its conversion into a solid. At high temperatures, the substance is in a liquid state and molecules have much mobility, but if temperature is decreased at a sufficiently slow rate, they align themselves in a crystalline structure which is the minimum energy state. On the other hand, it has been observed that if the liquid is cooled too rapidly, the outcome is an amorphous solid with a higher internal energy.

SA attempts to mathematically capture this process of controlled cooling and apply it to combinatorial optimization problems. The cooling process is formulated as the search of the solution implying a lower cost (energy). Every new solution is generated by applying a slight perturbation over the current one. Likewise, from a physical viewpoint, there is some non-zero probability of reaching a higher energy state. As a consequence uphill movements are allowed with a certain probability too, which decreases as the temperature is lowered. Thanks to this strategy, the algorithm is able to escape from local minima, especially at the beginning of the optimization and facilitating a more efficient exploration of the solutions space. The process is summarized in Table 2.2, previously defined notation F_{cost} and $N(S)$ has been used.

The quality of the final solution depends on aspects such as the initial heating or generation of the starting solution, the cooling strategy, the criteria to generate the neighborhood of solutions, etc. In general, a trade-off is always present between the quality of the result and execution time.

Table 2.2: Basic SA schema.

1.	Obtain initial solution S and temperature T
2.	Obtain initial cost: $C \leftarrow F_{cost}(S)$
3.	Generate new solution $S' \in N(S)$
4.	$C' \leftarrow F_{cost}(S')$
5.	Accept S' as the current solution S with probability P
	$P = exp[(C - C')/T]$ if $C' \geq C$
	$P = 1$ if $C' < C$
6.	If equilibrium condition has not been reached, go to 3
7.	Update temperature T
8.	If termination criterion has not been reached, go to 3.

SA is indeed the algorithm chosen for the *Automatic Planning* proposal in this dissertation and further details on it and its adaptation to the particular problem are given in Chapter 4.

The algorithm is currently considered a powerful optimization tool and it is being widely used at many levels of telecommunications engineering. Along Section 2.2.3 its use on 3G/3.5G *Automatic Planning* is revisited, however it has also been used in other contexts of radio planning. It is one of the main strategies to solve efficiently the frequency allocation problem in GSM systems [DAKR93; BK99] and satellite networks [SSSMBC04]. In the context of Wireless Local Area Networks (WLANs), it has been used to decide the optimum location of Access Points (APs) [KU02]. Its utilization is not only restricted to the wireless access network but it has also been successfully used to optimize the tree hierarchical structure among the different entities in the core network, also called as the hub location problem [MG04; HSG00].

Tabu Search

The origins of this second technique are in the 70s although it was not till the 80s that was presented as it is currently known. The work by F. Glober in [Glo86] is considered to be the first reference on Tabu Search (TS).

The underlying idea in TS is that in order to improve the exploration efficiency, it is necessary to keep track of the previously evaluated solutions. Thus, not only neighbor solutions are visible but also the recent history of the search. In fact a *tabu list* is a short-term memory which contains the solutions that have been visited in the last n iterations, where n is a parameter to adjust and it is called the *tabu tenure*. Thanks to these tabus, going back to previously visited solutions is prevented and loops are avoided.

The management of the tabu lists is the key point of the algorithm. Too short lists do not avoid the possibility of cycling, on the other hand, too long lists require

Table 2.3: Basic TS schema.

1.	Obtain initial solution S and Tabu List $T(S)$
2.	Record best solution $S^\star \leftarrow S$
3.	Generate new solution $S' \leftarrow \arg\min [F_{cost}(S')]$ $S' \in N(S) \setminus T(S)$
4.	$S \leftarrow S'$
5.	Update Tabu List $T(S)$
6.	if $F_{cost}(S) < F_{cost}(S^\star)$ then $S^\star \leftarrow S$
7.	If termination criterion has not been reached, go to 3

much memory and the algorithm becomes so strict that exploration can become inefficient. In some cases more than one tabu list is employed, whereas a short one contains the short-term history, the long one tracks older trajectories. A variation of the algorithm prohibits solutions that have certain attributes, this allows tracking more past solutions without too much memory consumption. However it may also imply missing interesting solutions that have not been explored. To avoid this the "aspiration" mechanism is included, which permits tabus to be exceptionally accepted if they allow finding solutions which are better than the currently-known best solution.

Because of the close dependence between the algorithm success and the correct adjustment of this amount of parameters, TS is not so popular as SA. However, to some extent, it has also been applied with success in certain optimization problems in mobile communications systems. For example in the frequency allocation problem [SRH01] or in the hub location problem [GBD01]. Table 2.3 summarizes the steps of the basic algorithm.

Genetic Algorithms

GAs were invented in the mid-70s by John Holland [Hol75] who was inspired by the model of biological evolution. Specifically, these algorithms use the principle of natural selection to solve optimization problems.

One of the differences with previously explained algorithms is that GAs start with several initial solutions, normally generated heuristically, and next they are submitted to a simulated evolution process. In particular, the algorithm starts by selecting certain solutions from the generated set according to a predefined criterion. By means of a recombination process, new "daughter" solutions are created again. The daughters are evaluated according to rules of acceptance and eventually may be "mutated" (slightly modified) with a usually low probability (around 1%). These new solutions are finally inserted in the solutions pool and can be used for future recombination. In this way, results closer to the optimum solution are obtained.

Table 2.4: Basic GA schema.

1.	Define population size $\|\Sigma\|$
2.	Obtain initial set of solutions $\Sigma = \{S_1, S_2, \ldots, S_{\|\Sigma\|}\}$
3.	$C_i \leftarrow F_{cost}(S_i), 1 \leq i \leq \|\Sigma\|$
4.	Generate set with best solutions $\Sigma^\star = \{S_1^\star, S_2^\star, \ldots, S_{\|\Sigma^\star\|}^\star\}, \|\Sigma^\star\| < \|\Sigma\|$
5.	Crossover($\Sigma^\star$)
6.	Mutate($\Sigma^\star$)
7.	$C_i^\star \leftarrow F_{cost}(S_i^\star), 1 \leq i \leq \|\Sigma^\star\|$
8.	Replace worst solutions in Σ with $\Sigma^\star$
9.	If termination criterion has not been reached, go to 3

One of the drawbacks in such algorithms is the multitude of parameters that must be adjusted: crossover and mutation probabilities, population (pool of solutions) size, number of generations, and so on. Nevertheless, its use in all fields of telecommunications has been massive and there is a great deal of literature in which authors make use of them to solve a great variety of problems. For example, in the field of planning and deployment of mobile communication systems, GAs have been used in the frequency allocation problem [WW02], AC algorithms [XCW00], optimal location of APs in WLANs [MVC03], optimal assignments of Nodes-B to Radio Network Controllers (RNCs) [QP08] or routing optimization [PJ03], among others. Table 2.4 summarizes the steps of the basic schema.

Other Metaheuristics

There are other minority mechanisms which enjoy less popularity and have been used to solve specific problems. For example, the greedy randomized adaptive search procedure is a quick execution algorithm which iteratively constructs the solution [FR89]. It has been used to design an enhanced cooperative communication method in wireless ad-hoc networks [COPR05] and to solve the frequency allocation problem [LPRR00]. Another example is the ant colony optimization [Dor92], which uses several agents or "ants" to explore the solution space and find locally interesting areas. This algorithm has been used to solve the frequency allocation problem [LBAN07] and in self-configuration mechanisms in ad-hoc networks [KC05].

2.2.3 Parameters with an Important Impact on the Network Performance

As it was previously explained, optimizing 3G/3.5G network capacity requires the adjustment of several parameters and processes of the radio planning process. In this sense, *Automatic Planning* research was initially focused on the automatic design of the network layout, that is to say on the automatic election of BS site locations, number of sectors and its azimuth orientation. Later on researches have focused

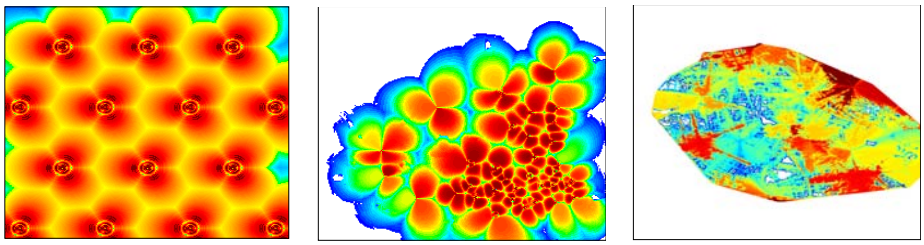

(a) Hexagonal (b) Realistic (c) Real city

Figure 2.2: Comparison of theoretical and realistic layouts.

on designing automatic algorithms to configure BSs. Along next paragraphs, the impact of these parameters is explained and research on its automatic adjustment is revised.

Base Station Positioning

The hexagonal cell model introduced by MacDonald [Mac79] has been widely used in academic and scientific studies of different cellular systems (Figure 2.2(a)). In practice, environments are not regular and propagation conditions and capacity requirements contribute to destroy any regular cell pattern (Figure 2.2(b), particularly in urban areas in which buildings and streets conduct signal propagation (Figure 2.2(c)). Furthermore, the available set of sites is a finite number and thus geometrical layouts are difficult to be respected. A deployment like this is often impractical and it is necessary to find strategies that make possible selecting the best set of sites considering the specific propagation conditions, offered traffic, desired coverage, etc.

With the deployment of 3G networks, the layout design is usually conditioned to a preexistent 2G network because operators try to cosite every new Node-B as far as possible. In addition, infrastructure sharing among different operators is currently much more usual. Thus, the problem should be formulated as: Given a discrete set of possibilities, which are the sites that maximize coverage and capacity while minimizing the number of new acquisitions and thus costs?.

Many jobs have been published proposing automatic algorithms to solve this problem. It has been tackled under different perspectives, including the use of combinatorial optimization algorithms. However, many of them do not provide details on the technique and just indicate which one was used. This is an important issue because, most metaheuristics require several parameters and functions to be adjusted and without this information results can difficulty be reproduced. [KFN02] is an interesting work because it provides very accurate data on how SA was applied to the problem.

A group of researchers from Politecnico de Milano (E. Amaldi, A. Capone, et

al.) has intensively studied the problem and published more than ten works at international conferences, journals and contributions to the COST Action 273 [COS]. They have mainly developed TS based strategies and other simpler search techniques. The optimization criterion chosen to properly locate sites depends on the link (UL or DL) that is considered dominant and therefore the type of traffic that is more likely to be served. When a mostly symmetrical traffic is assumed, the study focuses on the UL [ACM01], otherwise the objective function is defined by the DL [ACMS03].

In [WRH04] a step further is taken and the problem is reformulated to achieve several goals at once (multiobjective problem). Specifically, coverage and cost (minimum number of transceivers required) are jointly optimized. By applying a GA, it is pursued to achieve the solutions that belong to the Pareto front achievable through this type of formulation [Coe01]. It should be noted that there are very few jobs in the literature addressing the problem under this viewpoint. The results are interesting and easily measurable since a set of optimal solutions are presented and thus comparison is possible among them.

As a final remark, it is worth mentioning that so far this has been the most studied problem in the context of radio planning optimization.

Sectoring

Under the concept of sectorization both sector orientation and antennas beamwidth are included. Initially, these two parameters are chosen according to coverage criteria and as an efficient manner to reduce interferences among cells. However, if traffic is heterogeneously distributed, sectorization can be used to increase capacity by means of load balancing. This can be done through a shift in the azimuth angle or by reducing and increasing the width of adjacent sectors [Ahm02].

The work in [SY01] proposes a method to find the sectorization which guarantees minimum transmitted power in the UL. Given that the proposal needs to know the position of the terminals with precision, the technique is proposed to be used in wireless communications systems with fixed terminals, as for example local multipoint distribution systems. In future wireless systems, it will not be unusual the presence of Global Positioning Systems (GPS) in the UEs, so if users positions are exactly known in real time, this mechanism could be easily extended to mobile systems. However, the extra UL signalling may be a serious drawback.

A further step in this direction is to change the whole shape of the horizontal radiation pattern and not just the width or azimuth angle. In this way, the diagram is adapted to traffic conditions. Its synthesis is easy, as for example with a least mean square error criterion. It must be said, however, that these strategies are proposed as adaptive and therefore existing works will be commented in forthcoming sections.

Tilting Antennas

One of the optimization strategies that has been used more in the past is adjusting the tilt of antennas at BSs. By changing the elevation angle, energy can be concentrated in the target area and interferences towards (and from) other cells can be reduced. So a correct adjustment can imply both a coverage improvement and interferences reduction. This last point is particularly important in WCDMA systems in which isolation among cells is paramount because of a frequency reuse factor of 1. Downtilting can be performed mechanical or electrically, however a detailed description is delayed to Section 3.3, where a study is carried out to quantify the effect of this parameter in UMTS networks. Subsequent paragraphs review existent works dealing with downtilt to optimize radio access networks in mobile communication systems.

Initial studies on downtilt variation addressed the problem of minimizing cochannel interference in FDMA systems, thereby yielding a better SIR. However, in this dissertation only works that aim at optimizing (W)CDMA based systems are revised. In this sense, the different research works can be categorized in different topics.

- **Hotspot traffic relief**. Initial works investigate how downtilting allows alleviating traffic congestion in cells with one hotspot. This way the final capacity in the evaluated system is increased. The feasibility of this strategy is demonstrated in [WCW98], which makes use of mechanical downtilt and [KLKW00], which utilizes electrically tilted antennas.

- **Mechanical downtilt gains**. A second group of works focuses on quantifying the gains of mechanical downtilt in generic systems. Thus, [Bun99] makes an UL study and concludes that expected gains are between 15% and 20% when antennas angles are optimized. The work also concludes that intercell interference is the main factor that determines the optimum angle and that intercell separation or antenna heights do not appear to be critical factors in the effects of downtilt. However these ideas are contradicted by a more recent work [NIL05] which concludes that capacity gains obtained by downtilting are directly proportional to antennas height and are reduced with site spacing. The gains obtained by means of mechanical downtilting in the DL are investigated in [NL04] making use of 6-sectorized cells.

- **Comparison between mechanical and electrical downtilt**. With the introduction of electrical downtilt, several works studied the differences that both strategies had on radio planning results [For02]. Critical variations are not detected, being the main one wider softer handover areas in the mechanical case, in which sidelobes are not sloped down [NIL05]. Nevertheless, other features such as improved flexibility, precision, etc. make of electrical downtilt a more interesting option (see Chapter 3).

- **Electrical downtilt and *Automatic Planning***. Currently, most papers that somehow consider downtilt deal with the electrical option. However, and

because of their interdependence in the final effective cell shape, downtilt angles are usually jointly adjusted with pilot powers (described in next section). The authors in [LSWA00] started their study by investigating optimum angles in a realistic scenario and extending these results to design an *Automatic Planning* mechanism in [WSK02]. A LS based algorithm is proposed to optimize the angles in a cell by cell manner. The search tries to find the angle which best fits traffic conditions. Although the algorithm performs correctly, it is likely that the approach could be enhanced by substituting the LS method by one metaheuristic considering all cells simultaneously and not evaluating them sequentially. Along next chapter it is investigated how interdependencies among cells imply that a joint optimization can be much more efficient.

Finally, dynamic strategies are lately being proposed so that tilt angles are continuously adapting to traffic conditions. Since these approaches are out of the scope of the (static) *Automatic Planning*, the reader is referred to Section 2.3.

Pilot Power

Pilot signals or CPICH in the UMTS case have two basic objectives. First, this channel is used to enable channel estimation and second, it is used by cell selection and HO processes. UEs are only served by those cells that are received with enough quality in their CPICH signals. So intuitively, it can be learnt that it is a key planning parameter in both coverage and capacity maximization. Further details on this channel and its impact on the system performance are described and studied in next chapter, in Section 3.2.

Pilot powers optimization is difficult when performed in an ad-hoc manner. Besides, it can become tedious, costly, and time consuming when they involve repeated drive tests and measurements, likewise local adjustment cannot guarantee a consistent result. Because of interdependencies among cells in CDMA based networks, the adjustment problem should be ideally addressed considering all the cells in the area to optimize. Hence, several researchers have proposed different *Automatic Planning* techniques. In particular, Table 2.5 compiles several relevant works and their main features are listed in a comparative manner. Publications derived from this thesis are also listed at the end of the list.

In summary, it can be observed that most of the works are focused on the DL. In particular, several of them aim at minimizing the required CPICH powers while guaranteing coverage. The reduction in power also tends to benefit DL capacity. On the other hand, when data channels are considered one of the main objectives that is usually pursued is achieving DL load balancing. This way, cells containing a hotspot transfer part of its UEs to nearby ones, so that transmission powers are leveled. However, the UL effects are usually missed and techniques do not take UL requirements into account. The works in which *n/s* is indicated do not clearly specify this fact. Next chapter shows that, from an UL viewpoint, transferring UEs from one cell to another must be done carefully in CDMA systems because of the unitary frequency reuse and load balancing strongly depends on the propagation

Table 2.5: Comparison of pilot and tilt static optimization techniques.

Paper	Year	System type	Optimized link	Metrics considered by the optimizer			Algorithm	Pilot / Tilt of Antenna
				UEs interference	% Handover	% Coverage		
[KCL99]	1999	CDMA	both	no	no	yes	Rule based	pilot
[Hur02]	2002	FDMA	DL	yes	yes	yes	SA	pilot + tilt
[WSK02]	2002	CDMA	DL	yes	no	no	LS	tilt
[VY03]	2003	CDMA	DL	no	no	yes	Math. Prog.	pilot
[SGH03]	2003	CDMA	DL	yes	no	yes	Rule based	pilot
[GJCT03a]	2003	CDMA	n/s	yes	no	no	Rule based	pilot + tilt
[GJCT03b]	2003	CDMA	n/s	yes	no	yes	Rule based SA	pilot + tilt
[GJT04]	2004	CDMA	n/s	yes	yes	yes	GA	pilot + tilt
[SY04]	2004	CDMA	DL	no	no	yes	Math. Prog.	pilot
[LZY05]	2005	CDMA	DL	yes	no	yes	Rule based	pilot
[SVY07]	2007	CDMA	DL	no	no	yes	Math. Prog.	pilot
[GLRO03a] [GLRO03b]	2003	CDMA	both	yes	yes	yes	SA	pilot
[GLRO04a]	2004	CDMA	both	yes	yes	yes	SA	pilot
[GLRO04b]	2004	CDMA	both	yes	yes	yes	SA	pilot + tilt

loss between each UE and the serving BS and its UL load factor. As a consequence, sometimes the best option cell is the loaded one and transferring UEs to a less loaded one not only does not provide any benefit, but also can seriously impair UL performance. Particular details on some of the works in the table are given next.

Minimizing the required pilot powers for a certain covered area is a single objective problem smartly addressed by means of mathematical programming in [VY03; SY04; SVY07]. These studies are coverage focused and UL effects are not considered, SHO areas are neither guaranteed or evaluated after the mechanism is applied. With the same objective, a rule based strategy is proposed in [KCL99], where pilot powers are adjusted in a cell by cell basis but taking into account SHO constraints. Another rule based strategy is presented in [LBSR99] but in this case the objective is to reduce pilot polluted areas, which is missed in the previous ones. This has an indirect impact on the network capacity because interferences due to pilot signals are minimized. The mechanism is not only simulated but its results are also successfully implemented in a real network.

The works enumerated in the previous paragraph are more focused on CPICH coverage optimization. The work in [SGH03] proposes an algorithm composed of two parallel modules. Whereas the first one aims at optimizing coverage, the second one pursues to adjust pilot powers to balance the DL load among cells. The algorithm iteratively increases or reduces BSs powers in 0.5 dB steps after comparing the DL load with a certain threshold value. An interesting aspect of this work is that simulations have been done for different levels of knowledge on the traffic distribution. From a system with a lot of resolution in which traffic is known at a pixel level to a system with very low resolution in which the density of users is only known for extensive areas covering several cells. The differences in the algorithm outcomes are not very high and so it could be applied without such a precise knowledge of the traffic distribution.

Metaheuristics are used in [GJCT03b] and [GJT04], in particular a geometrically cooled version of SA and GAs which succeed to improve the number of correctly served UEs. In the most refined version the algorithm actively searches to achieve load balancing among cells and both pilot powers and downtilts are modified according to previously defined rules. UL and DL cell load are evaluated by the algorithm but their definitions are not directly indicated.

2.3 Dynamic Planning and Automatic Tuning

During the last years mobile communications market not only has grown but also it has started to diversify thanks to their improved capabilities. New products and services are being offered and future cellular networks will offer an even higher amount of services, partly promoted by the migration to IP Multimedia Subsystems (IMS). All this causes important fluctuations in offered traffic, aggravated by the temporal and spatial users behavior. Short-term traffic variations are going to be absorbed by RRM mechanisms: Power control, scheduling and adaptive modulation

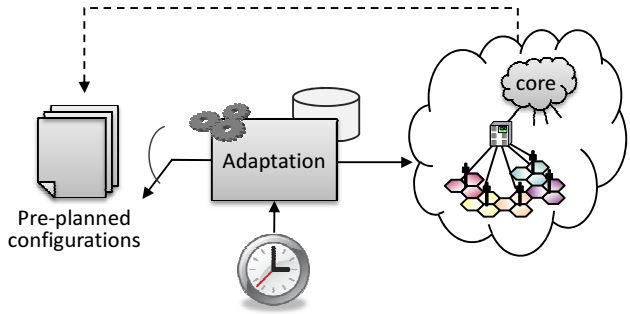

Figure 2.3: Open-loop optimization based on *Automatic Planning*.

are clear examples of that. On the other hand, when looking at aggregate variations, it can be observed that intermediate and long-term changes also appear. Inevitably this results into a dynamics in load and resource demand that is a challenge for the radio network planning engineer. Traffic conditions evolve along time and so does the optimum radio plan.

Although *Automatic Planning* strategies are static in essence, they might well be a first step towards *Dynamic Planning* and optimization. *Automatic Planning* can be executed offline, being fed by real data from the network. This way many cases and situations can be analyzed and pre-planned. Given this, the network would switch among the different optimized cases according to a preestablished temporal pattern for example at different days during one week or even at different hours in the same day. This would represent somehow an open-loop dynamic optimization [BBD+05], graphically described by Figure 2.3.

However the more frequent traffic variations are, and the higher its dynamic range, the less effective open-loop strategies based on *Automatic Planning*. This motivates investigations on dynamic techniques able to autonomously adapt to short and mid-term changes in a closed-loop manner. Indeed, measurements from the network will be turned into appropriate Key Performance Indicators (KPIs) and will feed the closed-loop optimization (Figure 2.4). These strategies are aimed to fill the optimization temporal gap between existent RRM algorithms and seasonal optimizations.

The research community is showing an increasing interest in the development of these strategies and several authors propose algorithms for the control of specific network parameters. First proposals have dealt with planning parameters such as pilot powers levels and antennas configurations, for these cases the denomination *Dynamic Planning* is used in this dissertation. However, many efforts are lately concentrating on dynamic auto tuning of RRM parameters mainly in the parameters that control the AC and SHO algorithms. In this second context, the term *Automatic Tuning* and *Automatic Tuning Systems* has been preferred.

These mechanisms reduce network sensitivity to changes in the assumptions done during the planning process and they aim at reducing infrastructure costs

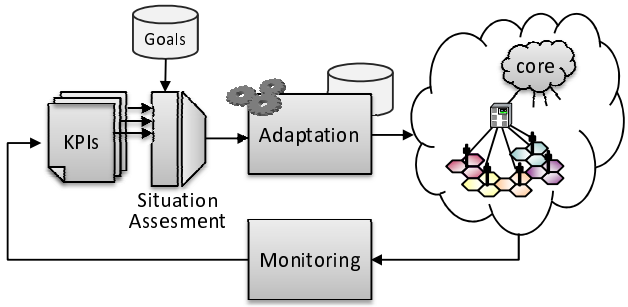

Figure 2.4: Closed-loop optimization

while ensuring QoS under time-varying conditions and without human intervention. Because of this last feature, networks making use of them are also know as self-organized or self-optimized networks [SNBH00]. A self-organized network can be defined as a system that responds to its contour conditions autonomously, detecting changes and reacting accordingly. Hence, it must extract the maximum possible information not only from instantaneous conditions but also considering trends and behaviors in larger temporal windows. From this information, it has to decide how to change different parameters to guarantee optimum performance. Several research projects and consortiums have made contributions in this research line, some of the main exponents are: AROMA [ARO], CELTIC-GANDALF [GAN], MONOTAS [MON] and SOCRATES [SOC].

Self-organization goes beyond a throughput or network performance improvement, it enhances operability, allows a faster rollout, reduces OPEX, planning efforts, failures, etc. A fully autonomous network is a challenging objective and 3GPP has started to standardize this feature in its Release 8 [3GPf; 3GPg]. Self-configuration tasks are paramount in deployments using home BS (femtocells), which are expected to be usual in the Long Term Evolution (LTE) context. In this possible forthcoming framework, BSs have to be real plug-and-play devices and interference coordination with existent and new nodes is mandatory.

2.3.1 Dynamic Planning.

Dynamic Pilot Powers Variations

One of the first strategies that is proposed in this sense is dynamic pilot power variations to achieve real time cell coverage changes and transfer UEs from one cell to another. This strategy succeeds if there is a high enough density of active UEs which appear and disappear in a particular area. If the density is high but without changes along time, *Dynamic Planning* is not justified. In that case, (static) *Automatic Planning* is the solution to deal with complex load imbalances. Moreover, the success level of this type of proposals is also closely coupled to the utilized Spreading Factors (SFs). Intuitively, it can be thought that if one cell is highly

loaded because of just a small group of UEs with a high rate (low SF) over a classical DCH, real time changes in the coverage area are not going to achieve a smooth load balancing. Given this, most of existent literature aim to enhance the performance of multicell scenarios with one of the cells containing a hotspot. A second comment is that, similarly as with static algorithms, in general proposals are based on DL load balancing and the UL is again usually missed.

A rather relevant work is [VHPH02a] which proposes a technique based on heuristic rules to optimize pilot powers and improve DL performance. Periodical updates of pilot powers are done aiming at balancing the load among cells while keeping total transmission power below a certain threshold. The same authors propose a second technique in [VHPH02b], in this case a cost function is defined depending on the load difference between the cell under study and its limiting ones. The function is constantly kept minimized by means of the gradient method. Whereas the throughput gains are important in the first case, in the second approach the benefits are notably lower. It is worth mentioning that in these studies coverage levels are a secondary constraint and that is why a reduction is obtained when the algorithms are running. The work in [LYLC05] goes one step further and poses the problem more realistically considering AC algorithms in the study; [PUAL97] also takes into account the call blocking rate to take decisions on pilot power levels.

Many of the published papers do not take into account the influence of UEs location in the cell and hotspots are indirectly supposed to be homogeneously distributed in the affected cell. In this sense, the work in [ZBNH02] investigates dynamic load balancing in a more general and rigorous way and several ideas are indicated to better identify a hotspot cell susceptible of successful traffic shedding. The proposed mechanism consists of two phases, firstly the identification is performed, and secondly, the target cell to which UEs are going to be redirected is selected. Pilot power from both cells are modified in steps of 1 dB until the desired reassignment of UEs is achieved.

One drawback of dynamically shrinking or extending cells through pilot power variations is generating coverage problems. Also there can be an increased probability of handover failure if changes are not perfectly coordinated among cells. Moreover several thresholds and power levels in UTRAN are derived from CPICH transmission powers. An alternative technique without these drawbacks is modifying the parameters controlling SHO areas, as explained later.

Dynamic Antenna Configuration

With regard to antennas configurations, authors propose both adaptive sectorization and downtilting, and indeed many recent patents exist in this respect. Expectable gains from the first parameter are analytically studied in [SY01], but it is not until [NDF04] that an adaptive sectorization mechanism is proposed. Certain azimuth angles are preprogrammed and antennas commute among according to traffic distribution. [LOP03] and [DBC05] are systems that dynamically change sector sizes by means of semi-smart antennas, the sector size is inversely proportional to the

DL offered load so that all load sectors remain as balanced as possible. In a more complex manner, the work in [DBC03] proposes a real time synthesis of diagram patterns and actions are taken to force different horizontal cuts.

Concerning dynamic downtilting, its benefits are validated in this dissertation in Chapter 3 and also in other works such as [PBS04]. Mechanisms to dynamically change tilt are usually based on simple iterative searches that adapt angles to traffic distributions [Cal06; WBJN06].

As with pilot powers, one of the drawbacks of these strategies is potential coverage problems and handover failure. Taking this into account, [AJLD+04] proposes a multiband system with two antennas operating at different frequencies. Whilst the first antenna is tilted in the long-term to follow the less dynamic traffic, short-term variations are controlled by the second one.

2.3.2 Automatic Tuning of RRM Parameters

The second group of automatic tuning algorithms is a more recent direction of research and deals with RRM parameters. General ideas on this topic can be found in [LWN06; NDA06] which validate its feasibility and demonstrate a significant increase in network capacity in comparison with default parameter settings. Most efforts have been focused on the parameters that govern AC and SHO algorithms.

It is worth mentioning that the integration of RRM parameters adjustment in the radio planning optimization process and the use of strategies that dynamically change the planning parameters imply that planning and RRM have partially merged and the line between both has become blurred.

Admission Control

Concerning AC, an automatic tuning of the maximum allowable load factor, or indirectly, of the measurements to calculate it, is proposed in several works. For instance, paper [HPVL03] controls the UL planned total received power target in a cell-by-cell basis, the proposed algorithm is very similar to the method presented in [LWN06]. The target value is auto-tuned in each cell based on the Block Error Rate (BLER) and blocking of Real Time, Circuit Switched (CS) calls and Non Real Time traffic queuing. A Look-Up-Table (LUT) is designed relating these three indicators with an adjustment decision (increase, decrease, etc). The metrics are calculated with straightforward functions considering that degrading a connection is 5 times "worse" than blocking a new one, and blocking is 4 times worse than queuing, which has a very small impact on the tuning. The same authors deal with the DL in [HV02] and extend the application of the algorithm to adjust the maximum power that can be devoted to a single DL link. Both papers are similar and just differ in the parameter to be tuned. The throughput increase is smaller (39%) in the DL than in the UL (50%) when compared to that obtained with fixed default parameter settings. Finally, paper [PDGA04] also deals with load target auto tuning in a very

similar way but taking dropping and blocking rates as inputs. The authors assume an autonomous control unit for each sector that is fed by quality indicators from the sector itself and its neighbors. The control is again rule-based but quantified and represented by a matrix, which in essence contains a similar information to that in the two previous works. Each element of the matrix contains a correction value for a couple of blocking and dropping rates. Similar matrices are constructed for each neighboring cell and then all of them are aggregated to give a global decision. However, it is not deeply explained how these neighboring matrices are generated and examples of the mapping between rates and decisions are not given.

Soft Handover

Automatic tuning of SHO parameters is usually done aiming at load balancing by means of cells shapes modifications, so the objective is the same as in most pilot and downtilt related works. However, instead of acting over the measurements themselves, the different hysteresis thresholds that control the algorithm are varied. This way, the authors in [YGNT00; FN02; LCH05; LFYG05] propose automatic displacements of SHO areas so that loaded cells shed part of their UEs, which are naturally directed towards limiting cells. To achieve this, slightly different mechanisms are used but not all of them are applicable to UMTS networks.

For example, [LCH05; BHHPSS06] reduce SHO thresholds so that a cell with a hotspot is less appealing to nearby UEs and also it can expel some of its more external ones. This method, however, is only feasible for multi carrier CDMA systems, since the condition that triggers the reconfiguration is the percentage of occupied bandwidth. Similarly, the work in [YGNT00] designs an algorithm for CDMA systems but soft capacity is not considered. Nevertheless, these cases could be adapted to realistic UMTS systems with minor changes, just measuring the load factor and comparing it with a maximum allowable threshold.

The work in [LFYG05] is fully developed in the context of UMTS networks, in this case there is a direct mapping between different load levels and specific handover thresholds. The work is quite generalist in the sense that it does not give the definition of the considered load factor. This parameter is constantly monitored and thresholds are updated every 100 ms if needed. However, mechanisms to avoid ping-pong effect and excessive reconfigurations are missing. Thus, in a system with active UEs using different services, variations in load levels could impair the algorithm performance. This issue is not a problem itself because complementing the proposal with a filtering process would be straightforward. Finally, the authors in [FN02] make use of a second order gradient method so that the minimum of a predefined cost function is constantly tracked. This function relates handover thresholds with the blocking ratio and DL transmission power.

Previous works perform the network tuning by modifying the thresholds that govern the addition and dropping of cells. However, in the case of UMTS, the standard defines a parameter that can be easily used to make more or less attractive particular cells. This is the *Cell Individual Offset* (CIO), which is usually not con-

sidered for load balancing. More details on how this parameter affects on SHO is given Chapter 7. A second comment to existent work is that load evaluations are done considering just one link. However, SHO parameters impact on each link in an opposite manner and thus should be considered and optimized at the same time. This effect is studied in Section 7.3 and indeed this is the framework of the current proposal. The opposite effect is investigated and conveniently used to detect whether the UL or the DL is the limiting link and favor it so that congestion control algorithms are delayed. Also, among the novelties on this topic, an important one is the investigation of UL and DL behavior in front of variations of SHO parameters and some extra light is provided in the lack of consensus about gains or losses in the DL.

Chapter 3

Base Station Parameter Adjustment

3.1 Introduction

Prior to the design of any *Automatic Planning* strategy it is mandatory to investigate the effects of the variables to be optimized. In addition, interactions with other parameters must also be included in the study.

In the previous chapter it was shown that two of the parameters that have been used for optimization more often are the CPICH and downtilt of antennas. Indeed, modifications in both of them allow a controlled way of modifying the cell shape. This is the effect that is mainly considered by existent approaches that aim at transferring UEs between cells. However there are secondary effects in WCDMA wireless access networks that are usually missed and which imply that reducing the load in a cell is not as straightforward as just reducing its cell area.

This chapter focuses on the impact of these two planning parameters on the radio access performance and in particular, the study stresses effects beyond well known ones.

The chapter is organized in two differentiated parts. The first one deals with CPICH power variations and the second with downtilting. In both cases an introduction is given on their role in the network and how they impact in the outcome of the radio planning. Interactions with other parameters are studied in both the UL and DL and some considerations on UEs spatial distribution are given too. Conclusions from this chapter are a direct input to the *Automatic Planning* strategy proposed in the next one.

3.2 Impact of CPICH Power Variations

3.2.1 Introduction

In WCDMA FDD cellular systems, the CPICH is a DL channel broadcasted over the entire cell with a fixed and known channelization code (code 0) and transmitting a pre-defined bit sequence with a fixed SF of 256. Its transmission power is a cell-specific configuration parameter and must be adjusted taking into account that the channel participates in several important network processes:

- In conjunction with the Synchronization Channel (SCH), it allows determining the cell primary scrambling code during the cell search procedure [3GPj].
- It is used for measurements of signal quality and it also provides phase and path loss estimations and permits the discovery of other radio paths. All this information is used by the Rake receiver to improve other channels decoding. Optionally Nodes-B may broadcast one or more Secondary Common Pilot Channels (S-CPICH) and transmit them over specific areas of the cell, for example in multi-beam systems.
- CPICH is also used to evaluate the cells to be included in the Active Set (AS) and so it is a key factor in the SHO procedure. Thresholds, margins and parameters participating in the process are described in [3GPm] and are summarized in Chapter 7, Section 7.3. If the reader is not familiar with these, it is recommended a previous browsing of that section.

In order to carry out these functions, the quality of CPICH signals is evaluated in terms of Received Signal Code Power (RSCP) and E_c/I_0, which is the ratio of the received chip energy to the total power spectral density at the UE antenna connector [3GPh]. The $(E_c/I_0)_{CPICH}$ measured by UE k from BS j is given by:

$$(E_c/I_0)_{CPICH}(j,k) = \frac{\frac{P_{TX,CPICH}(j)}{L^{DL}(j,k)}}{\sum_{i=1}^{N_{BS}} \frac{P^{DL}_{TX,tot}(i)}{L^{DL}(i,k)} + n_{UE}(k)} \tag{3.1}$$

Where:

- $P_{TX,CPICH}(j)$: CPICH power transmitted by BS j.
- $P^{DL}_{TX,tot}(j)$: Total power transmitted by BS j, it accounts for control and data channels.
- $L^{DL}(j,k)$: DL link loss between BS j and UE k.
- $n_{UE}(k)$: Thermal noise power at UE k.
- N_{BS}: Number of BSs in the system.

According to the Third Generation Partnership Project (3GPP) a cell shall be considered detectable when $(E_c/I_0)_{CPICH} > -20$ dB [3GPh] but higher values are usually imposed to leave a margin for safety, typical values are -18 dB [VHPH02a] or even -12 dB [Gat05]. Given this requirement, CPICH transmission powers are usually set during radio network planning and reference values are typically between 5% and 15% of the total Node-B transmit power. A first estimation can be easily obtained just manipulating the previous expression:

$$P_{TX,CPICH}(j) = (E_c/I_0)_{CPICH}(j,k)\, L^{DL}_{max}(j) \left[\sum_{i=1}^{N_{BS}} \frac{P^{DL}_{TX,tot}(i)}{L^{DL}(i,k)} + n_{UE}(k) \right] \quad (3.2)$$

The UE k is supposed to experience the maximum allowable loss, $L^{DL}(j,k) = L^{DL}_{max}(j)$, it is at the cell edge. This value can be estimated for example, by means of link budgets.

Since interference is perceived as an increase in the noise at the receiver, the previous equation can be expressed in terms of the noise rise at k, $\Delta n_{UE}(k)$, or more precisely, in terms of its measured load factor, η^{DL}_{edge}, which represents the perceived load in a more comfortable range, between 0 and 1:

$$\begin{aligned} P_{TX,CPICH}(j) \quad = \quad & (E_c/I_0)_{CPICH}(j,k)\, L^{DL}_{max}(j,k)\, n_{UE}(k) \\ & \left\{ 1 + \left[f^{DL}(j,k) + \frac{1}{\rho(j,k)} \right] \left[\frac{1}{1+f^{DL}(j,k)} \frac{\eta^{DL}_{edge}(k)}{1-\eta^{DL}_{edge}(k)} \right] \right\} \end{aligned} \quad (3.3)$$

This expression is derived in Appendix A.

Since these values depend on the particular UE geographical position (variations can occur in different points of the cell edge), the expression is just an approximation that should only be used in preliminary preoperational phases of radio network planning. Furthermore, it also depends on $f^{DL}(j,k)$ which is the quotient between the intercell and intracell power measured at k and considering its link with BS j. This parameter is also highly dependant on the UE position and the combination of services used in each cell.

Concerning $\rho(j,k) \in [0,1]$, it represents the orthogonality factor. In particular, intracell interference is calculated as the summation of powers transmitted by the BS towards the rest of users in the cell $\left(P^{DL}_{TX}(j,i), \forall i \neq k\right)$ plus the power devoted to control channels $c(j)$, both terms measured at k. Ideally, the interference should be zero, because of the use of orthogonal codes [HT02], Orthogonal Variable Spreading Factor (OVSF) family codes in the UMTS case. However, in practice, part of this orthogonality is lost due to multi-path propagation. The effective interference is then characterized by a fraction of the total power through ρ, whose value depends on the type of environment and on the power delay profile of the channel, in particular

$\rho = 1$ defines a situation with full loss of orthogonality.

More refined values for $P_{TX,CPICH}(j)$ are found by means of simulations and using realistic digital terrain models and loads distributions. Drive testing measurements also help to detect discrepancies between the real load and f factors and their estimations, and thus they allow finding coverage holes, pilot polluted areas, or a lack of enough RSCP that would cause difficult channel estimation.

Nevertheless, CPICH not only provides coverage or a means for channel estimation, $(E_c/I_0)_{CPICH}$ is also a key parameter in UTRA SHO and its measurement determines the cells to be included in the AS. The procedure is an event triggered mobile evaluated handover in which the network orders the UE to add a cell to its AS according to events derived from measurements on different received CPICH signals. Given this, it may be inferred that traffic can be transferred from one cell to another by means of CPICH power variations. Because of the frequency reuse of 1, these variations can lead to an increase or a reduction in the global interference level and so to capacity degradation and improvement respectively. A final comment is that pilot power variations just affect the powers of other common control channels that are derived from it so that their joint coverage is coherent. This is an important difference with respect to modifications in the downtilt of antennas, this last case permits the aforementioned transfer of UEs but additionally it does imply a modification in all transmitted powers and received intercell interference.

Along next section, a quantitative analysis on the impact of CPICH powers is done. Variations on power levels are evaluated to test the required margin that implies significant transfers of UEs among cells. Also, an UL and DL analysis is performed to investigate variations in users' connections, in UL and DL load factors and in the maximum achievable capacity, among other network indicators.

3.2.2 Quantitative Analysis

This analysis is performed by means of static system level simulations in a realistic and heterogeneous scenario that consists of 13 cells and where propagation losses are based on real measurements from a GSM network operating in the 1800 MHz band. Details on the scenario and the simulation platform can be found in Appendix B. All figures and results are the outcome of executed simulations.

The first set of simulations have been done with a fixed number of UEs (250) using a 12.2 kbps conversational service, whose features can be found in the same appendix. The type of services is not particularly important because initially the analysis aims at evaluating the influence of CPICH power variations over traffic distribution and connections between UEs and specific BSs.

Increasing or decreasing the pilot power of a particular cell implies that UEs are going to listen to it in a better or worse manner. Thus, the number of times a cell appears in the users' AS and, consequently, the number of links established with it is directly proportional to its CPICH level. In particular, Figure 3.1 shows the probability that the central cell and nearby ones are included in the users' AS.

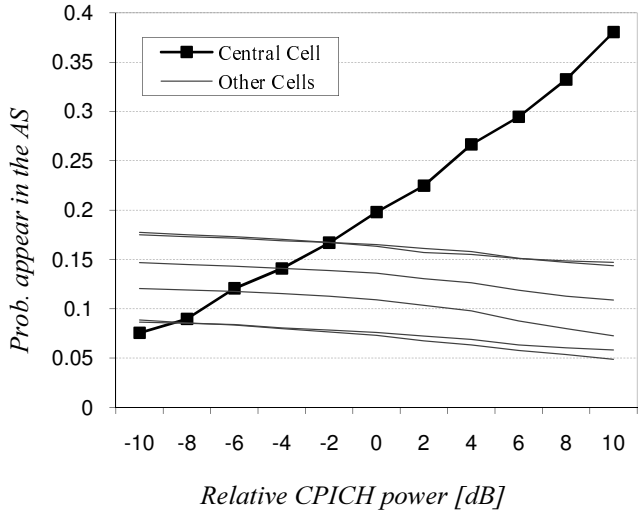

Figure 3.1: Probability of being included in the AS for different CPICH powers.

This probability is represented for different relative values of the central cell CPICH power. Thus, when the x-axis indicates 0 dB, all cells are transmitting with the same power. A wide margin of values is represented but these simulations are done for relatively low traffic loads, around 50% in the worst case (central cell) when CPICH powers are equal. Otherwise, it must be taken into account that devoting too much power to pilot powers can mean a significant reduction in DL capacity because of power shortage. On the other hand, a reduction without coordination with neighbor cells can generate coverage holes.

From the figure it can be observed that traffic transfer is feasible even for the smaller variations. It is noticeable that changing the pilot implies capturing or expelling users from or towards several cells. The impact is much higher on the central cell because the other ones are just affected in the portion of its boundary that limits with the modified cell. Hence, to transfer users from one cell to another it is more effective reducing the pilot power of the loaded cell and not increasing the power of the limiting ones, of course, as long as coverage holes do not appear. This second option would have an impact in a higher number of cells, all those neighbor of the modified ones. The increase or decrease of UEs in one cell by means of pilot power variations depends on their geographical position, and if there is a high concentration of users in a specific area of the cell, a smooth transfer is complicated.

The election of SHO parameters has a direct influence on the possibility of transferring (eventually balancing) traffic among cells. The notation to define each AS configuration is ($\mathcal{N}$,*AddWin*) where $\mathcal{N}$ indicates the maximum number of cells and *AddWin* is the addition window expressed in dB and considered equal to the drop window. Details on the SHO algorithm an the impact of these parameters can be found in Chapter 7.

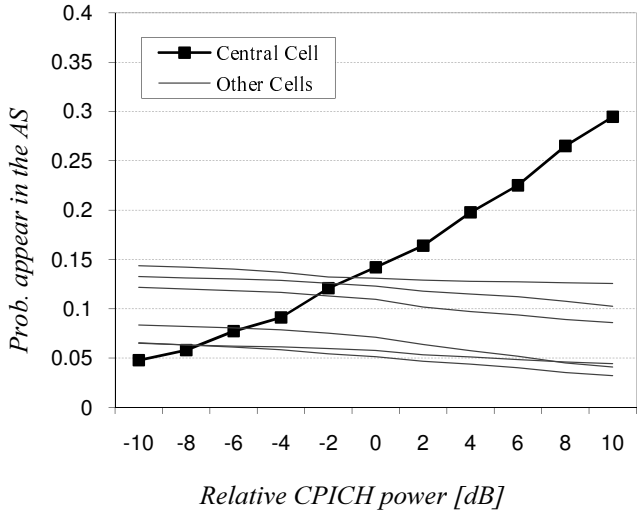

Figure 3.2: Probability of being included in the AS for different CPICH powers and AS (2,2).

Pilot variations are more effective to include or exclude BSs from the AS if both $\mathcal{N}$ and *AddWin* are adjusted with high values. Figure 3.1, which was done with a (3,6) AS configuration can be compared with Figure 3.2, which considers (2,2). It can be seen that the central cell needs 4 dB extra in the second case to obtain a 0.2 probability of appearing in the ASs.

These two graphs give a first level information. In fact, there is a direct relation between these values and the number of DL connections. On the other hand, the relationship with the UL is not so direct. UEs are supposed to be connected to the BS that requires less power from them. In fact, the UE adjusts its transmit power based on the combination of received transmit power control commands (TPCs) from all BSs in the AS. In the conventional scheme a UE in SHO decreases the UL transmit power whenever it receives the corresponding TPC from at least 1 BS belonging to the AS. On the other hand, if TPCs are 'up' (=1) or 'no change' (=0) and the mean of the received TPCs is bigger than 0.5, the power is increased [3GPj]. Hence, UEs are always transmitting at the minimum possible power.

Given the previous paragraph, it has been represented the evolution of UEs connected with the central cell in Figure 3.3. It can be observed how the number of UEs is higher for an AS (2,2). Paradoxically, with this configuration, the probability of appearing in the ASs was lower. The reason behind this is that UEs are not able to transmit to other new cells because of reduced *AddWin* and $\mathcal{N}$. With larger SHO areas, UEs are able to select among a wider number of BSs and reduce its UL transmission power, so indirectly this helps to reduce the impact of bad adjustments in pilot powers. In fact, it can be seen that variations in the number of UEs are sharper with smaller AS parameters. On the other hand, too many BSs in the AS implies more DL resources and an increased SHO overhead. This UL

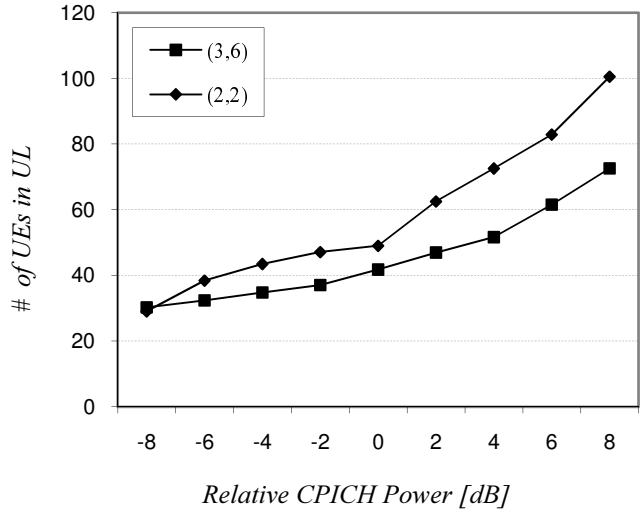

Figure 3.3: Number of UEs connected with the central cell for different CPICH powers.

and DL capacity trade-off is investigated in Chapter 7 and a mechanism to solve it is proposed. As a conclusion it can be stated that, even though $(E_c/I_0)_{CPICH}$ is eminently a DL measurement, since ASs are finite in size, UL considerations must be taken into account to adjust CPICH powers in order to maximize capacity. This idea is further explored in next chapter.

Once SHO parameters are selected and fixed, any future variation on the pilot powers would displace SHO areas and so it would impact on SHO overhead and the number of established links. Differences before and after reconfiguring the powers would be particularly significant if UEs are very heterogeneously distributed inside cells. For the simulated case, Figure 3.4 shows the probability that ASs contain more than 1 BS for different relative values of the pilot power and 3 AS configurations. It is clear that variations are not so significant and in the worst case (3,6) they just evolve from 30% to 35%.

Keeping in mind that the final objective is to achieve a maximization of the system capacity, it must be indicated that wrongly adjusted pilot powers can lead to a relevant degradation of the network. UL capacity is directly related to interferences at BSs, which can be understood as a noise rise in the BS, $\Delta n_{BS}(j) = P^{UL}_{RX,TOT}(j)/n_{BS}(j)$. However, in general and as previously stated, by using the load factor η, the cell load is represented in a more comfortable range, between 0 and 1:

$$\eta(j) = 1 - \frac{1}{\Delta n_{BS}(j)} = \frac{P^{UL}_{RX,TOT}(j) - n_{BS}(j)}{P^{UL}_{RX,TOT}(j)} \tag{3.4}$$

Thus, when the system is empty $\eta = 0$ and the received UL power just equals

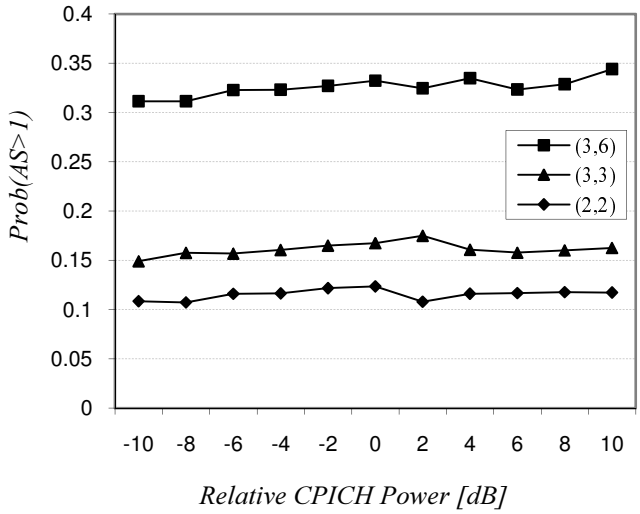

Figure 3.4: Probability that AS contains more than 1 BS for different CPICH powers.

the receiver noise. On the other hand, the higher the interference, the closer η is to 1. The limit $\eta = 1$ means a theoretical situation (pole capacity) in which all UEs in the cell should transmit an infinite power.

Figure 3.5 shows a first result in this sense, it is represented the UL load factor for the central cell and two more cells at different distances, a nearby cell and a faraway one. It can be observed that there exists an optimal power value for the central cell. However it is interesting to note that wrong adjustments not only affect on closer cells but they can also significantly impact faraway cells because of the propagation of the interferences effect.

For very low pilot powers, even though several UEs are transferred to other cells, there is a negative effect on the cell load. The explanation relies on those UEs that must transmit a higher level of power in the new cell and so eventually generate more interference to the central one. This way, the maxim that dictates that transferring users to other cells reduces the own cell load must be considered with caution. Although relationships between pilot variations and capacity are analyzed later, it can be noticed that despite its higher load, the optimum CPICH power for the central cell is not far from the others.

Regarding DL load factor, several definitions are possible. For example, an analogy with the UL can be done and calculate it as the averaged individual load factor at each UE. These individual factors are calculated from the perceived specific noise rise at each UE. Each value is conveniently weighted by its contribution to the power

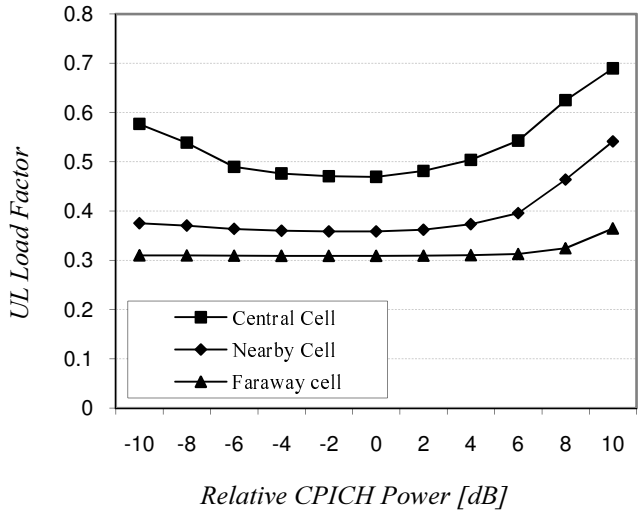

Figure 3.5: UL load factor for different CPICH values.

consumption in the BS and so contribution to DL interferences:

$$\begin{aligned} \eta^{DL}(j) &= \sum_{\substack{k=1 \\ i \in j}}^{N_{UE}(j)} \left(1 - \frac{1}{\Delta n_{UE}(k)}\right) \frac{P_{TX}^{DL}(j,i)}{P_{TX,tot}^{DL}(j)} \\ &= \sum_{\substack{k=1 \\ i \in j}}^{N_{UE}(j)} \frac{I_{Inter}^{DL}(j,k) + I_{Intra}^{DL}(j,k)}{I_{Inter}^{DL}(j,k) + I_{Intra}^{DL}(j,k) + n_{UE}(k)} \frac{P_{TX}^{DL}(j,i)}{P_{TX,tot}^{DL}(j)} \end{aligned} \tag{3.5}$$

Where:

- $N_{UE}(j)$: is the number of UEs with BS j in its AS.
- The summation is calculated over the UEs connected to BS j, which is indicated by '$i \in j$', where i is the summation index.
- $\Delta n_{UE}(k)$: noise rise at UE k.
- $P_{TX}^{DL}(j,k)$: DL transmitted power from BS j to UE k.
- $I_{Inter}^{DL}(j,k)$: inter-cell interference measured at UE k in its link with BS j. It is understood that j is included in the AS of k.
- $I_{Intra}^{DL}(j,k)$: intra-cell interference.
- $n_{UE}(k)$: total thermal noise power measured at UE k.

This first expression gives an idea about the load level measured by UEs but its main disadvantage is that when the BS has reached its 100% of available traffic

power, its value might not be 1. For this reason, the quotient between the used traffic power and the maximum available one is chosen as the DL load indicator. A second advantage of this definition is that it can easily be obtained by the BS, whereas the first one requires that each UE reports its measurement to the BS:

$$\varsigma^{DL}(j) = \frac{P^{DL}_{TX,tot}(j) - c(j)}{P^{DL}_{TX,max}(j) - c(j)} \tag{3.6}$$

Where $P^{DL}_{TX,max}(j)$ is the maximum power available at BS j.

Figure 3.6(a) shows the evolution of the DL load indicator for different pilot powers of the central cell. It can be observed that in this case it exists a monotonous increase with the pilot level. As the BS gets new users, it has to serve them and consequently its available traffic power is reduced. Besides, the increment in the signalling power also contributes to reduce this availability faster and faster. For lower pilot values, the load factor of nearby cells is slightly increased and the effect is distributed among all limiting cells. If some of those adjacent cells were under high load conditions this action could jeopardize its power availability. However, in general, reducing the CPICH power to unload the DL of a particular cell is effective but at the cost of degrading nearby ones. Finally, Figure 3.6(b) shows the same situation but using as load measurement the definition in Equation (3.6), it is verified how this indicator is not so representative.

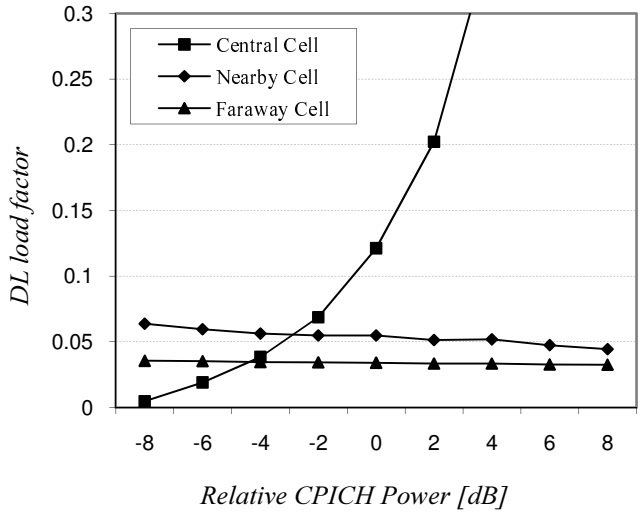

(a) DL load factor

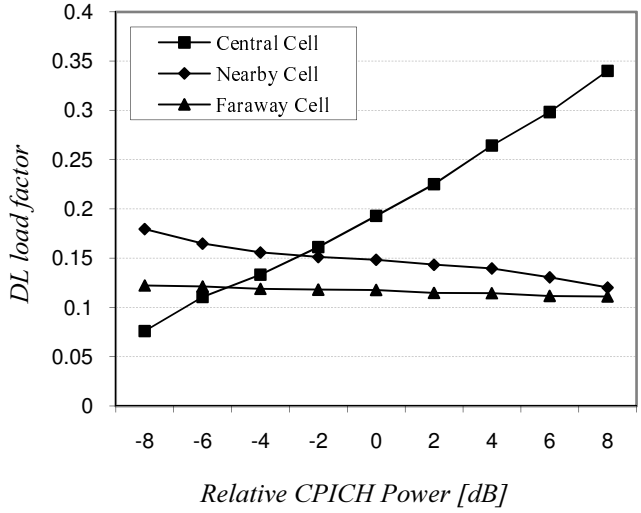

(b) Averaged UE DL load factor. Eq. (3.6)

Figure 3.6: DL load factor for different CPICH powers.

3.2.3 Impact on System Capacity

Throughout this section a more extensive study is made to evaluate the impact of pilot powers variations on the system capacity. Initially, the study is focused in the UL, in which maximum capacity conditions have been defined as the situation when one of the cells has 5% of UEs in degraded mode, that is to say users not reaching the target E_b/N_0.

Figure 3.7 represents the UL capacity for different values of the central cell pilot power. This has been simulated for different AS configurations to evaluate their impact on the optimal CPICH power election.

From the figure, one of the first conclusions that can be drawn is that optimum CPICH values are not very dependant on AS modifications. In most cases, maximum capacity is obtained when the pilot power of the central cell is just 1 dB below the others. When Hard Handover (HHO) is implemented, case (1,0), an extra 2 dB reduction is needed to force a better reassignment between UEs and cells. With the other configurations all users in the SHO area chose the better cell in a natural manner.

Thus, with HHO a finer adjust is needed to find the optimum configuration because wrong configurations quickly degrade capacity. In this sense, it is noticeable that, increasing SHO areas allows controlling capacity degradation when the central pilot is very incorrectly adjusted. For example, in the simulated scenario whereas capacity reduction is 35.4% for the HHO case, it is just 11.0% if a (3,6) configuration is applied and considering a 6 dB displacement from the optimum value. Again, larger SHO areas permit a wider set of election and UEs transmit according to the BS that requires less power from them. In fact, UL capacity increases with the size of the AS, regardless of the CPICH power combination. However, the relation between capacity and SHO parameters is not investigated until Chapter 7. Conversely, if AS parameters are not chosen to maximize UL capacity, with a correct setting of pilot powers the capacity loss is lower. For example, in the simulated scenario, when CPICH powers are optimally adjusted, variations between AS configurations reach 15.8%, otherwise capacity differences can reach up to a 37.5%.

DL maximum capacity can be seen in Figure 3.8, which shows that the optimum configuration corresponds to a central pilot power 2 dB lower than the rest. This result is consistent with the fact that the central cell is more loaded. DL capacity is very sensitive to increases in the pilot power beyond the optimum adjustment since this means more power devoted to signalling and so less to traffic. On the other hand, reductions from the optimum imply less degradation because expelled users are distributed among the limiting cells. Nevertheless, with pilot reductions coverage issues might arise.

Similarly, as it happened in the UL, higher $AddWin$ and $\mathcal{N}$ lead to less sensitivity to wrong adjustments in pilot powers. In this case, the reason is that wider SHO areas imply a larger set of UEs whose power is provided by several cells, so the effect of a user out of its optimum cell is shared. With HHO, CPICH variations imply the entrance or exit of users that must be fully served. On the other hand,

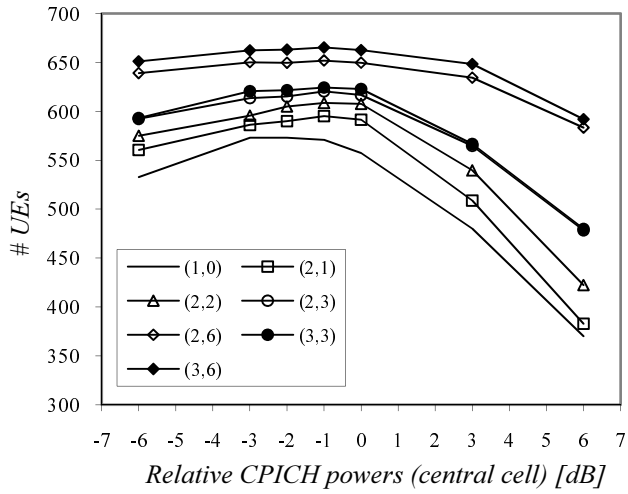

Figure 3.7: UL maximum capacity for different CPICH powers and AS configurations.

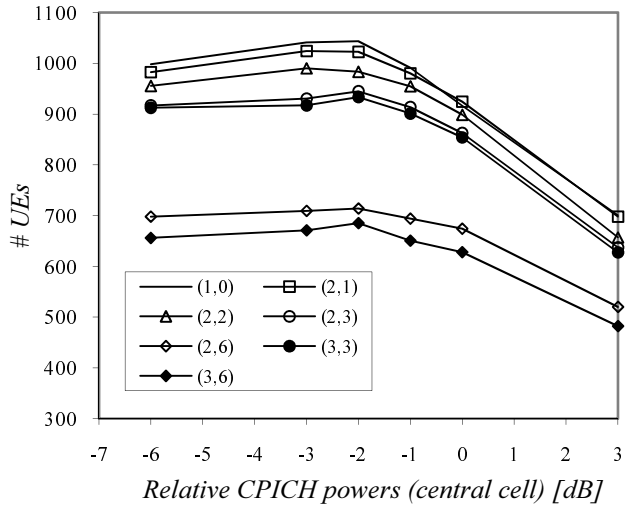

Figure 3.8: DL maximum capacity for different CPICH powers and AS configurations.

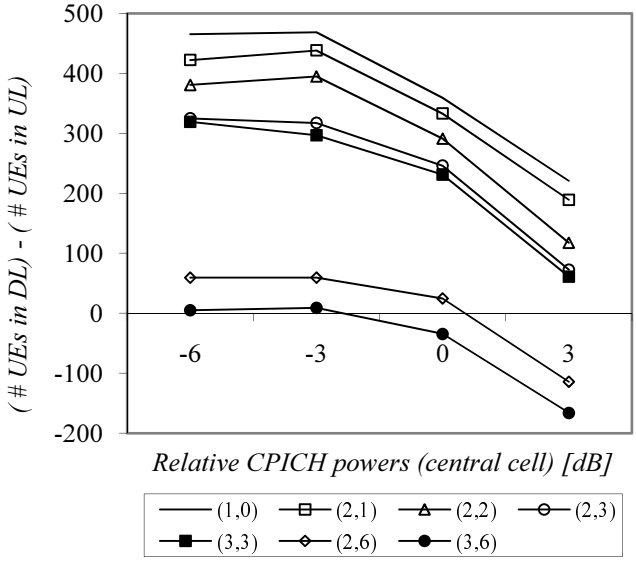

Figure 3.9: Difference in number of simultaneous UEs between DL and UL under maximum capacity conditions.

although higher ASs imply a reduction in the dependence with pilot variations, absolute values of DL capacity are worse (see Chapter 7 for an extended analysis on this topic).

Finally, Figure 3.9 aims at comparing the UL and DL unbalance of each configuration. It shows the difference between the maximum number of users in the DL and in the UL. Thus, the positive area indicates those configurations of pilot powers and AS in which the UL is the limiting link in the system. The negative area represents the opposite case. By properly adjusting the combination of pilot powers and SHO parameters a correct balance between the UL and DL capacity can be achieved.

Relative values and trends are the important data in the simulations. Absolute values are not representative because they are specific of the simulated scenario. And thus, for example, if asymmetrical services were considered, DL capacity values would be reduced but curves would maintain their shape and therefore conclusions would be the same. This statement is corroborated by Figure 3.10 which is an example of DL capacity when UEs are considered to use an asymmetrical service, in particular the DL rate is increased to 144 kbps. Curves show the number of simultaneous UEs that can be supported by the system.

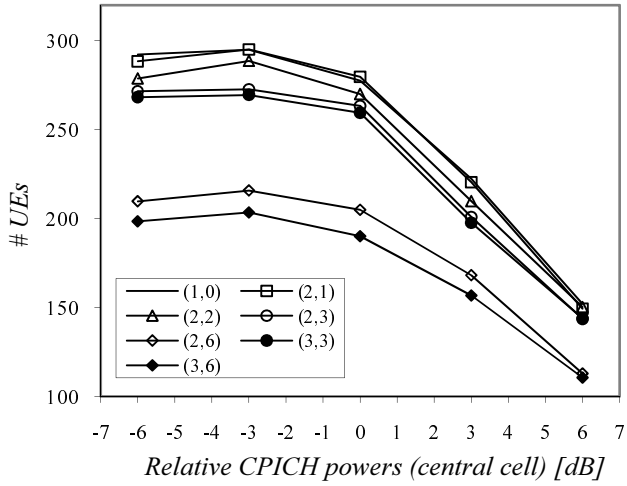

Figure 3.10: DL maximum capacity for asymmetrical service.

3.3 Impact of Downtilted Antennas

3.3.1 Introduction

Initially, antennas were just simple radiant elements, however with the wide deployment of GSM networks and the important increase in the number of users, new alternatives were developed and manufactured. Radio planning engineers asked for antennas with an improved flexibility and more precise coverage areas which boosted an important technological evolution during the nineties. Actually, one of the optimization strategies that has gained more momentum in the recent past is the adjustment of the tilt of antennas.

By changing the elevation angle, energy can be concentrated in the target area and interferences towards (and from) other cells can be reduced. That is why it is considered a cost effective method to provide both coverage improvement and interference reduction.

Interference reduction is particularly important in WCDMA systems in which isolation among cells is essential because of a frequency reuse factor of 1 which causes mutual interference among cells. That is why the downtilt of antennas is one of the most important planning parameters to be optimized. Furthermore, 3G networks can benefit from the technological development making use of electrical downtilt which is currently offered by antenna manufacturers.

Mechanical downtilt was the predominant method used in 2G systems, where the tilt was physically applied to the antenna. Its adjustment was carried out by means of field tests and long term statistics on the network performance. Changes should be made manually and thus any variation in the environment that required a modification in the tilt angle meant that an operator had to physically go to the site

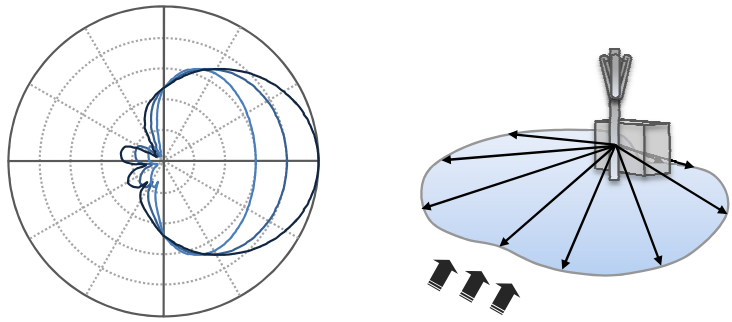

(a) (b)

Figure 3.11: Coverage variation with a mechanically tilted antenna.

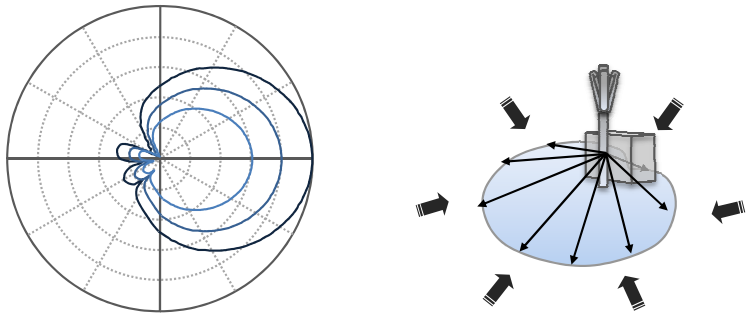

(a) (b)

Figure 3.12: Coverage variation with an electrically tilted antenna.

to readjust it. That is to say, there was an important lack of flexibility and reaction capacity in front of unexpected alterations in the system. Mechanical downtilt shows several other drawbacks, for example it is only effective in the forward direction and has no effect on side radiation, it also moves rear lobe upward. Figure 3.11 graphically shows the resultant coverage footprint of a mechanically tilted antenna.

With electrical downtilt the diagram pattern is modified by adjusting the relative phases of individual radiation elements in an antenna array. The main lobe inclines for all azimuth angles and, thanks to this, interference is controlled in all directions and in a more precise way (Figure 3.12). First versions of antennas supporting this feature still required an operator to adjust them in the site. However, soon appeared remotely controlled electrical tilt antennas, which are the latest development and offer the desired flexibility. This means new possibilities in UMTS radio planning and in fact, 3GPP has introduced a new interface named *Iuant* which shall facilitate controlling the tilting of antennas from the O&M subsystem [3GPo].

3.3.2 Effects on Capacity Indicators

Along this section it is studied the effect that downtilting has on several performance indicators. As with CPICH configuration, detailed results, beyond than well known effects, have been obtained.

One of the drawbacks of the realistic scenario used in the previous section is that UEs are characterized by their propagation losses and not by their coordinates. This allows scattering them realistically but geographically speaking the scenario is blind and UEs positions are not known, moreover indoor and outdoor users are mixed. Hence, downtilt modifications cannot be implemented and the 3GPP based scenario in Appendix B, Section B.3 has been used instead. Electrical downtilting is used by all BSs.

The first set of simulations aim at evaluating how different performance and capacity indicators evolve with different downtilt angles and which considerations must be taken to define an optimum angle. The effect of UEs spatial distribution is investigated as well. For this purpose, several load scenarios have been defined:

- Scenario with low load: this corresponds with the 500 UEs case.
- Scenario with medium load: 1000 and 1500 UEs.
- Scenario with high load: from 1600 to 2000 UEs.

All load conditions have been simulated for different downtilt angles, ranging from 0^o to 14^o in steps of 1^o. Results are recorded for the central cell.

Figure 3.13 represents the evolution of UL load factor for different number of UEs in the system and all possible downtilt angles. A downwards trend is observed for all cases up to 9^o, which represents an absolute minimum for most of cases. The reason behind this trend is a better isolation of intercell interference. In particular de optimum angle is achieved when the first radiation null is directly pointing to a higher amount of intercell UEs. For the same reason, if the antenna is downtilted further, the second main lobe contributes to a reduction in the link loss with intercell power and the load factor rises again. In fact, when 11^o are applied, the second main lobe is directly pointing to adjacent cells and that is why a local maximum appears. However, this behavior is different for the three most loaded cases because several UEs reach their maximum power and have a degraded connection. In addition, with the highest angles it is well known that coverage and SHO areas issues arise. As a complementary result, Table 3.1 shows the evolution of the percentage of the simulated area without coverage or the number of cells included in the AS. As expected, both coverage and SHO areas are indirectly proportional to downtilt angles.

It is also interesting to note that downtilt effects increase with the system load. The higher the number of UEs, the sharper the fluctuations. This is logical since more interference is included or expelled with every degree of angle variation.

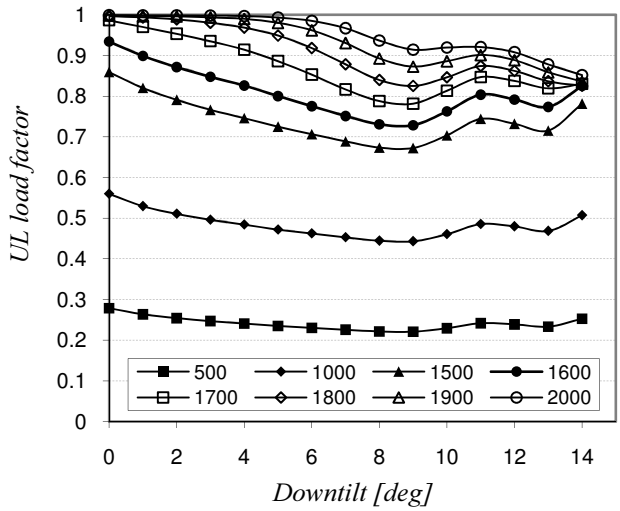

Figure 3.13: UL load factor for different number of UEs in the network and downtilt angles.

Table 3.1: Number of cells in the AS for different downtilt configurations.

Downtilt (deg)	No coverage (%)	1 cell (%)	2 cells (%)	3 cells (%)	4 cells (%)
0	0.00	79.02	17.81	3.09	0.09
2	0.00	81.50	15.88	2.55	0.07
4	0.00	82.37	15.34	2.21	0.07
6	0.00	82.87	15.14	1.93	0.06
8	0.00	83.54	14.69	1.75	0.02
10	0.74	82.79	15.04	1.44	0.00
12	3.67	80.17	14.29	1.87	0.00
14	6.60	82.37	10.95	0.08	0.00

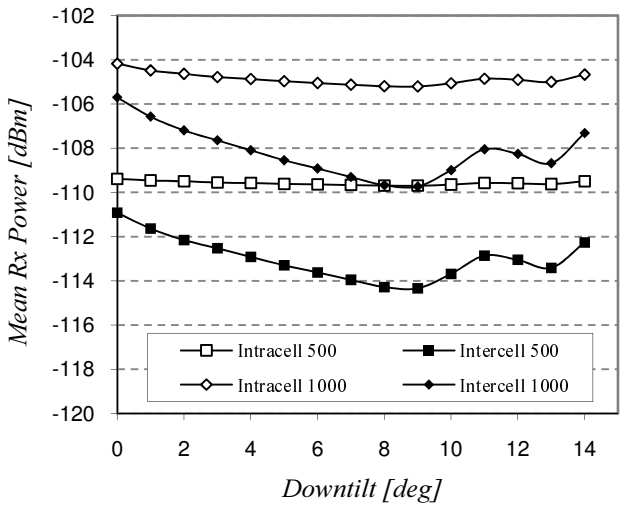

Figure 3.14: Intercell and intracell received power for different load conditions and downtilt angles.

The close interdependence among downtilt angles, UL load factor and intercell interference can be observed in Figure 3.14. In particular, it represents both the intra- and intercell received power measured at the BS, which are the two interference contributions of the UL load factor of a cell. Regarding intracell interference, it is fixed by the power control and E_b/N_0 targets. Therefore, variations only appear whenever the number of UEs (or the corresponding service mix) that transmit to the BS change. Unless effects such as coverage holes, degraded UEs, etc. appear, variations in UL load factor follows intercell interference levels, and thus the optimum from an UL load viewpoint is the one that minimizes intercell interference, which is reduced up to 4 dB in the best represented case (Figure 3.14). This reduction reaches 20 dB for the most loaded scenario (not represented).

Given this, downtilting is an effective technique to reduce the UL noise rise, with a minimum in 9º for this scenario. However, UL transmission power depends on both the noise rise and the link loss and the global effect determines the final required power. Figure 3.15 represents the mean UL transmission power as a function of the downtilt angle and for the different simulated cases. Two different SHO configurations are presented to also assess the impact.

From the figures, the power also decreases with the downtilt until a minimum is reached, however this optimum value evolves with the system load and in most cases it does not match with the optimum for the UL load factor. With a low number of UEs in the network, the noise rise is less significant and it is link losses that determine the required power to a greater extent. With 9º of downtilt many cell users are out of the main radiation lobe and lower angles are better options. As the load increases, so does intercell interference and it becomes the dominant factor in the power adjustment. As a consequence the angle that guarantees minimum

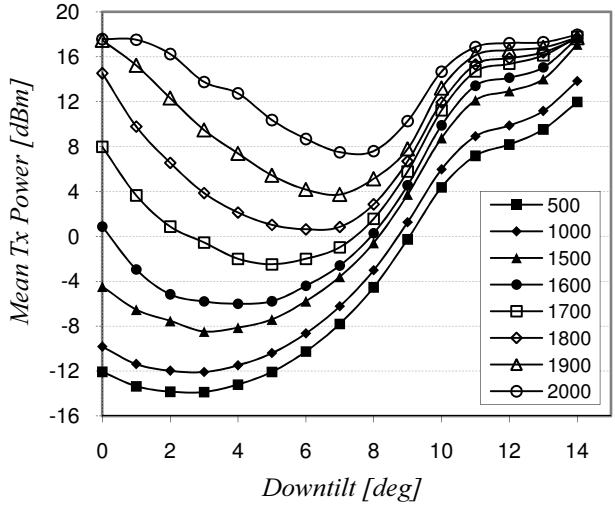

(a) AS=(1,0)

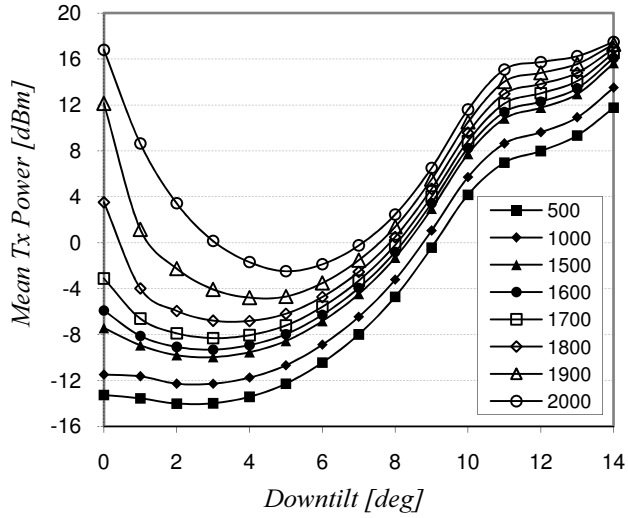

(b) AS=(3,3)

Figure 3.15: UL transmitted power for different load conditions, downtilt angles and SHO configurations.

transmission power is closer to 9º. Comparing both SHO configurations, it can be seen how a higher number of BSs in the AS benefits the UL and then the required UL power increases more slowly with the number of UEs. This is true as long as the downtilt angle is adjusted in its best value, otherwise there are no clear benefits in one or the other option. Out of this expected effect, downtilt variations impact in the same way both cases.

The minimization of transmission powers implies that UEs are further from its maximum and so the QoS of their links can be improved. However, in this case slight modifications in the system load imply that the optimum condition is changed and important differences in the required power arise. Comparing the values from different curves at a fixed downtilt angle, it can be seen that the closer the angle to the optimum load factor, the less the changes in the required powers. For example, for the lower case load, the angle should be adjusted at 2º, however if the load in the area increased in four times along the day, differences in required power would reach 30 dB. On the other hand, a downtilt of 9º would imply just a difference of 10.5 dB in the worst case (HHO). In this last situation the system is planned to be in a more steady situation but at the cost of requiring higher levels of power when the load is low, up to 14 dB in the simulated scenario.

Since the represented power is the mean value, when it gets closer to 21 dBm (considered as the maximum available power at UEs) it is expected that the percentage of UEs having reached this limit increases. Figure 3.16 shows this fact by representing the probability of having more than 5% of users in degraded mode. It can be seen how adjusting low angles in a fixed manner can lead the system to very poor performance when the load increases. In the worst case, sloping down antennas to 2º can imply that 30% of users are unable to achieve their $(E_b/N_0)_{target}$. Again, it is shown how selecting higher angles lead the network to a configuration dealing better with changes in the number of active UEs. Finally, as expected, the lower the load in the system, the less sensitive this indicator is to bad selections in configured angles.

Regarding the DL, optimization from the transmitter and cell viewpoints is the same. In particular, Figure 3.17 shows the power transmitted by the BS for the different scenarios, downtilt angles and comparing a (3,3) SHO configuration with a HHO one. The optimum tilt is between 8 and 9º and without changes for different load conditions, thus it can be considered coincident with the UL when this one is adjusted to minimize the load factor. Furthermore, variations from 3º to 9º are just 0.75 dB in the (3,3) case and 0.5 dB in the (1,0). Consequently, unless the DL is the limiting link, dynamic variations to benefit the UEs transmission power and QoS could yet be executed without and important impact on the DL. Comparing both handover configurations, the cell is benefitted in the DL when using a HHO strategy and the system is more robust to not optimized downtilt angles. This effect, to be addressed in in Chapter 7, is opposite to that in the UL and already appeared Section 3.2.3.

Given this, it can be concluded that optimum performance can only be achieved by introducing remote and electrically controlled antennas, which arise as an inter-

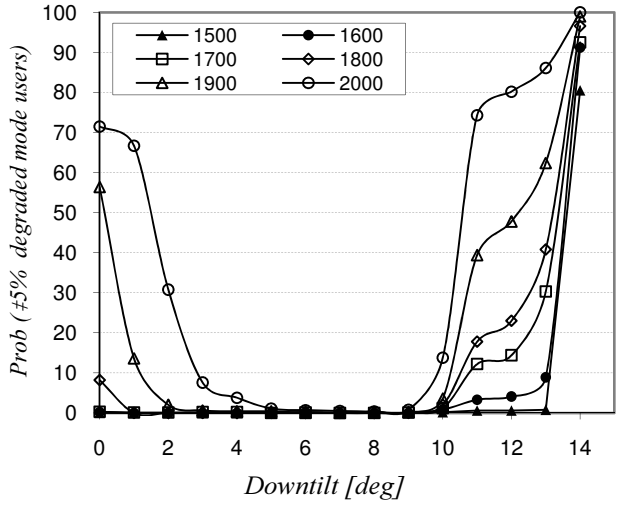

Figure 3.16: Probability of having equal or more than 5% of UEs in degraded mode.

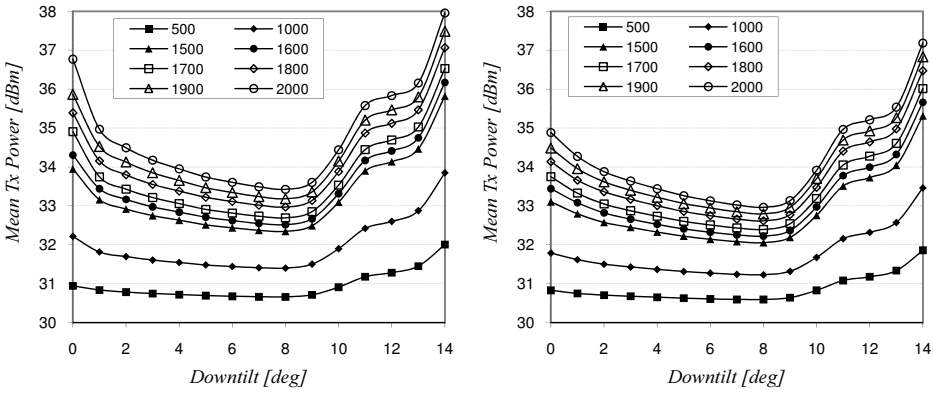

(a) AS=(3,3) (b) AS=(1,0)

Figure 3.17: DL transmitted power for different load conditions, downtilt angles and SHO configurations.

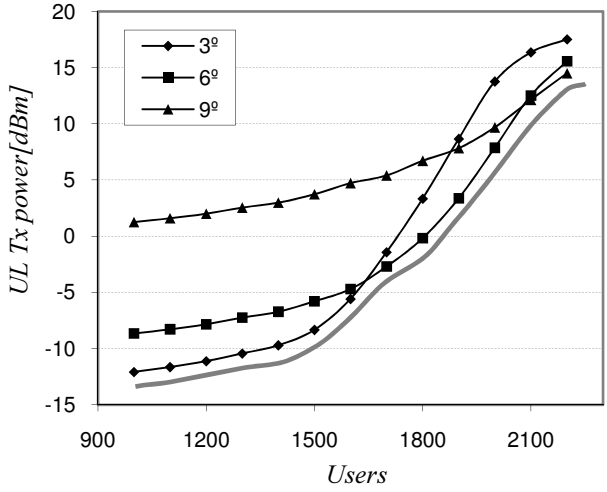

Figure 3.18: Optimal functioning by means of electrical and remotely controlled downtilting.

esting option to operators. Angles should be modified as the load conditions evolve along time in order to assure optimal functioning. Moreover, as traffic patterns tend to be repetitive in time, operators could pre-program the different optimum angles. Figure 3.18 shows an example of operation in which the minimum angle step is chosen equal to 3°. The lower envelope of the 3 curves combination determine the mean required UL transmission power as the number of UEs in the system, or group of cells, grows.

3.3.3 Considerations on UEs Spatial Distribution

All UEs inside a cell coverage area are not equally affected by the downtilt of the antenna, those nearer to the site will not perceive the same gain than those that are in the cell edge. In order to obtain a wider perspective of powers evolution Figure 3.19 represents the evolution of the UL transmission power histograms for a scenario with 1500 UEs.

The existence of optimum angles is emphasized with this representation, but other effects can be also observed. For instance, the standard deviation increases with the angle, long queues appear in the histograms representing UEs nearest to the BS. It can also be seen that when a downtilt higher to 7° is applied, the increases in transmitted powers are sharper. This is because of the entrance of the first radiation null in the cell and the second main lobe pointing towards the adjacent cell, which constitutes the worst possible configuration in terms of both propagation losses and interference.

It is clear that differences in powers are highly dependant on the position of UEs with respect to the antenna but also to its main radiation lobe. This is graphically

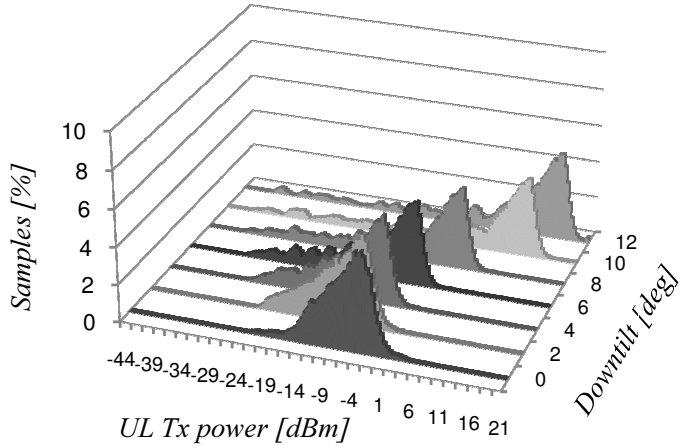

Figure 3.19: Histogram of UL transmitted power for different downtilt angles.

shown by Figure 3.20, which shows the transmitted power as a function of the distance between the UE and the Node-B for different downtilt angles. To obtain this plot, a test user is simulated following a straight line in the direction of the antenna azimuth and being forced to be connected to the evaluated cell irrespective of its position.

This figure illustrates why the standard deviation in the previous histograms increased with the angle. The higher the angle, the wider the range of variation in transmitted powers. It can also be seen how the radiation null just before the direction of maximum gain contributes to important increases in power. For example, users at 150 m from the Node-B experience a difference of 20 dB in their powers when 0º of tilting is compared with just 3º. Thus, further gains can be obtained if phased array antennas are used not only for electrical downtilting but also to provide null filling.

This figure also reveals how the optimum angle position depends on the actual cell size. For example, considering just the 4 represented cases, if the cell has a radius higher than 350 m the optimum angle is 3º from a transmission power viewpoint. However, for cells with a radius smaller than 250 m that would be the worst case. Finally, for cells below 100 m a 14º downtilt appears to be the best option. Thus, optimization of downtilt is a key factor to improve microcell deployment. Rural areas, in which macrocells are wide and traffic is low can be adjusted in a more static fashion.

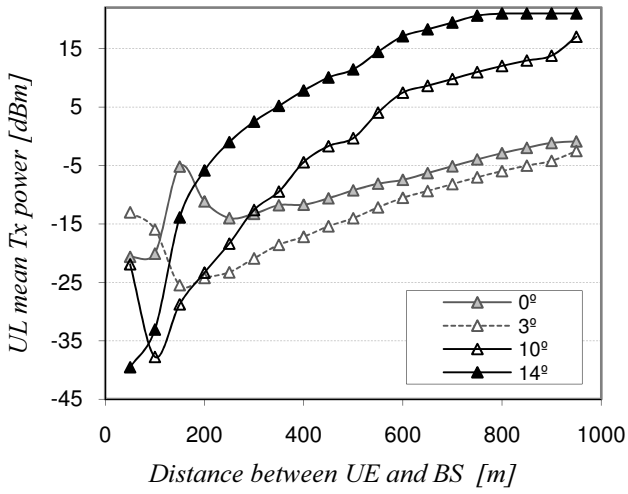

Figure 3.20: UL transmitted power as a function of the distance between UE and Node-B for different downtilt angles.

3.4 Concluding Remarks

The impact of CPICH power variations and downtilt angles on UMTS based systems has been studied in this chapter. The study goes beyond well known facts and interactions with other parameters are also investigated.

The study starts by analyzing the CPICH. Its participation in the cell selection and SHO procedures determine its preliminary adjustment by means of standard link budgets. In this sense, it has been shown an analytical example providing a closed expression to estimate the required value.

By means of simulations (in a real and in a synthetic scenario), it has been quantified the transfer of UEs by using CPICH power variations, the technique is effective to reshape cell areas and even small changes have a noticeable impact.

Regarding interactions with SHO, although the number of DL connections are directly proportional to the value of AS parameters $\mathcal{N}$ and *AddWin*, paradoxically the number of UL connections is smaller because UEs have more possibilities to transmit to better option cells. From this, it has been observed that higher SHO parameters help to reduce the impact of wrongly adjusted, or just non-optimized, pilot powers.

Once SHO parameters are fixed, it has been quantified how AS sizes are changed by CPICH power variations. Although the scenario has a quite heterogeneous distribution of UEs, variations are present but are not very significant, and SHO overhead is maintained. Hence, only uncoordinated changes of pilot powers could jeopardize this aspect.

Load variations have been investigated for both UL and DL. Concerning the

UL, the maxim that dictates that transferring UEs to other cells contributes to reduce the own load must be taken carefully. There is an optimum pilot adjustment that implies a proper assignment of UEs into cells and once these values are left, interference increases, regardless the pilot is increased or decreased. Even faraway cells are impacted by a wrongly adjusted pilot and so the whole area to optimize must be studied as a whole.

Regarding DL load variations, after comparing two definitions on the DL load factor, the analysis shows that there exists a monotonous increase with the pilot level, reinforced by the extra power consumption of control channels. On the other hand, reducing the CPICH power to unload the DL of a particular cell is effective but at the cost of degrading nearby ones. As seen in the previous chapter, many published works perform DL based balancing in scenarios with one hotspot. If the scenario has a more heterogeneous distribution this rule of thumb must be taken carefully and the whole area to optimize should be studied simultaneously. This is one of the requisites in the designed proposal in next chapter.

The impact of pilot power variations on system capacity represents the second part of this study and its main conclusions are summarized next:

- Optimum CPICH values are not very dependant on AS modifications.
- Higher SHO parameters cause a less sensitive network to wrong adjustments in CPICH powers and capacity degradation is less relevant. HHO requires a finer adjust of power and small variations cause important capacity reductions.
- Conversely, a correct setting of pilot powers promotes reducing the differences in capacity among different SHO parameters. So it contributes to minimize the capacity reduction when these are not optimally adjusted.
- DL capacity is more sensitive than the UL to increases in pilot powers beyond the optimum value. Reductions imply far less capacity degradation but coverage issues must be considered.
- By properly adjusting CPICH powers and AS parameters, capacity balancing between UL and DL can be achieved.

Downtilt of antennas is the second planning parameter that has been investigated. This technique appears to be particularly appropriate for 3G networks using a unitary frequency reuse, the reason is two-fold: first to increase isolation among cells and second because of the recent technological evolution that permits remotely controlled electrical tilt through new interfaces such as *Iuant* from 3GPP.

Coverage and interference variations caused by downtilt variations have been previously addressed in the literature. Along this chapter, new detailed results are given in the framework of UMTS systems and its performance optimization. Different performance indicators have been evaluated for different electrical downtilt variations in a scenario of variable load and the main conclusions are listed next:

- Not only the main lobe slope down is important but also the relative position of the first radiation null and secondary lobes with respect to UEs from limiting cells.
- From the previous point, a correct minimization of intercell interference leads to the optimum angle in terms of UL load factor, considered as the optimum from the whole cell viewpoint.
- However individual UL transmission powers depend on both the noise rise and the link loss. It is the global effect what determines the final required power. For this reason, in general, the optimum angle from UEs viewpoint does not match with the optimum from a cell viewpoint. Actually, both configuration are only the same for high loaded scenarios.
- Adjusting angles to reduce required UL transmission powers permits increasing the UE perceived QoS but at the cost of being in a more instable situation. Slight changes in the system load imply important power increases and the probability of having UEs in degraded mode grows rapidly. On the other hand, minimizing the load factor yields a more steady system but at the cost of requiring higher levels of power when loads are not particularly high.
- DL effects are simpler to analyze and conclusions on the optimum angles match with the UL load study.

Given the previous points, in order to design a static *Automatic Planning* algorithm, angles should be optimized from a cell viewpoint, so that both UL and DL performs correctly under variable load conditions. However, by introducing remote and electrically controlled antennas, angles could be dynamically modified according to traffic patterns mapped to a timetable. In that case, whenever the UL is the limiting link, optimal angles from UEs viewpoint could be tracked and achieve the best possible network performance.

The worst possible downtilt adjustment implies having the first radiation null pointing towards the cell and the second lobe pointing towards the adjacent ones. This is an important issue in *Dynamic Planning* strategies that change cell sizes by only adjusting CPICH powers and which do not consider the spatial distribution of UEs after having reshaped the cell. In fact final figures show that optimum angles are very dependant on cell sizes and important capacity degradations are obtained if downtilts are not accordingly adjusted.

As a final comment, it is worth mentioning that modifications in both pilot and downtilt permit a controlled way of changing the cell shape. Nevertheless their effect is noticeable different. Pilot variations just imply a change in the power assigned to control signals and also have an influence on the reliability of UEs channel estimations. On the other hand, downtilt variations have a direct impact upon the power UEs and BSs have to transmit, the radiated interference and also interference levels listened from other cells. In this sense, using CPICH power variations to achieve UEs transfer among cells looks more appealing than downtilt variations, that appears to be much more indicate to control transmission powers and interference.

Chapter 4

Automatic Planning Based on Simulated Annealing

4.1 Introduction

Along the previous chapter it was analyzed the influence of the CPICH power levels and downtilt of antennas on the capacity of the network. It was shown that variations on these parameters play a major role on the optimization of the radio access network and several guidelines for their adjustment and the reduction of load levels were devised.

The use of equal pilot powers and downtilt angles would be the best solution in terms of interference in an ideal scenario with perfectly uniform user distribution, equal path loss conditions and only one service, which imply homogeneous traffic among all cells. Although this design can be intuitively predicted, the idea is analytically addressed in [AHNPM01], which demonstrates that this uniform network layout with equal-sized cells is optimal for that theoretical case, and that capacity degrades significantly if loads are not balanced.

Unbalanced traffic distributions in realistic environments might lead some groups of cells to congestion whereas other ones could be remaining with a much lower load. This unbalance can be produced by non-uniform users distribution and by non-uniform services distribution. In this sense, from the previous chapter it is clear that variations in CPICH powers and downtilt angles are potentially good strategies to improve capacity by reshaping effective cell areas. In particular, it can be predicted the existence of a group of CPICH powers and downtilt angles such as traffic is effectively equalized among cells and a higher capacity is achieved.

Along this chapter an *Automatic Planning* strategy is designed and assessed to adjust both parameters. From the study in the previous chapter, it is necessary to optimize jointly all the target cells and to consider realistically UL requirements.

Indeed this is one of the novelties of the proposal since this link is usually missed in the literature, as was pointed in Chapter 2.

After this introduction, the chapter states the problem analytically and stresses the importance of correctly assigning cells to UEs in the UL. Next section gathers the principles of the proposed solution and fully describes the *Automatic Planning* strategy. The fourth section presents results and the discussion. Finally the chapter is closed by conclusions.

4.2 Problem Statement

4.2.1 Comments on Load Balancing

Load balancing is often addressed just as a transfer of users from a loaded cell to another one with less users. Although this approach can be effective in FDMA based systems, in CDMA networks this is not so straightforward. Because of a frequency reuse of 1, forcing the handover of certain UEs into a less loaded cell does not guarantee an improvement in terms of interference in the mother cell. When talking about load balancing or rather, about capacity maximization, BSs should be configured so that the resulting effective cell areas imply that UEs connect to the cell requiring the less power level and then that maximizes capacity by minimizing both interferences and load. Actually, one of the conclusions in the previous chapter was that reducing the pilot power of a loaded cell could potentially cause a poorer performance in the loaded cell.

Given this, a cell selection process that is only based on CPICH RSCP does not account for DL interference and it is only appropriate under low load conditions. On the other hand, standard $(E_c/I_0)_{CPICH}$ criterion does take into account interference and is more suitable for CDMA systems, where capacity and coverage are so coupled. RSCP measurements are important from a coverage viewpoint during drive testing because areas with high RSCPs but low E_c/I_0 levels are very susceptible of being pilot polluted, which in turn causes coverage problems. However, this measurement does not consider any UL interference information.

UEs always transmit to the BS that requires less power, as explained in Section 3.2.2, but the AS is finite and the included cells could not be the best option. Thus, it is desirable that CPICH powers are adjusted so that the number of optimum assignments is maximized and interference is reduced. This also yields an UL coverage improvement because each UE is more likely to have enough power to meet its individual $(E_b/N_0)_{target}$. However, as it was stated in Chapter 2, many of existent algorithms often neglect the interaction between coverage and capacity, they do not take into account the UL behavior and their cost functions are mainly focused in DL coverage, which may be worthless if capacity is not optimized as well.

4.2.2 Analysis of UL Requirements

In order to achieve a certain Bit Error Rate (BER) at a given connection, a minimum received E_b/N_0 must be guaranteed. This determines the transmission power P_{TX}^{UL} of a certain UE k to its serving BS s_k. Indeed, the E_b/N_0 target is related with this value through the next equations:

$$\frac{E_b}{N_0}(k, s_k) = \frac{P_{RX}^{UL}(s_k, k)}{I^{UL}(s_k, k) + n_{BS}(s_k)} \frac{W}{R_b(k)} = \frac{P_{TX}^{UL}(k) / L^{UL}(j, k)}{P_{RX,tot}^{UL}(s_k) - P_{RX}^{UL}(s_k, k)} \frac{W}{R_b(k)} \tag{4.1}$$

Where:

- $P_{RX}^{UL}(j, k)$: Power received from UE k at BS j.
- W: Channel bandwidth.
- $R_b(k)$: Bit rate associated to UE k.
- $I^{UL}(s_k, k)$: UL multi-user interference power received by the connection between k and s_k, accounts for both inter- and intra-cell interference.
- $n_{BS}(j)$: Thermal noise power produced by the receiver of BS j.
- $P_{TX}^{UL}(k)$: Power transmitted by UE k.
- $L^{UL}(j, k)$: UL link loss between UE k and BS j.
- $P_{RX,tot}^{UL}(s_k)$: Total received power at s_k. It includes signal, all interferences and noise.

Consequently, $P_{TX}^{UL}(k)$ is expressed as:

$$P_{TX}^{UL}(k) = \frac{P_{RX,tot}^{UL}(s_k) L^{UL}(k, s_k)}{1 + \frac{W}{\frac{E_b}{N_0}(k, s_k) R_b(k)}} \tag{4.2}$$

Since interference increases the apparent noise, the previous equation can be expressed as a function of the noise rise Δn_{BS} at the serving BS:

$$P_{TX}^{UL}(k) = \frac{n_{BS}(s_k) \Delta n_{BS}(s_k) L^{UL}(k, s_k)}{1 + \frac{W}{\frac{E_b}{N_0}(k, s_k) R_b(k)}} \tag{4.3}$$

From here, it is evident that an increase in Δn_{BS}, or equivalently in the number of UEs, implies a higher transmission power to achieve the desired E_b/N_0. Since the UE is limited in power, this can eventually be translated into a loss of coverage. In

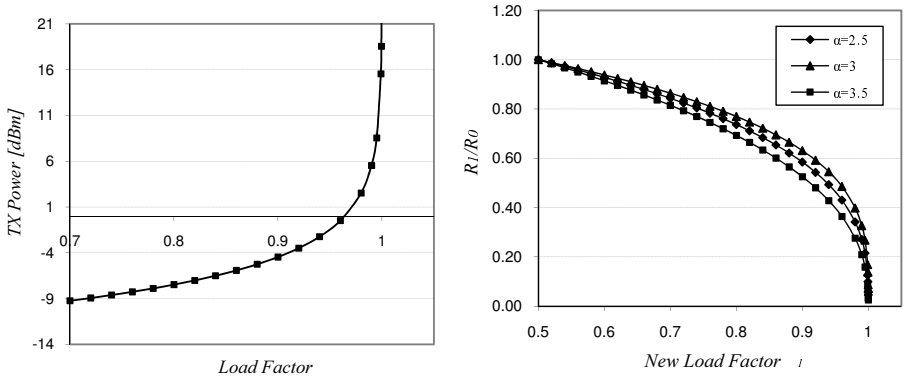

(a) Transmission power as a function of cell load factor.

(b) Cell radius variation with increasing load factor.

Figure 4.1: Quantification of UL load factor effects.

general, as explained in the previous chapter, the UL load factor is preferred and so the expression becomes:

$$P_{TX}^{UL}(k) = \frac{L^{UL}(k, s_k)\, n_{BS}(s_k)}{1 + \frac{W}{\frac{E_b}{N_0}(k, s_k) R_b(k)}} \frac{1}{1 - \eta(s_k)} \tag{4.4}$$

The UL load factor is an essential parameter in AC algorithms not only to control interferences but also the coverage variation margin. Figure 4.1 is included as an example to quantify load factor effects on transmission power and coverage variations. In particular, Figure 4.1(a) represents the transmission power as a function of η and it can be observed that, after a quite linear evolution, the required power rapidly increases with the load level. It is assumed a SF of 64, $n_{BS} = -104$ dBm, $E_b/N_0 = 5$ dB and a link loss of 86 dB.

On the other hand, considering that the propagation loss exponent is α, the coverage variation induced by load changes can be quantified. Considering that the load evolves from η_0 to η_1, the cell radius also changes from R_0 to R_1 according to next expression:

$$\frac{R_1}{R_0} = \left(\frac{1 - \eta_1}{1 - \eta_0}\right)^{\frac{1}{\alpha}} \tag{4.5}$$

As an example, Figure 4.1(b) shows the evolution of R_1/R_0 considering that the cell load increases from $\eta_0 = 0.5$ to different values of η_1 (ordinates). Three propagation loss exponents α are considered. Even though these graphs show a monotonous decrease in coverage, in practice, for high values of η, required transmission powers are higher than the maximum possible. This means that connections are eventually

dropped and so interference is regulated, preventing cell breathing from reaching a null coverage level.

Given the previous paragraphs, UL requirements can be summarized as follows:

$$\text{Minimize} \quad \sum_{i=1}^{N_{UE}} P_{TX}^{UL}(i) \tag{4.6}$$

$$\text{Subject to} \quad P_{TX}^{UL}(k) \geq \frac{L^{UL}(k,s_k)}{1+\frac{W}{\frac{E_b}{N_0}(k,s_k)R_b(k)}} \left(\sum_{\substack{i=1 \\ i\neq k}}^{N_{UE}} \frac{P_{TX}^{UL}(i)}{L^{UL}(i,s_k)} + n_{BS}(s_k) \right) \quad 1 \leq k \leq N_{UE}$$

$$\text{and} \quad 0 \leq P_{TX}^{UL}(k) \leq P_{TX,max}^{UL}(k) \quad 1 \leq k \leq N_{UE}$$

Where:

- N_{UE}: Number of UEs in the system.
- $P_{TX,max}^{UL}$: Maximum UL transmission power of UE k.

Making the next change of variable, which is the Signal-to-Signal-plus-Interference-plus-Noise ratio (in future sections this physical meaning is extended, in the current development, it is just used to simplify final expressions and thus no further details are given):

$$\gamma'(k,s_k) = \frac{1}{1+\frac{W}{\frac{E_b}{N_0}(k,s_k)R_b(k)}} \tag{4.7}$$

The E_b/N_0 constraint can be rewritten as:

$$P_{TX}^{UL}(k) \geq \gamma'(k,s_k) \left[\sum_{\substack{i=1 \\ i\neq k}}^{N_{UE}} P_{TX}^{UL}(i) \frac{L^{UL}(k,s_k)}{L^{UL}(i,s_k)} + n_{BS}(s_k) L^{UL}(k,s_k) \right] \tag{4.8}$$

Or similarly:

$$P_{TX}^{UL}(k) \geq \mathbf{\Theta_k^{UL}} \mathbf{\Pi_{TX}^{UL}} + \gamma'(k,s_k) n_{BS}(s_k) L^{UL}(k,s_k) \tag{4.9}$$

Where $\mathbf{\Pi_{TX}^{UL}}$ is a vector containing the UE's transmission powers P_{TX}^{UL} and $\mathbf{\Theta_k^{UL}}$ is a vector with individual elements as follows, being $\delta_{k,i}$ the Kronecker delta:

$$\mathbf{\Theta_k^{UL}}(i) = (1-\delta_{k,i})\gamma'(k,s_k) \frac{L^{UL}(k,s_k)}{L^{UL}(i,s_k)} \tag{4.10}$$

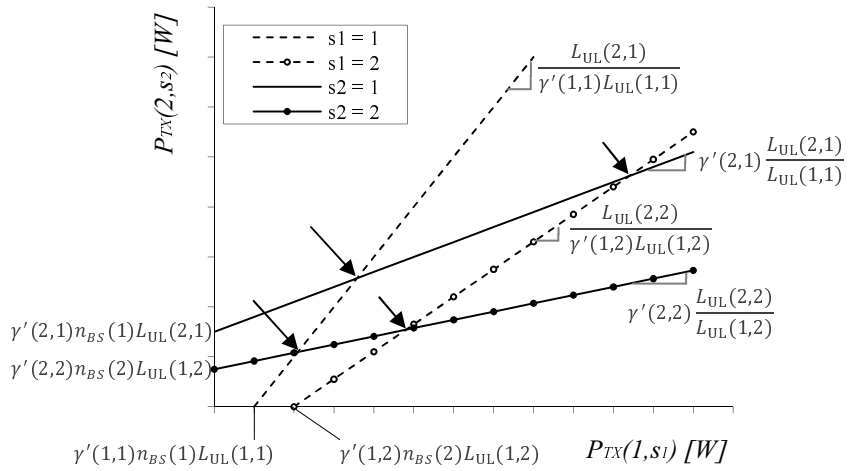

Figure 4.2: Relationship between transmission powers for a system with 2 UEs and 2 BSs.

The number of possible assignments between UEs and BSs, is $N_{BS}^{N_{UE}}$, where N_{BS} is the number of BS in the network. This number is an upper bound because many of the possibilities do not respect the individual power constraints and degraded UEs are possible as well. Among all configurations, the *Automatic Planning* algorithm should configure BSs so that a higher number of UEs include their best option cell in their AS, this way interference and load is minimized. For example, if a simple theoretic scenario of two UEs and two BSs is considered, the number of possible assignments is 4 but only one of them implies minimum transmission powers and interference. Figure 4.2 shows this situation graphically. Each straight line represents the minimum required power of user k to communicate with base j as a function of the transmitted power of the other user. Regarding the attenuation levels, it has been considered that UE 1 is closer to BS 1, and UE 2 closer to BS 2. Therefore $L^{UL}(2,1)/L^{UL}(1,1) > L^{UL}(2,2)/L^{UL}(1,2)$. This condition establishes the slope of each line, which is indicated along with the crossing points with each axis.

Continuous lines indicate the transmission power of UE 2 as a function of that of UE 1, which is obviously higher when $s_2 = 1$. On the other hand, the discontinuous ones should be read as the transmission power of UE 1 for variations of UE 2. Thus, when there is no interference, i.e. $P_{TX}^{UL}(2, s_1) = 0$, then this power only depends on the noise at the BS, the link losses and the E_b/N_0, it equals $\gamma'(1, s_1)\, n_{BS}(s_1)\, L_{UL}(1, s_1)$.

The crossing points between each pair of lines are the possible four solutions depending on the BS included in the ASs and are indicated with four arrows. In this example it is easy to verify that powers are minimum when $s_1 = 1$ and $s_2 = 2$.

In a more general scenario and recalling Equation (4.4), it is not possible to make this type of representation. However, it is clear that noise rise induced by other UEs (indirectly the load factor η) and link losses determine the best cell for

UE k. The best BS j is the one that satisfies:

$$\min_{j}\left(\frac{L^{UL}(k,j)}{1-\eta(j)}\right) \quad 1 \leq j \leq N_{BS} \tag{4.11}$$

For example, if two BSs are considered, pilot powers should guarantee that UE k includes the first one in its AS if:

$$\frac{L^{UL}(k,1)}{1-\eta(1)} < \frac{L^{UL}(k,2)}{1-\eta(2)} \Rightarrow \frac{L^{UL}(k,1)}{L^{UL}(k,2)} < \frac{1-\eta(1)}{1-\eta(2)} \tag{4.12}$$

If α is the propagation loss exponent and $d(k,j)$ is the distance between UE k and BS j, the previous condition can be expressed as follows:

$$\left[\frac{d(k,1)}{d(k,2)}\right]^{\alpha} < \frac{1-\eta(1)}{1-\eta(2)} \tag{4.13}$$

From this relation, two conditions on the values of $\eta(1)$ and $d(k,1)$ can be derived:

- First, if it assumed that $\eta(2)$ is a fraction of $\eta(1)$, i.e. $\eta(2) = \beta\eta(1)$ with $\beta \leq 1$, then $\eta(1)$ can be expressed as a function of the distances and β as follows:

$$\eta(1) < \begin{cases} \dfrac{1-\left[\frac{d(k,1)}{d(k,2)}\right]^{\alpha}}{\beta\left[\frac{d(k,1)}{d(k,2)}\right]^{\alpha}-1} & \text{if} \quad \beta\left[\frac{d(k,1)}{d(k,2)}\right]^{\alpha} > 1 \\ \\ \dfrac{\left[\frac{d(k,1)}{d(k,2)}\right]^{\alpha}-1}{\beta\left[\frac{d(k,1)}{d(k,2)}\right]^{\alpha}-1} & \text{if} \quad \beta\left[\frac{d(k,1)}{d(k,2)}\right]^{\alpha} < 1 \end{cases} \qquad 0 \leq \eta(1) \leq 1 \tag{4.14}$$

  This condition represents the maximum load factor of BS 1 so that it remains as the best station for UE k. Figure 4.3 shows this condition graphically for two cases. The area represents the maximum value of $\eta(1)$ for different combinations of $d(k,1)$ and $d(k,2)$, it is assumed $\alpha = 3.76$. As expected, when both cells are equally loaded ($\beta = 1$) the area becomes step shaped. In this case, the best BS is always the closer to the UE, that is why for $d(k,1) < d(k,2)$ the condition is simply $\eta(1) < 1$ which is always accomplished. On the other hand, if the UE is closer to BS 2, the condition becomes $\eta(1) < 0$, which is impossible. For the second case ($\beta < 1$), BS 2 is more loaded and so the area shows that lower values of $\eta(1)$ are required to have BS 1 as the best option, even though the UE is closer to it.

- From Equation (4.11), a second condition can be derived to quantify the impact of η from another viewpoint. The maximum distance at which BS 1 remains as the best option can be expressed as a function of the load factors measured at both BSs. Thus, if the sites are separated by a distance D and

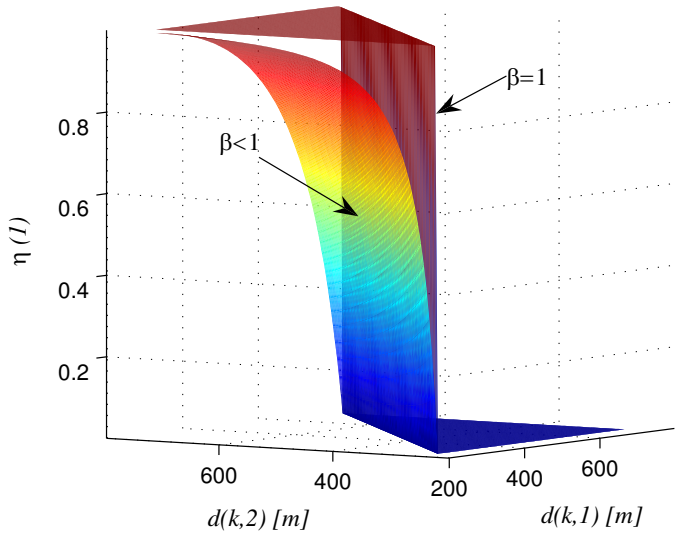

Figure 4.3: Maximum load factor that establishes BS 1 as the best option for UE k for different distances to BS 1 and 2.

assuming that the UE moves on the straight line connecting them, then its distance to BS 2 is easily found from its distance to BS 1, $d(k,2) = D - d(k,1)$, and the next condition is derived:

$$d\,(k,1) < \frac{D\left[\frac{1-\eta(1)}{1-\eta(2)}\right]^{\frac{1}{\alpha}}}{1+\left[\frac{1-\eta(1)}{1-\eta(2)}\right]^{\frac{1}{\alpha}}} \tag{4.15}$$

Which is graphically represented by Figure 4.4 assuming D =1 km. For a fixed $\eta(1)$, the area where BS 1 is the best option expands as $\eta(2)$ increases. Conversely, if $\eta(1) > \eta(2)$, then the maximum distance that implies that BS 1 is the best candidate decreases. As expected, whenever both cells are equally loaded, this distance is $D/2$.

Given the previous paragraphs the selection of a set of pilot powers or downtilt angles that improve the UEs assignment to BSs is very dependant on the different η values and this implies that the optimizer should consider all them jointly. It is not clear whether a reduction or increase of a particular cell area will imply an improvement or worsening of its performance without having the knowledge of surrounding BSs. Thus an strategy that considers all the elements simultaneously is definitely recommended.

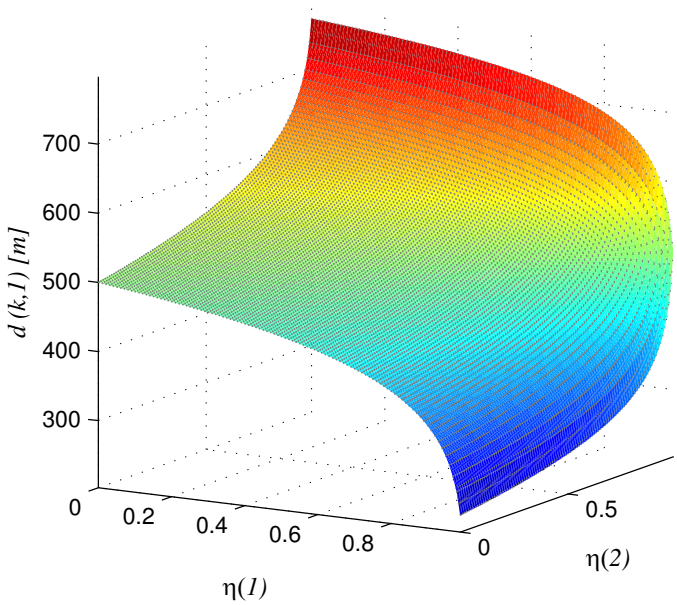

Figure 4.4: Minimum distance that establishes BS 1 as the best option for UE k for different load factors measured at BS 1 and 2.

4.3 Solution Principle

To design an *Automatic Planning* strategy dealing with CPICH powers and downtilt angles, the problem has been posed as the assignment of a finite set of possible configurations to BSs so that a cost function is minimized while respecting several constraints. Concerning downtilt, the cost function should follow what was indicated in the conclusions of the previous chapter and angles are optimized from a global cell viewpoint, which also guaranteed that both UL and DL are jointly optimized. Regarding CPICH powers, UL requirements are considered jointly for all target cells. The cost function in Equation (4.16) is used having to respect the subsequently indicated constraints. The problem is reduced to:

Minimize:

$$F_{cost}\left(S_i\right) = \frac{1}{N_{BS} N_{snap}} \sum_{j=1}^{N_{snap}} \sum_{k=1}^{N_{BS}} \eta_{S_i}\left(k\right) \tag{4.16}$$

Subject to:

- The percentage of target area without enough CPICH coverage should not be higher than 5%.
- The percentage of UEs not reaching the $(E_b/N_0)_{target}$ in a certain cell should not be higher than 5%.

- The number of BS under maximum DL capacity conditions cannot be greater than 1. This condition happens when one BS reaches maximum power.

N_{snap} is the number of snapshots considered during the optimization process. The proposal considers several snapshots of the network conditions because it is desirable that simulation evaluates the network ability to cope with multiple traffic requirements. Too many snapshots to analyze a wide extension of the network can imply prohibitive computational time. Finally, the subindex in η_{S_i} indicates that the load is calculated considering that BSs are configured according to solution S_i.

The range of possible CPICH powers has to be established considering that too high values can jeopardize DL capacity and too low values can promote the existence of many solutions lacking enough coverage. Since reference values for macrocells are typically around 10% of the total Node-B power, the selected range is [24, 33 dBm divided in steps of 0.5 dB. Regarding downtilt angles, the minimum value is set to 0º and the maximum is 9º, separated in steps of 1º, typical electrically controlled commercial antennas are considered [Kat] (see Appendix B and Section B.3). Although the selected antenna can be electrically adjusted with up to 10º, the 9º maximum has been chosen taking into account the results from the previous chapter (see for example Figure 3.15).

This type of resource allocation problems are known to be NP-complete and that means its resolution time is exponential with the problem size. Since there are so many possible combinations, evaluating all the space of solutions is impractical and the SA metaheuristic is proposed to cope with the problem.

4.4 Resolution with Simulated Annealing

SA was introduced in Chapter 2 as one of the algorithms that more popularity enjoys in the resolution of combinatorial optimization problems. It was also indicated its basic functioning that established an analogy with the cooling process of a liquid and conversion into a solid. A previous reading of this section is recommended since it gives an overview of the algorithm along with basic ideas of its functioning.

One of the paramount components of SA is the transition between solutions and the process that describes them. In particular, when the temperature is T, the probability that a system has a particular energy state is given by the Boltzmann-Gibbs probability distribution of statistical mechanics:

$$P\left(\text{Energy state} = x\right) = c_T \exp\left(\frac{-x}{k_B T}\right) \tag{4.17}$$

Where:

- c_T: Normalizing constant ($c_T > 0$).
- k_B: The Boltzmann constant (1.38×10^{-23}J/K).

Therefore, even with low temperature there is some nonzero probability of reaching a higher energy state. In the optimization problem, this is equivalent to uphill movements in the space of solutions and so worsening the cost function. However, this probability is reduced as the temperature decreases.

It was Metropolis [MRRT53] who first introduced this probability distribution to construct a means for simulation to study the state of a physical system at a fixed temperature. In particular, if a substance has a free internal energy E_i, the next potential state, in which the energy would be E_j, is generated by applying a small perturbation, for example the movement of a single particle. Then the Metropolis criterion assesses whether this state is accepted as the new one. The system goes to the new configuration if it has less internal energy in the new state ($E_j < E_i$), otherwise the probability of doing the change is $\exp\left[\left(E_i - E_j\right) / \left(k_B T\right)\right]$. In the case of combinatorial optimization problems, this rule is applied to the probability p_{ij} of accepting the transition from solution S_i to solution S_j as follows:

$$p_{i,j} = \begin{cases} 1 & \text{if} \quad F\left(S_j\right) < F\left(S_i\right) \\ \exp\left[\frac{F(S_i) - F(S_j)}{T}\right] & \text{if} \quad F\left(S_j\right) \geq F\left(S_i\right) \end{cases} \tag{4.18}$$

Where $F\left(S\right)$ is the cost function of a certain radio planning solution S and T is the temperature, which acts as a control parameter. Since T is decreased as the algorithm advances, the probability of uphill movements is also reduced along time, by the end of the simulation the algorithm is positioned close to the global minima and T is close to zero.

Given this, it seems logical to generate one new solution by applying the Metropolis criterion for each value of T. However, and continuing with the physical analogy, if the cooling is slow enough, the system can find a thermic equilibrium at each temperature level. These states can be achieved in the optimization process by applying the basic iteration many times with the same T and once the equilibrium is detected, the temperature is reduced again. Indeed one of the critical components of SA is the mathematical analogue of the rate of cooling in physical processes since it has a strong effect on the final success of the algorithm [Spa03].

A high level approximation of SA algorithm is plotted in the flow chart in Figure 4.5(a). Two parts are differentiated, first the search for an appropriate initial temperature T_0, which physically would correspond to the heating of the system to promote the movement of its molecules. The second part is the exploration itself of the solutions space to find the solution that optimizes the cost function. The individual block named "Search of Equilibrium" is the basic iteration of the algorithm at a certain T, it is depicted by the second flow chart, Figure 4.5(b).

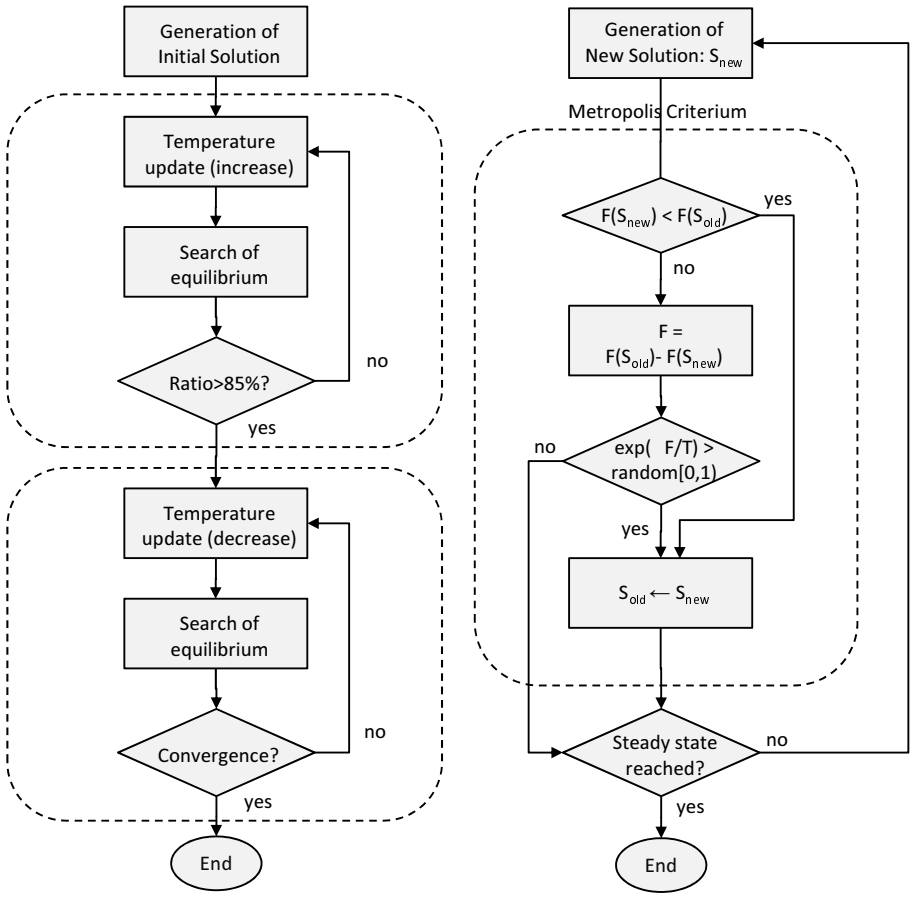

(a) SA. First approximation.

(b) SA. Basic iteration.

Figure 4.5: Flow charts of SA.

4.4.1 Determining the Initial Temperature

In order to make of SA a robust procedure, it is desirable that the quality of the final solution is independent of the initial one. Thus, the value of T_0 must be high enough so that most of transitions are accepted, otherwise the algorithm could be conditioned to be trapped in a local minima.

The initial value can be easily found starting with a small value of T_0 and multiplying it by a value greater than 1 until the ratio of accepted solutions is close to 100%. In the simulations of this work the search is stopped when this ratio is higher than 85%, as indicated in the flow charts.

In order to start the execution of the algorithm, it is needed an initial solution that already accomplishes with all constraints, that means a solution that already belongs to the feasible solution space, otherwise SA does not guarantee that all constraints are accomplished by the final solution. It can be thought as an algorithm that optimizes an existent solution and not as "solution creator" by itself. The cost of the initial solution is irrelevant. In the particular case of BS configurations, the easiest initial solution is the configuration that was estimated in early planning stages, by means of link budgets.

4.4.2 Generation of New Solutions

The generation of a new solution consists of a slight perturbation over the current one. This modification is done according to two random elections: one pilot power in the established range and one BS in the area to be optimized. The new cost value is recalculated and constraints are evaluated, whenever a constraint is not accomplished the solution is rejected, otherwise the Metropolis criterion is executed.

Regarding downtilt angles, initial simulations showed that choosing them randomly as well was impractical. The problem size augmented exponentially and so exploring the solutions space with SA required a prohibitive computational time. Moreover the algorithm wasted a great percentage of the time evaluating non valid solutions, not accomplishing constraints. This is because uncoordinated increases of angles and reductions in pilot powers led to important reductions of SHO areas and generation of deadspots. That is why downtilt angles are chosen in a more guided fashion by running a separate optimization module several times per cycle. This consists in choosing one random BS and evaluating all possible angles. The solution that implies a minimum cost is directly accepted without evaluating the Metropolis criterion. The number of downtilt optimizations within each temperature level is adjusted around 10. Thanks to this, it is later shown that the search performs correctly and configurations with a better performance are found without compromising the required computational time.

4.4.3 Algorithm Convergence and Cooling Strategy

Given how the problem has been presented, its resolution by SA makes that mathematically speaking, at each temperature level, it can be modeled as a homogeneous Markov chain. Indeed the algorithm can be characterized by a transition matrix $\mathbf{T}_T$ representing all transition probabilities for all the possible solutions at temperature T. The whole algorithm is described by an inhomogeneous Markov process that consists of the sequence of all the particular chains at each temperature level. For example, if it is assumed that there is a finite number N of possible solutions, then the transition matrix at temperature T is given by:

$$\mathbf{T}_T = \begin{pmatrix} 1 - \frac{1}{N}\sum_{k\neq 1} p_{1,k} & \frac{1}{N}p_{1,2} & \cdots & \frac{1}{N}p_{1,N} \\ \frac{1}{N}p_{2,1} & 1 - \frac{1}{N}\sum_{k\neq 2} p_{2,k} & \cdots & \frac{1}{N}p_{2,N} \\ \vdots & \vdots & \ddots & \vdots \\ \frac{1}{N}p_{N,1} & \frac{1}{N}p_{N,2} & \cdots & 1 - \frac{1}{N}\sum_{k\neq 1} p_{N,k} \end{pmatrix} \tag{4.19}$$

Being $p_{i,j}$ the transition probability from solution S_i to solution S_j defined by the Metropolis criterion in Equation (4.18). The terms have been conveniently normalized so that each row of the matrix sums 1. This yields the probability of not changing a certain solution S_i, which is given by $1 - \frac{1}{N}\sum_{k\neq i} p_{i,k}$. It is clear that $\mathbf{T}_T(i,j) = 0$ if $S_j \notin N(S_i)$, where $N(S_i)$ is the subset of new solutions that can be generated from S_i, i.e. its neighbor solutions. The transition matrix not only allows determining the probability of reaching each solution for one step of the simulation, but also across n steps through the matrix $\mathbf{T}_T^n$.

Thanks to this mapping, it has been demonstrated in [AK89] that the Markov chain associated with SA converges at T to a stationary probability distribution defined by the probability vector $\boldsymbol{\pi}_T$:

$$\lim_{n\to\infty} \mathbf{T}_T^n(i,j) = \boldsymbol{\pi}_T(j) \Rightarrow \lim_{n\to\infty} \mathbf{T}_T^n = \boldsymbol{\pi}_T \tag{4.20}$$

Thus, for any fixed temperature $T > 0$, if SA is executed for "a long time", the distribution of the associated Markov chain will be very close to $\boldsymbol{\pi}_T$. Once this equilibrium is reached, the temperature can be decreased again to further improve the solution. In particular, two general modes of convergence exist towards the global minimum or minima:

1. In the first mode, convergence is guaranteed if T is decreased until zero but executing each Markov chain for an infinite time, so that the stationary distribution is reached at every level.

2. In the second mode, convergence is achieved if temperature is reduced so that it approaches to zero in a logarithmic manner, i.e. if temperature at level n fulfills $T_n \geq T_0/\ln(1+n)$, where T_0 is the initial temperature level and n is a

counter of the already executed levels.

If one of these update rules is hold, then $\boldsymbol{\pi}_T$ converges to the optimal vector $\boldsymbol{\pi}_T^\star$ which represents a uniform probability distribution among all the global minima. Although both modes of convergence require infinite computing time, many works have used fast cooling algorithms and demonstrate that SA is a highly efficient metaheuristic for a wide variety of combinatorial problems (see Section 2.2.2). The slower the temperature is decreased, the higher the probability of reaching the global optimum.

Given this, for a slow enough cooling strategy, if stationarity is achieved at level n, in the next one $(n+1)$ the number of required iterations will be lower because both Markov chains are going to be very similar and stationarity appears sooner. Hence, and outlining the importance of having a long enough iteration at T_0 the authors in [AK89] propose as the most appropriate cooling update the following:

$$T_{n+1} = \frac{T_n}{1 + \frac{T_n \ln(1+\delta)}{3\sigma_n}} \tag{4.21}$$

Other options have been used in the literature being the geometric cooling the most typical one because of its easy implementation: $T_{n+1} = \beta T_n$, $\beta < 1$. In the present work, however, the temperature has been updated as proposed in Equation (4.21) because it is mathematically demonstrated that it preserves the convergence theory as much as possible.

The aggressiveness in the reduction of T_n can be controlled with δ so that simulation time can be adjusted to the available one. On the other hand, σ_n represents the standard deviation of the cost evolution with temperature T_n and its importance is described in next paragraphs.

The update should be executed whenever a certain stationarity is detected for a given level. However, monitoring this condition demands a very high computational cost and more practical empirical rules have been derived. For example, for the previous cooling algorithm, it is found in [AK89] that a good stationarity condition is executing the Metropolis criterion as many times as the dimension of N (set of neighbor solutions) for a given solution. In the case of study, this value can be estimated by the product of N_{BS} and the number of possible CPICH powers: $1 + \left(P_{TX,CPICH,max} - P_{TX,CPICH,min}\right) / \Delta P_{TX,CPICH}$. The resultant value is in fact an upper bound since several combinations are not valid solutions because they do not respect constraints. This rule-of-thumb works properly and an exact election of this value is not so critical because the temperature reduction is inversely proportional to σ_n, thus if the update is done too soon, σ_n will be high and the decrease will be lower and viceversa. That means the cooling schema would react to some extent if the equilibrium condition had not been very accurately chosen. This is graphically shown by Figure 4.6 which represents Equation (4.21) for different values of σ_n.

A second comment that can be drawn from the figure is that the higher the

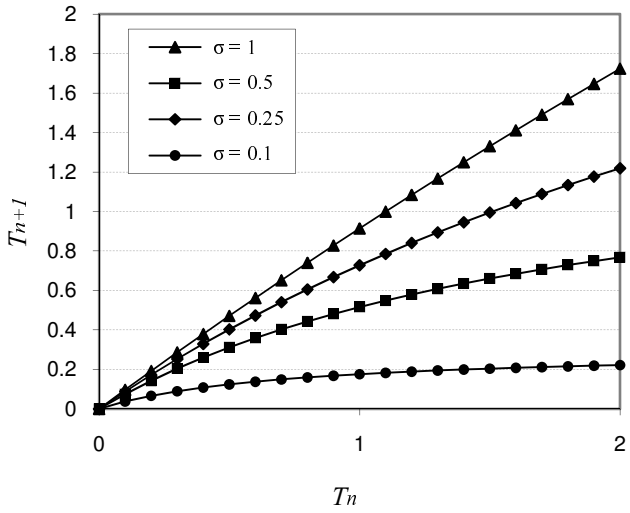

Figure 4.6: Graphical representation of the cooling schema for different values of σ_n.

temperature, the higher the reduction as well. When the algorithm is supposed to be near the optimum, the temperature decrease is slower. In fact, an infinite time is required to reach $T = 0$ and therefore a convergence criteria different from that must be defined. In this case, it is taken into account the ratio of accepted solutions by the Metropolis criterion at a certain temperature level. The algorithm is considered to have finished when this ratio is less than 1%. At this point cost variations are very low and no more significant gains are obtained.

4.5 Results

The proposal has been tested by means of system level simulations. Two heterogeneous scenarios are considered, with cells with important load levels. The first one is synthetic the second is a realistic one based on real measurements from an existent network.

4.5.1 Synthetic Scenario

The first scenario is a synthetic one whose main features are described by Appendix B in Section B.3. In order to provide more heterogeneity to it, the deployment layout is not exactly regular and site positions have been shifted by a bidimensional uniform random variable represented by a square of 100×100 m^2. Antenna heights were also randomly chosen between 25 and 35 m.

Regarding UEs distribution, a total of 700 are scattered according to the heterogeneous distribution depicted by Figure 4.7. Darkest areas indicate a probability of

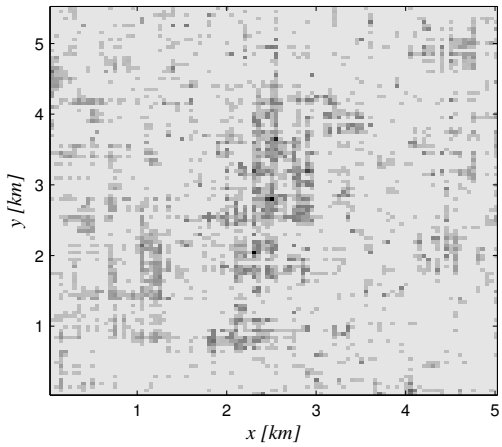

Figure 4.7: Density of users for the synthetic scenario.

Table 4.1: Simulated service mix in the synthetic case.

Type of Service		UEs %
Voice	12.2 kbps	70%
	12.2 kbps (50 km/h)	15%
Data	64 kbps	11%
	144 kbps	2.5%
	384 kbps	1.5%

active UEs four times higher than in the lighter ones. Finally, the 5 different services listed in Table B.2 (Appendix B) are used considering the service mix indicated by Table 4.1.

The flow chart in Figure 4.8 shows a first level of the basic steps executed during the optimization. It can be noted that for small variations of CPICH powers a new solution can have the same cost as the previous one. That happens when all AS remain without changes and it permits not executing the UL power control. The DL has to be evaluated always because any variation in pilot powers means variations in the DL interference pattern and thus in the CPICH coverage probability. Also devoting more power to CPICH signals implies a reduction in the power available for traffic.

Several results have been obtained with this first scenario, with and without executing the downtilt optimization module. From Figure 4.9 it can be seen the mean UL load factor η for all the cells in the system before and after optimization. The heterogeneity of the scenario is clear and sharp variations among load factors of different cells can be noticed. Those cells with a particularly low load are the ones at the border and cover smaller regions because of the specific dimensions of the simulated area. Border effects are not important since the interest is not on the absolute values but on the relative ones.

With the number of scattered UEs, several cells are highly loaded, however their AC algorithms have been disabled so that the gains introduced by the optimization can be observed. Results show that SA succeeds in obtaining a globally better network performance. The number of cells with a load factor higher than 0.8 is reduced from 18 to 7 when the pilot powers are optimized and this number if reduced to 4 when the downtilt module is also running. The algorithm indeed finds a configuration of parameters so that interference is minimized and consequently,

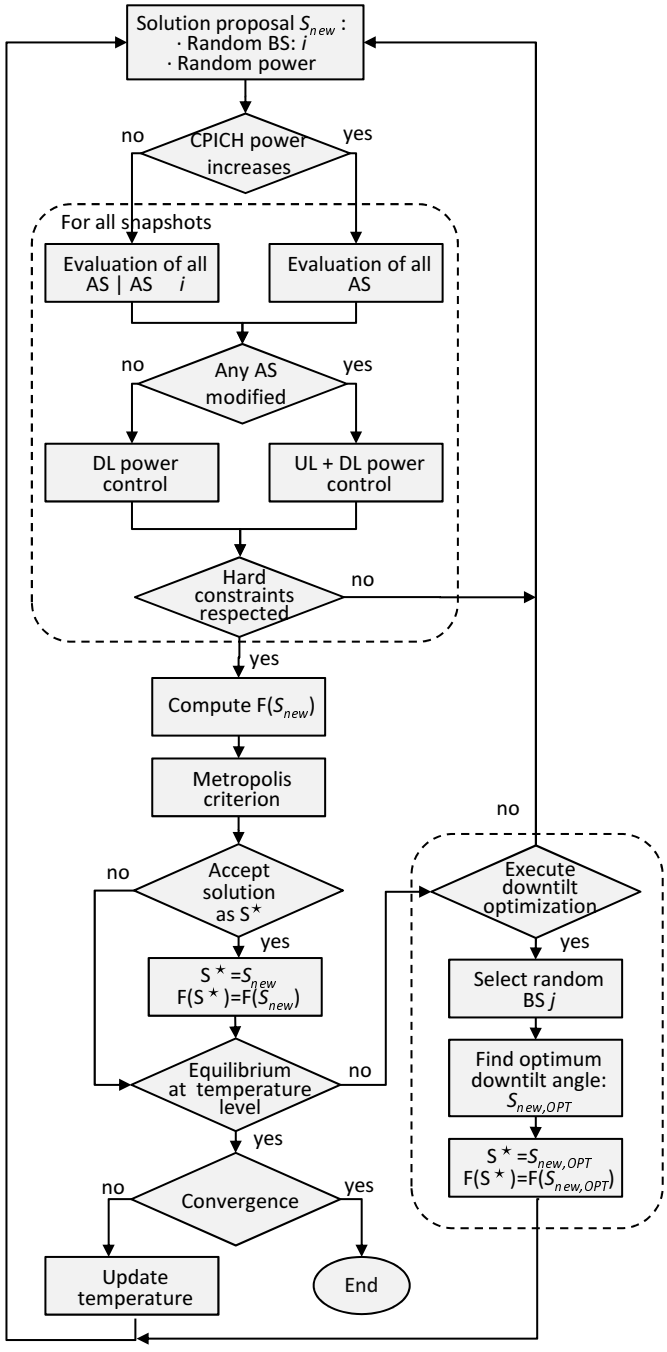

Figure 4.8: Flow chart of optimization process.

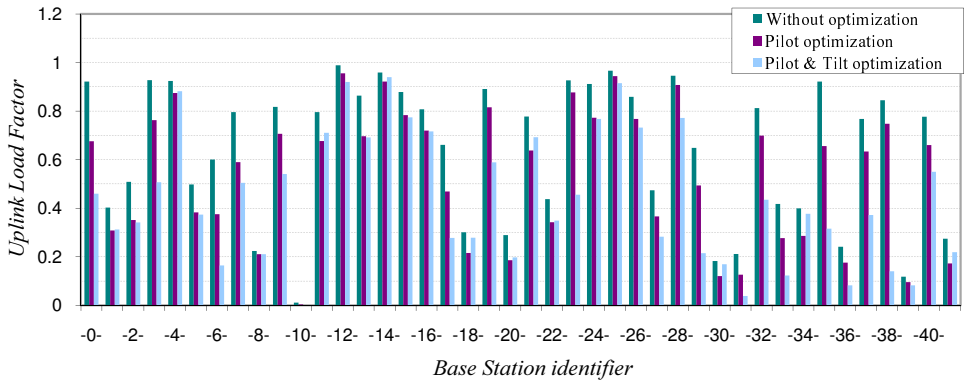

Figure 4.9: UL load factor before and after optimization.

capacity can be increased. It can also be seen that executing the downtilt module does not guarantee a reduction in the 100% of cells when compared with the option without it. However, the global benefit in the network is far superior. In this sense, it is recalled a result from the previous chapter: Modifying downtilt angles can imply an important reduction in the transmission powers of those UEs in the cell area which causes a reduction in the interference transferred to other cells, but in some cases this is at the cost of increasing the own UL load factor because intercell interference is received better as well. The combination of both effects, link losses reduction and interference increase determines the final outcome of the angle modification.

Figure 4.10 shows a comparison of the cost evolution for both optimization options. For the version that considers both pilots and angles, two cases are plotted. The difference lies in the number of samples that the algorithm spends in each temperature level, 750 or 4000. The first case corresponds to the value adjusted considering the previously explained rules and the second one is an overestimation to test the benefits of further increasing the computational time. The horizontal continuous line indicates the original cost value, when all BSs in the area to be optimized are homogeneously configured, for example with the help of link budgets. The fast initial increase corresponds to the search of the initial temperature, which reveals that the initial configuration could be clearly worsened. Once the temperature has been found, a downward trend appears until the end of the search.

According to the curves, when introducing downtilt analysis, the cost is reduced in an extra 18%. Actually Figure 4.11 reveals how it can help to the annealing process by representing the cost evolution in the samples executed at a certain temperature level T_n. Once the temperature is sufficiently reduced, the algorithm starts to converge towards suboptimal solutions but thanks to local downtilt optimizations, it is guided out of those relative minima and it is positioned in new areas of the space of solutions. As a result, better final configurations are found.

Going back to Figure 4.10 and comparing the cases with different number of samples per temperature level, a slight gain is obtained when 4000 samples are

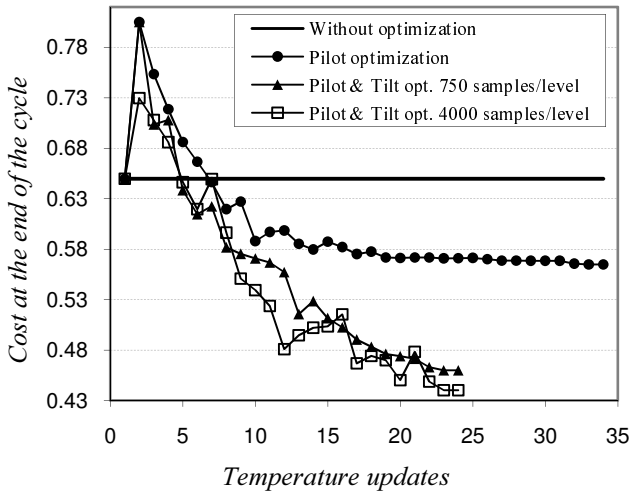

Figure 4.10: Cost evolution for different optimization options.

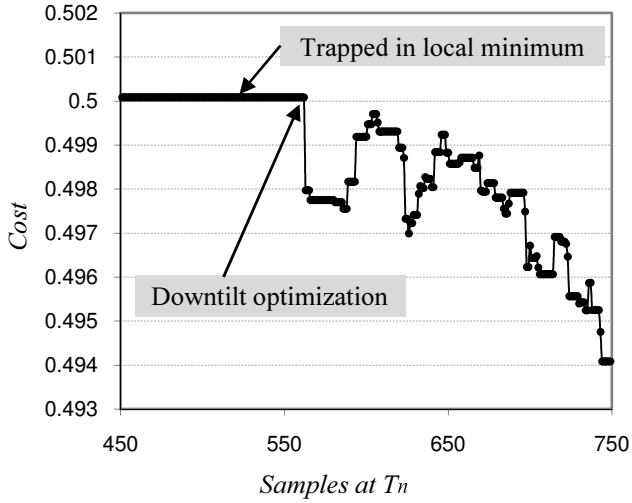

Figure 4.11: Effect of intelligent local downtilt optimization.

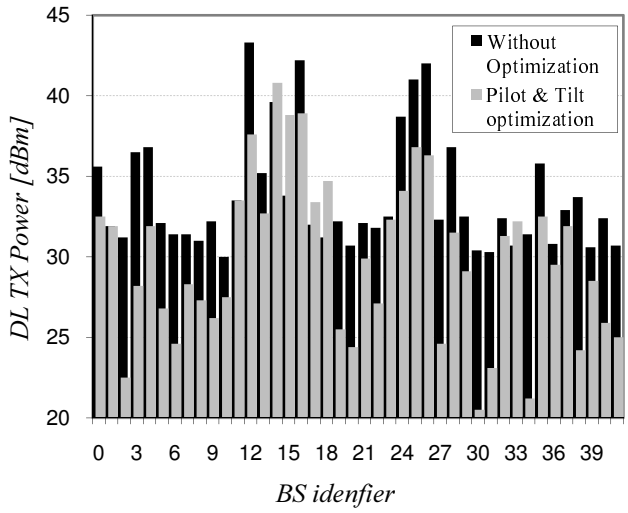

Figure 4.12: DL transmission power before and after optimization.

used. This is at the price of multiplying by more than 5 the computational time. The obtained gain is consistent with the fact that SA tends to better solutions as search time tends to infinite, however higher gains are more and more difficult to obtain. Shorter simulations were also run, for example, for a rather small number of samples (75) results were around a 27% worse than the 750 case.

The average DL transmission power has also been reduced, from 35.6 dB to 32.7 dB. Individual cell levels, however, are more indicative and they are represented in Figure 4.12, where an irregular gain can be seen. The cells that cover the more loaded area are numbers 12, 14, 16, 24, 25 and 26, which are the ones situated in the center of the scenario. These cells required DL transmission powers close to its maximum (43 dBm) and, as shown in the figure, the optimization permits reducing these values in most cases (all except ♯14). This is because of a better assignment between UEs and BSs, but also because several CPICH powers are reduced and consequently less power is devoted to signalling.

Since the scenario has many BSs, it is difficult to analyze all the relationships between each BS and its limiting ones, this aspect is more clearly seen in the second scenario. Nevertheless, some particular cases can be commented. For example, Figure 4.13 compares the probability that a UE has a certain cell in its AS for the three basic cases: without optimization, only modifying pilot powers and optimizing both pilots and tilts. This is done for two significant cells, one in the loaded area (♯26) and another limiting with the first but serving far less UEs (♯15). These values are accompanied by Table 4.2 which contains the final CPICH powers and tilt angles for these two cases.

It can be seen how cell 26, reduces the probability of appearing in the AS, which is done by reducing its CPICH power and increasing nearby ones, as for example cell 15. This however cannot be taken as a rule-of-thumb, because as seen in the

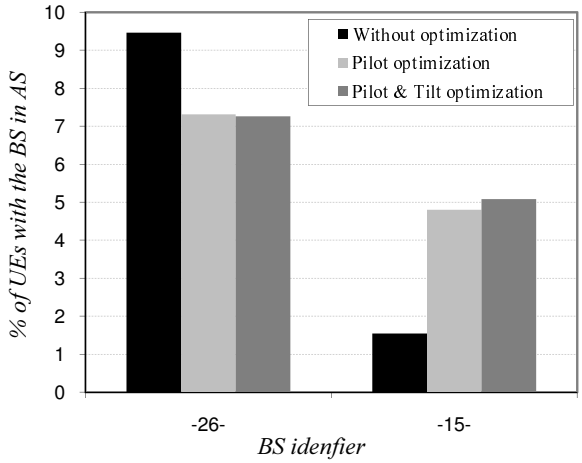

Figure 4.13: Probability that a cell appears in AS.

Table 4.2: Final CPICH powers and downtilt angles.

Cell id.	CPICH pow. [dBm]	Tilt [º]
26	24	3
15	32	4

Table 4.3: Changes in SHO areas due to the optimization.

AS size	% of UEs		
	Without opt.	Pilot opt.	Pilot & Tilt opt.
1	75.6	72.1	81.3
2	21.39	21.57	16.6
3	3.01	6.33	2.1

previous chapter, this reduction can lead to a worse assignment of UEs into cells and so to a reduced capacity. In fact, there are some central cells that do not change significantly is effective areas but improve in both UL and DL because of actions taken in nearby ones. Although the differences in the number of links indicate that effective cell areas have been changed, SHO areas are well guaranteed by the new configuration, this is shown by Table 4.3, which contains the probabilities of being connected to one or several BSs before and after optimization, important changes are not observed.

Downtilt angles contribute to reduce the required transmitted power and modify generated and received interference. However, two cases can be commented, firstly the cell in the bottom part of the scenario, which have a smaller area to cover because the scenario is cut. In this case the algorithm applied downtilt angles of 8 and 9º, which are quite high but adequate to that situation, where UEs are close to the Node-B. On the other hand, the upper cells have a wider potential area to serve and the algorithm applied in most of the cases a 0º angle, consistent with the coverage constraint.

4.5.2 Realistic Scenario

The second scenario is the same as in the previous chapter, a realistic and heterogeneous one based on that described in Section B.2 (Appendix B). That is a 13 cells layout based on real attenuation measurements from a GSM network operating in the 1800 MHz band.

The traffic distribution is not exactly the same as indicated in the Appendix and has been partially changed in the current set of simulations to help analyzing the final solution. In particular, the probability that a UE operates at a certain radioelectrical region, or area in which a BS is the best received in terms of CPICH RSCP, has been set equal in all cells but one. This cell has a probability four times higher than the rest. Although this fact, UEs out of the hotspot are not uniformly distributed in the space because, once a radioelectrical region has been assigned, the real probabilities of the subregions are maintained according to the measurements.

As indicated in the previous chapter, one of the drawbacks of this scenario is that UEs are characterized by their propagation losses and not by their coordinates, the scenario is blind and UEs positions are not known, furthermore indoor and outdoor users are mixed. This way, downtilt modifications cannot be implemented and the proposal has been tested omitting that optimization module. On the other hand, the number of BSs to optimize is smaller and that is why the power step between possible CPICH levels is reduced to 0.1 dB.

The first results contained in Figure 4.14 show that the algorithm also succeeds in this real network. As with the synthetic scenario, the cost reduction is plotted (Figure 4.14(a)) and also the comparison of load factors before and after optimization (Figure 4.14(b)). Without optimization there were 6 cells whose load factor was comprised between 0.7 and 0.8, after the optimization, they all are reduced far below this range. However, the more loaded cell, identified by 8-33, does not improve significantly. Indeed, the particular position of geographical UEs may spoil any possible inclusion of new BSs in the AS and so a BS reassignment, and if they are very close to the Node-B, it is likely that the best cell is always the original one with no other possibilities of improvement. This type of situations can only be further improved by rearranging the layout or introducing new cells.

Figure 4.15 gives extra information about the obtained gains since it represents the histogram of the UL load factor for 4 of the cells in the system before and after the optimization process. The improvement is clear in both mean and standard deviation.

Since this scenario is smaller in size than the previous one, and despite the heterogeneous distribution of UEs, the analysis of the final solution is somehow easier than in the previous scenario. Figure 4.16 shows the combination of pilot powers obtained by the algorithm. The power assigned to 8-33 is lower, consistent with the fact that more traffic was deliberately scattered in its corresponding radioelectrical region.

It is worth mentioning that, assuming that CPICH coverage is guaranteed, it

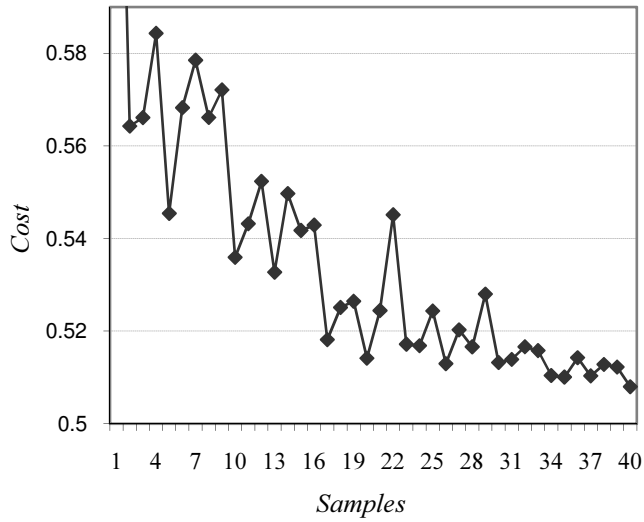

(a) Cost reduction during the optimization process

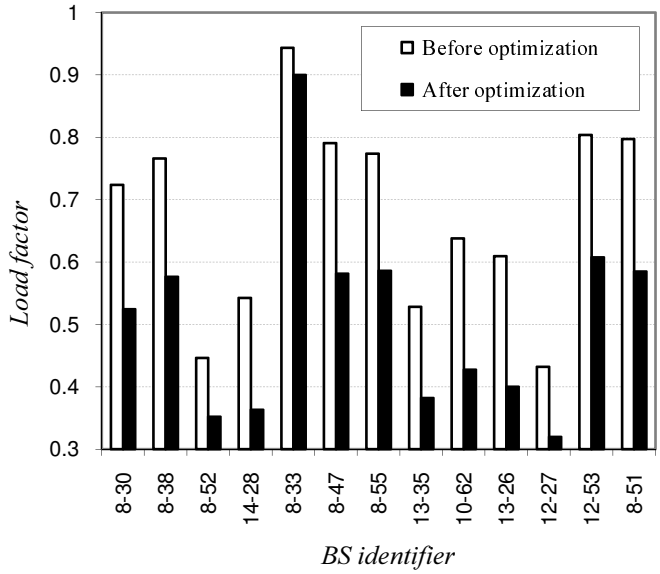

(b) UL load factor in the optimized BSs before and after optimization

Figure 4.14: Gains obtained by SA in the realistic scenario.

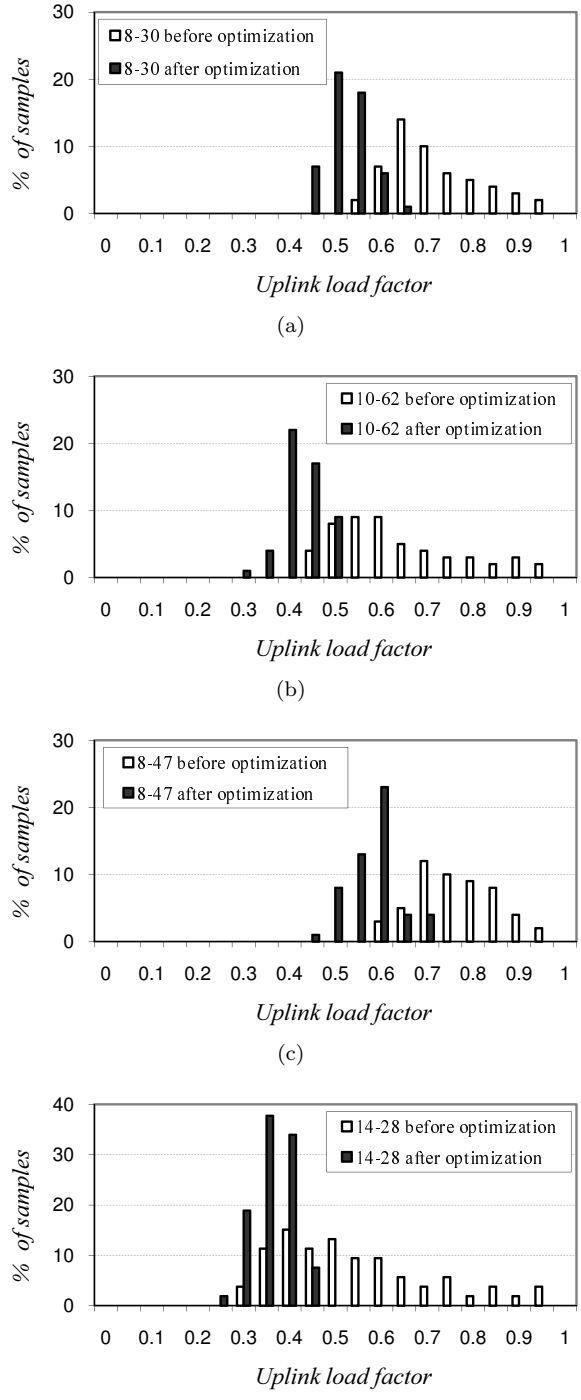

Figure 4.15: Histogram of UL load factor for 4 random BSs in the system.

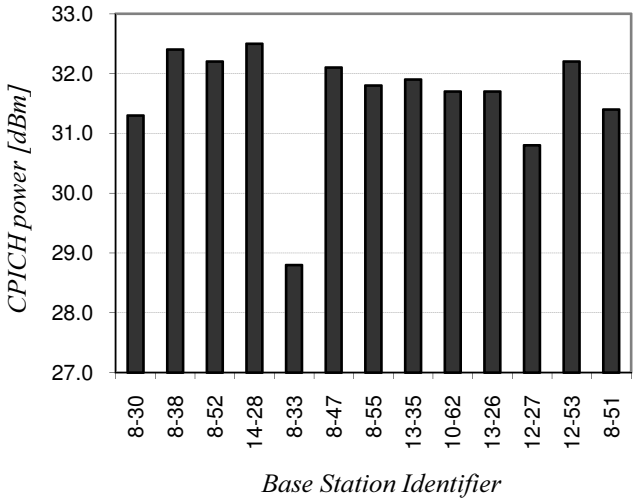

Figure 4.16: Pilot power proposal for realistic scenario.

is the relation among pilot powers the responsible of traffic equalization. So, once this is obtained, the transmitted powers can be iteratively reduced to minimize DL interference up to the point in which coverage would start to reduce. Unnecessary power for signalling channels is always to the detriment of data ones.

The final plots just intend to show the behavior of some of the internal parameters controlling the algorithm. Thus, Figure 4.17 shows the evolution of the temperature (relative to its maximum initial value) and the correspondent acceptance ratio, which decreases almost linearly. This behavior is desirable because a concave curve would have meant an excess of samples exploring the solutions space with a high temperature or a shortage of samples with lower levels. Similarly, a convex shape is not desirable either and both cases would have result in worse solutions.

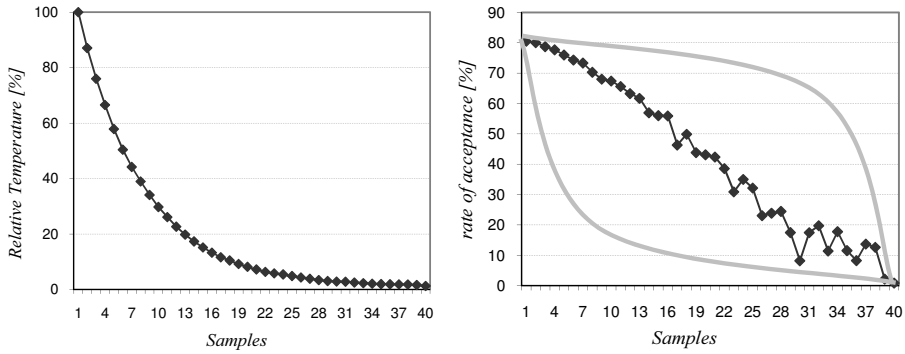

(a) Temperature evolution

(b) Acceptance ratio evolution and undesired behaviors

Figure 4.17: Evolution of SA parameters.

4.6 Concluding Remarks

Along this chapter a novel optimization technique based on SA has been proposed and investigated with the objective of automatically planning optimal configurations for BSs. In particular, the two parameters that were studied in the previous chapter, CPICH powers and downtilt angles, have been object of optimization. These two parameters were shown to be good candidate strategies to improve the assignments of UEs to BSs so that UL and DL transmission powers are minimized and capacity can be eventually increased.

Load balancing is usually addressed as the transfer of UEs from a loaded cell to a nearby one with less connections. However in CDMA systems this rule is not so straightforward and forced handovers might imply even more interference and degradation for the mother cell. The 3GPP E_c/I_0 cell selection criterion takes into account DL interference, but UL measurements are not considered and thus the BSs included in the AS may not be the best option. Moreover, most of automatic planning proposals address CPICH power adjustments just as a coverage improvement method but potential capacity increases are not studied or only exploited to alleviate the traffic of a cell containing a hotspot and surrounded of cells with much less traffic. Indeed, coping with heterogeneous traffic distributions and adjusting the planning parameters to maximize capacity for a given covered area is the key objective behind the proposal in this chapter.

Among all possible configurations, the automatic tuning algorithm should configure BSs so that a higher number of UEs include their best option cells in their AS. The existence of this optimal configuration has been analytically addressed along with the dependence on link losses and load factors. Its impact has been quantified showing how a far away cell may be more appealing to a UE provided that its load is low enough and viceversa. This way it can be predicted an optimal combination of pilot powers and downtilt angles so that UEs are correctly equalized among cells,

transmission powers are reduced and capacity is improved.

The problem has been posed as an optimization one, in which a cost function is minimized subject to constraints on coverage, QoS degradation and DL power consumption. Because of its NP-completeness feature and the size of the space of solutions, the SA metaheuristic has been used for its resolution.

After explaining the parallelism with the annealing physical phenomenon the Metropolis criterion, responsible for uphill movements in the space of solutions, has been introduced and the effect of the control parameter named *Temperature*. High and low level representations of the algorithm have been presented through flow charts showing that the algorithm accounts for two phases, one that sets the initial maximum temperature level and another that is the optimal solution search itself.

To find an appropriate initial temperature value, solutions are iteratively generated until the algorithm ratio of acceptance surpasses an 85%, which guarantees independence between the initial and last solution.

The generation of new solutions is done by applying a random modification in the pilot power of a random BS and AS modifications are evaluated to test whether it is required to simulate UL and DL power control. On the other hand, downtilt angles account for its own optimization module to avoid evaluating too many invalid solutions. In particular, this module is executed several times during the annealing search and selects one BS at random and looks for the angle that best fits the currently accepted solution.

According to studies on the convergence of SA to the optimal solution, two general modes of convergence exist but they both require an infinite computational time. Given this, a finite in time cooling strategy that preserves the convergence theory as much as possible has been chosen. Its dependence with the standard deviation of the cost during the previous temperature level provides a capacity of reaction if the equilibrium condition that controls the temperate update rate is not very accurately selected.

The proposal has been tested in two heterogeneous scenarios with cells with important load levels, a synthetic one and a realistic one based on real measurements from an existent network. Results show that the proposed *Automatic Planning* algorithm succeeds in enhancing planning configurations and an improved network performance is obtained. Thus, for the first scenario the number of cells with a load factor higher than 0.8 was reduced from 18 to 4. In the second one, the number of cells with a load higher than 0.7 was reduced from 7 to 1. A greater cost reduction is achieved when both parameters are jointly optimized. In particular, downtilt optimizations guide the algorithm towards new and better areas in the solutions space and prevent it from getting trapped in local minima. The cost function is reduced an extra 18% when antenna angles are considered as well. However, executing the downtilt module does not guarantee a reduction in 100% of cells because reducing link losses of served UEs in a cell, and thus the generated interference, can be at the cost of increasing the received intercell one. On the other hand, DL transmission powers were reduced in 3 dB on average and those cells close to its maximum power

gained a clear extra margin.

Extending iterations beyond the equilibrium condition implies slightly better solutions but requiring much more computational time. Thus, for instance, a simulation 5 times longer just gave an extra 4.3% gain in terms of cost. On the other hand, quick simulations degrade the outcome significantly, for example a simulation around 10 times shorter implied a cost loss of 27 %.

In the synthetic scenario, the final solution has been analyzed for significant BSs in the network, in the realistic the complete final solution has been provided, however rules of thumb are difficult to obtain because of the strong interactions among cells.

The algorithm failed in improving significantly the performance of the cell containing a hotspot in the realistic scenario. This reveals that UEs reassignments can be done to some extent. For instance, if UEs are close to the site, it is likely that the best cell is always the original one, unless nearby ones have a load factor close to zero. In this case, some gains can be obtained with downtilt angles, but in general further important improvements can only be achieved by rearranging the layout or introducing new cells.

Finally some internal parameters of the algorithm were analyzed showing a correct decrease of the rate of accepted solutions.

As SA is rather time consuming (several hours in an updated computer for general use), an often and continuous execution is impractical, the proposal belongs to the group of (static) *Automatic Planning* strategies. However, as it was explained in Chapter 2 this type of algorithms could be complemented by a pattern recognition system so that mid-term traffic patterns are tracked and adjusted parameters are conveniently applied according to a predefined timetable.

Chapter 5

Effect of Repeaters on WCDMA Radio Network Performance

5.1 Introduction

Mobile communications systems often work under high heterogeneous conditions in both time and space domains. However their optimization is not just a technical challenge, the intense competition among operators implies that they need to expand and improve their networks as cost effectively as possible. In this sense, repeaters are equipment of special interest. In comparison with full BS, *non-regenerative* active repeaters are much cheaper because, in the simpler case, they are just bidirectional amplifiers and that is why the rational for using them is basically cost.

On the other hand, *regenerative repeaters* are actually receiver-transmitter pairs that get the signal, demodulate it, obtain the bit stream, and remodulate and transmit it amplified and cleaned of noise. These devices are mainly used in long haul digital communications and in fact, BSs themselves, can be considered as a particular case of regenerative repeaters. Thus, they are aimed at signal consistency over these long links and are not necessarily used for cost reasons. This dissertation deals with non-regenerative active repeaters, hereinafter called simply *repeaters*.

Repeaters not only become interesting to operators to fill in coverage holes or spread the service area to a wider area [LL00], they also permit alleviating hotspots and defining distributed cells to reduce interference and improve the network capacity [RE04]. In a nutshell, repeaters enable reaching more subscribers while optimizing the investment. Tables of expenses (CAPEX and OPEX) are given in [Tay03] based on operator costs in Stockholm (Sweden), considered representative of a urban European market. The comparison with standard cells shows that repeaters

can indeed generate important costs savings to operators.

In the context of radio planning and optimization of WCDMA networks, not many studies in the literature have analyzed in depth the effects when deploying repeaters. This is reflected in the fact that network planning enhancement proposals based on these devices sometimes ignore their particularities in a WCDMA context. For example, [RSW06] considers ideal repeaters with no noise amplification. This effect is also missed in [RE04] but in this case, it is justified by using low gain repeaters, however this is at the cost of limiting the validity of the study to scenarios where BSs have one single repeater with a low internal gain. Other works make detailed DL analysis but omit the UL, [BNL05; BNI+06]. Moreover, in most cases the analysis only considers one repeater, which is not the case in several of the last advances in radio planning with repeaters, such as distributed Node-B architectures aiming at load balancing, [WQDT01].

The usage of non-low gain repeaters or structures with multiple repeaters can desensitize the BS and it requires a careful planning. This leads to several effects regarding coverage and capacity that are usually not taken into account in the existent literature and their study is the focus of this chapter after an introductory part. In particular, Section 5.2 provides important definitions and a classification of the different types of repeaters and Section 5.3 discusses some of the reasons that make repeaters appealing to WCDMA based networks. Next, capacity and coverage effects are investigated, analytically modeled and simulated:

- Regarding capacity, the noise rise induced by repeaters undeniably has a negative impact, circumstance that did not happen in FDMA based 2G systems. Indeed, one of the main novelties of this chapter is a holistic and general theoretical study on system capacity with repeaters deployment in a multiservice environment with a general heterogeneous layout and taking into account AC. In particular, a compact closed expression for the admission region is presented in Section 5.4, suitable for a system where the users belong to an arbitrary number of different service classes. This generic analysis could be used for both the deployment of mobile communication systems and the implementation of suitable AC mechanisms. From this study a trade-off between capacity and coverage arises. This is analyzed both theoretically and by means of simulations in Section 5.5. The adjustment of those parameters with a major impact is discussed to derive useful planning guidelines for operators.

- Regarding coverage, since the noise floor of the donor BS is raised, there is a shrinkage of its effective coverage. Obviously the loss is clearly compensated by the new coverage area of repeaters themselves, as represented by Figure 5.1 in a qualitative manner. In addition, this effect is not likely to appear in dense urban environment where link losses are low and the network is capacity limited. However, when that is not the case, deploying repeaters can induce the appearance of deadspots in the donor cell. In this sense, Section 5.6 derives an analytic expression that relates the donor cell radius before and after connecting repeaters to it. This analysis is based on that in [SM07], which is generalized by considering a scenario with multiple services and a

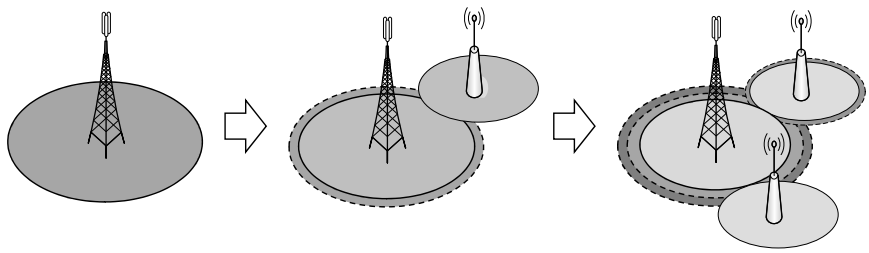

Figure 5.1: Coverage reduction in the donor cell because of repeaters deployment.

heterogeneous users distribution.

Finally, concluding remarks close the chapter.

5.2 Classification and Definitions

Repeaters are basically Radio Frequency (RF) heads which receive one or more carriers from the donor BS, and re-transmits them to a remote location. Considering how this process is done, two types of repeaters can be established.

1. *On-frequency repeaters or Iso-frequency repeaters.* This is the simplest case, they basically are bidirectional amplifiers connected to two antennas. The donor antenna is installed under the coverage of the BS and subsequently the signal is amplified and retransmitted (Figure 5.2). One of their main advantages is that they can be virtually installed anywhere as long as it provides a suitable mounting area with a power supply, without the need of an equipment room.

   Antenna isolation is an essential issue for the performance of this type of repeaters since they can act as oscillators under certain circumstances. The feedback path is formed between its two antennas and, to guarantee an adequate protection against self-oscillation, the coupling loss between the two repeater ports should be at least 15 dB higher than the repeater gain [3GPd]. Appropriate alignment of null radiation points in the diagram pattern, vertical separation between antennas and modifications in the environment around antennas (e.g. use of shielding grids) are mechanisms that can help to increase isolation. Nevertheless, repeaters will use an Automatic Gain Control (AGC) system as a fall back to prevent this self-oscillation. AGC would function if, for some reason, the isolation between ports is reduced during the network operation. Further details about repeaters gain adjustment and AGC functioning are given in Section 5.4.2.

2. *Remote sectors* consist of antennas and respective amplifiers. As indicated by their name, they are located remote from the BS shelter to which are linked via a link that can be of different types of conduit, e.g. microwaves, fiber optics,

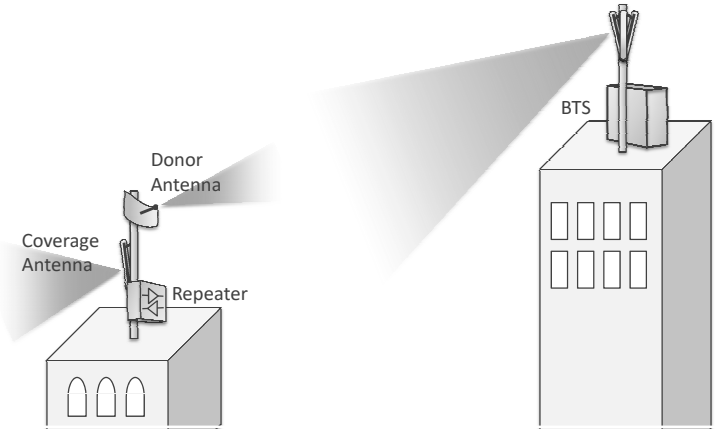

Figure 5.2: On-frequency repeaters.

coaxial cable, copper twisted pairs or optical wireless links. In this second type of repeaters, a new equipment denoted as *donor unit* is needed. It is directly connected to the BS and it is responsible of adapting the RF interface to the link. In the other end, the *remote unit* converts back the signal to mobile wireless frequencies and transmit them to UEs through the coverage antenna (Figure 5.3).

There can be more than one remote sector (this also applies to on-frequency repeater) connected to the BS. On the other hand, there can also be more than one BS, which may be of different operators, in one specific location or BS hotel.

Regarding the different types of conduits that can be used in the link between donor and remote units, repeaters can be classified in three big groups [WC01].

(a) *RF repeaters.* When the link between the donor and the remote unit is radio based, the frequency band to chose for transmission is one of the most important issues. Desirably, It must be one of those that the operator already exploits. If the radiolink does not over-interfere with the rest of the mobile network, it is possible to interchange the UL and DL WCDMA bands and use them as DL and UL respectively. Thanks to this transposition users will not connect to the network through the radiolink. Another option is using 5 MHz of the GSM band if it is available to the operator. The advantage of this second approach is that the interference would be around 13 dB lower than in WCDMA, since the channels are 22 times smaller in the first system. In any case, frequency planning must always be done carefully and taking into account this new source of interference.

(b) *Fiber Optic Repeaters* also denoted by the generic term *Radio over Fiber* (RoF). This case is formed by a combination of a RF repeater and optical

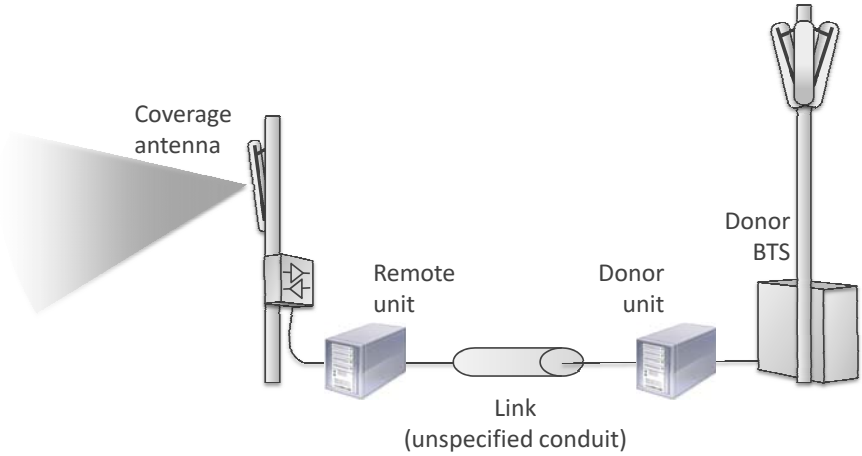

Figure 5.3: Deployment of remote sectors.

transceivers (laser diodes and photodiodes) that enable signal transmission through optical fibers. This type of repeaters is very appropriate for areas where the geography does not allow having Line of Sight (LOS) between the donor and remote units, they are also suitable if the intended coverage area is far from the donor BS and for RF distribution in buildings. Indeed they make possible covering distances several km away from the donor BS (Figure 5.4). The main RoF architectures are:

i. Direct modulation of the laser diode with the RF signal.
ii. Idem, but with previous downconversion of the radio signal to Intermediate Frequency (IF).
iii. Downconversion plus digitalization for digital transmission through the fiber.

The first approach is the simplest one but requires monomode fiber cables. On the other hand, in many indoor environments it exists multimode fiber for the connection of floor distributors with campus (or building) distributors and so the second approach would be more suitable, at the expend of an extra complexity. Finally, the third architecture can work well over both types of fibers and it has all the advantages of digital transmission, nevertheless it is the most complex and expensive [WWW+04].

The same authors in [WWW+04] propose an optical switching architecture to dynamically activate and deactivate remote sectors, thus achieving a dynamic cell shape. B. Lanoo et al. go one step further and develop this idea in several papers (being perhaps [LCPD07] and [LCPD06] the most representative) to design a novel RoF based architecture in which moving cells supply high transmission rates to users inside trains. Instead of the train moving along a fixed repeater cell pattern, the authors consider a cell pattern that moves together with the train, so that handovers

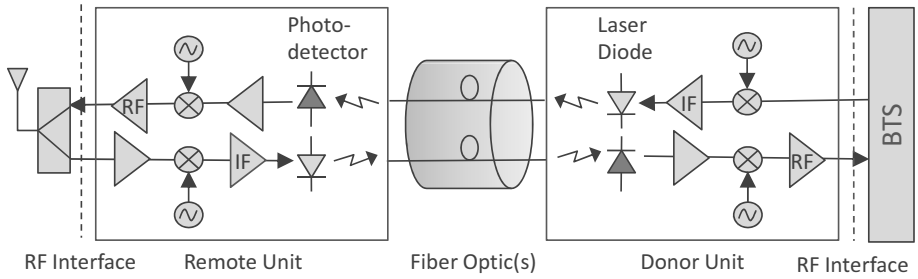

Figure 5.4: Basic structure of fiber optic repeaters.

are minimized. Preliminary simulations demonstrate the feasibility of this concept. The idea of (de)activating remote sectors was also proposed in [CCB01] but in a RF repeaters environment. However, in this case the reason was the reduction of noise at the BS receiver.

In case it is desired to transmit more than one subcarrier, a multiplexing mechanism is mandatory. Subcarrier Multiplexing (SCM) is a viable method in the DL. However, since several frequency conversions must be done, phase noise on oscillators must be carefully considered so that the final phase error in the UMTS signal is not excessive. Although more expensive than SCM, Wavelength Division Multiplexing is also a feasible option, particularly for the UL, since SCM shows several problems in that direction [DU92].

(c) Other alternatives as for example repeaters over coaxial cable or copper twisted pairs are also viable but allow shorter link distances, up to 300 m in the first case and 100 m in the second one. That is why repeaters with this type of backhauls are mainly used indoors. The process of transmission is similar in both cases: firstly the WCDMA signal is shifted to IF, next, it is digitalized and finally it is transmitted through the cable. Echo cancelers are used in twister pairs to differentiate transmission paths. In the coaxial case, UL and DL are separated through the use of different IFs. Phase equalizers are not rare because of the phase distortion caused by coaxial cable.

Finally, optical wireless based repeaters are also gaining focus lately. This technique has matured in the last years and permits establishing links through laser transmission in free space between the donor and remote units [WB01]. Since clear LOS is required, its usability is restricted to limited distances and acceptable weather conditions (particularly non-foggy regions). Its main niche market is dense urban environments. Since a conduit is not needed and the transmission band does not require a license. Thus, fast deployment and cost are its advantages along with wide bandwidth, interference immunity and security.

From the previous paragraphs it can be seen that repeaters can be categorized as well in devices for indoor or outdoor purposes. The main difference between them

is the transmission power, until 20 dBm approximately in the first case, and up to 43 dBm in the second one. The cabinet and complexity of installation is also an obvious difference between them.

5.3 Repeaters in WCDMA Mobile Networks

At this point, it is already possible to comment why repeaters are expected to play a major role in mature WCDMA systems than in 2G systems. The section covers the most important reasons.

- Installation of coverage extension repeaters in 2G FDMA systems requires a review of the frequency plan of the network. Incorporation of repeaters in WCDMA networks does not require large scale replanning, but just local parameter retuning. The WCDMA repeater serves users with the same pilot channel as its donor BS. The UEs served in this area interact with the donor BS in the same way as those connected directly. They receive and respond to the same AC, power control, handover and other RRM algorithms.

- Since adjacent cells share the same frequency, repeaters are a cost-effective option to reduce inter-cell interference, particularly in environments with hotspots. If properly adjusted, they can reduce the coupling loss between the BS and UEs that are close to the repeater, [RE04].

- It has become increasingly more difficult for wireless operators to find locations for radio equipment. This is a particular problem in urban areas and remote sectors can become a solution for these cases. RoF and optical wireless are mature enough technologies to allow a dense deployment in these environments. Paper [GC04] describes two radio over fibre systems, for GSM and UMTS networks as well as results from field-tests aiming at indoors coverage improvement.

- The use of higher frequencies in WCDMA systems imply less favorable link-budgets in comparison with 2G and especially for high-bit-rate services. Repeaters can be key devices to guarantee these services indoors at a low cost. [BNL05; BNI+06] investigate DL gains in indoor hotspots by means of field tests. Conducted measurement campaigns reveal DL capacity improvements around 35%.

- Narrowband CDMA systems such as CDMAOne (IS-95) or CDMA2000 1xRTT (IS-2000) can reserve some channels for indoor coverage and thereby reduce the load of outdoor channels. This policy is impractical in most WCDMA cases, since operators have only a few WCDMA channels. These reinforces the suitability of repeaters in indoor environments.

- Finally, one issue with early repeaters was a lack of remote monitoring capabilities. During the last years, repeaters have improved in terms of O&M

capacities. Operators are now able to monitor the performance of these equipment, making them more appealing.

Unfortunately, since repeaters are not noiseless devices, their deployment has an impact on both the capacity and coverage of the donor BS. These effects were already posed in the introduction and are investigated in the rest of the chapter.

5.4 Feasibility Condition for the UL in a Multiservice Generic System with AC

5.4.1 Access Network without Repeaters Deployment

AC is a key RRM strategy in WCDMA systems. Since coverage and capacity are tightly coupled, a method that handles all new incoming traffic is mandatory. AC strategies decide whether a new RAB can be admitted or not according to a certain estimation of the current load. If the load stays below a certain threshold the new RAB will be allowed.

The load in a certain cell can be found by computing the load factor η. Details on this parameter and its relationship with planning parameters can be found in the two previous chapters. Equation (5.1) recalls one of the possible expressions to determine the value of the load factor for a given BS j.

$$\eta(j) = \frac{\sum_{k=1}^{N_{UE}} P_{RX}^{UL}(j,k)}{\sum_{k=1}^{N_{UE}} P_{RX}^{UL}(j,k) + n_{BS}(j)} \tag{5.1}$$

Where:

- N_{UE}: Number of UE in the system.
- $P_{RX}^{UL}(j,k)$: Power received at BS j from UE k.
- $n_{BS}(j)$: Thermal noise power at BS j.

Or equivalently:

$$\eta(j) = \frac{[1+f(j)] \sum_{\substack{k \in j \\ k=1}}^{N_{UE}} P_{RX}^{UL}(j,k)}{[1+f(j)] \sum_{\substack{k \in j \\ k=1}}^{N_{UE}} P_{RX}^{UL}(j,k) + n_{BS}(j)} \tag{5.2}$$

Where:

- The summations are calculated over the UEs connected to BS j, this is indicated by $k \in j$¸ being k the summation index.

- $f(j)$: Quotient between intercell and intracell power, measured at BS j.

On the other hand, in WCDMA systems a power control algorithm is present being composed of the so-called inner and outer loops. The former aims at adjusting the transmitted powers, so that a certain Signal-to-Interference-plus-Noise-Ratio (SINR) target before de-spreading for a user k is reached; this ratio is denoted as $\gamma^{UL,DL}(s_k, k)$, s_k being the BS that serves k. The latter intends to keep the quality of communications at a desired level in terms of BLER depending on higher layer requirements. The expression for $\gamma^{UL}(s_k, k)$ is straightforward in the case of a generic WCDMA system without repeaters deployment:

$$\gamma^{UL}(s_k, k) = \frac{P_{RX}^{UL}(s_k, k)}{[1 + f(s_k)] \sum\limits_{\substack{i=1 \\ i \in s_k}}^{N_{UE}} P_{RX}^{UL}(s_k, i) - P_{RX}^{UL}(s_k, k) + n_{BS}(s_k)} \tag{5.3}$$

In order to simplify subsequent expressions, let define the parameter ϕ^{UL} as the Signal-to-Signal-plus-Interference-plus-Noise-Ratio (SSINR) measured in the UL:

$$\phi^{UL}(s_k, k) \equiv \frac{\gamma^{UL}(s_k, k)}{1 + \gamma^{UL}(s_k, k)} = \frac{P_{RX}^{UL}(s_k, k)}{[1 + f(s_k)] \sum\limits_{\substack{i=1 \\ i \in s_k}}^{N_{UE}} P_{RX}^{UL}(s_k, i) + n_{BS}(s_k)} \tag{5.4}$$

Then, after combining Equations (5.2) and (5.4), a new expression is obtained, which establishes a relationship between $\eta(j)$ and the summation of all the ϕ targets of those users connected with BS j. This second term is the Aggregated Signal-to-Signal-plus-Interference-plus-Noise ratio or $\Lambda(j)$:

$$\eta(j) = [1 + f(j)] \sum_{\substack{i=1 \\ i \in j}}^{N_{UE}} \phi(i) = [1 + f(j)] \Lambda(j) \tag{5.5}$$

This value has to be always lower than the maximum load factor η_{max} allowed by the AC, so that interference levels are kept sufficiently low and connections are not degraded. That means the next condition has to be accomplished by all the cells in the system:

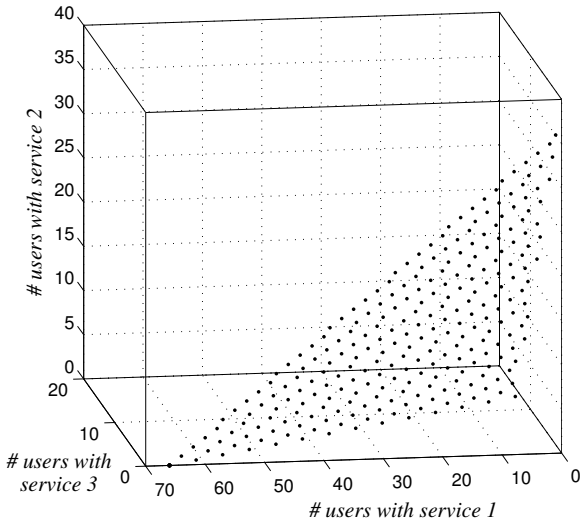

Figure 5.5: Discrete representation of admission regions.

$$\Lambda(j) \leq \frac{\eta_{max}}{1 + f(j)} \tag{5.6}$$

This condition states how many users of each type can be admitted without exceeding the maximum allowed load in the cell, or rather it defines an admission region. Note that the expression is general and independent on the type of service the users are using. The inequality defines a S-dimensional region, being S the number of services in the system (or more generically the number of types of users with different E_b/N_0 requirements). Geometrically speaking, the admission region defines a straight line for $S = 2$, a plane in a 3-dimensional space is defined for $S = 3$ and, in general, it defines an M-dimensional hyper plane. Nevertheless, the number of users is obviously an integer value, consequently admission regions are actually discrete. Figure 5.5 shows an example in which the maximum load factor η_{max} has been fixed to 0.8. Three services are considered and each axis corresponds to one of them. Services features can be consulted in Appendix B, Section B.3, in particular in the first three rows of Table B.2.

5.4.2 Access Network with Repeaters Deployment

Subsequently, a general deployment with the presence of repeaters in a multiservice scenario is considered. An analytical solution of the feasibility condition for the UL of a CDMA system is derived and compared with that in Subsection 5.4.1.

As it was previously pointed, repeaters are not noiseless devices, a certain noise rise appears at the BS whenever new equipment is installed. Consequently, some changes must be introduced in the previous expressions. Particularly, $\phi(k)$ becomes:

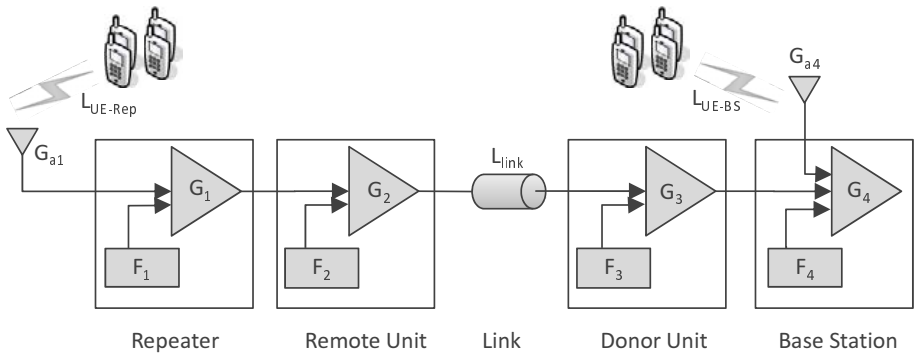

Figure 5.6: Example of cascaded stages, each one with its own noise figure and gain.

$$\phi(k) = \frac{P_{RX}^{UL}(s_k, k)}{[1 + f(s_k)] \sum_{\substack{i=1 \\ i \in s_k}}^{N_{UE}} P_{RX}^{UL}(s_k, i) + n_{BS}(s_k) + \sum_{r=1}^{N_{Rep}(s_k)} W(KT_0) F_g(r, s_k) G_g(r, s_k)} \tag{5.7}$$

Where:

- $N_{Rep}(s_k)$: Number of repeaters connected to BS s_k
- W: Channel bandwidth
- (KT_0): Reference thermal noise density (-174 dBm/Hz).
- $F_g(r, s_k)$: Global noise figure at the end of the transmission chain between repeater r and its donor BS, s_k in this case. Its calculus is straightforward by applying the Friis formula to compute the noise figure of a receiver composed of n cascaded stages, each one with its own noise figure F_x and gain G_x or losses L_x (Figure 5.6):

$$F_{receiver} = F_1 + \frac{F_2 - 1}{G_1/L_1} + \frac{F_3 - 1}{(G_1 G_2)/(L_1 L_2)} + \cdots + \frac{F_n - 1}{\prod_{x=1}^{n-1} G_x/L_x} \tag{5.8}$$

- $G_g(r, s_k)$: This parameter represents the global gain between the repeater and its donor BS, s_k in this case. It then considers the internal gain of the repeater itself, the gain of the transmitter in the link with the BS, the absolute loss in the link between the BS and the repeater, etc. In short, all the gains and losses of each one of the cascaded stages in the transmission chain:

$$G_g = \prod_{x=1}^{n} \frac{G_x}{L_x} \tag{5.9}$$

Before continuing with the mathematical development, some considerations on the adjustment of G_g must be pointed out.

Considerations on Repeaters and Backhaul Gains Adjustment

As seen, the value of G_g is a design parameter that allows controlling the noise level in the BS. Particularly, modifying internal repeaters gain, the transmitted noise can be limited. However, repeaters gain can only be adjusted in a particular range of values to bear in mind. Moreover, the impact on the coverage is another issue to consider.

Repeater UL and DL gains should be adjusted taking into account the particular net gain in backhaul transmission. In some cases, it is likely that backhaul conditions change over time and so the perceived gain between the repeater and the BS. So an AGC is mandatory to maintain a certain global gain value. Furthermore, there are cases in which UL and DL backhaul gains are difficult to keep equal (this is particularly true in fiber repeaters). Thus, repeater UL and DL gains, G_{Rep}^{DL} and G_{Rep}^{UL} do not necessarily have to be set equally since the objective is to ensure the same perceived global value in both links. If this is not possible and no actions are taken, there might be important inaccuracies in open loop type power control. As a consequence, some system processes would not work properly, e.g. UL Random Access Channel (RACH) transmissions in UMTS [3GPj]: Before any RACH access, the UE transmits a set of short preambles. This is done continuously until it receives and *Acquisition Indicator* from the Node-B, which signifies that the network has correctly detected one of them. In this process, the power of the first preamble is computed from the DL measurement and after each attempt, the UE updates its transmission power increasing the value in a power step $P_{i+1} = P_i + \Delta P$. Unbalanced UL and DL can cause starting with a very low power preamble and thus introducing a delay in the access of all UEs accessing the network from the repeaters coverage area. Moreover, after several preamble attempts the procedure is considered to have failed and it is not restarted after a certain *backoff time*. On the other hand, too high power levels in the preamble imply that UEs generate unnecessary interference levels which can extend over the time if the UE receive a NACK because of cell congestion or if there are collisions in the access. If it is not possible to balance both links, one solution is that the Node-B (or more generically the BS) broadcasts a different level of power so that the unbalance is compensated. However, this option would only be applicable if the BS just transmits through one remote sector, since G_g is not likely to coincide between different repeaters.

But AGC is not only a mechanism to compensate for unpredicted backhaul variations, it is also a fall-back mechanism to avoid self-oscillations in on-frequency repeaters 5.7. If the mechanisms devoted to increase coupling losses between the coverage and the donor antennas, $CL_{coverage \rightarrow donor}$ and $CL_{donor \rightarrow coverage}$, fail for some reason, AGC comes into play. As a consequence, and bearing in mind that isolation $\jmath$ between both ports must be at least 15 dB [3GPd], a limit must be set on the amplifier gain:

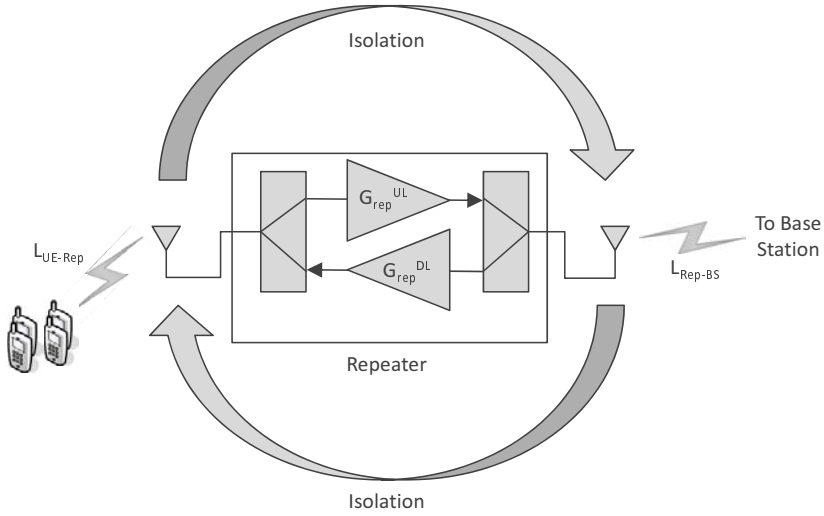

Figure 5.7: Self-oscillations in on-frequency repeaters.

$$\begin{aligned} G_{Rep}^{DL} \cdot CL_{coverage \rightarrow donor} &\leq \jmath \leq -15 \text{ dB} \\ G_{Rep}^{UL} \cdot CL_{donor \rightarrow coverage} &\leq \jmath \leq -15 \text{ dB} \end{aligned} \tag{5.10}$$

Note that coupling losses account for all the gains and losses between the amplifiers, they consider cable and connector losses, antenna gains and path losses between antennas.

In order to avoid amplifiers saturation, Equation (5.10) is subjected to a second condition. Indeed the maximum possible value for G_g is the quotient between the maximum transmission power of the repeater, $P_{Rep,max}$, and the BS, $P_{BS,max}$ (Equation (5.11)). Thus, once G_g is adjusted, the internal gain of the repeater, and so, its maximum transmission power are also fixed. These conditions are taken into account along the rest of the chapter.

$$G_g \leq \frac{P_{Rep,max}}{P_{BS,max}} \tag{5.11}$$

AGC is also necessary to avoid amplifiers saturation in front of unexpected high level powers, e.g. in the presence of high adjacent channel interference. Under these circumstances, there would be a reduction in the amplifiers gain, but consequently this would cause a loss of sensitivity and a coverage reduction.

Going back to Equation (5.7), because of the introduction of an extra noise power, the load factor must be also redefined as Equation (5.12) indicates. In addition, in order to compare with environments without repeaters, the number of

users has been maintained to N_{UE}. It is irrelevant if they have established their connection through the donor BS or one of its repeaters, the appropriate value of $P_{RX}^{UL}(j,k)$ would be equally adjusted by the power control, but just considering a different effective link loss. It is noticeable, that if repeaters are deployed, in the case of no UEs in the system, the load factor would not be zero because of the noise rise induced by the own noise of repeaters.

$$\eta(j) = \frac{[1+f(j)] \sum\limits_{\substack{k \in j \\ k=1}}^{N_{UE}} P_{RX}^{UL}(j,k) + \sum\limits_{r=1}^{N_{Rep}(j)} W(KT_0) F_g(r,j) G_g(r,j)}{[1+f(j)] \sum\limits_{\substack{k \in j \\ k=1}}^{N_{UE}} P_{RX}^{UL}(j,k) + n_{BS}(j) + \sum\limits_{r=1}^{N_{Rep}(j)} W(KT_0) F_g(r,j) G_g(r,j)} \tag{5.12}$$

In order to allow an easy comparison with Equation (5.6), an intermediate variable $\beta(j)$ is defined:

$$\beta(j) \equiv \frac{1 + \sum\limits_{r=1}^{N_{Rep}(j)} \delta F(r,j) G_g(r,j)}{\sum\limits_{r=1}^{N_{Rep}(j)} \delta F(r,j) G_g(r,j)} \tag{5.13}$$

Being $\delta F(r,j)$ the relationship between the global noise figure due to repeater r and that of its donor BS, $\delta F(r,j) \equiv \frac{F_g(r,j)}{F_{BS}(j)}$.

As a consequence, the next expression is obtained:

$$\beta(j)\,\eta(j) - 1 = \tag{5.14}$$
$$= \frac{[\beta(j)-1][1+f(j)] \sum\limits_{\substack{i=1 \\ i \in j}}^{N_{UE}} P_{RX}^{UL}(j,i)}{[1+f(j)] \sum\limits_{\substack{i=1 \\ i \in j}}^{N_{UE}} P_{RX}^{UL}(j,i) + n_{BS}(j) \left[1 + \sum\limits_{r=1}^{N_{Rep}(j)} \delta F(r,j) G_g(r,j)\right]}$$

Or equivalently:

$$\beta(j)\,\eta(j) - 1 = [\beta(j)-1][1+f(j)]\,\Lambda(j) \tag{5.15}$$

And thus, a new admission region is found and defined by:

$$\Lambda(j) \leq \frac{\beta(j)\,\eta_{max} - 1}{[\beta(j) - 1]\,[1 + f(j)]} = \tag{5.16}$$
$$= \frac{\eta_{max} - (1 - \eta_{max}) \sum_{r=1}^{N_{Rep}(j)} \delta F(r,j)\, G_g(r,j)}{1 + f(j)}$$

If this expression is compared with that in the case without repeaters, Equation (5.6), it can be observed that the new admission region is smaller, therefore the system capacity in terms of number of active users is reduced. The new capacity is the one that would be obtained in a network without repeaters but imposing a lower η_{max}. This effect is extended and analyzed by means of theoretical figures and simulations later on but it is clear that planning a WCDMA network with repeaters will not be such straightforward as in FDMA based 2G networks.

Thus, when considering the presence of repeaters, a new parameter $\xi(j)$, depending on the AC threshold η_{max}, can be defined:

$$\xi(j) \equiv \eta_{max} - (1 - \eta_{max}) \sum_{r=1}^{N_{Rep}(j)} \delta F(r,j)\, G_g(r,j) \tag{5.17}$$

And therefore the definition of the admission region can be re-written as follows:

$$\Lambda(j) \leq \frac{\xi(j)}{1 + f(j)} \tag{5.18}$$

Where $\xi(j)$ represents the equivalent η_{max} that should be imposed at BS j in an environment without repeaters to obtain the same new admission region.

The capacity reduction depends on the extra level of noise that is measured at the donor. The higher the number of installed repeaters, their noise figure or the global gain term, the smaller the admission region. This degradation also depends on the maximum allowable load factor: for higher thresholds, the reduction is smaller, unfortunately this is a rather fixed design parameter.

Conclusions in the previous paragraph are immediate as long as the relationship between the intra and the intercell power $f(j)$ is maintained after installing repeaters. This is accomplished, for example, by those situations in which repeaters are 'isolated' from the rest of the system, for instance when covering a tunnel or inside a building with high propagation losses. On the other hand, there are other situations in which the installation of these devices modifies $f(j)$. In these cases, the analytical expression of the admission region is identical but substituting $f(j)$ by the new value, $f'(j)$. The impact of $f'(j)$ on the new admission region should be evaluated for each particular scenario. For example, repeaters could transmit more intercell power to the donor BS and decrease even more the admission region.

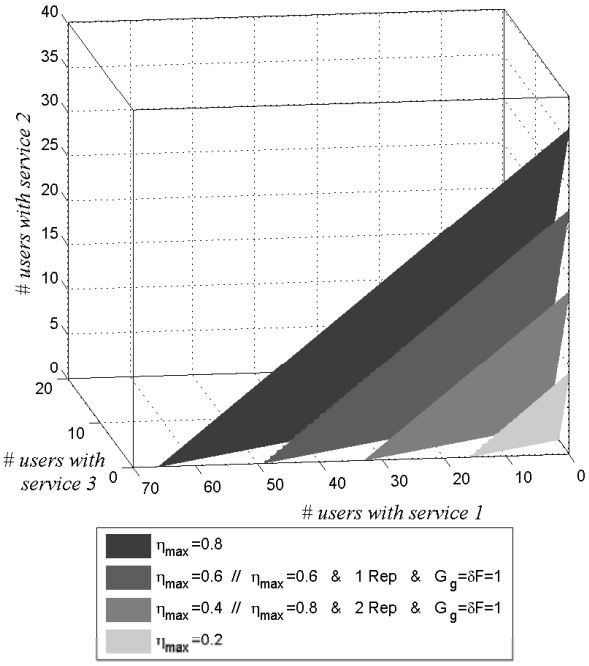

Figure 5.8: Correspondence of admission regions with and without repeaters.

Figure 5.8 shows some different examples of the facts that have been discussed. In this case, admission regions are represented as continuous planes (not discrete, as they actually are) to improve observation and analysis. Admission regions are plotted in a particular scenario with 3 different types of services (the same as in Figure 5.5) and values of η_{max}, although, as it was stated, the analysis is general and fully extensible to other cases. The darker graph represents those possible combinations of user types that would not exceed a load threshold of 0.8 when no repeaters are connected to the serving BS. The lighter the plane, the higher the number of repeaters. In those cases, gains in the transmission chain between repeaters and donor are set so that G_g is equal to 0 dB and repeaters noise factor is considered to be the same as in the donor BS. The reduction in the number of admissible UEs with the number of connected repeaters is clear.

If one repeater is installed, the admission region is equal to that in a situation without repeaters in which the maximum allowable load ξ is 0.6. If a second repeater is introduced, the equivalent maximum load ξ would be 0.4. Finally, the installation of four repeaters would imply such a noise rise in the donor BS that no users could be admitted in the cell. It is interesting to observe that thanks to the definition of the new parameter ξ, there is an easy manner to quantify the reduction and compare the network capacity before and after installing repeaters.

Figure 5.9 also helps to the analysis of the plotted admission regions since it

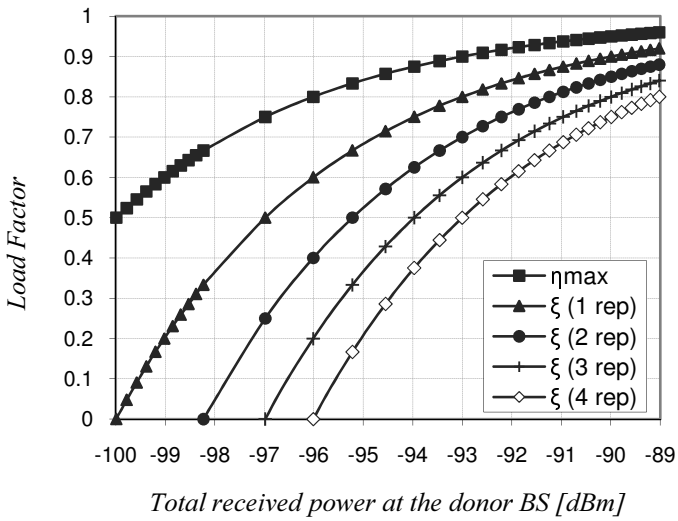

Figure 5.9: η_{max} and equivalent loads ξ as a function of the total received power at the donor BS.

shows the maximum allowed load factor η_{max} and the different equivalent loads ξ that would be obtained for different total received power at the BS. These curves permit an easy comparison of four situations, ranging from 1 to 4 repeaters, all of them with adjusted internal gains so that G_g is 0 dB. It can be seen that the higher the maximum allowed power at the receiver, the smaller the differences between η_{max} and the equivalent loads. Also, it can be seen those combinations of η_{max} and number of repeaters which would imply that no users can access the cell, for example, when 3 repeaters are installed and η_{max} must be below 0.75, or when installing 4 repeaters and imposing $\eta_{max} \leq 0.8$. Finally, these curves would be scaled by the term $(1+f)/(1+f')$ if the f factor was modified after installing the repeater, as indicated by Equation (5.18).

5.5 Capacity and Coverage Trade-off

From the previous expressions and paragraphs, it can be stated that:

$$\begin{aligned} \lim_{G_g \to 0} \xi(j) &= \eta_{max} \\ \lim_{N_{Rep}(j) \to 0} \xi(j) &= \eta_{max} \\ \lim_{\delta F \to 0} \xi(j) &= \eta_{max} \end{aligned} \tag{5.19}$$

This is logical, since all three situations tend to eliminate repeaters noise. However, whereas the third one is imposed by the equipment itself, the first and the second one can be decided during the planning process. Unfortunately, both imply a

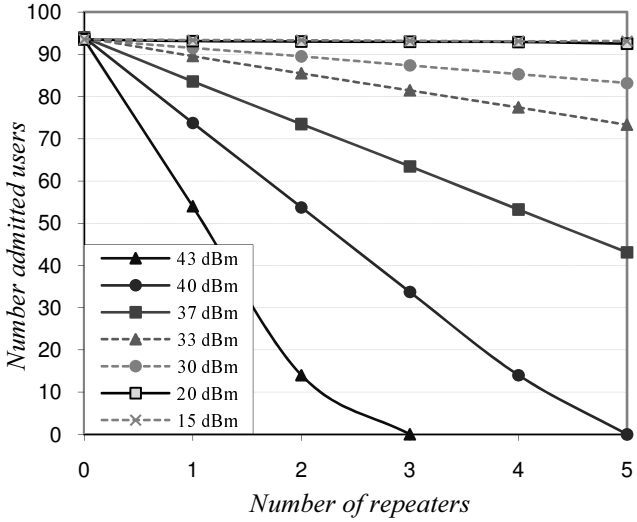

Figure 5.10: Number of admitted users for different number and types of repeaters.

decrease in the global coverage so a trade-off between coverage and capacity arises.

In order to analyze the impact of these parameters on the system performance, static system level simulations have been executed. That is to say, a significant amount of uncorrelated snapshots have been run to obtain statistics. The scenario is a modified version of the synthetic one in Appendix B. In particular, it is a road-like or railway one in which different numbers of repeaters are added to one BS to cover a certain target area. For radio propagation evaluation, the assumptions are the same as for the synthetic case. Regarding UEs services, the simulations consider the 5 possible types also described in the same Appendix. Finally, different realistic types of repeaters have been contemplated, with different maximum transmission powers $P_{R,max}$. In all cases their internal gain has been adjusted to the maximum value that guarantees no amplifiers saturation.

Figure 5.10 shows the number of admitted users by the BS as a function of the number of connected repeaters. It can be seen that the reduction in capacity is directly proportional to $P_{R,max}$ and the number of repeaters. For example, if repeaters transmit with the same maximum power as the BS (43 dBm) the global gain between the repeater and its donor is equal to 0 dB and therefore repeaters noise is not attenuated at all. This implies a high noise rise at the BS and consequently the admission region shrinks. In fact, it can be seen that, for certain configurations and number of repeaters, no users could access the system. On the other hand, very low power repeaters do not degrade capacity as long as their number is not over 5. In this sense, the impact of the global gain appears to be more important than the number of installed repeaters. This fact will be analyzed again later.

Regarding coverage, initially it has been evaluated in terms of E_c/I_0, measured on the pilot channel, which in the current simulations is realistically introduced

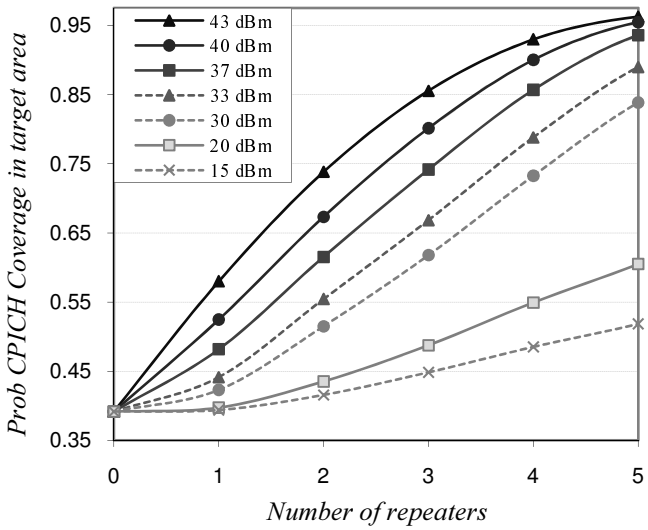

Figure 5.11: Probability of CPICH coverage in target area.

according to the UMTS standards. Thus, if the CPICH E_c/I_0 measured at one pixel is equal or higher than -12 dB with a probability higher than 95%, then that position is considered to be correctly covered by the signal.

Figure 5.11 shows the probability of CPICH coverage in the simulated target area. Curves reveal the expected trade-off and allow quantifying it. Those situations with higher capacity degradation are the ones with better pilot reception. Nevertheless, low power repeaters permit significant increases of with a minimum loss in capacity. This way, the trade-off can be mitigated by means of many low power repeaters. However, this fact might obviously jeopardize a third parameter to optimize: the network cost.

As explained in Section 2.2.1, UL and DL coverage must also be evaluated to guarantee service availability. In this sense, Figure 5.12 shows the average transmission power that a static voice user requires, an this is represented as a function of its distance to the BS. The black horizontal line shows the maximum available UL transmission power (21 dBm). However, the *test user*, evaluates the power even though when it is higher than the maximum in order to observe the difference. It can be seen that users would have to commute to a degraded mode from around 3500 m if no repeaters are installed in the scenario. In addition, 3 situations with 4 repeaters are shown and it can be observed that users have enough power until around 11 km with 43 dBm repeaters. With 30 dBm repeaters, some deadspots arise in the line between the donor and the last repeater and so repeaters should be placed closer. Finally, with 15 dBm repeaters, the extra coverage is very low.

Keeping these facts in mind, Figure 5.13 shows the probability that a service is available (that is, CPICH coverage is satisfactory and the power control does not require more than the maximum power in UL and DL). The figure represents the

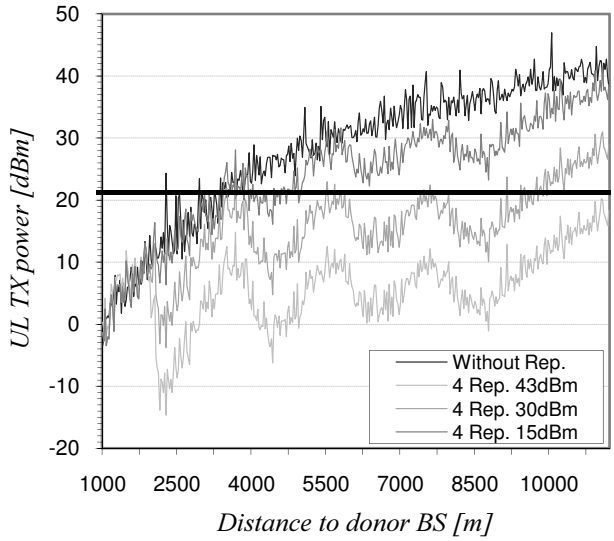

Figure 5.12: Average UL transmission power as a function of the distance to the donor BS.

values for repeaters with $P_{R,max}$ of 37 and 15 dBm. The notation S_i stands for service i, indicating the ith service in Table B.2, in Appendix B. It can be seen that the probability increases monotically with $P_{R,max}$ and the number of repeaters. However, as expected, both the absolute values and the increases are quite lower in the 15 dBm case, which shows modest improvements in the services availability.

The advantage of using low power repeaters is obtained from Figure 5.14, which shows those configurations (number of repeaters and $P_{R,max}$) that succeed in covering a certain target area (65% of the scenario) along with the reduction that they imply in terms of capacity. For example, if a 10% capacity reduction is tolerated, 4 repeaters with $P_{R,max} = 30$ dBm could be planned. But if degradation is desired to be below 2.5%, 6 repeaters with $P_{R,max} = 20$ dBm would accomplish the requisite. Finally, 12 low power repeaters ($P_{R,max} = 15$ dBm) achieves both the target coverage and capacity, which is reduced in less than 1%. Thus, even though these two last situations can partially control the trade-off and guarantee coverage and capacity, the cost of the network might invalidate the solutions.

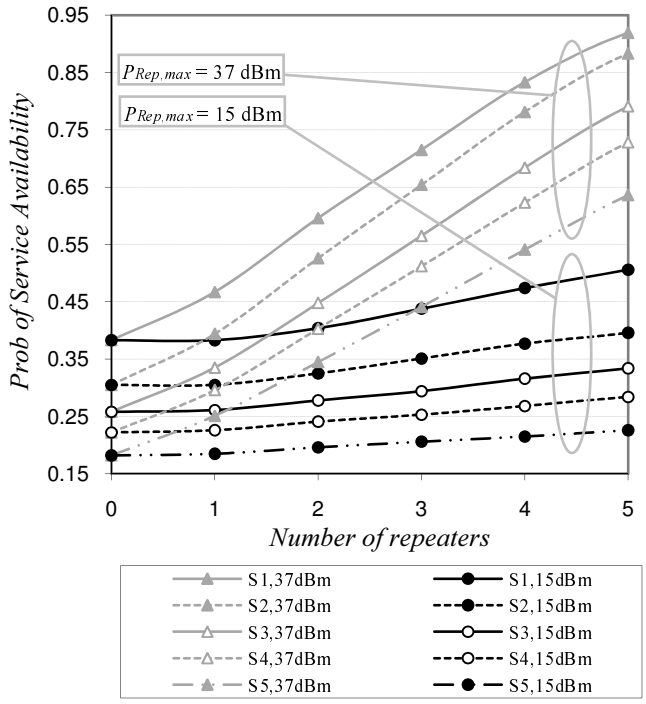

Figure 5.13: Probability of service availability.

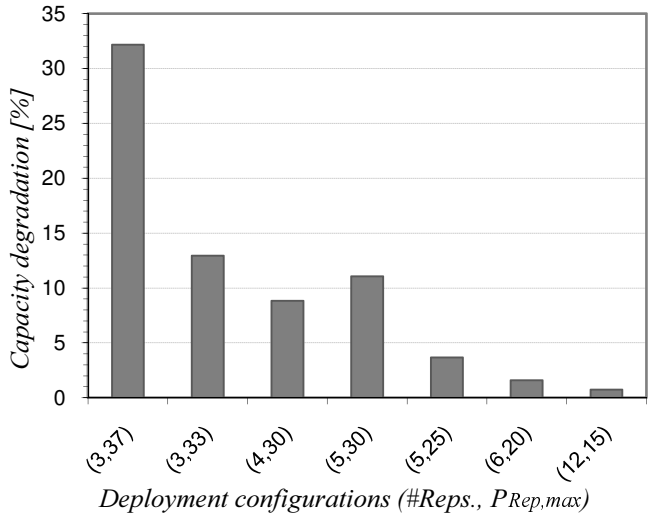

Figure 5.14: Capacity degradation when guaranteeing coverage at target area, for different number of repeaters and values of $P_{Rep,max}$.

5.6 Induced Cell Breathing in Donor Cells

When installing repeaters, operators must consider the global coverage, formed by the donor sector and the extra coverage from repeaters. This, of course, will be higher than the original one, indeed this is one of the reasons for installing repeaters and it was quantified in the previous section along with the trade-off with capacity. However, variations on the particular coverage of the donor BS must be considered as well.

This effect was already illustrated qualitatively by Figure 5.1, where a cell shrinkage is observed because of the new noise rise. In urban environments, this effect might not be problematic since the system is capacity limited and then UEs do not tend to reach their maximum power at the cell edge. Therefore an extra coverage margin is available and deadspots are not likely to appear in the donor cell. However, in suburban and rural environments, this effect can have an important impact, also indoor users in urban scenarios with high penetration losses.

Next paragraphs quantify and derive an analytic expression which relates the donor BS radius before and after connecting repeaters to it. In this case, the contribution is partial since this analysis follows the steps in [SM07] but generalizing it by considering a multiservice scenario and a heterogeneous distribution of users, with different users densities for each service. Therefore the particular coverage reduction can be predicted and repeaters deployment and their configuration can be done accordingly to avoid deadspots.

Combining Equations (5.1) and (5.4) it can be easily found the power required by the power control algorithm from user k as a function of the current load factor. For a cell without repeaters this is:

$$P_{RX}^{UL}(s_k,k) = \phi^{UL}(s_k,k)\, P_{RX,tot}^{UL}(s_k) = \phi^{UL}(s_k,k)\, n_{BS}(s_k)\, \frac{1}{1-\eta(s_k)} \tag{5.20}$$

If repeaters are installed, η is redefined as shown by Equation (5.12) and can be decomposed in two terms. The first one is the load from data traffic η_{traf} and the second one the extra load because of repeaters noise $\eta_{n,rep}$.

$$\begin{aligned}\eta(j) &= \frac{[1+f(j)]\sum_{\substack{k\in j\\ k=1}}^{N_{UE}} P_{RX}^{UL}(j,k)}{P_{RX,tot}(s_k)} + \frac{\sum_{i=1}^{N_{Rep}(j)} W(KT_0)\, F_g[r_i(j)]\, G_g[r_i(j),j]}{P_{RX,tot}(s_k)} = \\ &= \eta_{traf}(j) + \eta_{n,rep}(j)\end{aligned} \tag{5.21}$$

And the UL received power when repeaters are installed is given by:

$$P_{RX}^{UL}(s_k,k) = \tag{5.22}$$
$$= \phi^{UL}(s_k,k)\left(n_{BS}(s_k) + \sum_{r=1}^{N_{Rep}(j)} W(KT_0)\,F_g(r,s_k)\,G_g(r,s_k)\right)\frac{1}{1-\eta_{traf}(s_k)}$$

Since both situations are jointly considered in next expressions, notation x_0 will indicate the absence of repeaters. Besides, for the sake of simplicity the index s_k is omitted and presupposed.

Considering that the propagation loss exponent is α, a relationship between the radius of the donor coverage area before and after installing repeaters, R_0 and R respectively, can be established:

$$\frac{R}{R_0} = \left(\frac{P_{RX,0}^{UL}}{P_{RX}^{UL}}\right)^{\frac{1}{\alpha}} = \left[\left(\frac{1}{1+\sum_{r=1}^{N_{Rep}}\delta F(r)\,G_g(r)}\right)\cdot\left(\frac{1-\eta_{traf}}{1-\eta_0}\right)\right]^{\frac{1}{\alpha}} \tag{5.23}$$

On the other hand, if $\rho_s(r,\varphi)$ is a function that represents the particular density of UEs using service s in the surroundings of the donor BS, being r and φ the distance and azimuth angle with respect to the BS, then the load factor in the absence of repeaters η_0 can be calculated as follows:

$$\begin{aligned}\eta_0 &= \frac{P_{RX,tot}^{UL} - n_{BS}}{P_{RX,tot}^{UL}} = \frac{(1+f)\sum_{k=1}^{N_{UE}} P_{RX}^{UL}(k)}{P_{RX,tot}^{UL}} \\ &= (1+f)\sum_{s=1}^{S}\frac{1}{1+\frac{W}{\left(\frac{E_b}{N_0}\right)_s R_{b,s}\nu_s}}\iint_{A_{1,0}}\rho_s(r,\varphi)\,drd\varphi \\ &= (1+f)\sum_{s=1}^{S}\zeta_s\iint_{A_{1,0}}\rho_s(r,\varphi)\,drd\varphi\end{aligned} \tag{5.24}$$

Where:

- S: Number of services in the system.
- $R_{b,s}$: Service s transmission rate.
- ν_s: Activity factor of service s.
- $A_{1,0}$: Coverage area of the donor BS when it has no repeaters.
- ζ_s: Contribution to the load factor of a UE with service s.

Without loss of generalization and in order to further simplify the expressions, a uniform distribution of UEs with service s is considered in each particular area (donor BS, repeater 1, repeater 2, etc) that form the effective cell ρ_s:

$$\eta_0 = (1+f)\,\pi R_0^2 \sum_{s=1}^{S} \zeta_s \rho_s \tag{5.25}$$

And from here, the expression for η_{traf} is straightforward. Indeed it is just a generalization of the previous expression accumulating the users in the coverage area of the donor BS and its corresponding repeaters ($\pi R_r^2 \rho_{r,s}$, for $1 \leq r \leq N_{Rep}$ and $1 \leq s \leq S$):

$$\begin{aligned} \eta_{traf} &= \eta_{traf,donor} + \eta_{traf,rep} \\ &= (1+f)\left[\pi R^2 \sum_{s=1}^{S} \zeta_s \rho_s + \sum_{r=1}^{N_{Rep}} \left(\pi R_r^2 \sum_{s=1}^{S} \zeta_s \rho_{r,s}\right)\right] \end{aligned} \tag{5.26}$$

Because of the cell breathing effect, the number of users in the coverage area of the donor BS is not the same after installing repeaters. Indeed the relationship between the load factors caused by these specific users is:

$$\frac{\eta_{traf,donor}}{\eta_0} = \frac{(1+f)\,\pi R^2 \sum_{s=1}^{S} \zeta_s \rho_s}{(1+f)\,\pi R_0^2 \sum_{s=1}^{S} \zeta_s \rho_s} = \left(\frac{R}{R_0}\right)^2 \tag{5.27}$$

Consequently, Equation (5.26) can be re-written as a function of R_r/R:

$$\begin{aligned}
\eta_{traf} &= \left(\frac{R}{R_0}\right)^2 \eta_0 + \eta_{traf,rep} = \eta_0 \left[\left(\frac{R}{R_0}\right)^2 + \frac{\eta_{traf,rep}}{\eta_0}\right] = \\
&= \eta_0 \left[\left(\frac{R}{R_0}\right)^2 + \frac{\sum_{r=1}^{N_{Rep}} \left(\pi R_r^2 \sum_{s=1}^{S} \zeta_s \rho_{r,s}\right)}{\pi R_0^2 \sum_{s=1}^{S} \zeta_s \rho_s}\right] = \\
&= \eta_0 \left[\left(\frac{R}{R_0}\right)^2 + \sum_{r=1}^{N_{Rep}} \left(\frac{R_r}{R_0}\right)^2 \frac{\sum_{s=1}^{S} \zeta_s \rho_{r,s}}{\sum_{s=1}^{S} \zeta_s \rho_s}\right] = \\
&= \eta_0 \left(\frac{R}{R_0}\right)^2 \left[1 + \sum_{r=1}^{N_{Rep}} \left(\frac{R_r}{R}\right)^2 \frac{\sum_{s=1}^{S} \zeta_s \rho_{r,s}}{\sum_{s=1}^{S} \zeta_s \rho_s}\right]
\end{aligned} \tag{5.28}$$

Although there is no straight relationship between the radii of repeaters coverage and that of the donor BS before installing repeaters, there is an expression that relates the radii when in both cases repeaters are considered. Indeed, given a certain load condition, the power control algorithm will require the same received UL power to guarantee the E_b/N_0. It does not matter if the user transmits through one repeater or directly to the donor BS. Thus, in the limit of the coverage area, when UE transmits at its maximum power $P_{TX,max}^{UL}$:

$$P_{RX}(k) = \frac{P_{TX,max}^{UL}(k)\, G_g}{L_{max,UE-Rep,r}} = \frac{P_{TX,max}^{UL}(k)}{L_{max,UE-BS}} \tag{5.29}$$

Being $L_{max,UE-Rep,r}$ and $L_{max,UE-BS}$ the maximum loss (at the limit of the cell) between the UE and the repeater r and donor BS respectively.

This leads to the following radii relationship:

$$\frac{R_r}{R} = \left(\frac{G_{a,BS}}{G_{a,Rep,r}} G_g\right)^{\frac{1}{\alpha}} \tag{5.30}$$

Where $G_{a,Rep,r}$ and $G_{a,BS}$ are the antenna gain of rth repeater and donor BS respectively.

Combining this expression with Equation (5.28), η_{traf} becomes:

$$\eta_{traf} = \eta_0 \left(\frac{R}{R_0}\right)^2 \left[1 + \sum_{r=1}^{N_{Rep}} \left(\frac{G_{a,BS}}{G_{a,Rep,r}} G_g\right)^{\frac{2}{\alpha}} \left(\frac{\sum_{s=1}^{S} \zeta_s \rho_{r,s}}{\sum_{s=1}^{S} \zeta_s \rho_s}\right)\right] \tag{5.31}$$

And thus, by substituting this into Equation (5.23) an expression is found which allows relating the radius of the coverage area of the donor BS before and after installing repeaters:

$$\frac{R}{R_0} = \left\{ \frac{1}{1 + \sum_{r=1}^{N_{Rep}} \delta F(r_i) G_g(r_i)} \cdot \frac{1 - \eta_0 \left(\frac{R}{R_0}\right)^2 \left[1 + \sum_{r=1}^{N_{Rep}} \left(\frac{G_{a,BS}}{G_{a,Rep,r}} G_g\right)^{\frac{2}{\alpha}} \Delta_r\right]}{1 - \eta_0} \right\}^{\frac{1}{\alpha}} \tag{5.32}$$

It must be noted that the expression can only be solved recursively and that the next final variable change has been made:

$$\Delta_r = \frac{\sum_{s=1}^{S} \zeta_s \rho_{r,s}}{\sum_{s=1}^{S} \zeta_s \rho_s} \tag{5.33}$$

An example is given next for a particular case in which $\alpha = 2.5$, $\eta_0 = 0.75$. Besides, UEs are uniformly distributed in all the scenario (not only in the particular coverage areas) and user densities are the same for all services, which leads to $\Delta_r = 1$. The antenna gains in the repeater and the donor BS are considered to be the same and also noise factors are equal. Finally, different types of repeaters have been considered, with different maximum transmission powers $P_{Rep,max}$. In all cases their internal gain has been adjusted to the maximum value that guarantees no amplifiers saturation. Thus, for example if $P_{Rep,max}$ equals $P_{BS,max}$, which is 43 dBm, then the repeater gain will be such that the global net gain G_g is 0 dB. If $P_{Rep,max} = 33$ dBm then $G_g = -10$ dB and so on. Under these circumstances, the evolution of R/R_0 is calculated and plotted in Figure 5.15. Different curves represent the different types of repeaters.

Figure 5.15 shows that for those cases in which repeaters have similar transmission power as the BS, the cell breathing effect caused by the repeaters noise rise is rather important. It can be seen that the most unfavorable situation corresponds with the case where repeaters are transmitting the same power as the BS (43 dBm). In this situation and with 5 repeaters connected, the coverage reduction reaches a 43%. On the other hand, the impact of low power repeaters is almost null, although the new extra coverage that they provide is smaller as well.

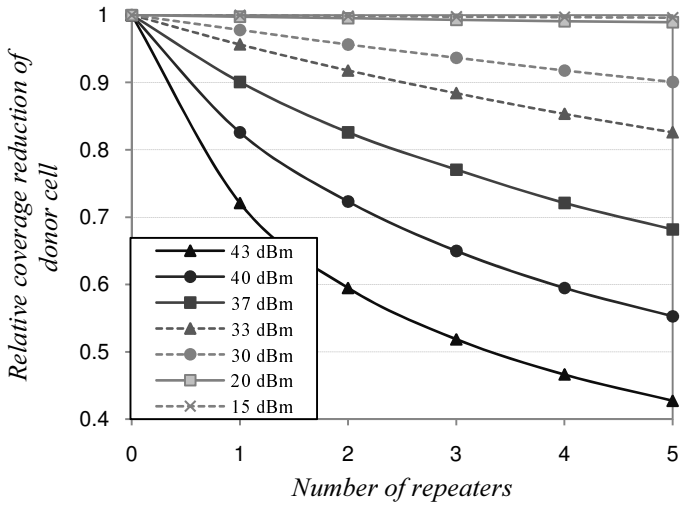

Figure 5.15: Coverage reduction of donor cell.

5.7 Concluding Remarks

Repeaters are a cost effective solution that permit extending the coverage and increasing capacity to some extent in cells with hotspots. Distributed Node-B configurations are also smart architectures that allow load balancing in highly heterogeneous scenarios, beating the optimization of BSs configurations. Several reasons make these devices particularly appealing to WCDMA based radio networks. On the other hand, new effects not present in FDMA based 2G systems imply that the radio planning process becomes more complex.

Most existent papers dealing with repeaters in WCDMA networks, ignore these effects or claim that their impact is not relevant. In this sense, the novelty of this chapter has been modeling them, quantifying their impact and deriving radio planning guidelines to enhance the final performance of the radio access network.

An analytic expression of the feasibility condition of a WCDMA mobile communications system with repeaters has been obtained. This has been done in a comparative manner with environments without repeaters deployment. The reduction in the admission region has been mathematically modeled and a compact, closed and generalist expression has been presented which allows easily obtaining the degradation in capacity that a given configuration of repeaters deployment would generate. This has been done through the definition of a new parameter representing the equivalent maximum load that should be considered in an environment without repeaters.

Planning WCDMA networks with repeaters implies a tradeoff between capacity and coverage, that is why introducing these devices will not be such straightforward as in FDMA based 2G systems. It has been found that the global gain (considering the internal repeater gain and all the backhaul gains and losses), the repeaters noise

figure and the number of repeaters itself are parameters with a high impact on this tradeoff. In addition, the higher the load threshold, the smaller the reduction. Finally, if the relationship between intra and intercell power is modified after installing repeaters admission regions are also modified, so particular attention should be paid to the placement of the repeaters antenna and its downtilt. If repeaters transmit more intercell power to the donor BS, admission regions are even further reduced. Additional conditions have to be taken into account if on-frequency repeaters are used to avoid self-oscillations.

Given this, the trade-off between capacity and the global coverage has been quantified by means of simulations and evaluating different types of repeaters. The global gain shows an important influence on capacity and service availability. With repeaters with a maximum power equal to the BS, a few units of these devices imply that no UEs can access the cell. On the other hand, by using a higher amount of low power repeaters it is possible to obtain relevant coverage increases but capacity problems are mitigated. This way, the trade-off is controlled but the main advantage of repeaters, cost, is jeopardized.

The last part of the chapter is devoted to the analysis of an effect also absent in most current literature: modifications on the donor cell coverage. Repeaters deployment in WCDMA system permit increasing the global coverage area but at the price of modifying the donor BS cell size. In dense urban environments, it is not expected an important impact because the network is capacity limited. But it is an important issue to consider in rural and suburban areas. Generalizing an existent previous work, an expression is given so that this particular coverage degradation can be predicted quantitatively in a heterogeneous scenario with an arbitrary number of available services. The final recursive equation is a useful tool which allows estimating the coverage reduction. Again, the higher the transmission power of the repeater, the worst the effects, and for example, if several repeaters are adjusted to have the same maximum transmission power as the BS, coverage reductions quickly get and surpass 50 %.

Chapter 6

Enhanced Analysis of WCDMA Networks with Repeaters Deployment

6.1 Introduction

In a mobile communications system with repeaters, signal contributions from the donor BS and from repeaters arrive through different paths, and those ones passing through a repeater are usually longer (both in spatial and time domains). This is because of the delay introduced by the link between the repeater and the donor BS, and the internal delay of the repeater itself. In fact, as explained in Section 5.2, the link can be established via various transmission media, such as fiber optic or copper, which show some advantages compared to radio, but also imply lower propagation velocities. On the other hand, the Rake receiver adapts to the channel delay profile [HT02] and just those components within a certain time window are constructively combined. Therefore, with the introduction of repeaters, when planning and designing WCDMA based access network the analysis must be revised. However, published studies always consider one of following assumptions:

1. Receivers get power just through the radio-link with the donor BS or through one of its repeaters. Other contributions are not considered in any way [CCB01; JCP+00; NLBL05].

2. All the contributions are always perfectly combined in the UE. Ideal maximum ratio combining (MRC) is applied [RE04; LL00].

The work in [PRO05] uses both assumptions but independently in different scenarios.

These assumptions are valid in the initial phases of the planning process. They allow obtaining theoretical and compact expressions and carrying out studies that provide preliminary values. However, the planning process of a network always reaches a point in which simulations over a digital terrain model is mandatory. It is at this point, when the above assumptions are not valid any more and it should be considered that, in comparison to traditional approaches, in real systems the Rake receiver has to measure a delay profile to designate the time offsets of the strongest signal components. Only those paths within a certain time window are constructively combined, the others not being considered and causing a certain level of *self-interference*. For example, BSs and UEs in UMTS can usually handle a 20 μs time delay between two paths [3GPd], and this value must be considered when repeaters are deployed, since UEs can incur into high levels of multi-path [LWN06].

Given this, one of the novelties of this thesis is a generic analysis, from a system level viewpoint, of a WCDMA system with repeaters. The objective is to derive compact expressions for the UL and DL so that transmission powers and other RRM parameters can be calculated without any of the previously mentioned simplifications. This permits an enhanced prediction of the network performance when studying and optimizing WCDMA networks with repeaters deployment. Moreover, a comparison with results obtained using existent approaches is also done. Different relevant parameters that characterize networks performance are evaluated and compared. The differences with respect to simplified analysis are remarkable, stressing the improvement provided by the proposed analysis.

Thus, whereas the previous chapter was devoted to a theoretical analysis of the impact of repeaters in WCDMA access networks and its optimization, this one investigates a new method to analyze a particular deployed network considering its specific and real path delays and the Rake receivers behavior.

The analysis is done along 5 sections. After this introduction, the model is explained, as well as the notation subsequently used. Next, along Sections 6.2 and 6.3 the mathematical approach is developed for UL and DL, some comments on final equations being also given. Numerical results and comparisons with existent approaches are analyzed in Section 6.4. Finally, concluding remarks close the chapter.

6.2 System Model

Let consider a mobile communications system consisting of any number N_{BS} of BSs, each one of them connected to any number of repeaters and being $N_{Rep}(j)$ the number of repeaters connected to BS j. The system layout can be completely generic, with no restriction on the spatial configuration and deployment of both the BS and the repeaters, and the links between BS and repeaters can also be of any nature. It is assumed that there are N_{UE} UEs in the network, spread all around the area under study without any restriction; there are no restrictions on the service the UEs can use, either. The expression to calculate the SINR $\gamma(s_k, k)$ is straightforward in the case of a generic WCDMA system without repeaters deployment (as indicated

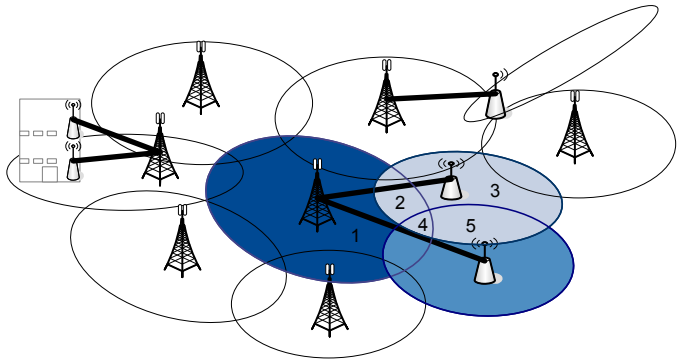

Figure 6.1: Different reception situations in an environment with repeaters.

by Equation (5.3) in the previous chapter), but, with the introduction of repeaters, the analysis has to be modified. All the different cases that should be considered to realistically plan the network are shown by means of an example in Figure 6.1. Indeed, based on the position of an UE with respect to the network layout, the signal could be received in different ways (numbered in the figure):

1. Directly from the donor BS.
2. Simultaneously from the donor BS and one repeater.
3. Just from one repeater.
4. From the donor BS and several repeaters.
5. From several repeaters.
6. All the previous ones in a SHO situation with other BSs or their repeaters.

For example, type 2 areas are defined as the zones in which the difference of propagation times of both received paths (in this case from one BS and one of its repeaters) is smaller than the Rake time window. Otherwise, one of the paths would generate a level of self-interference, which is nonexistent in a deployment without repeaters. In this sense, the position of the UE with respect to each BS or repeater, the internal delay introduced by the repeater, and the transmission media in the link between the donor and the repeater are of key importance.

Let define $\Gamma(j,k)$ as the set of mean link losses of the different paths between UE k and BS j:

$$\Gamma(j,k) \equiv \{L_1(j,k), L_2(j,k), \ldots\} \tag{6.1}$$

Where each element $L_i(j,k)$ of the set represents the absolute link loss of the i-th transmission path from UE k to BS j:

$$\Gamma(j,k) = \left\{ L_{UE-BS}(j,k), \frac{L_{UE-Rep}[k, r_1(j)]}{G_g[r_1(j), j]}, \cdots, \frac{L_{UE-Rep}\left[k, r_{N_{Rep}(j)}(j)\right]}{G_g\left[r_{N_{Rep}(j)}(j), j\right]} \right\} \tag{6.2}$$

Where:

- $L_{UE-BS}(j,k)$: Link loss between UE k and BS j.
- $L_{UE-Rep}(k,r)$: Idem but between UE k and a repeater r, $r_i(j)$ being the i-th repeater connected to BS j.
- $G_g(r,j)$: Global gain between repeater r and BS j.
- $N_{Rep}(j)$: Number of repeaters connected to BS j.

The subset $\Psi(j,k) \subset \Gamma(j,k)$ is defined as the one containing the paths that are constructively combined by the Rake receiver, that is, those within the Rake observing time window limits.

6.3 SINR Analysis

The objective of this subsection is to derive a generic expression so that transmission powers can be realistically found in order to achieve the system requirements. This is done for each link (UL and DL), valid for all types of system layouts, irrespectively of the position of the UEs with respect to the BS or the repeaters. The following points are devoted separately to each link.

6.3.1 Uplink

Taking the previous system model and definitions into account, the SINR for UE k in UL before de-spreading $\gamma^{UL}(s_k,k)$, can be written as:

$$\gamma^{UL}(s_k,k) \equiv \frac{\sum_{i \in \Psi(s_k,k)} P_{TX}^{UL}(k) / L_i(s_k,k)}{I^{UL}(s_k,k) + \tilde{P}_{RX}(s_k,k) + n_{BS}(s_k) + n_{RX,Rep}(s_k)} \tag{6.3}$$

Where:

- $P_{TX}^{UL}(k)$: Power transmitted by UE k.
- $I^{UL}(s_k,k)$: UL multi-user interference power received by the connection between k and s_k, for both inter- and intra-cells.

- $\tilde{P}_{RX}\left(s_k, k\right)$ Self-interference power of k at s_k, being generated by signal replicas from k that arrive with such a delay that fall out of the Rake window.

- $n_{BS}\left(j\right)$: Thermal noise power produced by the receiver at BS j.

- $n_{RX,Rep}\left(j\right)$: Received thermal noise power produced by all repeaters connected to BS j.

- These last two terms are constant and can be grouped in a single thermal noise term, denoted $n\left(s_k\right)$.

The numerator of Equation (6.3) is the constructive addition of the signal replicas that can be combined in the Rake receiver. On the other hand, the term $I^{UL}\left(s_k, k\right)$ takes into account all the possible paths of interfering signals for all users in the system. And finally, the self-interference level of k at s_k can be expressed as:

$$\tilde{P}_{RX}\left(s_k, k\right) \equiv \sum_{\substack{i \in \Gamma(s_k,k) \\ i \notin \Psi(s_k,k)}} P_{TX}^{UL}\left(k\right) / L_i\left(s_k, k\right) \tag{6.4}$$

Given this, Equation (6.3) can be rewritten as:

$$\gamma^{UL}\left(s_k, k\right) = \frac{\sum\limits_{i \in \Psi(s_k,k)} \frac{P_{TX}^{UL}(k)}{L_i(s_k,k)}}{\sum\limits_{\substack{m=1 \\ m \neq k}}^{N_{UE}} \sum\limits_{i \in \Gamma(s_k,k)} \frac{P_{TX}^{UL}(m)}{L_i(s_k,m)} + \sum\limits_{\substack{i \in \Gamma(s_k,k) \\ i \notin \Psi(s_k,k)}} \frac{P_{TX}^{UL}(k)}{L_i(s_k,k)} + n\left(s_k\right)} \tag{6.5}$$

Hence the useful received power at s_k from k (numerator) can be expressed as the product between the transmitted power and a certain term that only depends on propagation conditions. Then, it is possible to see the inverse of this factor as an 'effective' equivalent loss. Looking at the numerator, this term is calculated as the parallel (using an electrical equivalency) of the loss of the paths inside the time window of the Rake receiver. It can also be observed that this idea can be extrapolated to other terms of (6.5). Indeed, the self-interference can also be written as the transmitted power divided by another effective loss, which is evaluated as the parallel of those paths not being constructively combined at the Rake receiver. Finally, interference from any other UE m in the system is its transmitted power divided by the parallel of all paths between itself and the BS. Then, the following notation definitions are taken:

$$L_{ef\Gamma}\left(j, k\right) = \left(\sum_{i \in \Gamma(s_k,k)} \frac{1}{L_i\left(j, k\right)} \right)^{-1} \tag{6.6}$$

$$L_{ef\Psi}(j,k) = \left(\sum_{i \in \Psi(s_k,k)} \frac{1}{L_i(j,k)} \right)^{-1} \tag{6.7}$$

$$L_{ef\Gamma-\Psi}(j,k) = \left(\sum_{\substack{i \in \Gamma(s_k,k) \\ i \notin \Psi(s_k,k)}} \frac{1}{L_i(j,k)} \right)^{-1} \tag{6.8}$$

Which correspond, respectively, to the effective path loss of all possible propagation paths between k and j, the effective path loss of only the paths constructively combined within the Rake receiver, and the effective path loss considering the paths with such a delay that they appear outside the Rake time window. With this notation, some terms in Equation (6.5) can be simplified as:

$$P_{TX}^{UL}(k) \sum_{i \in \Psi(s_k,k)} \frac{1}{L_i(s_k,k)} = \frac{P_{TX}^{UL}(k)}{L_{ef\Psi}(s_k,k)} \tag{6.9}$$

$$\tilde{P}_{RX}(s_k,k) = P_{TX}^{UL}(k) \sum_{\substack{i \notin \Psi(s_k,k) \\ i \in \Gamma(s_k,k)}} \frac{1}{L_i(s_k,k)} = \frac{P_{TX}^{UL}(k)}{L_{ef\Gamma-\Psi}(s_k,k)} \tag{6.10}$$

$$P_{TX}^{UL}(m) \sum_{i \in \Gamma(s_k,k)} \frac{1}{L_i(s_k,m)} = \frac{P_{TX}^{UL}(m)}{L_{ef\Gamma}(s_k,m)}, \forall m | m \neq k \tag{6.11}$$

With these definitions, a more compact expression for $\gamma^{UL}(s_k,k)$ can be written:

$$\gamma^{UL}(s_k,k) = \frac{\frac{P_{TX}^{UL}(k)}{L_{ef\Psi}(s_k,k)}}{\sum_{i=1}^{N_{UE}} \frac{P_{TX}^{UL}(i)}{L_{ef\Gamma}(i,s_k)} - \frac{P_{TX}^{UL}(k)}{L_{ef\Psi}(s_k,k)} + n(s_k)} = \frac{\frac{P_{TX}^{UL}(k)}{L_{ef\Psi}(s_k,k)}}{P_{RX,tot}^{UL}(s_k) - \frac{P_{TX}^{UL}(k)}{L_{ef\Psi}(s_k,k)}} \tag{6.12}$$

Where $P_{RX,tot}^{UL}(j)$ is the total power received at j, including all the signal and thermal noise terms.

$$P_{RX,tot}^{UL}(j) = \sum_{i=1}^{N_{UE}} P_{TX}^{UL}(i)/L_{ef\Gamma}(j,i) + n(j) \tag{6.13}$$

Next, in order to further simplify (6.12), let define ϕ^{UL} as the UL SSINR:

$$\phi^{UL}(s_k,k) \equiv \frac{\gamma^{UL}(s_k,k)}{1+\gamma^{UL}(s_k,k)} = \frac{P_{TX}^{UL}(k)}{P_{RX,tot}^{UL}(s_k) \cdot L_{ef\Psi}(s_k,k)} \tag{6.14}$$

Thus, a compact and holistic expression that allows calculating the power that an UE must transmit to reach a certain SINR target is finally obtained:

$$P_{TX}^{UL}(k) = \phi^{UL}(s_k, k) \cdot P_{RX,tot}^{UL}(s_k) \cdot L_{ef\Psi}(s_k, k) \tag{6.15}$$

The required transmission power depends on the total amount of power received at the server BS, the effective path loss (parallel) of those paths within the Rake time window and the SINR target. It can be observed that the total effective loss, that is, considering all transmission paths, is also indirectly present through the total received power term.

It is obvious that the greater the number of repeaters, the higher the cardinality of Γ, but also, potentially, the cardinality of Ψ. This implies a decrease in $L_{ef\Gamma}(s_k, k)$ and consequently an interference increase; on the other hand, it could also imply a decrease in $L_{ef\Psi}(s_k, k)$ and therefore a reduction in the required power. Then, the global increase or reduction of $P_{TX}^{UL}(k)$ depends on the relative position of the BS and repeaters with respect to the users, not strictly only from a geographical viewpoint but also in the radiofrequency propagation domain.

From Equation (6.15), it is clear that the transmitted powers can be calculated by solving the N_{UE}th-order linear equations system formed by the application of this expression for each one of the UEs in the system. But, in general, N_{UE} is high, and so this type of *microscopic* approach requires a lot of computational power, especially if it has to be solved on a frame-by-frame basis. Nevertheless, a second relationship between $P_{RX,tot}^{UL}(j)$ and the individual UL transmitted powers was established in Equation (6.13), so that the complexity of the problem can be turned into a *macroscopic* approach, while clearly reducing the computational cost. Indeed, it can be written that:

$$P_{RX,tot}^{UL}(j) = \sum_{i=1}^{N_{UE}} \left[\frac{L_{ef\Psi}(s_i, i)}{L_{ef\Gamma}(j, i)} \cdot \phi^{UL}(s_i, i) \cdot P_{RX,tot}^{UL}(s_i) \right] + n(j) \tag{6.16}$$

Where Equation (6.15) has been used to substitute the numerator of the first term of (6.13). As a consequence, the dimension of the equations system can be reduced to N_{BS}, in the same way as it is usually done in WCDMA systems without repeaters deployment [Han99; MH01]. Since N_{BS} is far smaller than N_{UE}, the analysis is considerably reduced in terms of computational cost. The final linear equations system can be expressed in matrix notation as follows:

$$\mathbf{\Omega^{UL}} \cdot \mathbf{\Pi_{RX,tot}^{UL}} = \mathrm{N^{UL}} \tag{6.17}$$

Where $\mathbf{\Pi_{RX,tot}^{UL}}$ is a vector containing the unknowns, that is, the total received power at each BS:

$$\mathbf{\Pi_{RX,tot}^{UL}}(j) = P_{RX,tot}^{UL}(j) \tag{6.18}$$

$\mathbf{N^{UL}}$ is a vector with the total thermal noise power (received from repeaters and the BS itself).

$$\mathbf{N^{UL}}(j) = n(j) \tag{6.19}$$

And $\mathbf{\Omega^{UL}}$ represents a $N_{BS} \times N_{BS}$ matrix with individual elements calculated as follows, $\delta_{j,i}$ being the Kronecker delta:

$$\mathbf{\Omega^{UL}}(j,i) = \delta_{j,i} - \sum_{\substack{m=1 \\ m \in i}}^{N_{UE}} \frac{L_{ef\Psi}(i,m)}{L_{ef\Gamma}(j,m)} \cdot \phi^{UL}(i,m) \tag{6.20}$$

The summation is calculated over the UEs connected to BS i, which is indicated by $m \in i$, m being the summation index.

Note that the number of equations does not depend on the number of installed repeaters. Therefore, the computational cost to analyze the network with repeaters deployment is independent of their number, and it can be afforded using as much repeaters as needed without adding significant complexity to the network planning. Once the total received power has been calculated, the individual UE transmitted power can be calculated by using Equation (6.15).

UEs in SHO can be also considered with minor changes in the formulation, which is an additional usefulness. In order to take these users into account, the different BSs in the AS should be evaluated independently and, a posteriori, the connection that requires less power from the user should be selected. From an analysis viewpoint, if UE k has $\varepsilon(k)$ BSs in its AS, it would be characterized as $\varepsilon(k)$ independent UEs, each one connected to a different BS. Obviously, this indirectly implies a higher number of connections in the network and a more hostile scenario in terms of interference because:

$$\sum_{i=1}^{N_{UE}} \varepsilon(i) = N'_{UE} \geq N_{UE} \tag{6.21}$$

In this situation, it is necessary to solve the equations system twice. Firstly, a coarse adjust is done with all virtual connections. Subsequently, a refined one is required, once the optimum connection is chosen and the others are eliminated. Note that the BS that requires less power from the UE may not be the same as the best BS in the AS, which is selected according to CPICH E_c/I_0 levels.

6.3.2 Downlink

For DL, the objective of the analysis is to find a generic expression to evaluate the power that a certain BS j has to transmit to a given UE k, $P_{TX}^{DL}(j,k)$, in order to meet all users requirements. Similarly to UL, and using the same notation, it is

possible to write one single equation to calculate the SINR:

$$\gamma^{DL}(j,k) = \frac{P_{TX}^{DL}(j,k)/L_{ef\Psi}(j,k)}{I_{Inter}^{DL}(j,k) + I_{Intra}^{DL}(j,k) + n_{UE}(k)} \tag{6.22}$$

Where $I_{Inter}^{DL}(j,k)$ is the inter-cell interference, $I_{Intra}^{DL}(j,k)$ stands for the intra-cell one, and $n_{UE}(k)$ represents the total thermal noise power measured at UE k. In order to simplify notation, the same denomination for effective propagation losses has been used in both links, although these values may not match in FDD systems. Then, $L_{ef\Psi}(j,k)$ stands for the effective path loss from BS j to UE k considering only the paths that will be constructively added in the Rake receiver at k.

If the user is in SHO, $I_{Inter}^{DL}(j,k)$ depends on the specific BS link that is evaluated. Moreover, if j does not belong to the UE's AS, then $P_{TX}^{DL}(j,k) = 0$. Therefore, $I_{Inter}^{DL}(j,k)$ can be written as:

$$I_{Inter}^{DL}(j,k) \equiv \sum_{\substack{i=1 \\ i\neq j}}^{N_{BS}} \frac{P_{TX,tot}^{DL}(i)}{L_{ef\Gamma}(i,k)} \tag{6.23}$$

Where $P_{TX,tot}^{DL}(i)$ is the total transmission power of BS i including the power devoted to UEs and control channels.

Concerning, $I_{Intra}^{DL}(j,k)$, the interference measured by k at the link with j, and caused by the BS itself, it is the summation of powers transmitted by the BS towards the rest of users in the cell plus the power devoted to control channels $c(j)$, measured at k and taking into account the correspondent loss of orthogonality caused by multipath and characterized by the orthogonality factor $\rho(j,k) \in [0,1]$. It is recalled that $\rho = 1$ defines a situation with full loss of orthogonality and that if j does not belong to the AS of k, intra-cell interference is zero. A self-interference term can also potentially appear in DL, and it is also included as part of the intra-cell interference. Hence, $I_{Intra}^{DL}(j,k)$ can be expressed as Equation (6.25), where the summation is calculated over the UEs connected to BS j, indicated as '$i \in j$'.

$$\begin{aligned} I_{Intra}^{DL}(j,k) &\equiv \rho(j,k)\left[\frac{c(j)}{L_{ef\Gamma}(j,k)} + \frac{P_{TX}^{DL}(j,k)}{L_{ef\Gamma-\Psi}(j,k)} + \sum_{\substack{i=1 \\ i\neq k \\ i\in j}}^{N_{UE}} \frac{P_{TX}^{DL}(j,i)}{L_{ef\Gamma}(j,k)}\right] = \\ &= \rho(j,k)\left[\frac{P_{TX,tot}^{DL}(j)}{L_{ef\Gamma}(j,k)} + \frac{P_{TX}^{DL}(j,k)}{L_{ef\Gamma-\Psi}(j,k)} - \frac{P_{TX}^{DL}(j,k)}{L_{ef\Gamma}(j,k)}\right] = \\ &= \rho(j,k)\left[\frac{P_{TX,tot}^{DL}(j)}{L_{ef\Gamma}(j,k)} - \frac{P_{TX}^{DL}(j,k)}{L_{ef\Psi}(j,k)}\right] \end{aligned} \tag{6.24}$$

Note that the total power transmitted by a BS j, $P_{TX,tot}^{DL}(j)$, is expressed as:

$$P_{TX,tot}^{DL}(j) \equiv c(j) + \sum_{\substack{i=1 \\ i \in j}}^{N_{UE}} P_{TX}^{DL}(j,i) \tag{6.25}$$

If these expressions are substituted in Equation (6.22), a new expression for $\gamma^{DL}(j,k)$ can be obtained:

$$\begin{aligned} \gamma^{DL}(j,k) &= \frac{\frac{P_{TX}^{DL}(j,k)}{L_{ef\Psi}(j,k)}}{\sum_{\substack{i=1 \\ i \neq j}}^{N_{BS}} \frac{P_{TX,tot}^{DL}(i)}{L_{ef\Gamma}(i,k)} + \rho(j,k)\left[\frac{P_{TX,tot}^{DL}(j)}{L_{ef\Gamma}(j,k)} - \frac{P_{TX}^{DL}(j,k)}{L_{ef\Psi}(j,k)}\right] + n_{UE}(k)} = \\ &= \frac{\frac{P_{TX}^{DL}(j,k)}{L_{ef\Psi}(j,k)}}{P_{RX,tot}^{DL}(k) - \rho(j,k)\frac{P_{TX}^{DL}(j,k)}{L_{ef\Psi}(j,k)}} \end{aligned} \tag{6.26}$$

The total received power at k, $P_{RX,tot}^{DL}(k)$, has been used in the equation, being given by:

$$P_{RX,tot}^{DL}(k) = \sum_{\substack{i=1 \\ i \neq j}}^{N_{BS}} \frac{P_{TX,tot}^{DL}(i)}{L_{ef\Gamma}(i,k)} + \rho(j,k)\frac{P_{TX,tot}^{DL}(j)}{L_{ef\Gamma}(j,k)} + n_{UE}(k) \tag{6.27}$$

Similarly to the UL case, this expression can be manipulated and simplified. However, in this case the SSINR will not be directly used. Instead, a derived term $\phi_\rho(j,k)$ containing the orthogonality factor is defined:

$$\phi_\rho(j,k) \equiv \frac{\gamma^{DL}(j,k)}{1 + \rho(j,k) \cdot \gamma^{DL}} = \frac{P_{TX}^{DL}(j,k)}{L_{ef\Psi}(j,k) \cdot P_{RX,tot}^{DL}(k)} \tag{6.28}$$

Hence, it is possible to obtain the power that BS j should transmit to UE k. It is remarked that if j does not appear in the AS of k, $\gamma^{DL}(j,k)$ and $P_{TX}^{DL}(j,k)$, are equal to zero.

$$P_{TX}^{DL}(j,k) = \phi_\rho(j,k) \cdot L_{ef\Psi}(j,k) \cdot P_{RX,tot}^{DL}(k) \tag{6.29}$$

It can be seen that this expression is almost symmetrical to the one obtained for the UL, and that the conclusions drawn are applicable. This final equation allows finding the unknowns, $P_{TX}^{DL}(j,k)$, by solving a N_{UE}th-order linear equations system. Therefore, again, a dimensionality reduction will be an important issue to attain and a procedure similar to that performed for the UL is proposed.

The total received power by k can be found directly from the total transmitted power by all BSs, Equation (6.27). On the other hand, $P^{DL}_{TX,tot}(j)$ is the sum of the individual transmitted powers to the UEs connected to j plus the power devoted to control channels. Obviously, this sum cannot exceed the maximum power available at the BS, $P^{DL}_{TX,max}(j)$. Besides, a user with several BSs in its AS will contribute to all the summations of those BSs as:

$$0 \leq P^{DL}_{TX,tot}(j) \equiv \sum_{\substack{i=1 \\ i \in j}}^{N_{UE}} P^{DL}_{TX}(j,i) + c(j) \leq P^{DL}_{TX,\max}(j) \tag{6.30}$$

Given this, if Equation (6.29) is substituted in (6.30), the expression that permits a reduction in dimension of the problem can be found,

$$\begin{aligned} &P^{DL}_{TX,tot}(j) = \\ &= \sum_{\substack{m=1 \\ m \in j}}^{N_{UE}} \phi_\rho(j,m) \cdot L_{ef\Psi}(j,m) \cdot \left[\sum_{i=1}^{N_{BS}} \frac{P^{DL}_{TX,tot}(i) \cdot \rho(i,m)}{L_{ef\Gamma}(i,m)} + n_{UE}(m) \right] + c(j) \end{aligned} \tag{6.31}$$

And so, the problem can be posed as a $N_{BS}th$-order linear equations system:

$$\mathbf{\Omega^{DL}} \cdot \mathbf{\Pi^{DL}_{TX,tot}} = \mathbf{\Phi^{DL}} \tag{6.32}$$

Where $\mathbf{\Pi^{DL}_{TX,tot}}$ is a vector of dimension N_{BS} containing the unknowns:

$$\mathbf{\Pi^{DL}_{TX,tot}}(j) = P^{DL}_{TX,tot}(j) \tag{6.33}$$

$\mathbf{\Omega^{DL}}$ represents a matrix of dimension $N_{BS} \times N_{BS}$ with individual values calculated as follows:

$$\mathbf{\Omega^{DL}}(j,i) = \delta_{j,i} - \sum_{\substack{m=1 \\ m \in j}}^{N_{UE}} \left[\frac{L_{ef\Psi}(j,m) \cdot \rho(i,m)}{L_{ef\Gamma}(i,m)} \cdot \phi_\rho(j,m) \right] \tag{6.34}$$

And $\mathbf{\Phi^{DL}}$ is a vector of dimension N_{BS} with individual elements calculated as follows:

$$\mathbf{\Phi^{DL}}(j) = c(j) + \sum_{\substack{i=1 \\ i \in j}}^{N_{UE}} \phi_\rho(j,i) \cdot L_{ef\Psi}(j,i) \cdot n_{UE}(i) \tag{6.35}$$

Once the system is solved, individual transmission powers can be calculated for each UE with Equation (6.29). Since the resolution of the linear equations system can give impossible solutions not fulfilling the condition in (6.30), a standard iterative resolution method is mandatory as a complement to the approach.

In this way, a holistic description and analysis of WCDMA networks is given when repeaters are deployed. It is important to remark that all this analysis does not include any type of approximation regarding the combination of the signals at the Rake receiver and all the signal terms present in the system (both useful and interference). Therefore, it allows characterizing the system with the same computational cost as traditional approaches do, but considering the inclusion of repeaters in the system deployment and getting a higher accurate solution.

6.4 Numerical Results

In order to evaluate several performance indicators of a WCDMA network, and to quantify the differences obtained when using the proposed analysis with respect to usual approaches (which include some approximations and simplifications), simulations have been run. All the numerical analysis described in the previous paragraphs have been embedded in the simulator, along with the assumptions that were described in Subsection 6.2.

The number of UEs in the first set of simulations has been adjusted so that the number of users not reaching their E_b/N_0 target is 5% when using the MRC approach.

The study case scenario consists of a long road or railway with one BS and one repeater that has been used as a coverage extender. The distance between the donor BS and the repeater is 4 km and the repeater has been installed in the direction of maximum gain of the BS's antenna. The objective is to cover a long portion of the road or railway. The link between them is considered to be an optical fibre with refraction index of 1.48 in the core and a length of 4.5 km. It is considered that the fibre is not installed along a perfect straight line between the BS and the repeater since it is more likely to be part of a ring, continue a railway path, etc. The gains of the transmitter and receiver in the link and the internal gain of the repeater are adjusted so that there is no amplifier saturation at the repeater, which has the same noise figure and maximum available power equal to the BS. Other parameters regarding radio propagation, services characterization and the rest of assumptions are the same as in the synthetic scenario in Appendix B.

Results have been obtained considering different delays accumulated by the repeater and other active devices in the backhaul (from 5 to 11 μs). However, it is the difference between the absolute delays of the paths that is important. The same results can be obtained for smaller internal delays in the repeaters, but, for example, with a longer fibre. In subsequent graphs, all curves entitled MRC and SEL stand for the cases in which traditional approaches were used. Specifically:

- SEL: Power is considered to be received just through the radio-link with the BS or through one of the repeaters. Other contributions are not considered in any way. This case is different from our proposal even when only one path is recovered because SEL misses self-interference.

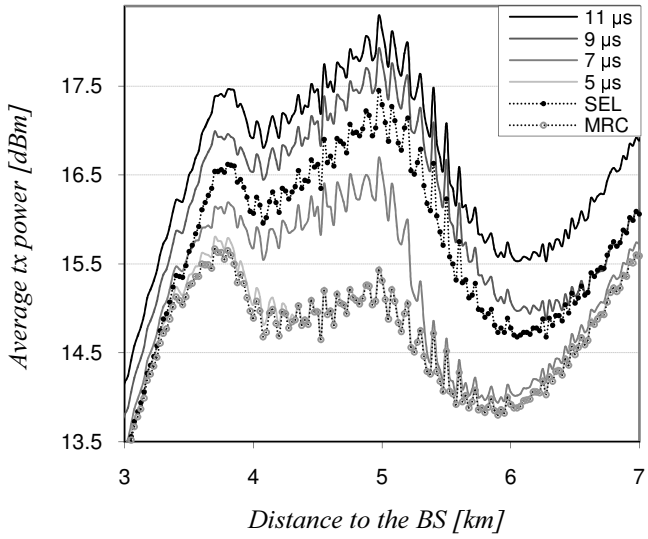

Figure 6.2: UL transmission power as a function of the distance to the donor BS, for traditional approaches and different internal delays at the repeater.

- MRC: All contributions are always perfectly combined in the UE irrespectively of their different delays. Ideal maximum ratio combining of all paths is applied. For references on SEL and MRC the reader is referred to subsection 6.

One of the first parameters to evaluate is the UE's transmission power as a function of the distance to the BS. This parameter is rather informative in such a lineal scenario. Thus, from Figure 6.2, all curves show an expected upwards trend in the required transmission power as the UE goes farther away from the BS and enters the repeater's area of influence. It can be observed that differences with respect to the full MRC approach reach up to 3 dB for the case of a repeater with 9 or 11 μs delay, because the path from the BS is out of the Rake time window (20 μs). This implies two facts: first, it puts in evidence the presence of a term of self-interference that causes an increase of the transmission power; second, in this situation, fewer paths can be combined, and therefore the attenuation suffered by the UE is greater than the one measured in a full MRC case. The percentage of area in which all the paths cannot be constructively combined is directly proportional to the repeater internal delay, therefore, the degradation observed with respect to the too optimistic traditional consideration will also increase. On the other hand, when the internal delay is 5 μs, there are very few areas in which all the paths cannot be combined, hence, results are very similar to the full MRC case. The error obtained when using a traditional approach keeps reducing with distance until reaching a constant value of 1.5 dB. Under some circumstances, inaccuracies of this order may not be tolerable.

On the other hand, if just the best path is considered (SEL case) and the repeater has an internal delay of 5 μs, an error around 2 dB occurs by the approximated

Table 6.1: Evolution of correctly served users for traditional approaches and different internal delays at the repeater.

Traditional Approach or Internal Delay	Users [%]
MRC	95.3
SEL	94.4
5 μs	93.9
7 μs	93.0
9 μs	89.5
11 μs	86.1

analysis along 1 km. The SEL curve tends to the MRC case when the UE is close to the BS. This behavior is coherent, since the propagation path through the repeater is more than 10 dB below than that of the path through the BS, therefore, this signal contribution can be considered negligible. Conversely, when the UE reaches the repeater and continues moving away from the BS, the curve tends to the 9 μs case. The curve does not tend to the 11 μs case because the SEL approximation only considers one path, the others not being taken into account, and then not generating any kind of interference. Between these two clear areas, the results are more or less accurate depending on the internal delay of the repeater and the actual possibility of some signal replicas to be out of the Rake window.

Since UEs are limited in power, the previous reasoning induces to think that there are also important differences in the forecast of the percentage of users not reaching their E_b/N_0 target (degraded users) between the traditional approaches and the proposed analysis. Some results for this evaluation are shown in Table 6.1, which actually shows the mean percentage of correctly served users. These values are obtained after analyzing all UEs at the end of each simulated snapshot. According to the full MRC or SEL approximations, around 95% of users can be correctly served, which is a typical design constraint. However, this value is reduced to 86% when the repeater has an internal delay of 11 μs. Therefore, the previous optimistic result might lead to accept as good an inappropriate system design when not using the proposed analysis. The differences are always higher compared to the MRC approach, which is the most optimistic as it considers that all paths are always constructively combined. Even with a repeater with very low internal delay (5 μs) a difference of 1.4% of users arises.

The curves on Figure 6.3 compare the normalized histogram of the DL transmitted power per UE obtained from the simulated samples. Since the orthogonality factor exhibits significant temporal variations [MGWK03], two typical cases [MMG05] of loss of orthogonality have been considered: in the first one, a coefficient equal to 0.6 is considered, and in the second one equal to 0.4, which is more common in low

dispersive channels. In this case, the most optimistic traditional approach (MRC) is compared with the enhanced proposal considering a worst case commercial repeater with 11 μs delay. It can be observed that the standard evaluation leads to a smoother error with respect to UL, since just a percentage of the total intra-cell power acts as interference. Nevertheless, this error increases with the orthogonality factor. In particular, for $\rho = 0.6$ the histograms are 1 dB displaced, but the value is quite smaller in environments with $\rho = 0.4$. The error is negligible as long as the accumulated delay in the link and repeater is under 5 μs, or if comparisons are drawn with the SEL case.

The same situations are subsequently evaluated in terms of coverage. Figure 6.4 and Figure 6.5 show the probability of coverage for each spatial point or pixel in the scenario. A pixel is considered to have coverage as long as it accomplishes these four conditions:

- The ratio of received energy per chip to the total power spectral density at the UE antenna connector E_c/I_0 measured on the pilot channel is higher than -12 dB. The pilot channel is realistically introduced according to UMTS features and so it allows UEs to execute cell selection and SHO procedures [3GPh] as well as estimate channel conditions.
- Once the UE has selected the cell, it has enough power so that the UL E_b/N_0 target is reached.
- Similarly, to reach the DL E_b/N_0 target, the UE does not need more power than the maximum allowed level per connection.
- The BS is not transmitting at its maximum transmission power, so it can serve new UEs.

Along the simulation and at the end of each snapshot, UEs and BS adjust their transmission powers. Under these load conditions, and before configuring a new sample, a test UE analyzes all the pixels in the scenario and assesses the four conditions. This UE is transparent to the system and does not generate interference, i.e., it just acts as an evaluator and allows finding the probability of coverage for each pixel in the system realistically, without approximations.

It can be seen that, when the full MRC approach is used, with $\rho = 0.4$ the coverage is supposed to be guaranteed in every point between the BS and the repeater. However, when considering the real delays of the paths, a clear loss is obtained, especially in the repeaters area of influence. With the proposed evaluation, certain zones turn out to demand more power than the available one and as a consequence connections are degraded or dropped. Since interference is also increased, the evaluated levels of E_c/I_0 on the pilot signals are affected too. These differences are much sharper when an orthogonality factor of 0.6 is considered. These are shown by Figure 6.5 and the analysis reveals that the proposed layout would be clearly inappropriate, but this conclusion would have not been reached if a standard evaluation had been performed.

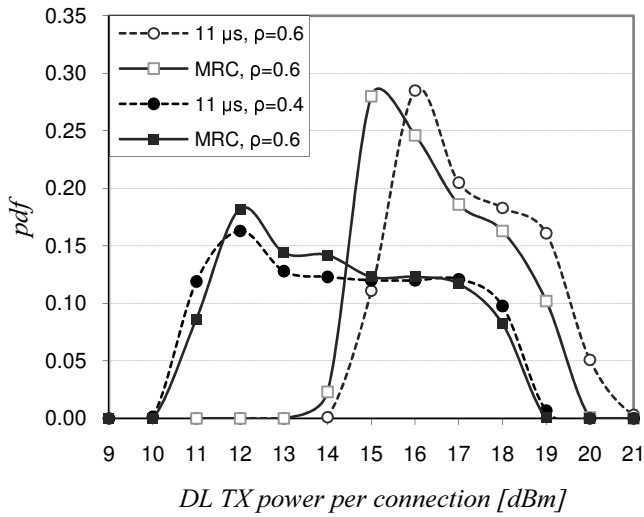

Figure 6.3: DL transmission power of individual connections, comparing the 11μs case with the traditional full MRC approximation.

It can also be noted that, when the new proposal is used, the coverage area of the repeater is not as regular as in the traditional case; there is a central zone in which the coverage is slightly extended. Indeed, it corresponds to the portion of the scenario in which all paths fall inside the window of the Rake receiver and the limit can be easily defined, it actually forms a hyperbola, because the scenario is flat. With traditional approaches, these variations cannot be appreciated, since the coverage does not depend on the internal delay of repeaters, devices in the backhaul, or the physical link itself with the donor BS.

Finally, admission regions for the network have been studied. An AC based on the UL load factor is considered. So, a new RAB can be admitted if the current load level stays below a certain threshold. In this set of simulations this maximum limit has been adjusted to 0.85, which implies a typical value of 95% of users correctly served when evaluating the scenario with traditional approaches.

In this sense, Figure 6.6 shows the number of users that could be admitted in the study-case scenario. It can be seen that those results obtained when considering traditional approximations are optimistic. Indeed, when actual differences in delays are considered, the resulting admission region becomes smaller, being inversely proportional to the internal delay of the repeater. This degradation in capacity reaches the 8% when the repeater has an internal delay of 11 μs. Furthermore, it can be seen an almost identical result between the MRC and SEL cases. This is because the only difference between them is the effective attenuation that perceives the UE; on the other hand, the enhanced proposal also introduces self-interference terms, which have a direct and evident impact on the load factor (it is increased), and therefore, as it is shown, on the admission region size.

Given this, admission regions are not only reduced because of the extra noise

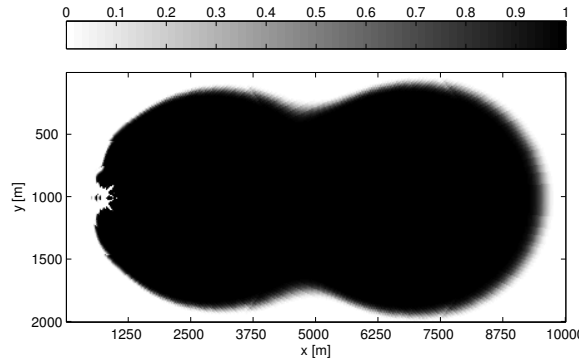

(a) Traditional full MRC

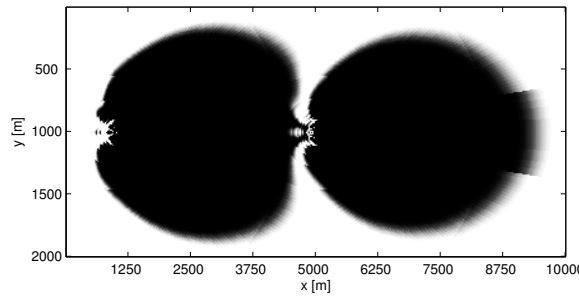

(b) Enhanced proposal

Figure 6.4: Probability of coverage for internal delay = 11 μs and $\rho = 0.4$.

rise introduced by repeaters, the potential existence of self-interference terms also reduces the number of UEs that a cell can serve. In the previous chapter, an expression was derived to find the new admission region when repeaters are deployed, but if the planned layout induces self-interference in a group of UEs, this equation becomes an upper limit. The real admission region is further reduced (as seen from Figure 6.6) and it is defined by the next mathematical expression:

$$\Lambda(j) \leq \frac{\xi(j)}{1+f(j)} - \frac{\sum\limits_{\substack{i=1 \\ i \in j}}^{N_{UE}} \tilde{P}_{RX}(j,k)}{P_{RX,tot}^{UL}(j)} \tag{6.36}$$

Similarly, the coverage reduction in the donor cell is also even higher if self-interference terms are present. The new mathematical expression modeling the relationship between the donor radius before and after installing repeaters is given next and should be compared with Equation (5.32), in the previous chapter:

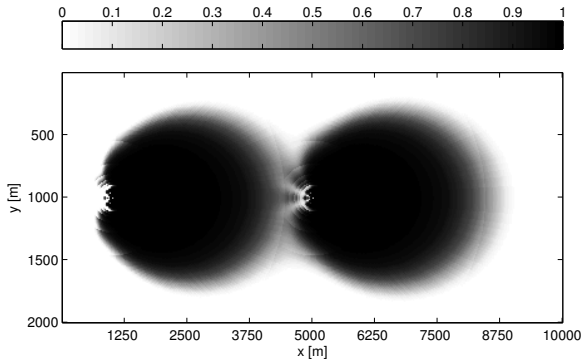

(a) Traditional full MRC

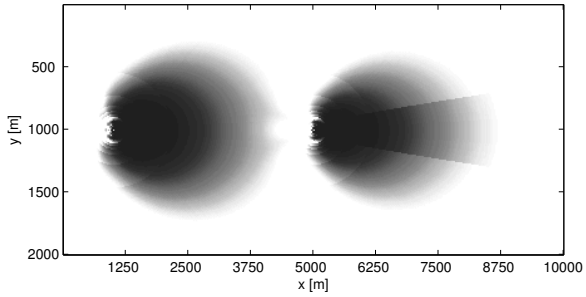

(b) Enhanced proposal

Figure 6.5: Probability of coverage for internal delay = 11 μs and $\rho = 0.6$.

$$\frac{R}{R_0} = \left\{ \frac{1}{1 + \sum_{r=1}^{N_{Rep}} \delta F\left(r_i\right) G_g\left(r_i\right) + \frac{1}{n_{BS}} \sum_{i=1}^{N_{UE}} \tilde{P}_{RX}\left(i\right)} \cdot \right. \tag{6.37}$$
$$\left. \cdot \frac{1 - \eta_0 \left(\frac{R}{R_0}\right)^2 \left[1 + \sum_{r=1}^{N_{Rep}} \left(\frac{G_{a,BS}}{G_{a,Rep,r}} G_g\right)^{\frac{2}{\alpha}} \Delta_r\right]}{1 - \eta_0} \right\}^{\frac{1}{\alpha}}$$

Thus, traditional approaches can give biased and optimistic results. The proposed analysis is concluded to be required for a proper system evaluation and planning.

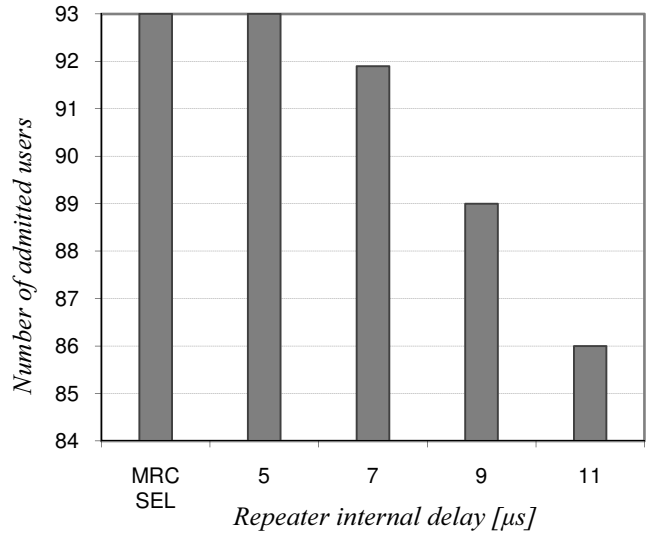

Figure 6.6: Admission region evolution for traditional approaches and different internal delays at the repeater.

6.5 Concluding Remarks

Along this chapter, a realistic analysis of WCDMA networks with repeaters deployment has been presented. A generic and compact expression for UL and DL evaluation is mathematically derived so that transmission powers and other RRM parameters can be calculated without simplifications. In particular, the effect of interference generated by signal replicas and the finite nature of the search window of Rake receivers are considered. This permits and enhanced analysis with respect to traditional approaches from a system level viewpoint. Furthermore, higher reliable and accurate predictions on network performance can be obtained, which can be very useful for network planning and management.

In the new mathematical approach, after defining different sets of mean propagation losses, effective equivalent losses have been introduced. These new definitions allow obtaining more compact and generic expressions. Similarly, for the same purpose, the SSINR in the UL and a derived term in the DL considering the ρ factor have been introduced so that the problem can be posed as an N_{UE}th-order linear equations system. However, thanks to the relationship between P_{TX} and $P_{TX,tot}$ (for the UL and DL), the dimension of the problem has been reduced and this has allowed its resolution with the same computational cost as in standard WCDMA systems without repeaters. Moreover, solving the obtained equations systems is independent of the number of repeaters and so the proposed approach does not introduce new extra computational cost, once the new propagation expressions are found.

Furthermore, with the help of simulations, a comparative study has been done

in order to test which are the major differences between the results obtained by the proposed analysis and those of traditional ones. Different performance indicators of WCDMA networks have been studied, being shown that traditional approximations may lead to unrealistic and too optimistic results. This, for example, could lead to accept bad planned networks as good designs. UL and DL transmitted powers have been evaluated, UL being the most affected link in terms of transmitted power with differences up to 3 dB. Because of the use of orthogonal codes, the differences in DL with respect to standard approaches are low, but more accurate metrics are obtained in scenarios with high loss of orthogonality. Figures on the number of non degraded mode users in the network would also be quite optimistic when traditional approaches are used; in the presented example this value evolved from 95% to 86% when using the proposed method. Important reductions of coverage have been observed when the realistic behavior of the paths is considered. Finally, admission regions have been also compared, showing, one more time, that traditional approximations lead to inadequate too optimistic results. In the simulated layout, reductions in the number of admitted users can reach 8% when the analysis is done with the presented proposal. Equations derived from the analysis in the previous chapter have also shown this degradation mathematically.

Chapter 7

Automated UL and DL Capacity Balancing

7.1 Introduction

Mobile networks are designed taking into account several target goals defined by operators at early stages of the planning process. These are essentially capacity, coverage, QoS and cost, and they determine the final decisions on the network planning itself, as seen in previous chapters. Static *Automatic Planning* strategies are sophisticated optimization tools which resort to cost functions to balance different trade-offs and optimize the planning outcome. However, due to the intrinsic characteristics of WCDMA and the great number of services offered by 3G networks, the radio channel is much more dynamic compared with, for example, the GSM system. The users scour through the network and constantly change between services with distinct characteristics. These traffic fluctuations can cause the impairment of the network performance and a significant degradation of the QoS may be observed, as a result the operator targets are not met. More flexibility, dynamism and reactivity are desired features to incorporate and this leads to the concepts of *Dynamic Planning* and *Automatic Tuning* which were introduced in Chapter 2.

The development of these strategies is showing a growing interest by the research community and several authors propose algorithms for the control of specific network parameters. Initially, proposals dealt with planning variables, however, recent efforts are concentrating on the auto tuning of RRM parameters. In this sense, from Chapter 2 it was learned that most contributions deal with AC and SHO. In the second case, the main pursued objective is achieving a real time load balancing among cells. However, load evaluations are usually done considering just one link, mostly the DL.

Investigation in Chapter 3 showed a close interrelation between these parameters and CPICH powers and downtilt angles, besides an UL and DL tradeoff appeared.

Thus, aiming at load balancing one link, without considering the effects in the other can yield an undesired outcome. In addition, because of services usage and users mobility, the network may evolve from UL to DL limited situations and vice versa. Given this, the framework of the current chapter is the investigation of UL and DL behavior in front of ASs variations. Results provide some extra light in the lack of consensus about gains or losses in the DL. From this study, an ATS is proposed to detect and correct UL and DL unbalance and SHO parameters are revealed as a feasible option to achieve this. Their opposing effect in UL and DL is investigated and conveniently used to jointly maximize the system capacity. This treatment is novel in the existent literature on UMTS optimization.

Some of the factors that determine which is the limiting link in a FDD CDMA based system are investigated in [KJ00]. In particular, the authors mainly study the signal quality required for each link, the effectiveness of the power control algorithm and the spatial distribution of UEs. Paper [YCC06] investigates to which extent capacity can be balanced by guaranteeing a certain SHO probability in a given cellular system. In particular authors obtain similar results to those in Subsection 7.5.1, their conclusions are in line with some of this thesis contributions [GLRS+03] and [GLSPR+07].

Not many other works deal with this problem considering the FDD mode. Other existent proposals cope with the UL and DL unbalance considering the Time Division Duplex (TDD) mode, as for example in [JJ99] which constitutes a relevant reference in this sense.

Next sections describe a mechanism to favor the limiting link and delay or avoid congestion control algorithms. Eventually, capacity is improved around a 30% in the simulated scenarios with different combinations of services. The pros and cons of modifying the thresholds that control the decisions taken by the algorithm are also investigated. Finally, along the chapter, complimentary results obtained in different scenarios are also obtained so that the generality of the proposal is tested.

Given this, after this introduction the chapter starts with a high level description of the functional architecture that has been used. Section 7.3 gives a more insight view on the problem and describes the solution principle. Next section comments on the scenario that has been designed for the study. Results are shown along Sections 7.5.1, 7.5.2 and 7.5.3 which also describe each of the stages of the functional architecture. Finally, the chapter is closed by conclusions.

7.2 Functional Architecture

The functional architecture for the ATS consists of three main blocks, named *Control algorithm*, *Learning & Memory* and *Monitoring* and two interfaces, one with UTRAN and the second with stored reference values. Whereas UTRAN provides access to the RRM parameters and measurements, the reference source provides the operator's concept of QoS and network performance. A conceptual representation of this structure is presented in Figure 7.1.

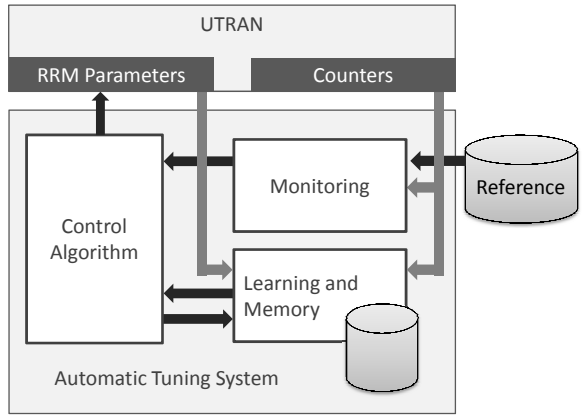

Figure 7.1: On-line Automated Tuning System. Functional Architecture.

The UMTS ATS creates a statistical feedback loop between network measurements and RRM parameters. The network is constantly monitored; selected parameters are placed into memory for statistical analysis and compared with the reference source. When any of the cells does not meet the reference criteria, the tuning algorithm is started. Thus, the radio network tuning process becomes an automatic one. Each of the constituting blocks are explained next in more detail:

- **Learning & Memory:** This block can be seen as a data-base that accumulates statistical information concerned with the network performance (memory). It is also responsible for finding out trends in the network behavior (learning). This entity will also be used to adjust the rules or the steps that govern the control algorithm.

  The *Learning* process can be executed online or offline. Furthermore, if it is executed without human intervention, one would talk of self-learning. Several works have dealt with this specific topic and a combination of neural networks plus fuzzy logic rules is accepted to be a good combination for that purpose [Wer92]. The tuning of the rules that control the ATS should not be confused with the tuning of the UTRAN parameters themselves. In most cases there is no need to change these rules along time once they have been found.

- **Monitoring:** This block is responsible of obtaining information from the network and processing it adequately to obtain KPIs that give a better understanding of the real state of the network and help the control block to take adequate decisions.

  In must be noted that *Automatic Planning* algorithms can simulate and obtain statistics about global performance indicators which allow knowing the exact outcome of a given optimization action. For instance, the maximum capacity in the network. However, in the context of ATSs, performance must be evaluated in real time and so this kind of measurements are bound to be unavailable. In particular, in order to obtain a KPI the following steps are taken:

  - Performance indicators measurement.
  - Data filtering to overcome instantaneous fluctuations.
  - Combination of filtered data and calculation of final KPIs.

  Next, KPI values are compared with the thresholds that define the operator's QoS concept and an alarm is triggered when they are not met. Eventually, KPIs could be transferred to the O&M system in constant time intervals or in near real time for additional monitoring, however this action is out of the ATS processes.

  Regarding the selection of measurements from UTRAN, each optimization case must be considered separately but the election should desirably take into account 3GPP definitions on performance related data. These are mainly grouped into radio-related measurements and protocol event counters [Kre06]. Whereas the second group information is somewhat reduced (mainly described in [3GPq]), a much better situation is found when looking for definitions of the first group. While [3GPk] defines measurement parameters themselves, [3GPh] is focused in how they must be reported. For example it contains reporting ranges, how the measurements are encoded in signalling messages, etc. In the context of UMTS Rel'99, the most important radio measurements in [3GPk] are summarized next [Kre06]:

  - Measurements related to a cell and reported from Node-B:
    * Received total wideband power and consequently the UL cell load factor.
    * Transmitted carrier power and so the DL cell load factor.
    * Preambles of RACH: number of connection request attempts. Also the number of rejected attempts.
  - Measurements related to single connections:
    * SINR and measurement difference with respect to SINR target. Eventually UEs in degraded mode.
    * Power transmitted by a single cell on a dedicated physical channel and therefore the difference with respect to the maximum allowable power.
    * Round trip time on the radio interface (Uu interface).
  - Measurements from UE:
    * CPICH E_c/I_0.
    * Power received on a DL dedicated physical channel.
    * Received Signal Strength Indicator (RSSI).
    * Reports on several events (see Section 7.3).

- **Control Algorithm:** This last stage receives the alarm from the *Monitoring* block and, with the information provided by *Learning & Memory*, decides on the actions to take, which may compromise the change of RRM parameters.

  Regarding which network element holds intelligence and generates reconfiguration orders, three strategies can be defined:

- A centralized strategy, wherein a central element receives information regarding the whole network (or a great part of it). In this case, optimization can take into account all existent interdependencies among cells. On the other hand, signalling between monitoring devices and this central control can be excessively high. Moreover, delays should be considered if real time functioning is desired.
- Pseudo-centralized strategies, wherein intermediate elements in the network hierarchy, e.g. RNCs, take decisions over the group of Nodes-B that they control. Actually, information can be shared among these devices to achieve a better understanding of the whole network performance.
- Finally, most of the existent works propose distributed topologies in which decisions are taken at Nodes-B. Unless an information sharing mechanism is implemented, decisions hardly take into account the state of nearby cells and therefore this strategy is not the best option for certain cases (as for example when trying to balance load among cells). On the other hand signalling is minimum.

In subsequent sections details will be given on the mapping that is proposed for the three ATS blocks in the specific problem of balancing UL and DL capacity.

7.3 Problem Statement and Solution Principle

Nowadays UMTS operators fix uniformly their RRM parameters during the planning process and make re-adjustments considering long-term effects. That static configuration may suit the network conditions and guarantee a perfect balance between UL and DL in certain cases. However, in 3G systems, new data applications, different services usage and users mobility imply important and frequent fluctuations in traffic patterns and as a result UL and DL requirements do not remain constant. Specific RRM settings could favor a particular link at a specific time and thus, variations along time can spoil the network performance.

An ATS can cope with this problem if designed with a monitoring subsystem able to trigger an alarm whenever one of the links starts to degrade significantly. On the other hand, the control block should modify RRM parameters so that the network can favor the limiting direction and delay congestion control mechanisms.

SHO parameters are the set of variables to be modified by the proposed ATS. These parameters are typically adjusted in a static fashion so that they suit the general network conditions. However, the SHO process is not the same in both transmission directions. In the UL, selection diversity is used (as long as the two cells do not belong to the same Node-B) and it is well accepted that SHO brings benefit to both the individual links and the whole system. In the DL, mobiles receive power from all cells participating in the handover and just see the different signals as multipath components that can be coherently combined, this provides the benefit of macrodiversity. Although the individual link quality can be improved by

this fact, during the SHO process, extra DL resources are needed and so there is a trade-off between the individual link gain and the additional resource consumption. Moreover, there are quite a few parameters that impact on the link that limits the system capacity, particularly on the DL. Some examples are the loss of orthogonality because of the delay spread profile, the maximum power that the operator devotes to a particular DL connection, the power allocation for each cell in the AS, the geographical distribution of UEs, type of services that are mostly used, etc. The first parameter, can be well characterized, the second and third ones are design parameters to be chosen by the operator, but the UEs behavior is not constant, it evolves along time and can make inappropriate certain SHO configurations.

The performance of UMTS SHO algorithm is closely related to the adjustment of different thresholds and hysteresis margins. While the UE is in connected mode, it continuously monitors the E_c/I_0 over the different CPICHs and reports to the network whenever certain conditions on this measurement are accomplished. So, in essence, it is an event triggered mobile evaluated handover: The mobile runs the handover algorithm, informs the network whenever certain events happen but final decisions are provided by the network. If the network cannot be consequent with the reported event, for example when a certain BS cannot be included in the AS because of a lack of resources, the algorithm commutes to a periodic reporting mode. In this case, the measurement is sent periodically until the AS update can be executed or until the measurement condition is no longer fulfilled or a defined maximum possible number of reports has been sent.

Thresholds, margins and parameters participating in the handover process are described by [3GPm]. Concerning UE measurements, several events can be generated, being the most important ones summarized next:

- **Event 1A**: The UE generates a report to add a new BS to the AS if its corresponding measurement $(E_c/I_0)^{new}_{CPICH}$ is higher than that of the best received station $(E_c/I_0)^{best}_{CPICH}$ minus a certain window, normally also known as macrodiversity window or addition window ($AddWin$).

$$(E_c/I_0)^{best}_{CPICH} - [(E_c/I_0)^{new}_{CPICH} + CIO^{new}] \leq AddWin \tag{7.1}$$

  Where CIO^{new} is the Cell Individual Offset of the new cell. This parameter is optional and can be added to favor the entry of the BS to the AS. In particular, whenever an AS update is signalled from the network, a new set of neighbor cells is informed along with their particular CIOs. This parameter is also present in the next events and with identical function.

  In order to avoid too excessive reporting and ping-pong effects due to many neighboring cells, all reporting events can define a time-to-trigger period, that is to say, the event is only generated if the criterion is accomplished for a certain period of time.

- **Event 1B**: This event is intended to eliminate one BS from the AS. The UE generates the corresponding report when the E_c/I_0 difference between the best station and the outgoing one is higher than a new margin called drop

window ($DropWin$). This parameter is set relative to the addition window, usually around 2 dB higher to establish a certain hysteresis.

$$(E_c/I_0)_{CPICH}^{best} - \left[(E_c/I_0)_{CPICH}^{outgoing} + CIO^{new}\right] \leq DropWin \tag{7.2}$$

- **Event 1C**: If the signal from a new BS is bigger than that of the weakest BS in the AS plus a margin window denoted as replacement window ($RepWin$), the UE sends a report to the network so that an order is responded to execute the replacement. The next criterion must be accomplished:

$$(E_c/I_0)_{CPICH}^{new} + CIO^{new} \geq (E_c/I_0)_{CPICH}^{outgoing} + CIO^{outgoing} + RepWin \tag{7.3}$$

- Other events include the replacement of the best cell and particular $(E_c/I_0)_{CPICH}$ measurements becoming better or worse than an absolute threshold.

Taking these paragraphs into account, it can be predicted that an *AddWin* configured to a too low value yields a reduction in SHO areas and can cause the terminals to connect to a cell which may not be the best option (i.e. the one that would request less power to achieve the E_b/N_0 target). This implies increased UL interference, poor quality and a rise in blocking and congestion. Note that dropping can also grow because of power outage. On the other hand, too high values would cause a reduction in the DL capacity because of increased transmitted powers due to many links, eventually, insufficient codes could lead to blocking as well. The same effects appear with variations in the $DropWin$, however, since this parameter is derived from the *AddWin* only variations in this one will be done in forthcoming sections. It is remarkable that these ideas can also be extrapolated to the maximum number of cells that are allowed in the AS, subsequently called $\mathcal{N}$. Note for example, in Figure 7.2 how the SHO areas are extended when increasing the *AddWin* from 3 to 6 dB. This simulated example is a realistic scenario in which $\mathcal{N}$ is set to 4, but there are regions in which more cells could be included respecting the *AddWin* conditions. Under these assumptions the SHO area is increased from 21 to 29%. This particular example makes use of one scenario from the MORANS initiative, already mentioned in the Introduction of the dissertation.

Finally, regarding $RepWin$, its variations represent a lower influence on the network capacity and it equally affects UL or DL. It should be set low enough to avoid replacements being executed so slowly that suboptimal configurations are maintained and so the previous effects appear, but also high enough to reduce unnecessary and frequent replacements and signalling overhead.

Given this, *AddWin* and, with lower impact, $\mathcal{N}$ are good candidates to manage load imbalances between UL and DL and favor one or the other link when congestion problems appear. Indeed, the proposed ATS is based on this idea and automatically modifies those parameters to achieve the objective. The proposal is designed taking into account the functional architecture described in Section 7.2. In particular, Sections 7.5.1, 7.5.2 and 7.5.3 describe the different stages of blocks, *Learning & Memory*, *Monitoring* and *Control* respectively.

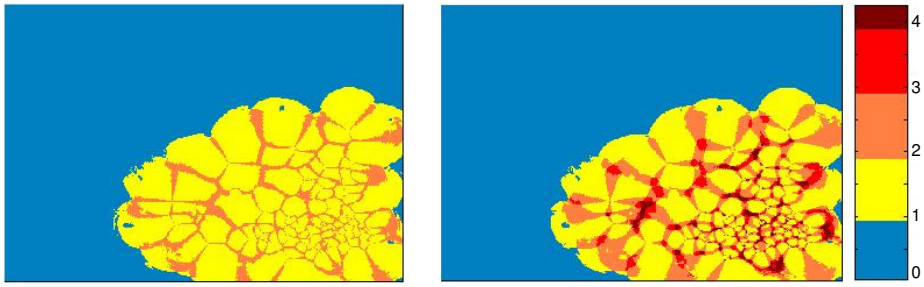

(a) *AddWin*=3 dB (b) *AddWin*=6 dB

Figure 7.2: Number of cells included in the AS.

7.4 Scenario and Simulation Conditions

The scenario to be evaluated is the 3GPP based, urban and macrocellular one described in Appendix B, Section B.3. Regarding the service mix, two situations are considered. The first one represents a scenario with all UEs of voice type. The second situation has 20% of terminals using a symmetric 64 kbps data service and the remaining 80% maintains the voice service. The transition between the two previous scenarios is simulated and the service mix change is done gradually during the first two-thirds of the observation time. 1100 pedestrian UEs move randomly around the network according to the mobility model described in the same appendix. Finally, regarding, SHO implementation, the optional additional time-to-trigger has been set to zero, which means that all events are reported as soon as they occur.

7.5 ATS Description and Results

7.5.1 Learning & Memory Stage

In an operating network, the process of gathering real data to accumulate statistical information and find and update trends corresponds to the *Learning & Memory* block. By means of simulations this process is approximated. Actually, these results could be eventually used as an *Initial Training* previous to the real learning from network data. Thus, in order to evaluate the behavior of both links under different service mix cases, maximum capacity in UL and DL is calculated, which is defined as the situation when at least one of the cells has 5% of UEs not reaching the E_b/N_0 target.

Figure 7.3 shows the evolution of capacity for different values of *AddWin* (in dB) and two possible values of $\mathcal{N}$, 2 and 3.

Several facts are observed. Firstly, the opposite impact in UL and DL, whereas

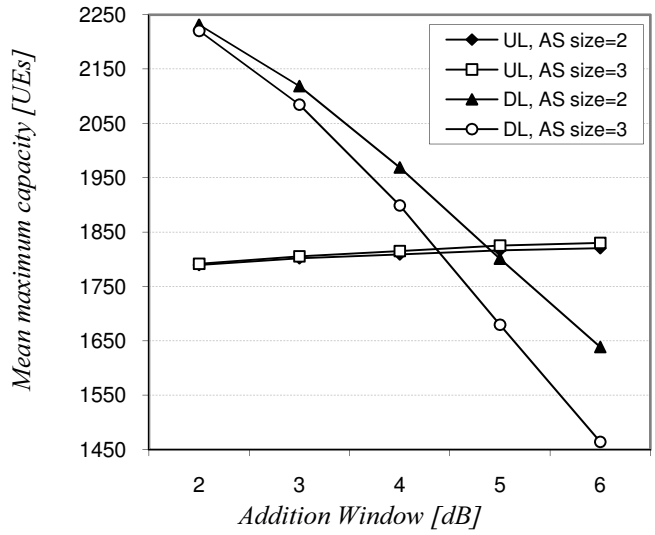

Figure 7.3: Maximum capacity for different configurations of SHO parameters (100% voice UEs.)

the UL capacity increases with higher values of SHO parameters, the DL worsens. Variations in the DL are far sharper and an erroneous adjustment can reach capacity reductions of around 30%. Conversely, bad adjustments lead the UL to just a 3% loss, which is logical since the load is evenly distributed and so in the central area of the scenario, opening the AS does not provide new cells with lower loads and demanding less power to UEs. Nonetheless, in an environment with a more heterogeneous users distribution, variations in UL capacity are much more evident. An example is shown in Figure 7.4(a) where UL fluctuations are much more important. In this case, users are distributed according to the spatial distribution in Figure 7.4(b), where the darker color indicates a higher density of UEs.

In general, what fixes capacity is the minimum value between UL and DL, and, in particular, the important points are those wherein curves cross (UL and DL remain balanced). Among crossing points, the one with a higher ordinate defines the system maximum capacity. According to simulations in the reference homogeneous scenario, a configuration around a maximum $\mathcal{N}$ of 2 and an *AddWin* of 5 dB, subsequently denoted as (2,5), might be a general possibility to be chosen by operators. Given the optimum point, the network remains UL limited for configurations that imply less BSs in the AS and, conversely, it gets DL limited when there are more. With different spatial distributions variations in the optimum are low and the new optimum would be situated at (2,5.5). This value is going to be much more dependent on the services being used and its corresponding UL or DL requirements and that is why the study has been focused on this aspect. Asymmetric data services will tend to displace the optimum value to the right, towards lower values of *AddWin* and $\mathcal{N}$.

The second traffic pattern with 80% of UEs using a voice service and 20% a

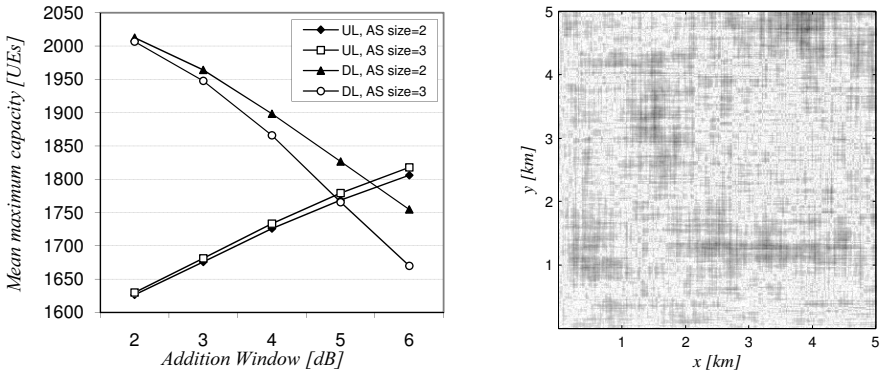

(a) 100% voice UEs

(b) Heterogeneous users density

Figure 7.4: Maximum capacity for different configurations of SHO parameters with heterogeneous users distribution.

64 kbps data service is simulated and Figure 7.5 shows that the DL is clearly now the limiting link for all simulated AS configurations except (2,2) and the optimum is now situated around (2,2.7). Furthermore, the prior selection (2,5) would now be one of the less appropriate possibilities. It can be noted that, for all scenarios, tuning the *AddWin* implies a higher impact than modifying $\mathcal{N}$. This second parameter shows a higher impact when *AddWin* is adjusted at its higher values.

As a conclusion, since services usage evolve along time, detecting the limiting link in real time and automatically tuning SHO parameters is bound to help to maximize the network performance and give an extra capacity margin to the loaded link before congestion control algorithms come into play.

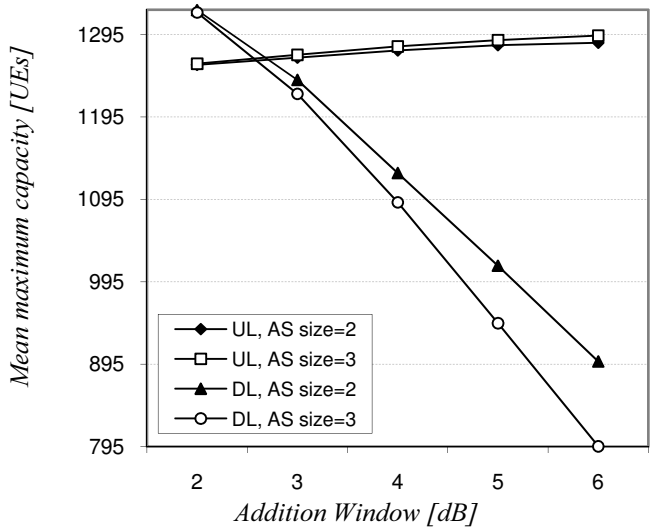

Figure 7.5: Maximum capacity for different configurations of SHO parameters (80% voice, 20% data UEs.)

7.5.2 Monitoring Stage

In order to select appropriate KPIs for the monitoring stage, an initial test was done without implementing the ATS. In particular, Figure 7.6(a) shows the evolution of the DL transmission power in the central cell. In this case, no tuning is done and SHO parameters are fixed to the optimum value when all UEs are of voice type (2,5). Along the simulation, the service mix evolves as described in Section 7.4.

It can be seen that the maximum power is reached several times at the end of observation time, so the level of generated interference to neighboring cells is maximum. Since the scenario is very homogenous, incoming interferences are high as well. Nevertheless, the level of degradation of a certain cell is quantified with the percentage of UEs reaching the required E_b/N_0. These data are gathered in Figure 7.6(b) which represents the percentage of UEs that the central cell is able to serve correctly. Initially, the cell is able to serve the 100% of UEs that have it in their AS but there is a point in which the network cannot manage so many UEs. Degradation appears once a certain number of UEs commute to the data service and the scenario becomes DL limited. The UL adjusted parameters lead the cell into a situation of instability in which most of UEs are in degraded mode. Regarding the UL (not plotted), all UEs reach the required E_b/N_0.

There is a correlation between the variations in the number of UEs with the cell in their AS and the slow variations of the graph. The main downwards trend, however, is motivated by the change in the service mix. Fast variations are caused by the whole system dynamics which cause changes in interference levels. Note that degraded UEs appear even though the maximum power is not reached. The reason

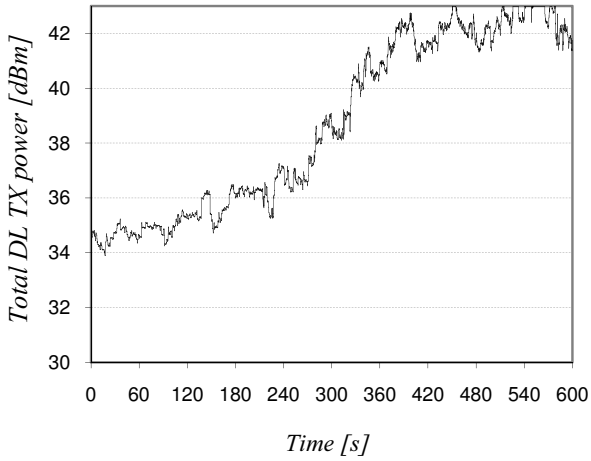

(a) Evolution of central cell DL transmission power

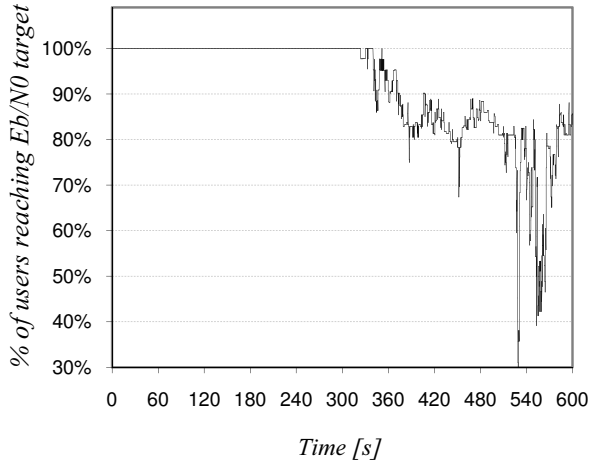

(b) % of UEs reaching E_b/N_0 target (central cell)

Figure 7.6: Evolution of central cell DL transmission power and % of correctly served users.

is the 30 dBm limit in the power that can be devoted for a single connection. A certain combination of high load factor and propagation loss may imply that a UE cannot meet this requirement.

Figure 7.7 shows three snapshots of the simulation. The graph 7.7(a) is a snapshot at the beginning of the simulation, 7.7(b) is an intermediate point in the observation time and 7.7(c) shows a snapshot closer to the end of the simulation. At the beginning, all users are served without problems (users are painted at their geographical situation with grey color), but as the number of data users increase,

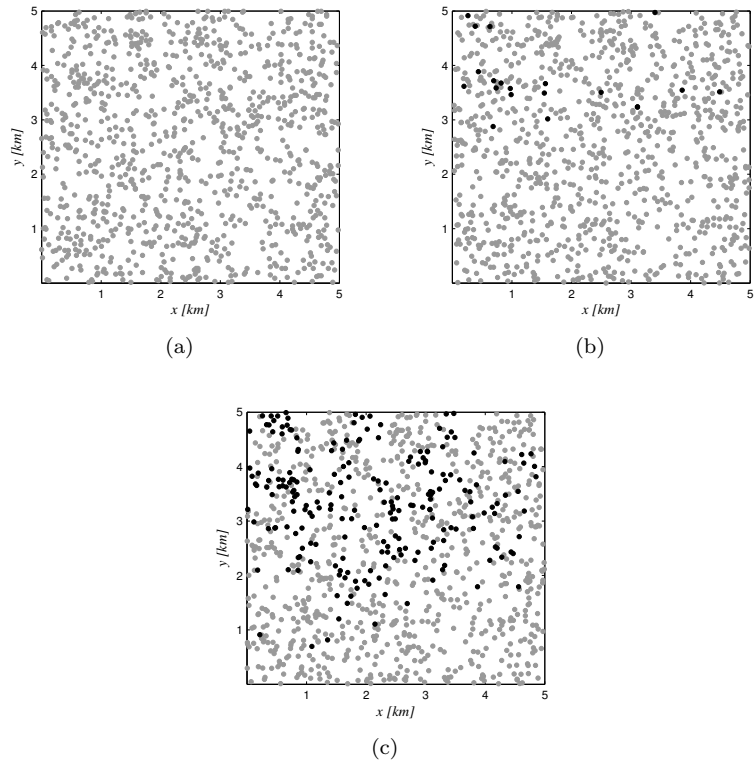

Figure 7.7: Distribution of correctly served (grey) and degraded users (black) for three different moments of observation time.

the number of them not reaching their E_b/N_0 target increases as well (plotted in black).

From this, a secondary conclusion is also derived, the total transmission power, or similarly the DL load factor, does not behave as a valid KPI because it does not characterize the cell performance by its own. Consequently single connections powers evaluations are preferred in the following. These permit monitoring individual connections with exact precision but at the cost of requiring more computational cycles. Thus, the next two KPIs are defined and monitored in a cell-by-cell basis:

- **KPI-A:** Percentage of mobiles that require more power than a certain threshold. The comparison reference is a percentage of the maximum power that can be devoted to one connection. Three thresholds have been evaluated. Case-1 considers 80% of the maximum power, case-2 uses 90% and, finally, case-3 employs 100%.

- **KPI-B**: Counter of the number of continuous frames in which KPI-A is ac-

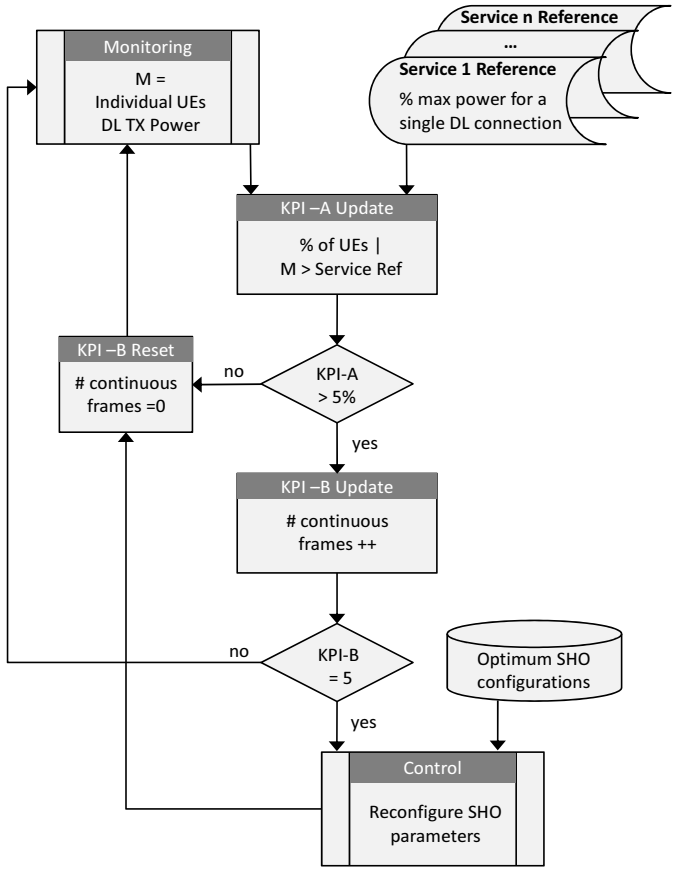

Figure 7.8: Flow chart of the ATS.

complished for 5% of users, in fact this acts as a filtering window. Whenever this counter reaches 5, the control block is triggered.

A graph, showing the triggers generated by these KPIs will be shown in next section, along with complete ATS results.

Finally, the whole process can already be described. The corresponding flow diagram is shown in Figure 7.8. Note that applied parameters are selected according to the *Learning* stage results, i.e. the optimum configurations (2,5) and (2,2.7).

7.5.3 Control Stage

The control block sends an AS reconfiguration order to all those UEs connected to the cell that triggers the mechanism. Note that reconfigured UEs maintain the new parameters until another order is received or the connection finishes. If new active

users enter the cell after one reconfiguration, they will maintain their original AS, no changes will be applied on them. Therefore a cell with frequent handover (for example with high speed mobiles entering and leaving) will tune SHO parameters often in short periods of time.

Figure 7.9(a) represents the transmission power evolution of central cell during observation time for the three simulated cases. Comparing with Figure 7.6, the most important difference is that DL transmission power is now always kept below 41 dBm, more than a 2 dB gain is obtained even for the less restrictive case (100%) and instability is never reached. Thus, the gains of ATS are obvious. Graphs show a general upwards trend, coherent with the fact that the service mix evolves to a more demanding DL situation. However, the trend is not continuous and downwards steps appear each time the observed cell or a nearby one triggers a reconfiguration command.

Figure 7.9(b) is a zoom at the end of the observation time and just for cases 1 and 3 to improve the readability of the graphs. By using the most conservative of the approaches (80%) the system is able to react faster to the service mix change, and the DL transmission power is kept around 3 dB below the case without ATS. So, an extra gain of 1 dB is often obtained when comparing with case 3 (100%). In case 1 (80%), cells activate the *Control* block earlier making transmission power decrease faster. The reason is the variation in the number of UEs the cell has to serve which causes a reduction in the consumption of DL resources. Actually, Figure 7.10(a) shows this fact by representing the evolution of UEs with the central cell in its AS. No ATS and cases 1 and 3 (80% and 100%) are plotted, the intermediate case is again avoided to facilitate the reading. It can be observed the decrease in the number of users because of the reduction in the value of *AddWin*. This action implies that several users exclude the BS from its AS. From the graph, it can be also observed that time of responses are slightly different and consequently different number of SHO reconfigurations are executed in each case.

Given this, Figure 7.10(b) represents the evolution of KPI-B, i.e. the counter of continuous frames with 5% of users reaching the threshold power. Note that all cells are aggregated in the figure. It can be seen, that case-1 (80%) starts triggering the control block before (of course, this was expected from the evolution of the corresponding curve in Figure 7.10(a)), and commands are slightly more distributed. On the other hand, case-3 (100%) starts triggering later and commands appear concentrated in time and slightly less often. Whereas case-1 executed 17 reconfigurations in the system, case-3 only fulfilled 13.

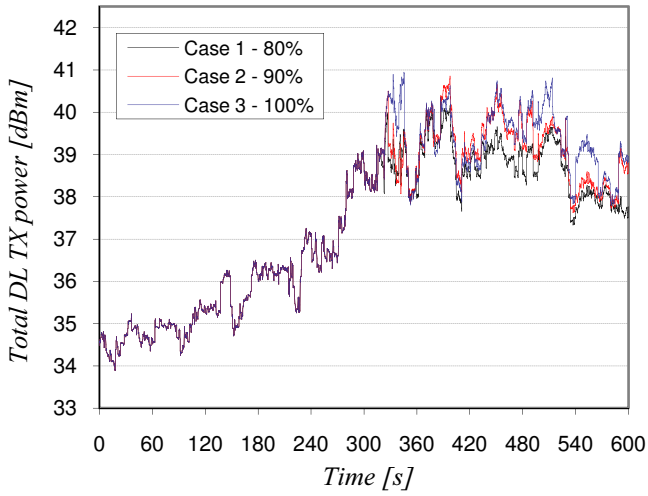

(a) Central cell DL transmission power during all observation time for all ATS cases

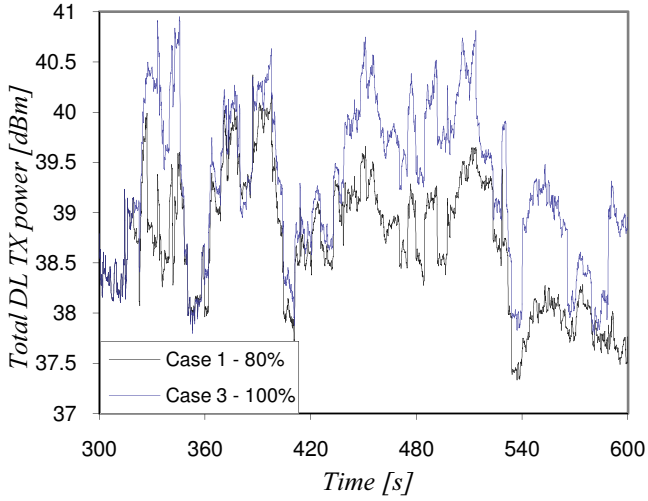

(b) Central cell DL transmission power at the end of observation time for case 1 (80%) and 3 (100%)

Figure 7.9: Central cell DL transmission power for different ATS study cases.

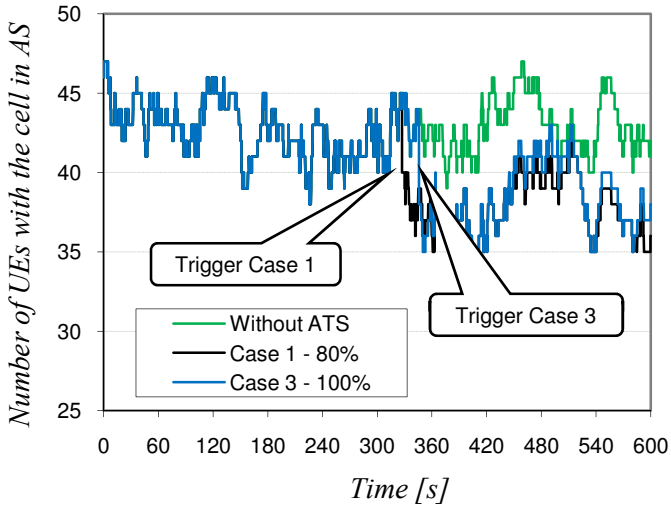

(a) Number of UEs with the central cell in its AS

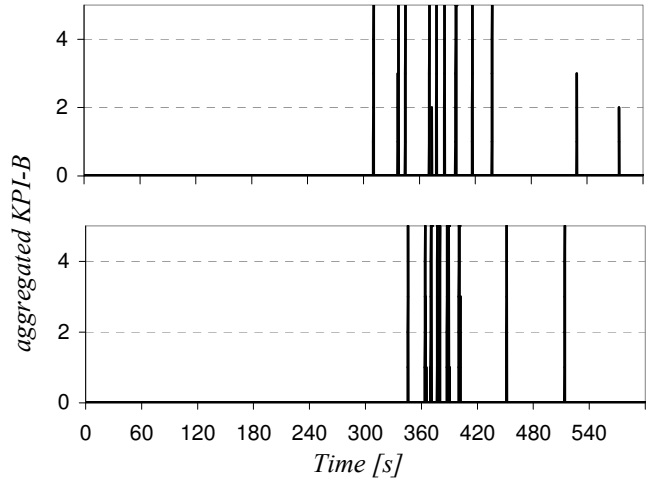

(b) Central cell DL transmission Power at the end of observation time for case 1 (80%) and 3 (100%)

Figure 7.10: Number of UEs with the central cell in its AS and aggregated KPI-B.

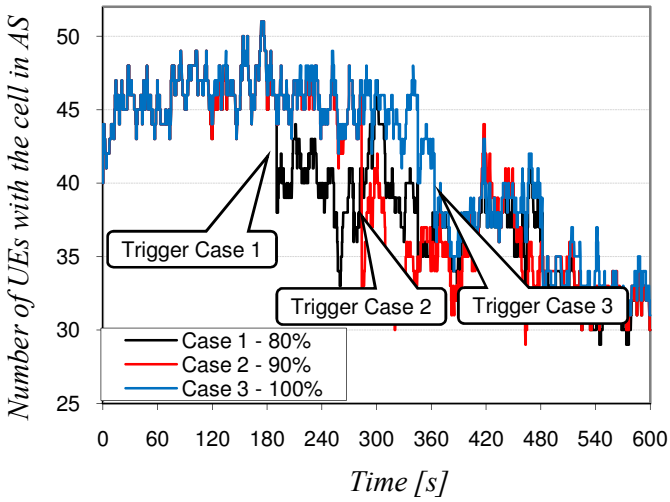

(a) Number of UEs with the central cell in its AS

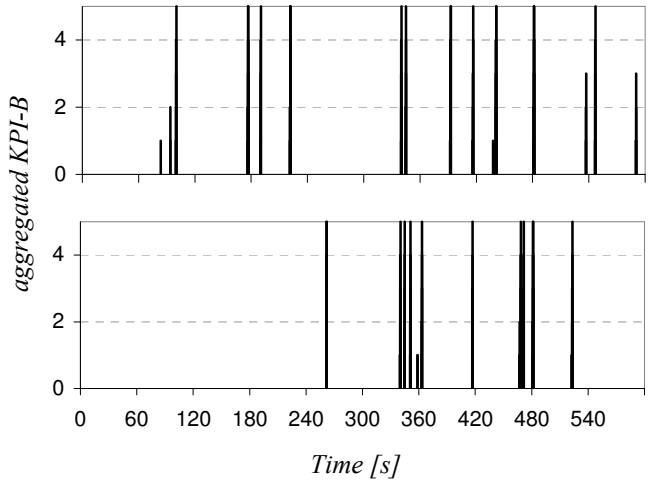

(b) Evolution of KPI-B (aggregated for all cells)

Figure 7.11: ATS performance (heterogeneous scenario).

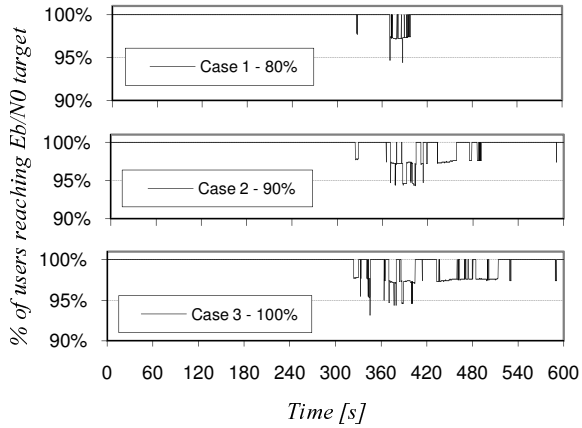

Figure 7.12: Evolution of % of UEs reaching their E_b/N_0 target.

Since the scenario is quite homogenous the commands are relatively concentrated for all cases. Moreover, in the central cell, case 1 and case 3 order a first reconfiguration with around 30 seconds of difference, which is coherent with the fact that all cells are increasing their load simultaneously (service mix evolves for all users in the scenario, and these are homogenously distributed). Nevertheless, if the service mix change would have taken longer (the current observation time is 10 minutes) this difference would have been accordingly scaled. Next, as an extra example, similar figures are given to show the behavior of the ATS proposal in a heterogeneous scenario. From Figure 7.11(a) it can be seen that now, the trigger starts much earlier for case 1. The situation in which many users are reaching their maximum power is maintained for a longer time and that is why if a threshold equal to 100% is chosen the trigger starts later. Obviously, KPI-B continues updating earlier, but in this scenario cells reconfigurations are more spaced in time because they do not reach the required situation so coordinately as in the original example (Figure 7.11(b)).

Going back to the test scenario, Figure 7.12 shows the evolution of the percentage of UEs reaching their E_b/N_0 target. Whereas, in case 1, central cell almost never shows degraded UEs, this does not occur in case 3, agreeing with previous conclusions. In all cases degradation is always kept below 6% of UEs, so even case 3 is good enough to guarantee an acceptable performance in this scenario. Furthermore, the performance improvement introduced by the ATS is obvious if compared with Figure 7.6(b). Without ATS and just maintaining SHO parameters to the optimum level before the service mix changed, degradation reached 70%.

Finally, Table 7.1, quantifies the capacity gains that would be obtained if ATS is applied in different service mix situations. The first row corresponds to the previous example, i.e. a 100% voice users situation that evolves to a service mix with 20% of data users. Next rows contain cases with increasing number of data users. The table shows that ATS gains remain quite constant, between 25 and 30%.

Table 7.1: ATS gains for different service mixes.

% of Data UEs	Maximum Capacity Simultaneous UEs		Capacity Gain [%]
	Without ATS	With ATS	
20%	1014	1270	25.2%
30%	852	1115	30.9%
40%	730	929	27.3%
50%	641	839	30.9%

7.6 Concluding Remarks

Dynamic optimization of UMTS systems has been gaining a growing interest by the research community since it provides to the network more flexibility, dynamism and reactivity in front of time-varying conditions. In this sense, existent proposals can be grouped in two sets, those dealing with planning parameters and the ones that cope with variables governing RRM algorithms.

Because of new data applications, different services usage and UEs mobility, UL and DL requirements do not remain constant. However, most of the existent auto tuning proposals fail in studying UL and DL effects jointly and unbalance is hardly checked. In this context, the ATS proposed in this chapter aims at achieving a more balanced situation between UL and DL when one of the links is limiting the capacity. The final objective is delaying or avoiding congestion control mechanisms by favoring the degraded link. This approach is novel and not previously addressed, since most works dealing with CDMA UL and DL unbalance consider the TDD mode duplexing.

A functional auto-tuning architecture has been described to adapt parameters to service mix dynamics and overcome capacity problems. This architecture is composed of three blocks (*Learning & Memory*, *Monitoring* and *Control*) and two interfaces.

These blocks have been described and tested in the proposed particular case, showing an effective adaptation to changes in the combination of used services. From the *Learning & Memory* stage SHO parameters have been revealed as a feasible option to achieve the desired UL and DL balancing:

- In essence, increasing the number of cells in the AS favors the UL, whereas too many cells in the AS degrades the DL capacity because of increased transmission powers.
- Maximum capacity curves have been given for AS configurations and for different service mixes and spatial distributions. Crossing points between these curves determine the optimum parameters setting.

- If services usage is maintained, spatial user distribution has a low impact in the globally optimal configuration.
- On the other hand, introducing DL demanding services clearly displaces the configurations towards values that imply less cells in the AS so that the DL is favored.
- Since service mixes evolve along time, detecting the limiting link and tuning the SHO accordingly gives an extra capacity margin when congestion appears in UL or DL.

Two KPIs have been defined in the *Monitoring* stage to detect three different grades of congestion. In this sense, it has been taken into account the 3GPP definitions on performance related data.

From tests without implementing ATS, it is derived that DL transmission power is not representative of congestion in the cell, and percentages of the values of individual transmission powers have been used instead. A pre filtering counter has also been introduced to avoid ping-pong effect.

Simulations with different service mix cases show capacity gains around 30% when ATS is running. A dynamic study case in which DL started to jeopardize capacity by the end of the observation time has been simulated. By adjusting dynamic and appropriately the SHO parameters, a reduction in DL resources consumption is possible. In particular, the control algorithm acts in a totally distributed manner and parameters are modified in a cell by cell basis. This allows a margin in the available power, in particular between 2 and 3 dB. Thus, the approach is able to stabilize the network and delay congestion control mechanisms. Indeed, regarding the % of UEs in degraded mode, a reduction from 70% to 6% was obtained for the worst case.

Finally, among the three considered monitoring cases, the most conservative one reacts faster but generates more reconfigurations. The less conservative also guaranteed network performance but degradation of UEs was not uncommon, although limited within an acceptable range, mostly below 5%, with occasional peaks of up 6%.

Chapter 8

Performance Improvement of 3G/3.5G Networks through Dynamic Code Tuning

8.1 Introduction

Along the previous chapter the problem of load balancing between UL and DL was addressed. A strategy for supporting the limiting link was proposed and discussed, so that capacity is further maximized and congestion control mechanisms delay their actions when one of the links is overloaded. However, with the aim of providing higher rates to DL and UL, UMTS Rel'5 [3GPc] and Rel'6 [3GPb] introduce new improvements through HSDPA and its counterpart HSUPA (High-Speed Uplink Packet Access). Within this context, the objective of this new chapter is to analyze the potential improvements that could provide the incorporation of an ATS on the HSDPA technology when it is deployed coexisting with UMTS Rel'99. In this sense, along the chapter it is assessed to which extent it is worthwhile to make a dynamic management of its three most important resources: Devoted power, codes and percentage of users assigned to Rel'99 and HSDPA.

From the study, one of the first conclusions reached is that the benefits of HSDPA are so high that in general, there is no clear benefit in introducing an ATS to manage power or the percentage of UEs assigned to HSDPA, both can be handled by straightforward rules-of-thumb. However, code allocation deserves a further study. Indeed, the main novelty of this chapter is the proposal of a full ATS so that the number of codes assigned to HSDPA is dynamically adjusted according to the CQIs reported by the UEs. Thus, a mid-term reservation mechanism is designed to guarantee that HSDPA performs at its most efficient level while guaranteeing blocking and dropping criteria. The proposal follows the functional architecture described in Chapter 7.

8.2 HSDPA Overview and Challenges

HSDPA features provide a reduction in the cost per megabit through quite a smooth and simple update from pure 3G systems. In fact, many operators are offering some kind of broadband service, which is the consequence, or maybe the cause, that the demand for wireless data services is growing faster than even before. Indeed HSDPA is a first step towards a further boost of data services usage. New improvements to this technology have been defined at Rel'7 HSPA+ (also called Evolved HSDPA) [3GPe].

Rel'5 HSDPA has been designed with different performance enhancing features to support theoretical data rates up to 14 Mbps (28 Mbps in HSPA+ DL). New and fast mechanisms are introduced into the Medium Access Control (MAC) layer to adapt the data rate to propagation channel conditions, being mainly coding and adaptive modulation (QPSK / QAM-16, also QAM-64 in HSPA+), fast Hybrid Automatic Repeat Request (H-ARQ) and fast scheduling based on a shorter Transmission Time Interval (TTI) of 2 ms. In addition to this, the H-ARQ mechanism and the scheduler themselves are located in a new MAC sub-layer, denoted as MAC-hs. The MAC-hs is located in the Node-B which leads to an almost instantaneous execution of H-ARQ and scheduling decisions.

HSDPA also introduces some changes in the UTRAN physical layer. Whereas Rel'99 originally defined three different techniques to enable DL packet data, in practice the DCH over the Dedicated Physical Channel (DPCH) is the primary means of supporting any significant data transmission. The Forward Access Channel (FACH) transmitted on the Secondary Common Control Physical Channel (SCCPCH) is an alternative way though much more inefficient. It must be generally received by all UEs in a cell's coverage area and that is why high SFs (SF128 or SF256) are usually employed [CBG+06], moreover, macro diversity or fast power control are not supported. Finally, the third mechanism is the Downlink Shared Channel (DSCH) which was not widely adopted or implemented for FDD and was eventually removed from the specifications [3GPa].

With DPCH transmission, each user is assigned a dedicated OVSF code with a SF dependent on the required data rate. Precisely, one of the novelties that allows HSDPA achieving high data rates is the allocation of multiple codes to a single user. Indeed, to support HSDPA, three new physical channels have been defined [3GPi]. First, the High Speed Physical Downlink Shared Channel (HS-PDSCH) is a SF16 DL channel carrying the data payload and supporting both time and code multiplexing: Several UEs can be assigned to different HS-PDSCHs in the same TTI. Second, the High Speed Dedicated Physical Control Channel (HS-DPCCH) is an UL channel in which each operating HSDPA UE reports the acknowledgements of the packet received on HS-PDSCH and also the CQIs, which can be used by the Node-B scheduler to decide the next UE to be served and the associated Transport Format (TF). And third, the High Speed Shared Control Channel (HS-SCCH) is a fixed rate (SF128) DL channel used to communicate to UEs the scheduling and control information relating to each HS-PDSCH. It is remarkable that a HSDPA UE must always have an associated DCH to carry the UL user payload and to

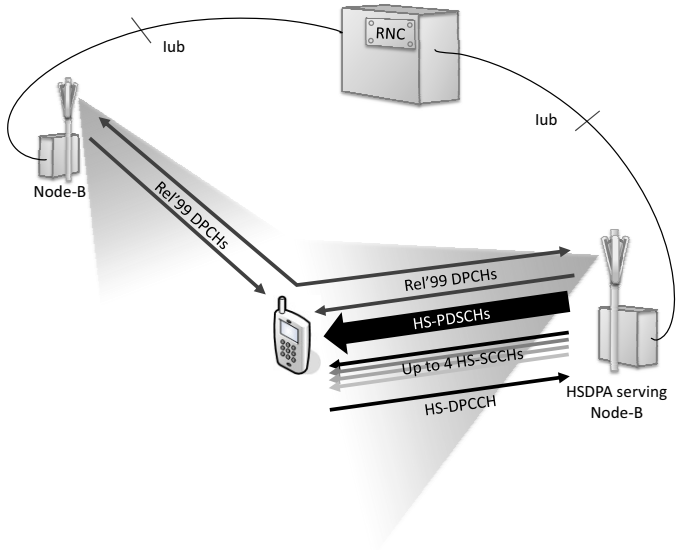

Figure 8.1: HSDPA associated channels in a SHO situation.

transfer the Layer 3 signalling. Whereas, the HSDPA specific physical channels do not support SHO, the associated DCH uses this mechanism normally. All these channels are graphically summarized by Figure 8.1 in which the UE is in a SHO area.

Apart from the improvements included in the standards, the RRM algorithms that are implemented in the vendor equipment are a key factor to the success of HSDPA. Since the design of these algorithms is not defined by 3GPP, several investigations are being carried out to find the best possible implementations. For example, thanks to the new 2 ms TTI, opportunistic schedulers are now a fairly interesting option to exploit the time-variant nature of the radio channel to increase the cell throughput. Indeed scheduling strategies are being the main focus of existent literature on HSDPA. Further details on this topic are given in Appendix C.

Other aspects susceptible of study and improvement are stated in [TWLK07], which propose practical considerations in realistic HSDPA deployments through lab and field testing. Among the technical features that are mentioned and susceptible of improvement, two of them are not usually addressed in the literature:

1. **Link Adaptation:** Regards to the aggressiveness in the TF selection. In this sense a trade-off exists between an under-use of cell capacity and a degraded performance because of excessive retransmissions. Conclusions from [TWLK07] recommend dynamic NACK rate target control.

2. **HS-DSCH Serving cell change:** Since macrodiversity is not considered in HSDPA, depending on the implementation, the transient period after a cell reselection can vary from a few milliseconds to several seconds, with the

consequent UE degradation. This aspect is out of the scope of this dissertation.

Finally, when a single carrier is shared between Rel'99 and HSDPA itself, mechanisms to efficiently manage shared resources must be designed and introduced to avoid disadvantaging one of the technologies. In particular, these resources are power and OVSF codes. Eventually HSDPA capable users could be susceptible of management and be directed to Rel'99 or HSDPA according to certain criteria. These three aspects are covered along Section 8.4. In particular, concerning power and UEs management, a study has been done with the help of simulations and straightforward engineering rules have been derived. On the other hand, automatic tuning based strategies are revealed to be good candidates to track the optimum code allocation along time and maximize the cell throughput while guaranteeing blocking and dropping criteria.

Since simulated examples soon appear in the text, the particularities of the scenario and simulation conditions are described in next section, prior to the study.

8.3 Scenario and Simulation Conditions

500 users have been spread around the scenario described in Appendix B.3. Unless the contrary is stated, 50% of users are supposed to use a high speed packet switched service and so, they are redirected to HSDPA when becoming active. The other 50% of users remain at Rel'99 and make use of one standard DCH.

Regarding HSDPA-capable terminals, twelve different categories exist [3GP1] offering maximum data rates ranging from 0.9 to 14 Mbps. These differences are due to the ability of the UE to support both QPSK and 16-QAM or solely QPSK. Also because of the maximum transport block size (TBS) transmitted in a single TTI as well as the inter-TTI interval, which can be 1, 2 or 3 ms. The maximum number of HS-PDSCHs that the UE can simultaneously decode also affects the maximum achievable rate. And finally, because of the number of soft bits that can be buffered by a UE in the active H-ARQ processes, which does not directly affect the peak data rate but the effective throughput. Simulations consider UEs of highest capabilities, i.e. category 10, which support both QPSK and 16-QAM, they can also decode up to 15 simultaneous HS-PDSCH codes with a maximum TBS of 27952 bits in one TTI with a TTI interval of 1 ms (i.e. consecutive HS-PDSCHs can be decoded) and with an incremental redundancy buffer size of 172800 bits. Regarding the traffic modeling, since the objective is to determine the maximum HSDPA capacity per cell, traffic buffers are assumed full during the simulation time. The service is considered to be a delay-tolerant and best effort one, so scheduling can be conducted without considering minimum requirements.

Rel'5 specifications do not stipulate power controlling HS-SCCHs and this decision is left to the infrastructure vendors. Avoiding this would lead to unnecessary power reservation and consequently to poorer throughput of data channels. Simulations consider that these channels are power controlled. Although a dynamic HSDPA power allocation is chosen for simulation, even in the case of presupposing

a fixed amount of HSDPA power, the quantity devoted to HS-PDSCHs would vary in a TTI basis and according to the radio channel condition of the UEs to be served.

Initially, users are considered to be uniformly spread around the network, nevertheless other mobility situations are also considered and are explained in the corresponding sections. The number of HS-SCCHs is kept to the maximum possible value, i.e. the minimum value between 4 and the number of HS-PDSCHs. Finally, the correspondence between the CQI values and the selected TFs was obtained from the AROMA research project, which is an IST Project from the *6th Framework Program of the European Community* [ARO].

It is worth remarking that in previous chapters, when considering Rel'99 based systems, traffic was quantified in terms of number of users and corresponding channel usage, each user was assigned a DCH. In HSDPA, however, because all user traffic is carried through a DL shared channel, a different approach to dimensioning is necessary. The important dimensioning output is now the average throughput. For example, interesting evaluation measurements for the operator are the average user throughput and average cell throughput. Indeed during the initial phases of HSDPA planning, the objective is to estimate the mean or maximum physical layer data rate achievable at the cell edge [TE06], [ZS05].

8.4 Planning and Deployment Aspects

Some specific aspects on implementing HSDPA are addressed in this Section and potential dynamic enhancements to be implemented as part of RRM algorithms have been evaluated. In particular, two different scenarios can be typically considered [CBG+06]:

1. **One-to-one overlay:** HSDPA is provided through a different and dedicated carrier, and, by means of an interfrequency handover, high speed UEs can be directed to the corresponding HSDPA carrier. However, the question that arises is if HSDPA capable users should be directly transferred to the high speed carrier or, on the other hand, if serving some of them by Rel'99 could imply a benefit, in particular a cell throughput benefit. Simulations have been run to evaluate this and Figure 8.2 shows the main result, the evolution of the cell throughput for different percentages of high speed users served by HSDPA. It must be recalled that 50% of the total UEs are considered to be HSDPA capable but only the value indicated by the abscissa is served by this technology.

   It can be observed how the central cell throughput increases as soon as UEs are transferred into HSDPA. Consequently, if the cell throughput is aimed to be maximized, traffic balancing should lie in that all HSDPA capable users are directly assigned to the HS carrier. Considering a different UE allocation would render into a reduction of the cell throughput.

   The new technology advantages are so clear that DCHs usage would be only justified when the service imposes hard constraints over delay and jitter and

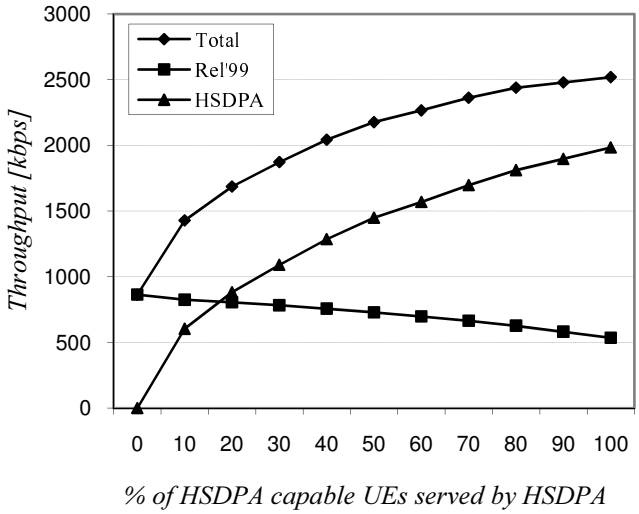

Figure 8.2: Cell throughput for different number of UEs served by HSDPA.

the HSDPA load is such that the required QoS cannot be granted by the scheduler. Therefore, the management is reduced to include an appropriate AC algorithm and a QoS aware scheduler.

The one-to-one overlay strategy is of simple management but at the expense of an inefficient use of the spectrum. Besides, using a different channel prevents users from using voice and high speed data services at the same time. Even though VoIP is a potential solution that is expected to be deployed widely in the future, operators will still face the problem of choosing how many radio channels at each BS should be devoted for HSDPA to support legacy terminals. Finally, the possible limited number of carriers per operator and the costs and issues associated with upgrading to a multicarrier network are important drawbacks as well.

A particular case of this scenario would be deploying the second carrier with HSDPA only in hotspots, where smaller, localized, high-demand areas are served by micro or picocells. In contrast with a macrocell environment, higher peak data rates can be achieved. Nevertheless, in indoor environments, HSDPA could only be enabled if the UE previously had coverage from the macrocell layer. Otherwise it would be unable to enter the network and execute the corresponding handover. This issue is an important drawback provided that the existing macrocell network has not a deep coverage indoors.

2. **Single carrier shared between Rel'99 and HSDPA:** In this second approach a single carrier shares all types of traffic. Spectrum is now more efficiently used but several issues not defined by 3GPP must be tackled carefully. In particular, the allocation of the two remaining basic resources to be shared between HS and Rel'99 users: Power and codes. Both topics are developed and studied in subsequent sections and, unless the contrary is stated, this de-

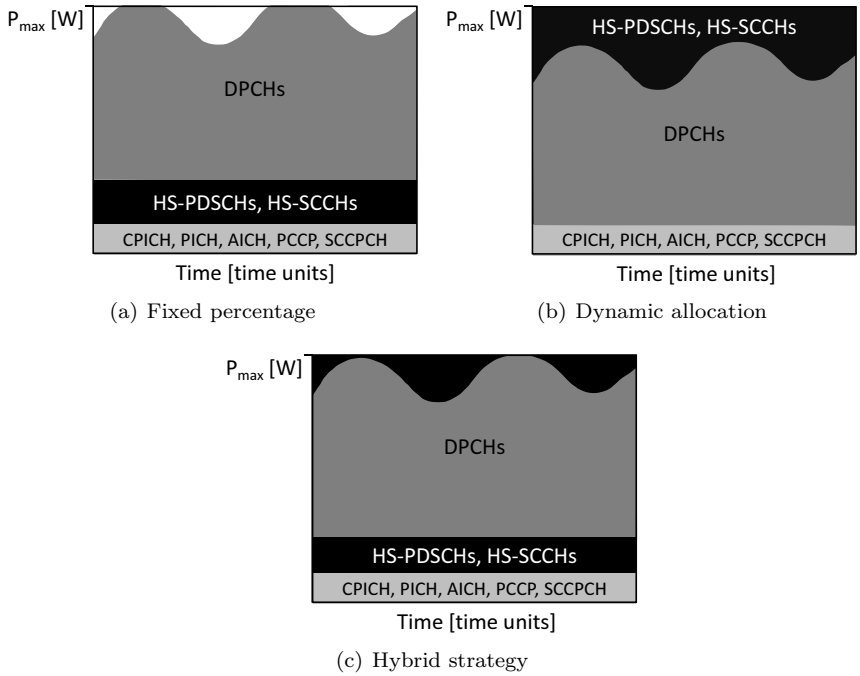

(a) Fixed percentage

(b) Dynamic allocation

(c) Hybrid strategy

Figure 8.3: Strategies for HSDPA power allocation.

ployment option (one shared single carrier) is the one considered in the rest of the chapter.

8.4.1 On the Automation of HSDPA Power Allocation

Regarding the power to be assigned to HSDPA, the usual strategies are:

1. Some providers design their equipment so that HSDPA power is fixed as a percentage of the total available DL power (see Figure 8.3(a) where P_{max} represents the maximum allowable transmission power).

2. Others allow a dynamic allocation on the basis of usage of non-HSDPA users. That is to say, HSDPA can only consume the power left by Rel'99 (Figure 8.3(b)). In certain cases, a margin below the maximum power in the Node-B can be adjusted to avoid excessive interference.

3. Finally, some authors propose fixing a minimum amount of planned power devoted to HSDPA and, if available, dynamically allowing more power up to a certain maximum threshold [MSS07] (Figure 8.3(c)).

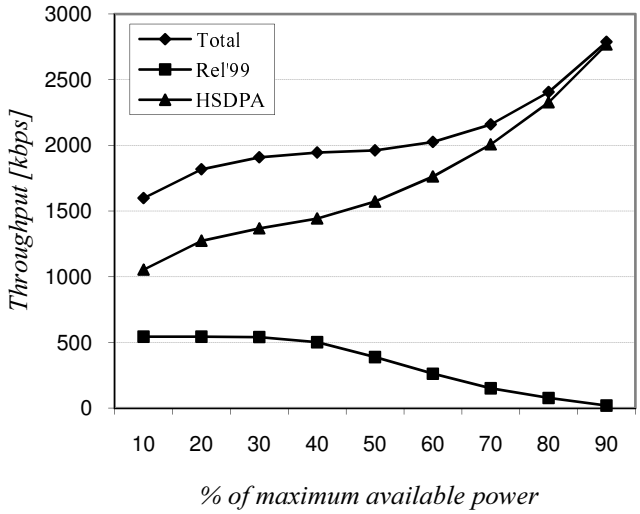

Figure 8.4: Cell throughput for different % of the maximum power allocated to HSDPA.

Approach 1 is not straightforward since the amount of power devoted to Rel'99 or HSDPA will tend to benefit one or the other type of users. This effect has been quantified by means of simulation. In particular Figure 8.4 shows the cell throughput when different percentages of the maximum power are allocated to HSDPA. It can be seen that the higher the HSDPA power, the better the total cell throughput is, but at the cost of degrading DCH connections. In this particular case, when 40% or more of the total power is reserved for HSDPA, the degradation probability is not null, the Node-B starts to lack power to correctly serve Rel'99 UEs.

In general, operators currently aim at guaranteeing DCHs required power. So, with approach 1, an estimation of the power to be consumed by Rel'99 must be previously done, for example by analyzing reports from Nodes-B. This analysis is subsequently done continuing with the same example. In particular, Figure 8.5 shows the Probability Density Function (pdf) and Cumulative Distribution Function (cdf) of the power that could be devoted to HSDPA once all Rel'99 UEs are served, that is to say, using approach 2. For this particular scenario, it can be calculated that the mean power used by HSDPA is close to 40 dBm. If this value is fixed and guaranteed, there will be resource shortage in DPCHs power control 50% of the time. A more acceptable value for the probability of degradation might be 3%, value that yields the reservation of 37.5 dBm for HSDPA. This corresponds to a 28.18% of the maximum available power (43 dBm). On the other hand, under these circumstances, in 97% of cases, Rel'99 UEs use less power but the extra amount will not be used by any channel. For example, according again to Figure 8.5, with a probability of 50% there would more than another margin of 37.5 dBm of unused power (probability of having equal to or more than $37.5 + 3 = 40.5$ dBm unused by Rel'99). Therefore, by fixing a certain amount of power, resources shortage can be controlled and take place with a minimum probability but at the cost of wasting an important part of them in an elevated percentage of the time as well.

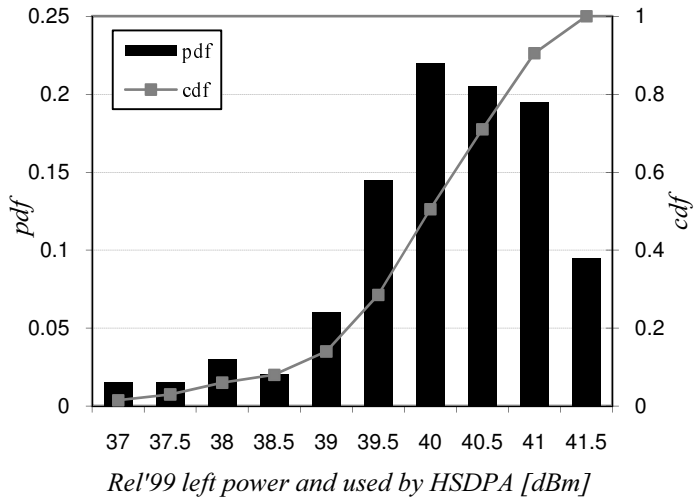

Figure 8.5: pdf and cdf of power devoted to HSDPA with a dynamic allocation policy.

Of course, one possibility to improve this static approach would be to define a long-term automatic tuning. Taking into account the expected needs of Rel'99 UEs, HSDPA power might be adjusted to a higher or lower level along time. Nevertheless, the point is that the finer this tuning is done, the closer it will be to approach 2, so it would be wiser and more natural adopting the second strategy directly.

Within approach 2, HSDPA users are served with a best server like policy. The available power is the remainder not being used by DCH channels and, as previously seen, allocating less power leads to poorer cell throughput. On the other hand, no peak throughput can be guaranteed at the cell edge, and an increase in the number of Rel'99 users implies a throughput and coverage decrease of high speed services.

Finally, strategy 3 is just a mixture of both approaches and tends to 1 or 2 just according to the adjustment of its thresholds.

From the previous paragraphs, there is no clear justification to investigate the adoption of an ATS to manage HSDPA UEs allocation or devoted power. All HSPDA capable UEs should be transferred to this technology to maximize the cell throughput but only if the scheduler is able to cope with delay constraints, which can be guaranteed by using a proper AC combined with a QoS aware scheduler. On the other hand, HSDPA should just consume the power left over by Rel'99 to guarantee DCH operation. Otherwise, to assure a certain HSDPA throughput at the cell edge, a fixed amount of power could be allocated but at the cost of losing maximum DCH performance. The value to reserve can be easily found by means of link budgeting. Simple and effective rules to dimension HSDPA to provide the required average data rate at a given coverage probability can be found in [ZS05].

8.4.2 On the Automation of HSDPA Code Allocation.

The final shared resource to be considered for analysis is the percentage of the OVSF code tree to be assigned to each technology. This aspect must also be carefully considered when deploying HSDPA over one existing Rel'99 carrier. The current subsection establishes the problem behind this topic and it is widely studied in the rest of the chapter.

The number of OVSF codes that are assigned to each technology must take into account different QoS requirements as for example cell throughput, throughput per user or blocking constraints. Since each HS-PDSCH uses a SF16 code, up to 15 codes could be allocated to HSDPA. However, this configuration in a single carrier would leave Rel'99 users with almost no codes or even without any of them. Figure 8.6 shows this situation graphically, it represents the utilization of the OVSF code tree when 15 HS-PDSCH are used. In this example, only one HS-SCCH is used and therefore, only one user could be scheduled at each TTI. So, the code tree occupation would even be worse if 4 HS-SCCH (maximum possible number) had been reserved. Moreover, for each active HSDPA user there must be an associated Rel'99 DCH (with a minimum SF of 256), so the full code tree occupation is obvious. Of course, 15 HS-PDSCH codes plus 4 HS-SCCH only leaves 2 SF256 codes free, so only 2 HSDPA UEs could be active and it would make no sense allowing 4 to be scheduled in one TTI. Under these circumstances, no codes would be available for Rel'99 UEs. With only one carrier in the cell, this configuration might only cohabit with Rel'99 UEs if a secondary scrambling code were used. This would be at the expense of extra interference because of the lack of orthogonality between channels.

So, given two certain amounts of traffic to be served between Rel'99 and HSDPA, the first question to answer is how the codes should be assigned to meet QoS targets. Besides, two more questions can be posed, firstly if this assignment is dependent on changes in traffic patterns, and secondly, if it should be considered for inclusion in the ATS of an evolved 3G network. These questions can be answered by analyzing the behavior of an operative network and deriving statistics to find trends. Likewise the previous chapter, static simulations are run whose results are covered along the next section. Once statistics and trends are obtained, it is shown that performance gains appear if the number of codes for HSDPA is not fixed to a particular value but changed dynamically according to certain KPIs. Given this, the complete ATS functioning is explained and studied.

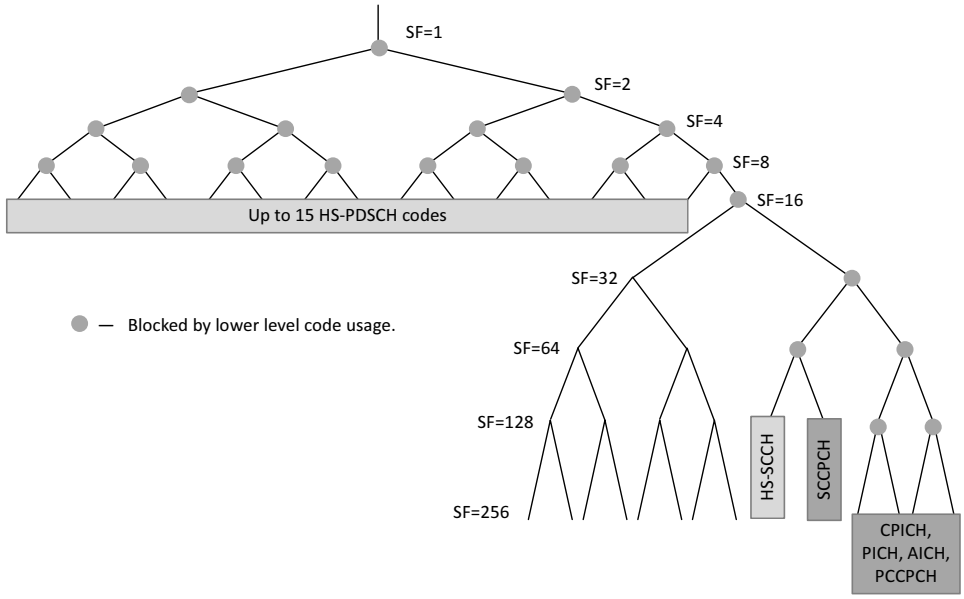

Figure 8.6: Example of OVSF code tree usage for a 15 HS-PDSCH reservation.

8.5 ATS Description and Results

8.5.1 Learning & Memory Stage

As it was stated with SHO ATS, in an operating network, the process of gathering real data to accumulate statistical information and find and update trends corresponds to the *Learning & Memory* block. Similarly to the former chapter, this process is approximated by means of simulations whose results could be eventually used as an "Initial Training", previous to the real learning from network data.

Cell Throughput Analysis with Different Code Allocations

Given the previous paragraphs, Figure 8.7 represents the mean throughput for both HSDPA and Rel'99 as a function of the number of codes assigned to HS-PDSCHs. The accumulated final throughput of the cell is also plotted.

Regarding the evolution of Rel'99 throughput it is fixed by the number of admitted users and starts to decrease as soon as blocking appears. For more than 4 codes assigned to HS-PDSCHs its contribution to the cell global throughput is far less important than that of HSDPA.

On the other hand, HSDPA throughput shows a monotonous increase until 8 codes are allocated. The initial upwards trend is very fast, particularly if compared with the evolution from 5 to 8 codes. This sharp initial increase denotes that most

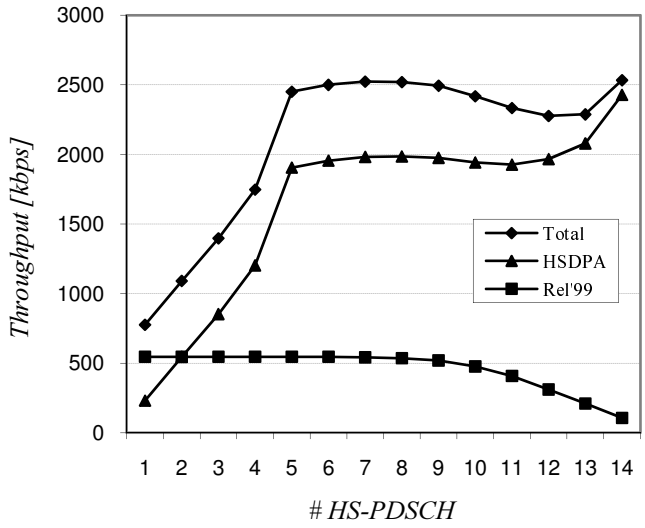

Figure 8.7: Throughput for different number of HS-PDSCH.

UEs report a CQI equal or higher than the first TF using 5 codes. That means individual peak rates equal or higher than 1.659 Mbps could be assigned to most UEs. However, due to the lack of codes, inferior TFs are used. Because of this, not all the power left by Rel'99 UEs can be used. This fact is illustrated by Figure 8.8 which depicts the evolution of HSDPA power. The particular values obtained in each snapshot and the mean is shown for each case. As expected there is a strong correlation between this graph and the HSDPA throughput. From 5 to 11 codes allocation, the power is maintained fairly constant both in mean and variance, most of the Rel'99 left power is being successfully used. The final power increase indicates that more power is available from Rel'99, the reason behind this is explained later.

The throughput increase is restrained after 5 codes assignment. This is due to UEs with CQIs allowing TFs with 7, 8, etc. HS-PDSCHs are not frequent. Furthermore, TFs do not have all the possible number of codes, for example none of them uses 6 HS-PDSCHs, the same happens with 9, 11, 13 and 14 values. Therefore, these combinations only give the chance to multiplex more users per TTI but will not contribute to rise the individual peak rates.

The final throughput increase for 12, 13 and 14 codes is justified by the growth in the transmitted HSDPA power. This extra power is justified by the rise in Rel'99 blocked UEs which means less UEs to be served by the Node-B. In fact, for more than 6 HS-PDSCH codes, the Rel'99 blocking probability starts to be non-zero.

Scheduling Considerations

The previous results were obtained considering a Round Robin (RR) scheduler. However trends and conclusions are rather independent on the algorithms and only

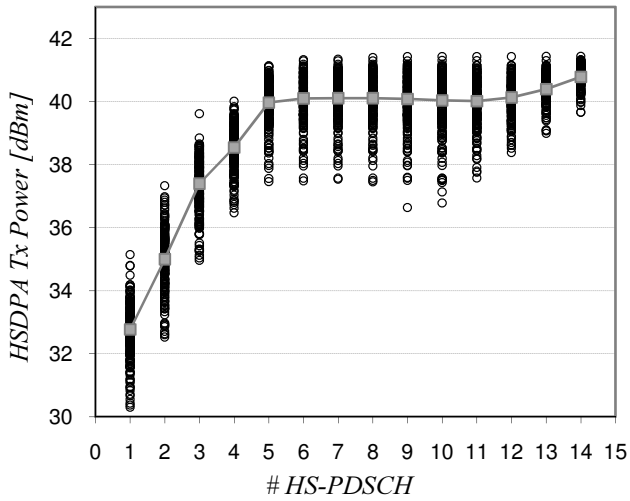

Figure 8.8: HSDPA power. Snapshot values and evolution of the mean.

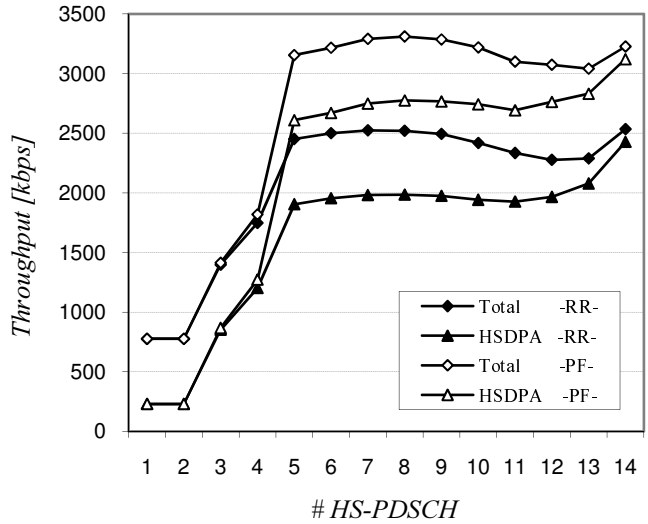

Figure 8.9: Cell throughput for different number of HS-PDSCH and scheduling policy.

absolute values are expected to change. Appendix C contains a description of current scheduling strategies. Differences between approaches are discussed and a review of the existent literature in the context of HSDPA is done. Given this, it is evident that the variety of scheduling strategies is huge but Proportional Fair (PF) and its variations arise as one of the most interesting options. For this reason, this algorithm was also incorporated to the simulator and results from Montecarlo tests were also obtained for this scheduler.

In particular, Figure 8.9 contains the evolution of the throughput for both PF

and RR. Rel'99 throughput has been omitted because curves are identical in both cases and do not provide new information, they can be easily derived. It can be observed that the new case passes through the same states as RR but with higher throughput values. The Figure also shows how the gain for allocating 8 codes instead of 5 is slightly higher in PF. Whereas in RR, this gain is just of 80 kbps, with the second scheduler reaches 166 kbps. In this sense, the results in [TWLK07] reveal that maximum PF gains in HSDPA scenarios are obtained under low mobility conditions, which is the case of current simulations (3 km/h). For stationary and vehicular conditions the gain is minimal and both curves would remain almost identical.

It is also noticeable that for a reservation under 5 codes, the throughput differences between both schedulers are negligible. Because of the lack of available codes, PF cannot take profit of good channel conditions and UEs are served under their possibilities.

Power Assignment in Multiuser Scheduling

The scheduler takes decisions on when to serve a particular user but it has also to rule the assignment of power. Particularly, taking into account that code multiplexing is supported by HSDPA, besides it is important the strategy used to allocate power levels when more than one UE is scheduled in one TTI.

When studying scheduling algorithms for HSDPA, most proposals consider one single user to be served in each TTI and therefore code multiplexing is usually missed. However, this strategy may not be optimal, particularly if there are delay constraints or if the traffic is too bursty, so that no single user may be able to fully use the available capacity. A recent contribution, [VB07], does propose a multiuser scheduling schema for CDMA packet data systems, sharing power among code multiplexed users and taking profit of this to increase cell throughput.

One of metrics aimed to be found is maximum capacity, and that is why buffers are considered full during the observation time. Despite this fact, there is another reason that leads single user scheduling to sub-optimality: the existence of a finite set of TFs. According to the reported CQI, the scheduler selects the best TF that guarantees the required Carrier-to-Interference-plus-Noise-Ratio (CINR). Consequently, a "quantification" is done and some resources are left, which might be potentially assigned to other terminals. The required CINR increases linearly in dB from TF to TF, so in linear units the differences between target CINRs increase as the TF is higher. Hence, the quantification is only noticeable for non low CQI values.

The adopted approach considers that, after the scheduling algorithm has prioritized users, the first one is served according to its reported CQI and the needed power is allocated to achieve the highest possible rate. Next, with the remaining power (if available), it is analyzed if a second (or third and fourth) UE can be served. This implies that the first scheduled user consumes power greedily and the next ones are a try to maximize the use of the total available HSDPA power. That is why these secondary users are not marked as "served" if the RR policy is being used

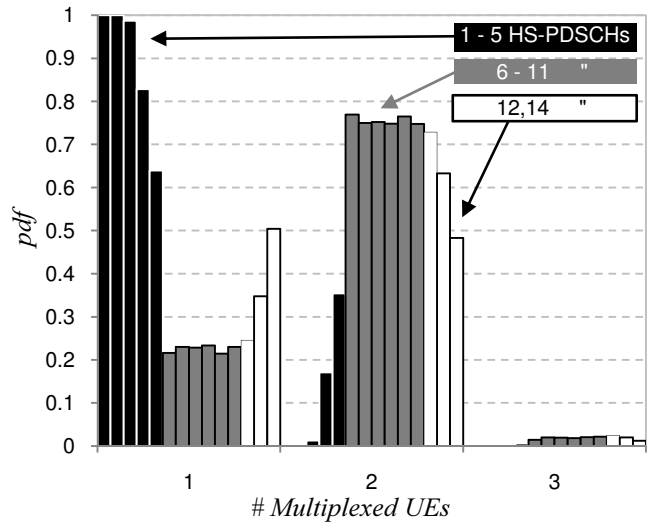

Figure 8.10: pdf of number of multiplexed UEs for different number of HS-PDSCH.

and could be again considered in the next TTI. If PF is applied the transmitted bits do contribute to the average throughput calculus needed to prioritize UEs.

Because of this criterion, multiplexing more than two users was hardly done. This can be seen in Figure 8.10, in which the probability of having 1, 2 or 3 multiplexed UEs is represented, the 4 UEs case is omitted because never occurred. From 1 to 5 HS-PDSCHs the pdf is plotted in black. It can be observed that, when allocating from 1 to 3 codes, the probability of serving more than one UE is practically null. In this cases the HSDPA available power is inferior, so eligible TFs correspond to lower peak rates, the quantification is low and the scheduler assigns a TF requiring a CINR very close to that derived from the reported CQI. No power is left for new UEs. When 4 and 5 codes are used, the probability of multiplexing two UEs increases up to 35%. But it is not until the 6 codes case, that a second HS-SCCH is clearly present. From 6 to 11 codes, the pdf is plotted in grey. As in the two previous figures, the behavior is maintained. This evolution is consequent with the power availability in each case and the fact that the users are homogeneously distributed, which implies a wider range of possible reported CQIs. Finally, cases 12 to 14 are plotted in white, more power is available for HSDPA and so TFs of higher rates can be assigned, the number of multiplexed UEs is slightly reduced. Finally, the probability of having 3 simultaneous UEs is so low that its contribution to the final mean throughput is negligible.

When considering PF, the probability of multiplexing more than one UE is reduced. Since the users are prioritized taking into account channel conditions, on average higher level TF are selected and more power is used per user. In particular, for 6 codes and more, the reduction is around the 20%.

From the previous paragraph an indirect fact can be derived. It can be stated

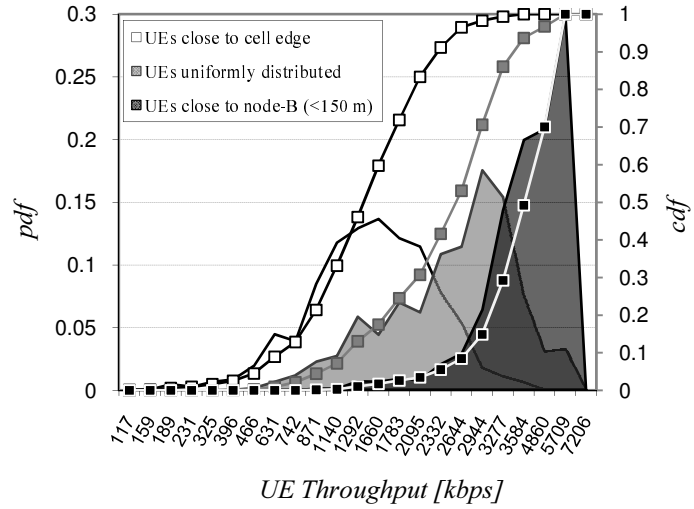

Figure 8.11: UE throughput pdf and cdf for different geographical distribution.

that if an ATS is designed to control the number of allocated HS-PDSCH, when the reservation falls below 4, the number of HS-SCCH could also be reduced from 2 (or 3) to 1. Although HS-SCCH occupy a small fraction of the OVSF tree (SF128), removing two HS-SCCHs might imply an extra SF32 code (Figure 8.6).

Going back to the analysis of throughput for different OVSF codes allocations, it should be taken into account that, in operative networks UEs are not always homogeneously distributed. In fact, certain cells can have most of their users concentrated in particular areas. So, the CQI reports can be different and consequently the HSDPA TFs, assigned data rates and the cell global throughput. This aspect is addressed along next Section.

Impact of Heterogeneous UEs Distribution

In order to quantify the impact of different channel conditions on the cell global throughput, results have been obtained for two extra scenarios. First, considering that most of UEs are positioned far from the Node-B and, second, UEs concentrated around the Node-B, at a distance inferior to 150 m. In this sense, Figure 8.11 represents the pdf and cdf of the individual UE throughput for the three considered situations, uniform distribution and both cases of user accumulation. The graphs consider an 8 HS-PDSCH allocation.

As expected, far away UEs report lower values of CQI which imply poorer throughputs. The closer the UEs to Node-B the higher the throughput per user. For instance, when UEs are concentrated in an area of 150 m radius from the Node-B the individual peak throughput is higher than 3.5 Mbps with a 50% probability.

In order to quantify the impact of these different channel conditions on the cell

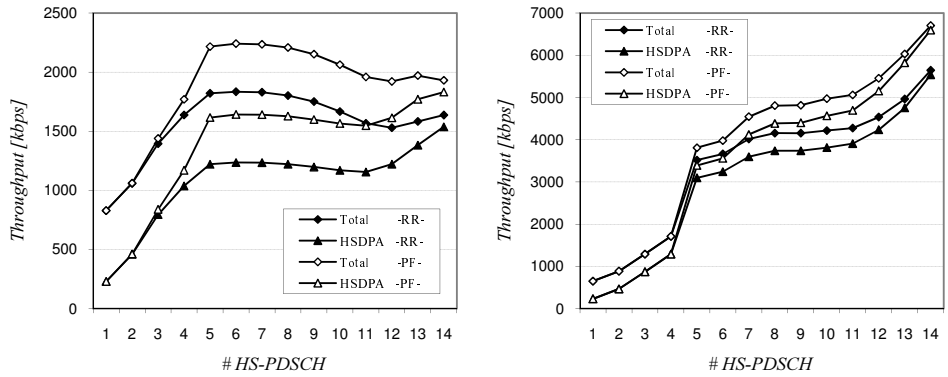

(a) UEs close to cell edge. (b) UEs close to Node-B (< 150 m).

Figure 8.12: Cell throughput for different number of HS-PDSCH and UEs distribution.

global throughput, Figure 8.12 represents its evolution for different allocations of HS-DPSCH. Both new scenarios with users close to the cell edge 8.12(a) and close to the Node-B 8.12(b) are represented. From the graphs, it can be observed that when UEs are mostly far from the Node-B, there is no gain in reserving more than 5 codes to HSDPA. Reported CQIs are low and those extra codes would be hardly used. In fact, assigning more than 7 codes would even imply an important reduction in the cell global throughput, up to 320 kbps.

On the other hand, having UEs close to the Node-B implies far higher levels of throughput and another optimum value for code allocation. In particular, the curves in the graph lead to the rule: The higher the number of HS-PDSCHs, the better. The 5 codes allocation does not represent a saturation point now and important throughput gains are obtained thanks to the UEs spatial distribution and the corresponding improved RF conditions. It can be compared the maximum average throughput of 2240 kbps obtained with PF scheduling when UEs are close to the cell limit with the 6702 kbps when they are close to the center, nearly the triple. Nevertheless, under these circumstances, it is blocking probability that upper bounds the number of codes to reserve, as it is studied along next section.

Given the previous paragraph, the optimum code allocation is fairly dependent on the users spatial distribution, or rather on their reported channel conditions. That is why CQI reports, and in particular its histogram, can be used to obtain which are the predominant channel conditions of HSDPA connections in the cell. In this way, whenever it is detected that RF channels improve, more codes might be reserved to HSDPA. If these conditions worsen, part of the code tree could be released since not only it would not give any throughput gain, but could even imply losses. Hence, the complete ATS proposal is depicted by the flow diagram in Figure 8.13 and next sections contain a description of its different steps.

To design an ATS capable of performing this intelligent reservation, it is neces-

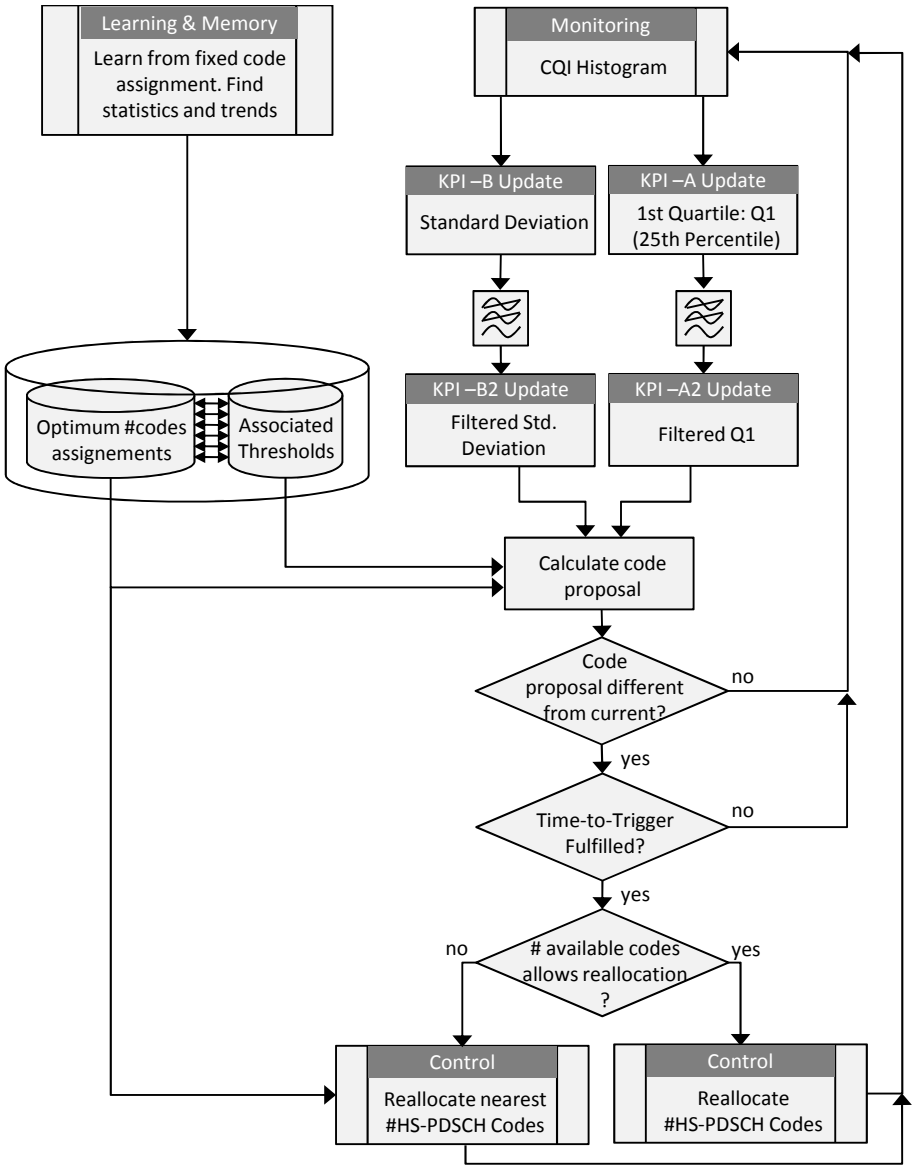

Figure 8.13: Complete ATS proposal.

sary to evaluate the effects that different codes selections have over several aspects of the network. This study is needed so that an upper limit to the number of allocable codes for HSDPA is established. Blocking was already mentioned and it is the first parameter to be studied. Subsequently, variations on SHO areas as well as induced degradation in Rel'99 UEs are investigated.

Effects on Blocking Probability

In this set of simulations, the assumed AC algorithm only takes into account the code tree occupation. No other criteria are introduced to avoid side effects that could hinder the analysis. It is important to comment that HSDPA blocking is also possible because HSDPA UEs also need an associated DCH, as was explained in Section 8.2. Assuming, that the OVSF is perfectly managed and appropriately updated to optimize its occupation, the number of free codes for an specific SF, $F(SF_i)$, can be easily found as the total number of codes ($=SF_i$) minus the occupation due to signalling from both Rel'99 and HSDPA, $Occ_S(SF_i)$, and the occupation of Rel'99 and HSDPA UEs, respectively $Occ_{R99}(SF_i)$ and $Occ_{HS}(SF_i)$. All this is summarized by Equation (8.1).

$$\begin{aligned} F(SF_i) &= SF_i - Occ_S(SF_i) - Occ_{R99}(SF_i) - Occ_{HS}(SF_i) = \\ &= SF_i - \left\lceil SF_i \left(\frac{3 + N_{HS-SCCH}}{128} + \frac{N_{HS-PDSCH}}{16} + \sum_{j=1}^{N_{serv}} \frac{N_{UE,j}}{SF_j} \right) \right\rceil \end{aligned} \tag{8.1}$$

Where:

- $\lceil x \rceil$ denotes the ceiling function, which returns the smallest integer not less than x.
- $N_{HS-SCCH}$ and $N_{HS-PDSCH}$ are the number of channels whose type is indicated by the subindex.
- N_{serv} is the number of different services, or rather, the number of different SFs used in the cell.
- $N_{UE,j}$ is the number of UEs using SF_j.
- Finally the number 3 in the first fraction numerator is the occupation of Rel'99 signalling channels, which corresponds to three SF128 codes as was shown in Figure 8.6.

Figure 8.14 shows the blocking probability for both Rel'99 and HSDPA UEs. According to this graph, HSDPA blocking probability starts to be non zero for 9 codes and above. Rel'99 users experience a higher blocking because they are more

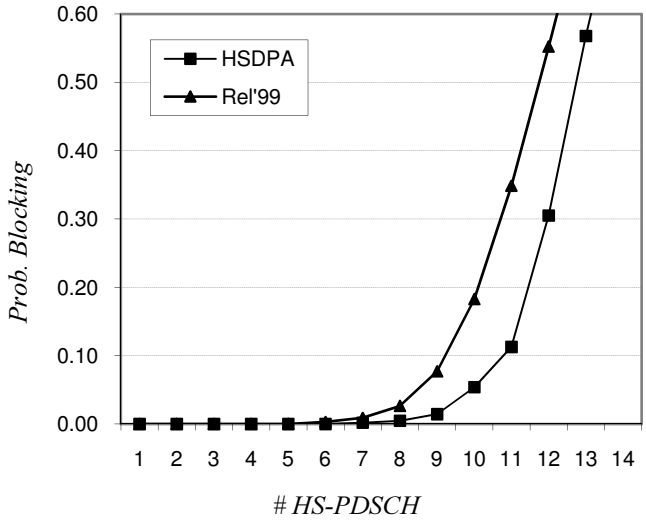

Figure 8.14: Blocking probability for Rel'99 and HSDPA users.

demanding in terms of code tree occupation, they use a 64 kbps data service with an associated TF having a fixed SF32 (vs. SF256 for HSDPA DCHs).

Therefore, using more HS-PDSCHs favors HSDPA throughput in general but also impacts negatively in its blocking indicators. For a higher number of codes allocated, the admitted HSDPA UEs can potentially use more channels and be served with a higher rate but at the expense of an increased blocking. Even a paradoxical behavior might appear for the more restrictive cases (12, 13 and 14 codes) and in fact it was present in a few simulated snapshots: Because of favoring too much HSDPA, no HSDPA UEs are able to access the cell. This happens when Rel'99 UEs occupy all the codes available for DCHs, which can easily happen if too many HS-PDSCHs are allocated. As a consequence, blocking is an important performance indicator to be considered as well when choosing the number of codes to be reserved, or rather, when choosing the range of codes the ATS has to consider.

Effects on SHO Areas and Degradation Probability

From a system planning viewpoint, it is remarkable that blocking caused by a too high reservation of HSDPA codes impacts the normal behavior of SHO in DCHs. Since not all cells in a network occupy the code tree at the same time, SHO users may be rejected by one cell but still access the system through another one in their Active Set (AS). The point is that the remaining cell can be far away and, because of the lack of macrodiversity, it is now forced to transmit 100% of the required power by the terminal. This causes more interference and a global worse situation which leads to less available power for HSDPA and more reduced CQI values, eventually a reduction in the HSDPA throughput is obtained (and thus in the total cell throughput) as can be seen from Figures 8.7 and 8.12(a) for the cases

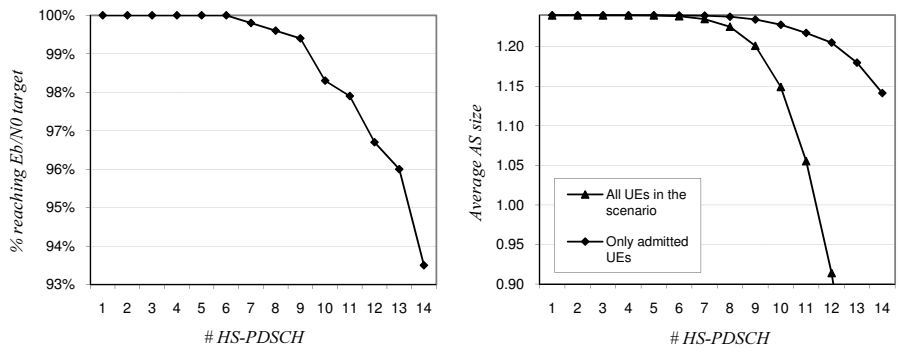

Figure 8.15: Evolution of degraded Rel'99 UEs (a) and AS size variation (b).

of 9, 10, 11 and 12 codes. Of course, intensified interference also causes increased degradation among Rel'99 UEs. This can be seen in Figure 8.15(a), which quantifies the appearance of DL degraded Rel'99 users because they demand more power than the maximum allocable to one single connection in the DL (the plot considers the uniform distribution case). The effect of a high HS-PDSCH reservation in the AS selection leads to an almost 7% of degraded UEs for the worst case.

On the other hand, Figure 8.15(b) quantifies the mean AS size variation for the case in which UEs are homogeneously distributed. It is given for both all UEs in the scenario and only those ones admitted in the system. The second case expresses the average AS size of admitted users, which is monotonously reduced with the number of codes from 1.25 to 1.14. However, the first case is more representative because it shows the global effect. When average AS sizes are inferior to one, admitted users are likely to drop when wandering around the network and commuting from one cell to another. Besides, SHO modifications can eventually affect UL performance as well. As was studied in Chapter 7, a reduction in the number of cells in the AS can cause the terminals to connect to a cell which may not be the best option (i.e. the one that would request less power to achieve the E_b/N_0 target). This implies increased UL interference, poor quality and a rise in congestion. Blocking would also rise if an UL load measurement was considered in the AC. Consequently, degradation in the UL must also be obtained to discard that the range of codes considered by the ATS is not needed to be further reduced. In the considered network, the 8 codes upper bound was maintained and no degradation appeared in the UL.

If the number of codes is augmented beyond 11, the reduction of HSDPA throughput because of increased interference is compensated by the effect of fully blocked Rel'99 users and an upwards trend is again obtained (see Figures 8.7 and 8.12(a)) for 11 to 14 codes allocations. When UEs are close to the Node-B (<150 m), interferences from other cells are inferior and these effects are very reduced.

Finally, all these values are even more emphasized if more HSDPA UEs operate

in the cell edge, and on the contrary, they are reduced if UEs are close to the Node-B, as can be indirectly observed in Figure 8.12.

Thus, it can be affirmed that the optimum code allocation to maximize throughput while ensuring blocking and dropping constraints is dependent on traffic patterns and mobile geographical locations. It has been observed that the number of codes to be assigned to HSDPA is tightly coupled with the channel conditions and so the monitoring must be designed taking this into account. If QoS requirements demand maximizing the cell throughput while maintaining blocking and degradation (eventually dropping) the maximum value that might be considered by the ATS is established by the latter, 8 in the considered scenario. Some code configurations (e.g. 10 and 11) are bad options for both Rel'99 and HSDPA jointly and should be avoided.

8.5.2 Monitoring Stage

Making an intelligent reservation based on the majority RF channel conditions permits maximizing the cell throughput. In fact, it is only necessary to know the channel status of HSDPA users and so, reported CQI measurements can be used as the first input to be taken into account. This data will be processed to obtain the final KPIs aiming to detect code reallocation situations.

With the objective of studying different alternatives and finding appropriate KPIs, dynamic simulations have been run. An observation time of one hour has been set, divided into three distinct parts. Initially users roam around the network according to the mobility model defined in Section 7.4. In the second third of the simulation, they move away from Nodes-B, towards the cells edge. Finally, on the last third of the observation time, users approach the central zone of the cell, defined as the area within a radius of 150 m. This behavior is intended to cover a wide range of situations, in the sense of reported CQIs. Figure 8.16 shows some snapshots of the geographical distribution of UEs along time.

On the other hand, Figure 8.17 represents the temporal evolution of the normalized histogram of reported CQI values, averaged every 500 ms. The three parts of simulation time can be clearly differentiated. Initially, the histograms show a high standard deviation since the UEs are situated very homogenously around the network and therefore around each particular cell. Furthermore, their movement does not contribute to generate significant accumulations in specific areas. As users concentrate on the cells edges, the standard deviation decreases and also the reported CQI values. These values increase again when users go towards the Node-B.

Following this figure, it can be observed that standard deviation can take high and low values along time. Consequently the evolution of the mean is only partially representative of the whole histogram behavior. Since the objective is to detect the RF characteristics of the "majority" of UEs in the cell, KPI-A is defined as the first quartile Q_1 (= 25th percentile) of reported CQIs. This way, it is known that 75% of UEs report better RF conditions than that threshold.

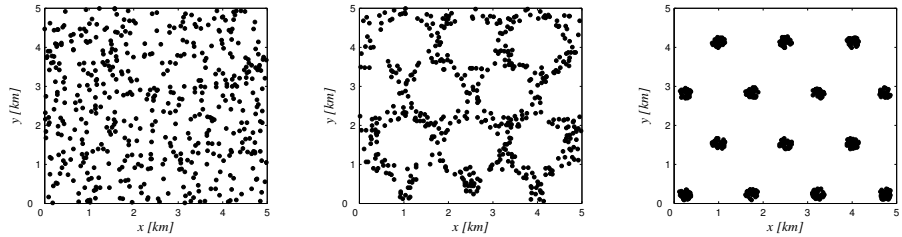

(a) Uniformly distributed (b) Close to cell edge (c) Close to Node-B (<150 m)

Figure 8.16: UEs geographical distribution for different moments of the observation time.

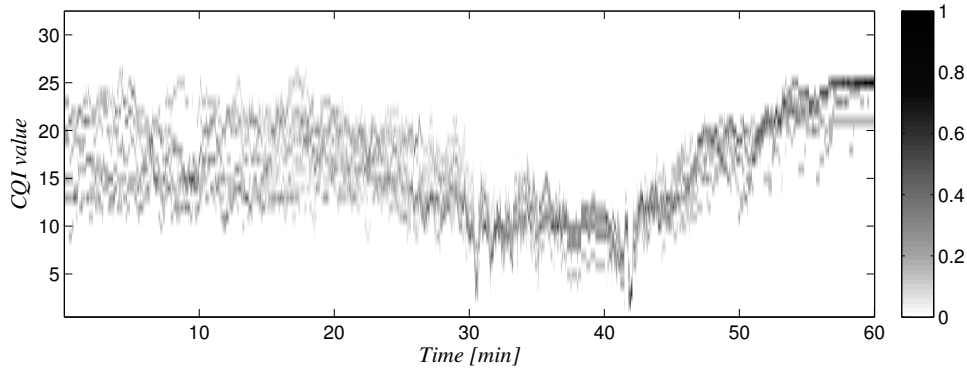

Figure 8.17: Evolution of CQI normalized histogram along time.

Even though Q_1 represents the majority of UEs, when dispersion is excessive, several UEs can report values well above Q_1 and decisions based on KPI-A can be too conservative. A high standard deviation σ_{CQI} is indicative that many UEs enjoy a radio channel much better than Q_1. That is why, in order to detect cases with high differences among link conditions, a second KPI is monitored, KPI-B=σ_{CQI}, whose impact is quantified later on.

8.5.3 Control Stage

From the reported CQI values and derived KPIs, a first step towards is to define which RF conditions imply an optimal allocation of 5 codes, because there is no gains with a higher number. And, second, in which situations the majority of perceived channel conditions are "so good" that allocating 8 codes is justified. Nevertheless a finer analysis can be done to define other cases. With this idea in mind, an analysis of 3 of the central cells has been done. Several simulations have been run with

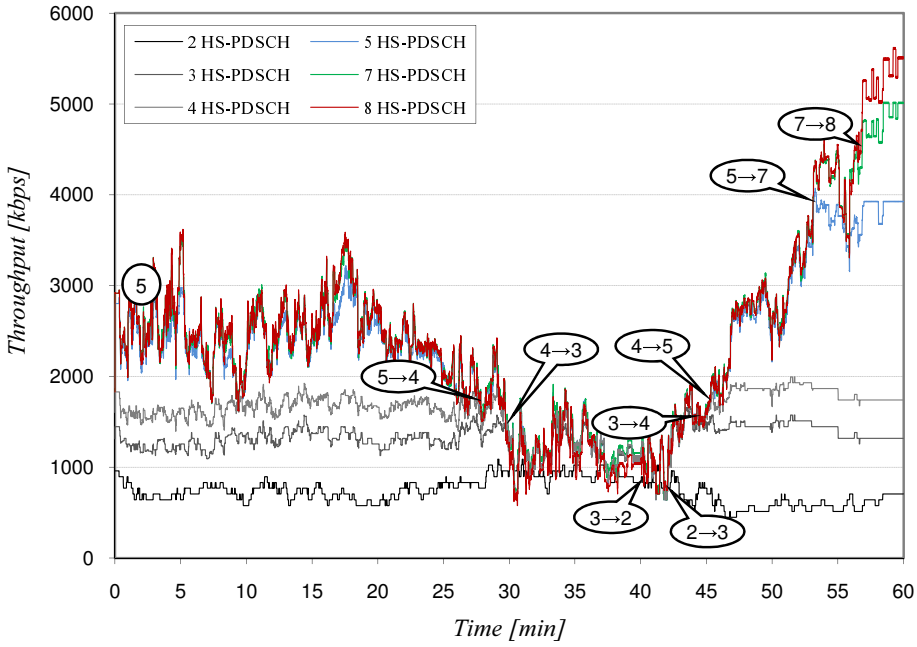

Figure 8.18: Averaged throughput for fixed code assignments and optimum commutation points.

different static codes allocation. Comparing each possibility with the others, the optimum commutation points is found. Figure 8.18 graphically shows the result of this analysis for one of the cells. Around those points the state of the CQI histogram was analyzed to derive the RF conditions in terms of KPI-A and B.

As was studied with static simulations, it can be observed that in certain cases there is no special benefit in increasing the codes reservation for HSDPA. But, in other situations, it does exist a clear throughput gain. In this way, the plotted bubbles indicate desirable points to commute from the current code allocation (first number in the bubble) to a new one (second number). That is to say, at those points the *Control* stage should receive an alarm from the *Monitoring* one and should reallocate codes according to the databases generated by the *Learning and Memory* block.

From the analysis of these cells a decision LUT has been defined relating the values of Q_1 with the number of codes to apply and the computed value of σ_{CQI}. The standard deviation is considered to be high when it takes a value greater than the 10% of the maximum reportable CQI (=30). An average variation of ± 3 units in the CQI values indeed imply diversified radio conditions among UEs. Under these circumstances, several UEs report a CQI fairly far from Q_1 (well over 3 units) and therefore the optimal number of available HSDPA codes should be superior to avoid a too conservative allocation that would lead to a throughput reduction. The final LUT is shown in Table 8.1.

Table 8.1: LUT used by the implemented ATS.

Q_1	# HS-PDSCH	
	$\sigma_{CQI} < 3$	$\sigma_{CQI} \geq 3$
≤ 7	2	3
≤ 9	3	4
≤ 11	4	5
≤ 17	5	7
≤ 21	7	8
> 21	8	8

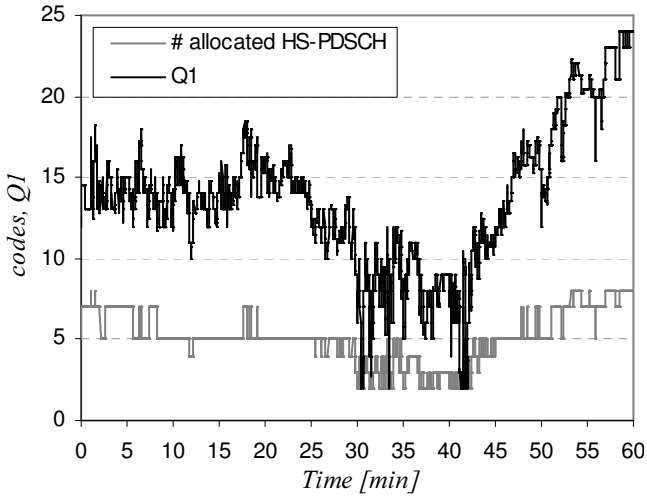

Figure 8.19: Q_1 and number of channelization codes to be assigned to HS-PDSCH.

Figure 8.19 shows the evolution of Q_1 along time as well as the number of codes to be set aside for HS-PDSCH if the value of Q_1 is directly evaluated in the proposed LUT. Reported CQIs show sharp and fast variations along their general trend and therefore a prior processing is needed to avoid an excessive number of codes reconfigurations. From the figure, too frequent reallocations along with and excessive ping-pong effect can be seen. Making excessive codes changes for just a short time is not desirable since they imply extra signalling in the Iub interface. Specifically, the channelization codes available for the HS-PDSCH packet scheduling in a cell are explicitly signalled by the RNC to the Node-B. This higher signalling is defined by [3GPn].

On the other hand, it is important to recall that one of the objectives to be met

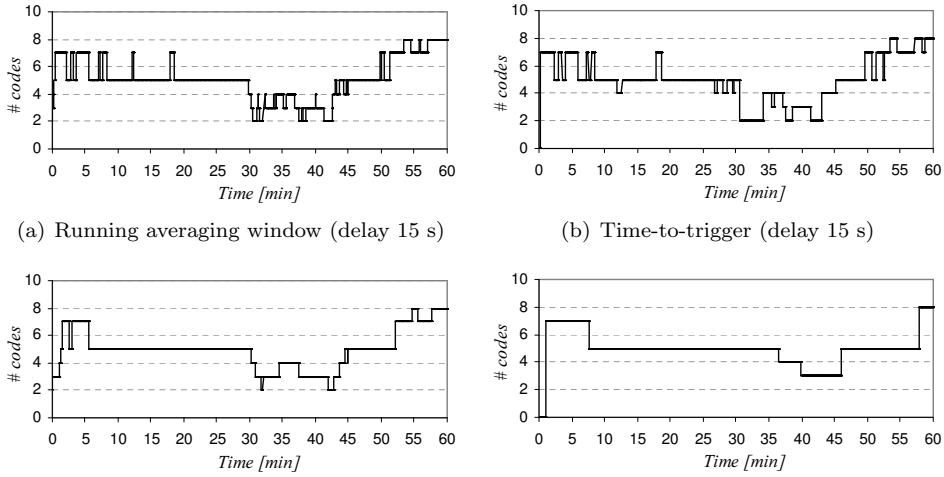

(a) Running averaging window (delay 15 s)

(b) Time-to-trigger (delay 15 s)

(c) Running averaging window (delay 60 s)

(d) Time-to-trigger (delay 60 s)

Figure 8.20: Central cell code allocations along time for different treatment of Q_1.

by the ATS is maximum simplicity so that it can be run continuously, in real time. Therefore extra calculations and mathematical manipulations with KPIs must be simple. The easiest option to avoid ping-poing is to use a classic time-to-trigger just as it was done in the previous chapter or in other RRM procedures of cellular networks, such as handover. Also, by means of a FIR filter, a running average can be obtained adding hardly extra complexity to the ATS. Both strategies are subsequently assessed.

In order to evaluate the effects of different averaging window sizes or the time-to-trigger durations and decide a proper value, different simulations have been run. Some examples are shown in Figure 8.20, which reveals, as it could be expected, a trade-off between the number of reallocations and the precision of the number of codes. The higher, the reallocations the more precise the system is, but also the higher the number of "false alarms" or codes that are allocated for just some units of seconds. This can be seen in Figures 8.20(a) and 8.20(b) where and averaging running window of 30 s and a time-to-trigger of 15 s is applied respectively. Note that time sizes are chosen so that the delay is the same, 15 s, with respect to the evaluated instant of time. These figures can be compared with Figures 8.20(c) and 8.20(d), which consider a 60 s delay and consequently, variations do not follow the evolution of UEs so accurately. This is particularly stressed in the Time-to-Trigger case, which takes longer to obtain a stable situation for 60 s because of rapid variations, however, false alarms are completely eliminated. On the other hand, in the running average case on Figure 8.20(c) some undesirable short allocations still appear.

Given this, in the final approach both strategies are concatenated and jointly used. So, after finding the mean and deriving the number of codes to apply, the allocation is only executed if a time-to-trigger is fulfilled. Definitive results measured

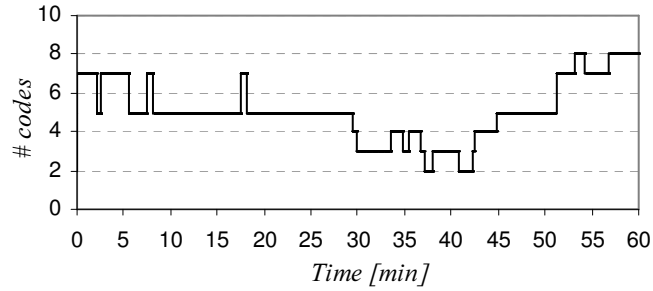

Figure 8.21: Final central cell code allocation. Concatenation of running average and time-to-trigger.

on the central cell are shown in Figure 8.21. The global delay is set to 30 s, coherent value to detect mid-term RF changes, as for example when UEs modify their spatial distribution along a day.

At this point, it is already possible to analyze the results obtained when the complete ATS proposal is running. It is important to note that each new allocation is always conditioned to codes availability and, if this is not possible, the nearest value is reserved and normal evaluation continues.

Figure 8.22 contains comparative results when the ATS is running and when a fixed allocation of 8 codes is applied, which was the maximum tolerable reservation estimated by means of static simulations and that implied maximum throughput. In particular, Figure 8.22(a) represents the blocking probability experienced by the central cell when the fixed strategy is implemented. Especially in the second third of the simulation, because of UEs being accumulated at the edges of the cell, and therefore at SHO areas, access requests are increased. The cell however does not have enough resources to support those new petitions and blocking rises dramatically up to values around 30%. On the other hand, the proposed ATS succeeds in keeping the blocking probability equal to zero. Precisely the number of assigned codes clearly descends when users are far away from the Node-B and their reported CQIs worsen. So, in this sense the gains are obvious and the automatic strategy clearly surpasses the fixed one.

Regarding the number of UEs that are not reaching their E_b/N_0 target, Figure 8.22(b) shows its evolution for a fixed allocation. As was studied in the *Learning & Memory* stage, the higher the number of codes, the higher the partial blocking and elimination of cells from the AS, which implies a worse interference pattern and a more likely DL degradation. If these values are compared with that from Figure 8.22(c), with the ATS running, it can be concluded that the proposed ATS also succeeds in reducing the number of degraded UEs.

The fact that the maximum value of 8 codes is permanently assigned is an advantage in terms of throughput when users are not particularly away from the Node-B and ASs are not affected. The ATS is a mid-term reservation mechanism that fits the number of HS-PDSCHs to the channel conditions of the majority of

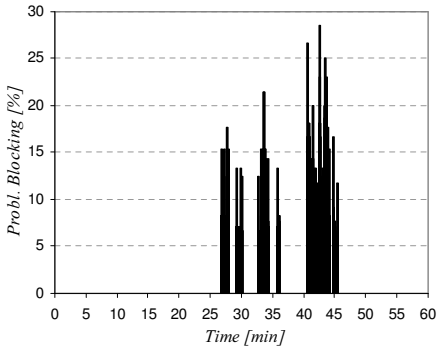

(a) Blocking probability (8 codes)

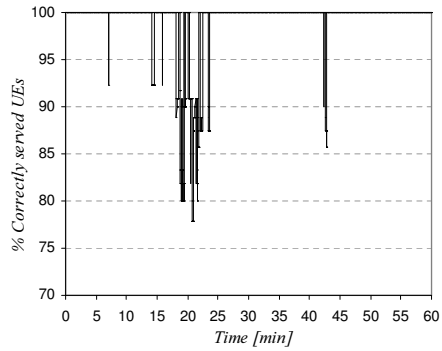

(b) % Correctly served UEs (8 codes)

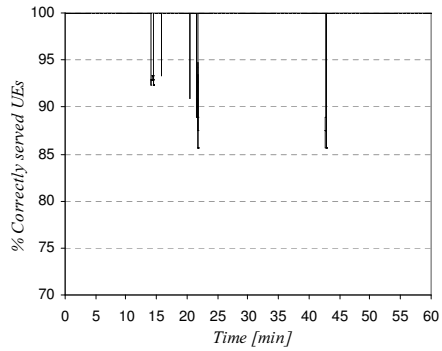

(c) % Correctly served UEs (ATS)

Figure 8.22: ATS results. Comparison against fixed 8 codes allocation.

users, however, one UE being especially close to the Node-B could be served with a higher throughput if more codes were devoted to HSDPA, not only 8 codes, but even 9, 10 and so on. Nevertheless, as seen, this would be at the cost of increasing blocking probability and therefore a globally worse network performance. Given this, it is expected that at certain moments, the throughput obtained with 8 codes is higher than that obtained by the ATS, since 8 is the maximum eligible number of codes in the considered scenario. In particular, Figure 8.23(a) contains the difference in throughput with respect to the fixed allocation. The global average of the graph is +18.7 kbps, value that quantifies the average loss for not using a fixed maximum code reservation policy. This loss can be tolerated if compared with the benefits in terms of blocking and dropping. In fact, in certain periods of time there are negative values (throughput gains), which appear when UEs are close to the cell edge and SHO areas are modified because of an excessive number of allocated HS-PDSCHs. On the other hand, in one peak of time there is a loss of 400 kbps, although this happens for just some units of seconds and the ATS quickly reacts and reallocates more codes for HSDPA.

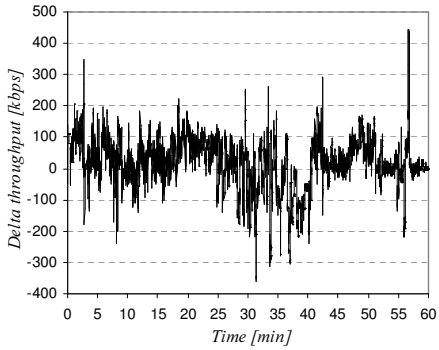

(a) 8 codes

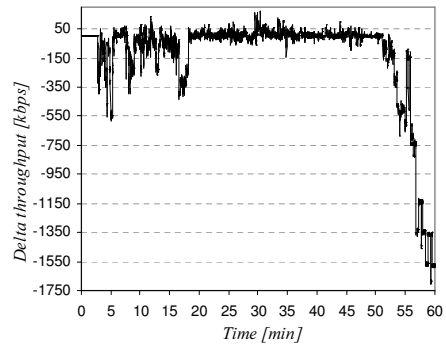

(b) 5 codes

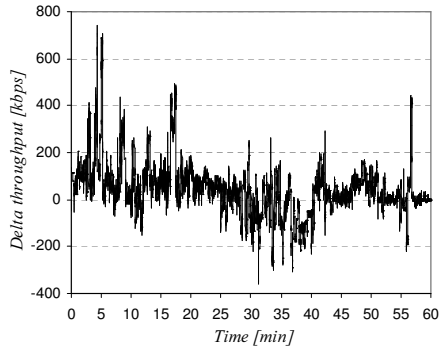

(c) 8 codes vs. ATS without considering σ_{CQI}

Figure 8.23: Throughput difference between ATS and fixed allocations.

If the throughput comparison is done with a more conservative fixed allocation that guarantees blocking and dropping, then the ATS stands out because of the throughput gains. This is reflected by Figure 8.23(b), which represents the throughput difference between a fixed 5 code allocation and the dynamic one decided by the ATS. Particularly when RF conditions improve, the fixed allocation implies throughput losses of up to 1750 kbps. Consequently, it can be concluded that the approach performs correctly and throughput levels are optimized while guaranteeing blocking and dropping indicators.

Finally, Figure 8.23(c) shows what would be the throughput variations if the ATS did not compute and did not take into account the value of σ_{CQI}. Again the comparison is done against the fixed 8 codes allocation and it can be seen that the results worsen those presented in Figure 8.23(a). In this case, the allocation is more conservative and UEs with high CQIs do not get the most of HSDPA. In certain short periods of time the differences reach 700 kbps. In particular, it can be observed that it is during the first third of the simulation when the ATS performs worse. During this period, users scour around the network homogeneously

and therefore the histograms computed for each cell show higher σ_{CQI} values (recall Figure 8.17). The average throughput loss in the whole observation time is just around 42 kbps and during the first time period it increases up to 115 kbps. This shows the importance of a good definition of the LUT and the consideration of second moment measurements to have a wider perspective of RF channel conditions.

8.6 Concluding Remarks

Although, HSDPA (and more generically HSPA) continues evolving through new 3GPP standard definitions, the RRM algorithms that are implemented in the vendor equipment are a key factor to its success and performance improvement. These algorithms are not defined by the standard and that is why several investigations are being carried out to find the best possible implementations. This chapter itself constitutes a contribution in this context.

The work has been presented in two differentiated parts. Initially, those aspects potentially improvable through RRM have been detected, being the HSDPA power allocation, code allocation, assignment of users to Rel'99 or HSDPA, scheduling policies, aggressiveness in the TF selection and aspects related to serving cell reselection.

The study was focused in the first three aspects, but it was concluded that, because of the benefits of HSDPA, in general there is no clear gain in introducing an ATS to manage power or the percentage of UEs assigned to HSDPA, both can be handled by straightforward rules-of-thumb:

- In order to maximize the cell throughput, all HSDPA capable UEs should be transferred to this technology but only if the scheduler is able to cope with delay and individual minimum throughput constraints. This can be guaranteed by using a proper AC combined with a QoS aware scheduler.
- On the other hand, HSDPA should just consume the power left over by Rel'99 to guarantee DCH operation. Otherwise, to assure a certain HSDPA throughput at the cell edge, a fixed amount of power could be allocated but at the cost of losing maximum DCH performance. The value to reserve can be easily found by means of simple link budgeting. Tradeoffs between the probability of degrading DCHs and the maximum cell-edge HSDPA throughput appear, so dynamic strategies are easier to manage and make the most of available resources.

The second part of the chapter is devoted to the investigation of dynamic code allocation. Codes from the OVSF tree is another of the resources to be shared when both technologies are deployed under the same carrier. Initially three questions were posed: First, how the codes should be assigned to meet QoS targets, second if this assignment is dependent on changes in traffic patterns and third, if code allocation should be considered for the inclusion in a UMTS ATS. To answer these questions

a detailed analysis was done by means of simulations. The cell throughput along with several collateral effects were studied for different codes allocation. This was done for different geographical UEs distributions and several engineering rules have been obtained:

- Effects on blocking probability: Blocking probability upper bounds the maximum number of codes to be considered by the ATS. Both HSDPA and Rel'99 blocking are proportional to the number of reserved codes. So, by favoring HS-PDSCHs too much, a negative effect also appears in HSDPA.

- Effects on SHO areas: An indirect effect of the previous point is that AS sizes are reduced if the number of allocated codes surpass a certain threshold, whose value depends on the Rel'99 TFs. This implies connections with Node-Bs that are not the best option in terms of DL power. As a consequence DL interference increases with the number of HS-PDSCHs. Of course, when fully blocked users are not negligible, DL power is again reduced, but with a clearly inadequate performance of the network.

- Effects on Rel'99 throughput and dropping: Rel'99 throughput is maintained but, degradation and eventually dropping are proportional to the number of HS-PDSCHs.

- Regarding scheduling policies, a revision of the state-of-the-art has been done in Appendix C and PF (and its variations) arises as one of the most interesting options for elastic traffic. Hence, this algorithm was also simulated and the previous conclusions (obtained with RR) are extensible to this case. The code range to be considered by the ATS can be slightly increased when UEs are uniformly distributed in the cell and PF is implemented. These differences tend to disappear when specific concentrations of users appear or if the maximum number of codes to be considered for HSDPA is less than 5.

- Power assignment and multiuser code multiplexing: The scheduler is also responsible for this aspect, which is typically missed in many of the HSDPA literature. However, in practical implementations should be considered to make the most of the available power. In the current dissertation, the first user is always served according to the reported CQIs and subsequent ones take profit of the remaining resources. The quantification that has to be done between the reported CQI and the selected TF, defines the remaining power for extra UEs. From 1 to 4 HS-PDSCHs, the probability of multiplexing more than one user is very low, so the ATS should allocate just one HS-SCCH. For higher numbers of HS-PDSCHs, multiplexing more than two users was hardly done. This probabilities are further reduced if PF is used.

- The optimum number of codes to be assigned to HSDPA is tightly related to UEs spatial distribution. For users concentrations far away from the Node-B there is no point in reserving more than 5 codes, this value can even be decreased as the cell size increases. A higher value does not improve HSDPA performance and codes are wasted and blocking probabilities are unnecessarily

increased in both technologies. On the other hand, when users are close to the Node-B (distance below 150 m) the number of codes to be allocated is just limited by the maximum allowable blocking probability. When UEs are homogenously distributed the optimum number depends on the cell size. In the presented set of simulations, since the scenario was a macrocellular one, it was closer to the "far away" case.

Given this, the proposed ATS makes mid-term reservations based on the majority of RF conditions in HSDPA UEs. Consequently, reported CQI measurements are continuously monitored and the corresponding histogram is computed. By means of dynamic simulations, the evolution of the histogram has been analyzed in a wide range of situations. From this analysis two KPIs were derived, which are the first quartile and the standard deviation of the histogram.

From the analysis of several central cells of the scenario, a decision LUT was defined and incorporated into the ATS. Thanks to this, the connection between the calculated KPIs and the codes to be applied by the *Control* block could be obtained.

A post-processing of the KPIs was revealed to be necessary to avoid too frequent reallocations and an excessive ping-pong effect. Two strategies were analyzed, a standard time-to-trigger and a FIR filter based running average. From this analysis a combination of both, introducing a 30 s delay was selected.

When comparing the performance of one network running the ATS against another with a fixed 8 code allocation, important benefits were obtained. Blocking was fully eliminated, whereas values near 30% where obtained with the static approach. Also degradation was clearly reduced. On the other hand, since 8 was the maximum number of codes in the range of the ATS, in certain periods of time the obtained throughput was inferior with the dynamic case. Nevertheless, the average loss of throughput was just 18.7 kbps. Conversely, when comparing with a conservative approach of 5 codes which guaranteed blocking and dropping, the ATS clearly succeeded in improving the cell throughput and gains raised up to 1750 kbps. Finally, the importance of including the standard deviation in the defined LUT was addressed. Missing this parameters leads the ATS to throughput losses up to 700 kbps in specific periods of time and when comparing with the 8 codes case.

Thus, it has been shown that the ATS proposal improves the performance of HSDPA networks coexisting with UMTS Rel'99. An optimum number of codes is allocated for each technology and, hence, the cell throughput can be optimized while minimizing both Rel'99 and HSDPA blocking probabilities and degradation below specific thresholds.

Chapter 9

Conclusions and Future Works

Radio network planning is continuously evolving along with access technologies. In this sense, the deployment of 3G/3.5G networks challenges traditional radio planning and optimization strategies. This is due to a new WCDMA access network and a more flexible conception in which lots of parameters have to be tuned subject to the discretion of the operator. The objectives pursued during the development of this Ph.D. thesis have been the realization of several contributions to the enhancement and optimization of the wireless access network of mature 3G/3.5G systems. Both static and dynamic mechanisms have been designed. New methods, guidelines and strategies of analysis have been proposed from a system level viewpoint and with the final objective of improving networks performance.

Challenges an open issues were derived by studying existent literature. The methodology followed during the investigation has been a combination of mathematical studies and simulations. Research has been organized in three parts.

Part 1.

As a step forward to standard optimization in which planning tools and drive testing were the basis, *Automatic Planning* strategies appear aiming at evaluating and optimizing multiple parameters jointly and considering interactions with other variables in the system. Performance indicators can be prioritized at will through the definition of cost functions that gather operators requirements. The ability to automatize a complex process allows adapting the network configuration easily to seasonal changes or slow demand variations. Opposite to *Dynamic Planning*, they are eminently static mechanisms that aim at obtaining an enhanced network configuration considering its average behavior. Nevertheless, shorter-term variations as weekly changes, could be tracked by applying algorithms results to different traffic conditions along time.

Because of non-linearities and dependencies among parameters, a purely mathematical approach is difficult to be applied when all variables and processes in the system are taken into account. The problem is a combinatorial optimization one and metaheuristics are good candidate techniques to its resolution. A review of these mechanisms has been done in the context of 3G networks along with those parameters with a higher impact on the final system performance and that are susceptible of optimization.

BS positioning and azimuth orientations to create optimum network layouts were initially studied, this dissertation focuses in the configuration of BSs. CPICH powers, downtilt of antennas and interactions thereof with SHO are the focus of the first part of the study because of their impact on the effective cell shape and their ability to transfer and equalize traffic among cells. Their values are susceptible of optimization to improve capacity in heterogeneous scenarios without increasing the cost of the network.

Most of *Automatic Planning* proposals prior to the published contributions from this Ph.D. thesis mainly addressed CPICH power adjustments as a coverage improvement method but potential capacity increases were not studied or just addressed in the DL for very specific types of scenarios. Indeed, coping with heterogeneous traffic distributions and adjusting the planning parameters to maximize capacity for a given covered area is one of the marked objectives.

Load balancing was usually used as a strategy aiming at transferring UEs from a loaded cell to a nearby one with less connections. However one of the first conclusions from Chapter 3 is that this rule must be carefully considered if both links are aimed to be jointly optimized. These actions might imply even more interference and degradation. The comparison among studies showed that DL was the main focus of most of existent literature and UL considerations were missed. However, the study from Chapter 3 and the analytical development in Chapter 4 conclude in the high importance of considering UL requirements and proper adjustment of BS parameters. The final cell pattern should promote that the highest number of UEs include their best option cells in their AS.

New planning guidelines have also been derived and were considered in the design of the *Automatic Planning* algorithm. These are gathered next in a list that contains the questions that have been answered:

- ***CPICH participates in cell selection and SHO procedures. What is the effect of SHO parameters when traffic is equalized among cells by means of CPICH power variations?.***

  Interrelation with SHO is tight, in fact by planning higher SHO areas, network sensitivity to wrongly adjusted pilots is reduced. If HHO is implemented, a finer adjust is required and small variations in the pilots cause important capacity reductions. On the other hand, the closer the setting of CPICH powers to the optimum, the less the capacity degradation because of wrongly adjusted SHO parameters.

- ***Is the optimal configuration different for UL and DL?***

Differences in the optimum set of CPICH powers for UL and DL are a possible case but these can be reduced modifying SHO areas to favor the limiting link.

DL capacity is particularly sensitive to increases in pilot powers beyond its optimum value and it can rapidly become the limiting link if pilots are wrongly adjusted by excess. Reductions in CPICH powers imply far less degradation in DL capacity but coverage issues must be carefully considered. UL is particularly sensitive in front of wrong adjustments, either in excess or deficiency.

Unbalance situations between UL and DL can be solved through an intelligent adjustment of SHO parameters. A mechanism that copes with this aspect is proposed in the third part of the dissertation.

- ***Downtilt modifies cell areas, individual transmission powers and generated and perceived interference. Which is the impact of these on the optimal adjustment?***

  The study carried in this Ph.D. thesis concludes that, because of the unitary frequency reuse, not only the main lobe downtilt is important to improve cell isolation, but also the relative position of the first radiation null and secondary lobes with respect to UEs from limiting cells. This result directly implies that, in general, the optimum angle from UEs viewpoint does not match with the optimum from a cell viewpoint. Actually, both configurations are only the same for high loaded scenarios.

  Adjusting angles to reduce users transmission powers permits increasing the UE perceived QoS but at the cost of being in a more instable situation, with more intercell interference. Slight changes in the system load imply important power increases and the probability of having UEs in degraded mode grows rapidly. On the other hand, minimizing the load factor yields a more steady system but at the cost of requiring higher levels of power when loads are not particularly high.

  In order to improve the network at general level, optimization should be done considering cells viewpoint, so that both UL and DL perform correctly under variable load conditions. But, if remote and electrically controlled antennas are introduced, performance can be maximized if angles track the users optimum.

- ***Both parameters are feasible candidates to modify cell sizes. Can it be concluded that they are interchangeable techniques to force the transfer of traffic among cells?***

  No, pilot variations just imply a change in the power assigned to broadcast control signals and on the reliability of UEs channel estimations. On the other hand, downtilt variations have a direct impact upon the power UEs and BSs have to transmit and upon the generated and received interference. CPICH variations have a more controlled impact and less side effects. On the other hand, downtilt variations are more indicate to enhance transmission levels and interference.

- ***Is it possible to optimize CPICH powers without considering downtilt angles?***

> No, adjusting CPICH powers imply a reshape of effective cell sizes and the study concludes that optimum downtilt angles are very dependant on cell sizes. Important capacity degradations are obtained if downtilt of antennas are not accordingly adjusted. Changes in one cell can imply that the first radiation null starts pointing towards the own covered area and the second main lobe towards the limiting cells, which is the worst possible adjustment. Thus, both parameters should be considered jointly.

Given the results presented in this dissertation, it can be concluded that there is a group of CPICH powers and downtilt angles such as traffic is effectively equalized among cells and a higher capacity is achieved. The proposed *Automatic Planning* algorithm searches for this configuration so that the outcome of the radio planning process is optimized.

The importance of not missing UL requirements in the optimization process has been emphasized. In this framework, the existence of optimal BSs configuration has been analytically addressed and because of its NP-completeness feature and the size of the space of solutions, the SA metaheuristic has been used for its resolution. A rigorous treatment of the technique has been done to preserve the convergence theory as much as possible.

The devised *Automatic Planning* algorithm has been tested in a synthetic scenario with parameters equally adjusted by standard link budgets and in a real scenario with parameters provided by an operator. The proposal is able to improve the global performance of the network, represented by a cost function containing information on the load factor and subject to constraints on coverage, degradation of QoS and DL power consumption.

Greater cost optimizations (18%) are achieved when both CPICH and downtilt angles are jointly optimized. Downtilt optimizations are run in a particular parallel module to avoid the evaluation of a too high number of invalid solutions. Thanks to this module the algorithm is guided towards new and better areas in the space of solutions.

When downtilt is included, the algorithm may penalize one cell in order to obtain a globally better solution. Individual cell constraints could be easily included in a future work to prevent this actions in particular areas. However, more work is needed to study the implications that this may have in the global optimization.

Although the number of cells with high loads (> 0.7) is dramatically reduced in the simulated cases, UEs reassignments can be done to some extent. This is due to the finite nature of the number of UEs and their geographical position. Distributed cell shapes with repeaters deployment is a possible solution to the last situation.

Extending simulations beyond the equilibrium condition implies slightly better solutions but requiring much more computational time. A simulation 5 times longer just gives an extra 4.3% gain in terms of cost. On the other hand, quick simulations degrade the outcome significantly. A simulation 10 times shorter implied a cost loss of 27%.

Due to the required computational time, an often and continuous execution of the proposal is impractical. However, it might be used as a first step towards *Dynamic Planning*. The algorithm can be executed offline, being fed by real data from the network. This way many cases and situations can be analyzed and pre-planned. The network would switch among the different optimized cases according to a preestablished temporal pattern for example at different days during one week or even at different hours in the same day. In a future work, this simple mechanism can be further improved by the addition of a pattern recognition system. For example, it is well known that neural networks are powerful pattern classifiers with good generalization properties. This last feature is particularly interesting in *Dynamic Planning* because it means that the network is able to give a good response to situations that were not used during its training.

Regarding downtilt adjustments, future studies should consider dense urban environments. In these cases diffraction over buildings and guided propagation imply that angle variations might have an effect different to the expected one. Up to the knowledge of the author, there are no publications dealing with this topic.

Although 3G/3.5G networks are continuously evolving, for example with HSPA+ and EV-DO Rev B (Evolution-Data Optimized Revision B), LTE is the current landscape of the 3GPP Radio Access Network standards. Vendors and operators expect to deploy this standard in some years from now, but uncertainties about how to manage the resources, dimension the network, coexistence of the new standard with previous infrastructure, etc. are still open issues to be investigated and that will be key for the success of this new technology. Among the different RRM procedures, the optimization of the MAC scheduling/priority handling is perhaps one of the most important aspects to address. Scheduling will have to be supported by other techniques that contribute to interference mitigation. In this sense, the configuration of BSs will play a key role and advanced radio planning techniques considering antennas orientation and effective cell sizes must be tested in the new scenario. An adaptation of the proposed *Automatic Planning* algorithm appears to be feasible and necessary so that scheduling can make the most of it. Aspects such as *Fraction Frequency Reuse* will have to be considered as well.

Part 2.

Repeaters are a cost effective solution that permit extending the coverage and increasing capacity to some extent in cells with hotspots. Distributed Node-B configurations are also smart architectures that allow load balancing in highly heterogeneous scenarios, beating the optimization of BSs configurations.

On the other hand, new effects not present in FDMA based 2G systems imply that the radio planning process becomes more complex. Most existent papers dealing with repeaters in WCDMA networks, ignore these effects or claim that their impact was not relevant. That is why the research work was focused in modeling them, quantifying their impact and deriving radio planning guidelines to enhance the final performance of the radio access network. If in the first part of the dissertation

simulations and tests were complemented by mathematical analysis, in this case it is the opposite. The methodology that has been followed is mostly analytical and equations are supported by system level simulations.

Results can be grouped in three points:

- An analytic expression of the feasibility condition of a WCDMA mobile communications system with repeaters has been obtained. This has been done in a comparative way with environments without repeaters deployment. The reduction in the admission region has been mathematically modeled and a compact, closed and generalist expression has been derived. This result allows obtaining easily the expected capacity degradation that a given deployment with repeaters can generate by itself. This has been done through the definition of a new indicator representing the equivalent maximum load that should be considered in an environment without repeaters to obtain the same capacity. Thus, this generic analysis could be used for both the deployment of mobile communication systems and the implementation of suitable AC mechanisms.

- From the previous analysis, it is concluded that planning WCDMA networks with repeaters implies a tradeoff between capacity and coverage, that is why their planning and deployment require careful adjustments. The parameters found to have the highest impact on this tradeoff are: Global gain (considering the internal gain at the repeater and the rest of gains and losses in the backhaul circuit), noise rise at the BS due to repeaters and number of repeaters. Unless these values are very low, effects on capacity are very relevant and cannot be missed in any analysis. Besides, if intercell interference is increased after installing the nodes, admission regions are further reduced, so particular attention should be paid to the placement of antennas and their downtilt. If on-frequency repeaters are used, additional conditions arise to avoid self-oscillations. It is also concluded that the tradeoff can be partially controlled by using low power repeaters, capacity problems are mitigated, but more devices are needed to cover the same target area, so the main advantage of repeaters, cost, is jeopardized.

- A side effect that is very absent in the literature is the modification of the donor cell coverage, which is present in scenarios that are not capacity limited. An existent work has been generalized so that this degradation can be quantified in scenarios with heterogeneous users distributions with arbitrary number of services. If several repeaters are adjusted to have the same maximum transmission power as the BS, coverage reductions quickly get and surpass 50%.

Another contribution of the thesis is the proposal of a new methodology to analyze WCDMA networks with repeaters deployment from a system level viewpoint, considering realistically path delays and the behavior of Rake receivers. This allows an enhanced analysis with respect to traditional approaches from a system level viewpoint. The proposed equations system has a dimension equal to the number of BSs to be evaluated and it is independent of the number of repeaters. This

way the proposal does not introduce new extra computational cost, once the new propagation expressions are found.

Compact expressions are derived for UL and DL so that transmission powers and other RRM parameters can be calculated without any of the traditional simplifications. Results show more reliable and accurate predictions on network performance. Not taking into account these effects implies erroneously optimistic metrics such as:

- Transmission powers: UL is the most affected link with differences up to 3 dB, differences in the DL are lower because of the use of orthogonal codes. The higher the loss of orthogonality, the higher the difference in the metric.
- Percentage of users in degraded mode.
- Coverage, both the global and donor's.
- Admission regions, which are mathematically redefined to show this degradation.

The use of repeaters in LTE networks may allow new topological structures where high data rates are provided in areas far from the BS. The use of guard intervals in OFDM allows using signal replicas constructively (from the donor and corresponding repeaters). However, locations inherited from previously planned technologies might force the use of too high guard intervals to avoid self-interference, with the corresponding throughput degradation. Conversely, fixing a certain interval defines the set of feasible positions to install repeaters. All these aspects are object of a potential future work. Experience and studied methodologies from Single Frequency Networks in Digital Video Broadcasting might be a useful start point.

One of the shortcomings of using repeaters in WCDMA networks is the difficulty of equipping them with some "intelligence", because information requires to be despread. Since this does not happens in LTE, the conception of distributed cell may be well extended beyond the coverage improvement and new distributed RRM opportunities appear.

Part 3.

Regarding the network capacity to adapt itself to time-varying conditions. Slow and aggregate demand variations may be absorbed thanks to the flexibility introduced by *Automatic Planning* strategies. On the other hand, RRM algorithms allow a finer adjust through real time adaptation to active UEs requirements. However, more levels of variations can be defined to maximize the utilization of the radio interface. In this sense, *Dynamic Planning* and *Automatic Tuning* aim at covering this intermediate time scale, of seconds and up.

The final objective is a network that fully plans and tunes itself. This is indeed challenging but following the divide-and-conquer idea, investigations are currently focusing on particular aspects of the network. Existent proposals can be grouped

in two sets, those dealing with planning parameters and the ones that cope with variables governing RRM algorithms.

Capacity unbalance between UL and DL is a fact that already arouse in the first part of the thesis. This effect is aggravated by the dynamism of new services usage, the appearance of new data applications and UEs mobility. All these lead to UL and DL requirements variable in time. Conversely, many of the existent auto tuning proposals do not study UL and DL effects jointly and unbalance is hardly checked. In this context, this Ph.D. thesis proposes an ATS with the objective of detecting whether one of the links has capacity problems and favor it to delay congestion control actions.

A functional auto-tuning architecture has been described to adapt parameters to service mix dynamics and overcome capacity problems. This architecture is composed of three blocks (*Learning & Memory*, *Monitoring* and *Control*) and two interfaces.

From the *Learning & Memory* stage SHO parameters (*AddWin* and $\mathcal{N}$) have been revealed as a feasible option to achieve the balancing objective. Increasing the number of cells in the AS favors the UL, whereas too many cells in the AS degrades the DL. Although several combinations of these parameters yield balanced situations, only one of them also implies maximum capacity. In this sense, the service mix in the target area has the most relevant impact on this configuration and users spatial distribution has a lower effect.

Regarding *Monitoring*, KPIs have been defined taking into account 3GPP definitions on performance related data. From tests without implementing ATS, it is derived that DL transmission power is not representative enough of congestion in the cell, and percentages of the values of individual transmission powers have been used instead. A standard time-to-trigger has also been introduced to avoid ping-pong effect. Finally, three monitoring cases have been considered

The *Control* stage acts in a totally distributed manner and parameters are modified in a cell by cell basis. Speed of reaction can be increased with a more conservative *Monitoring* but at the cost of increasing the number of reconfigurations.

Simulations with different service mix cases show capacity gains around 30% when ATS is running. The investigation is closed by a dynamic study case in which DL started to jeopardize capacity by the end of the observation time. Adjusting dynamic and appropriately the SHO parameters, a reduction in DL resources consumption is possible. This allows a margin in the available power, in particular between 2 and 3 dB. Thus, the approach is able to stabilize the network and delay congestion control mechanisms. Indeed, regarding the % of UEs in degraded mode, a reduction from 70% to 6% was obtained for the worst case.

Although more dynamic simulations would complement these results, tests with data obtained from real networks and implementation in an operative one is the natural path for this research.

The last objective of the thesis is to analyze the potential improvements that

could provide the incorporation of an ATS when the HSDPA technology is coexisting with UMTS. Although HSDPA continues evolving through new 3GPP standard definitions, the RRM algorithms to be implemented in the vendor equipment are not defined by the standard and are a key factor to its success and performance improvement.

In this sense, it is assessed to which extent it is worthwhile to make a dynamic management of its three most important resources: devoted power, codes and percentage of users assigned to Rel'99 or HSDPA. From the study, one of the first conclusions reached is that the benefits of HSDPA are so high that in general, there is no clear benefit in introducing an ATS to manage power or the percentage of UEs assigned to HSDPA, both can be handled by straightforward rules-of-thumb:

- In order to maximize the cell throughput, all HSDPA capable UEs should be transferred to this technology but only if the scheduler is able to cope with delay and individual minimum throughput constraints. This can be guaranteed by using a proper AC combined with a QoS aware scheduler.
- On the other hand, HSDPA should just consume the power left over by Rel'99 to guarantee DCH operation. Otherwise, to assure a certain HSDPA throughput at the cell edge, a fixed amount of power could be allocated but at the cost of losing maximum DCH performance. The value to reserve can be easily estimated by means of simple link budgeting. Dynamic strategies are easier to manage and make the most of available resources.

However, code allocation deserves a further study. Thus, before proposing the ATS itself, a detailed study on capacity has been done and the several engineering rules have been obtained. They give answer to next questions:

- ***How codes should be assigned to meet target performance?.***

  The maximum number of codes that can be assigned to HSDPA and so considered by a potential ATS is upper bounded by the target blocking probability and Rel'99 degradation.

  Both HSDPA and Rel'99 blocking are proportional to the number of reserved codes. Therefore, by favoring HS-PDSCHs too much, a negative effect also appears in HSDPA.

  DL Rel'99 degradation is induced when SHO cannot perform freely due to an excess of codes devoted to HSDPA in a certain cell.

- ***Is this assignment dependent on changes in traffic patterns?.***

  Yes, in fact the optimum number of codes to be assigned to HSDPA is tightly related the reported CQIs and hence, to UEs spatial distribution. For users concentrations far away from the Node-B there is no point in favoring HSDPA. A high number of codes does not improve its performance and codes are wasted. Blocking and dropping probabilities are unnecessarily increased. On the other hand, when users are close to the Node-B the number of codes to

be allocated is just limited by the maximum allowable blocking probability. When UEs are homogenously distributed the optimum number depends on the cell size.

- ***Should it be considered for the inclusion in a UMTS/HSDPA ATS?.***

  Yes, given that traffic loads evolve along the network during a day, a mid-term reservation mechanism is a feasible solution to guarantee maximum throughput while ensuring blocking and dropping constraints Thus, it is proposed a full ATS to dynamically allocate HS-PDSCHs in HSDPA systems is proposed.

Regarding scheduling, a revision of the state-of-the-art has been done, two strategies have been compared showing the same answers to previous conclusions. Only changes in the number of users multiplexed in one TTI were observed.

The basis of the functional architecture is the already explained three-block based structure. The proposed ATS makes mid-term reservations based on the majority of RF conditions in HSDPA UEs. These are characterized by the first quartile of the histogram of CQIs and its standard deviation, which are the set of KPIs. By means of an analysis of several cells using different fixed codes allocation a decision LUT was defined. This connects the KPIs with the corresponding number of codes to be allocated by the *Control* stage. A pre-filtering of KPIs is included to avoid too frequent reallocations and an excessive ping-pong effect, a standard combination of a time-to-trigger plus a FIR filter based running average is shown to perform correctly.

Results reveal that the proposed mechanism improves the performance of HSDPA networks coexisting with UMTS Rel'99. An optimum number of codes is allocated for each technology and, hence, the cell throughput can be optimized while minimizing both Rel'99 and HSDPA blocking probabilities and degradation below specific thresholds.

After these results, that define and confirm the mechanism, a future work consists of studying the generality of the obtained LUT or studying to which extent rules of thumb can be obtained to easily adjust it to any possible scenario.

Self-configuration tasks are paramount in deployments using the femtocell concept, which are expected to be usual in the LTE context. In this possible forthcoming framework, BSs have to be real plug-and-play devices and interference coordination with existent and new nodes is mandatory. Investigations of mechanisms that set-up CPICH power, antenna orientation, SHO parameters and neighborhood relations according to the actual location and environment is one of the logical next steps after this thesis.

As a final reflection, in addition to research contributions, a system level simulation tool has been developed. Although simulation is very present in the research on mobile communications systems, the author would like to emphasize the flexibility and complexity of the platform, accounting and supporting multiple options and whose main features are gathered in Appendix B. This conforms indeed a valuable tool with an easy update to follow the research work in the context of LTE.

Appendices

Appendix A

Preliminary Estimation of CPICH Powers

Along this annex an analytical expression is derived to relate the required CPICH power with a given E_c/I_0 target at the cell edge. This analytical expression is useful to estimate the value in early stages of the planning process.

The objective is to find a closed expression that only depends on the load perceived by the UE k at the cell edge, the relationship between intra and intercell interferences f^{DL} and the loss of orthogonality suffered by the intracell interference ρ.

Equation (3.2) is taken as starting point. This expression relates the required CPICH power with received power from all cells and the noise at the UE. It is recalled that the E_c/I_0 is measured at the antenna connector, before despreading:

$$P_{TX,CPICH}(j) = (E_c/I_0)_{CPICH}(j,k)\, L^{DL}_{max}(j) \left[\sum_{i=1}^{N_{BS}} \frac{P^{DL}_{TX,tot}(i)}{L^{DL}(i,k)} + n_{UE}(k) \right] \tag{A.1}$$

Where:

- $P_{TX,CPICH}(j)$: CPICH power transmitted by BS j.
- $P^{DL}_{TX,tot}(j)$: Total power transmitted by BS j, it accounts for control and data channels.
- $L^{DL}(j,k)$: DL link loss between BS j and UE k.
- $n_{UE}(k)$: Thermal noise power at UE k.

This expression may be evaluated in terms of the noise rise induced by interferences

or similarly by the load factor measured by the UE at the cell edge, both parameters are related as follows:

$$\eta_{edge}^{DL}(k) = 1 - \frac{1}{\Delta n_{UE}(k)} \tag{A.2}$$

Similarly:

$$\eta_{edge}^{DL}(k) = \frac{I_{Inter}^{DL}(j,k) + I_{Intra}^{DL}(j,k)}{I_{Inter}^{DL}(j,k) + I_{Intra}^{DL}(j,k) + n_{UE}(k)} \tag{A.3}$$

Where:

- $I_{Inter}^{DL}(j,k)$: inter-cell interference measured at UE k in its link with BS j. It is understood that j is included in the AS of k.
- $I_{Intra}^{DL}(j,k)$: intra-cell interference.
- $n_{UE}(k)$: total thermal noise power measured at UE k.

It is worth mentioning that η_{edge}^{DL} is measured after despreading and it is a measure of the interference perceived by the data connection. Given this, since SHO benefits from macrodiversity and so all BSs in the AS are simultaneously transmitting to the UE, $I_{Inter}^{DL}(j,k)$ depends on the specific BS of the AS that is evaluated and it is calculated as indicated next:

$$I_{Inter}^{DL}(j,k) \equiv \sum_{\substack{i=1 \\ i \neq j}}^{N_{BS}} \frac{P_{TX,tot}^{DL}(i)}{L^{DL}(i,k)} \tag{A.4}$$

Where N_{BS} is the number of BS or cells in the system.

As explained in Chapter 3, Section 3.2.1, intracell interference suffers a loss of orthogonality due to multi-path propagation and ρ is the factor that models the effect. On the other hand, intracell power accounts for data transmissions and the power devoted to control channels $c(j)$, consequently it can be expressed as follows:

$$\begin{aligned} I_{Intra}^{DL}(j,k) &\equiv \rho(j,k)\left[\frac{c(j)}{L_{max}^{DL}(j,k)} + \sum_{\substack{i=1 \\ i \neq k \\ i \in j}}^{N_{UE}(j)} \frac{P_{TX}^{DL}(j,i)}{L_{max}^{DL}(j,k)}\right] = \\ &= \rho(j,k)\left[\frac{P_{TX,tot}^{DL}(j)}{L_{max}^{DL}(j,k)} - \frac{P_{TX}^{DL}(j,k)}{L_{max}^{DL}(j,k)}\right] \end{aligned} \tag{A.5}$$

Where:

- $N_{UE}(j)$: is the number of UEs with BS j in its AS.
- $P_{TX}^{DL}(j,k)$: DL transmitted power from BS j to UE k.
- The summation is calculated over the UEs connected to BS j, which is indicated by '$i \in j$', where i is the summation index.

Then, the required $P_{TX,CPICH}(j)$ can be found:

$$\begin{aligned} P_{TX,CPICH}(j) &= (E_c/I_0)_{CPICH}(j,k)\, L_{max}^{DL}(j,k) \\ &\quad \left[I_{Inter}^{DL}(j,k) + \frac{1}{\rho(j,k)} I_{Intra}^{DL}(j,k) + \frac{P_{TX}^{DL}(j,k)}{L_{max}^{DL}(j,k)} + n_{UE}(k) \right] \\ &= (E_c/I_0)_{CPICH}(j,k)\, L_{max}^{DL}(j,k) \\ &\quad \left\{ \left[f^{DL}(j,k) + \frac{1}{\rho(j,k)} \right] I_{Intra}^{DL}(j,k) + \frac{P_{TX}^{DL}(j,k)}{L_{max}^{DL}(j,k)} + n_{UE}(k) \right\} \end{aligned} \tag{A.6}$$

Where $f^{DL}(j,k)$ is the quotient between the intercell and intracell power measured at UE k and considering its link with BS j:

$$f^{DL}(j,k) = \frac{I_{Inter}^{DL}(j,k)}{I_{Intra}^{DL}(j,k)} \tag{A.7}$$

The term $P_{TX}^{DL}(j,k)/L_{max}^{DL}(j,k)$ can be estimated by standard link budgeting. It can also be ignored because during the initial cell search process the UE has not yet established a data connection. Eventually the minimum required E_c/I_0 target could be increased to guarantee successful measurements when performing SHO.

On the other hand, from Equation (A.3) and (A.7), $I_{Intra}^{DL}(j,k)$ can be expressed as a function of the measured load factor at the cell boundary η_{edge}^{DL}:

$$I_{Intra}^{DL}(j,k) = \frac{1}{1+f^{DL}(j,k)} n_{UE}(k) \frac{\eta_{edge}^{DL}(k)}{1-\eta_{edge}^{DL}(k)} \tag{A.8}$$

And thus, CPICH powers can be finally established as indicated by the following expression:

$$\begin{aligned} P_{TX,CPICH}(j) &= (E_c/I_0)_{CPICH}(j,k)\, L_{max}^{DL}(j,k)\, n_{UE}(k) \\ &\quad \left\{ 1 + \left[f^{DL}(j,k) + \frac{1}{\rho(j,k)} \right] \left[\frac{1}{1+f^{DL}(j,k)} \frac{\eta_{edge}^{DL}(k)}{1-\eta_{edge}^{DL}(k)} \right] \right\} \end{aligned} \tag{A.9}$$

Appendix B

Scenarios and Simulation Platform

Along the first part of this Annex the scenarios considered for simulations are explained. Only the basic features are described because particularities in each simulation are explained in the corresponding section. For example, when HSDPA-capable UEs are introduced in the scenario or if repeaters are considered and the layout is modified, etc. The second part gives some details about the simulation platform that has been created during the development of this Ph.D. thesis.

B.1 Synthetic Scenario

This scenario is a 3GPP based, urban and macrocellular one [3GPp], with an area of 5.5×5 km^2 and 42 cells in a regular layout. The deployment scheme is assumed to be hexagonal. Sites in a row are separated by a distance of 1500 m. There are 42 cells in 14 trisectorial Nodes-B. Regarding propagation, a COST231-Hata model is used [DC99], considering a 2GHz carrier. For the shadowing model, the two dimensional model proposed in [FLC03]. This models does not consider a shadowing component independently for each user, and nearby ones have related values, situation that closely resembles reality. A correlation distance of 18 m, a standard deviation of 8 dB and a correlation coefficient between BSs of 0.5 have been considered.

Figure B.1 represents the minimum attenuation map and gives a vision of the layout. Two cases are represented antennas not being downtilted and when the tilt is 3º.

Unless the contrary is indicated, antennas are placed at a height of 25 m and radiation patterns from commercial antennas [Kat] have been used. Its main features are a gain of 18 dBi and 65º and 6.7º of horizontal and vertical beam width respectively. The chosen antenna can be electrically downtilted from 0º to 10º. Fig-

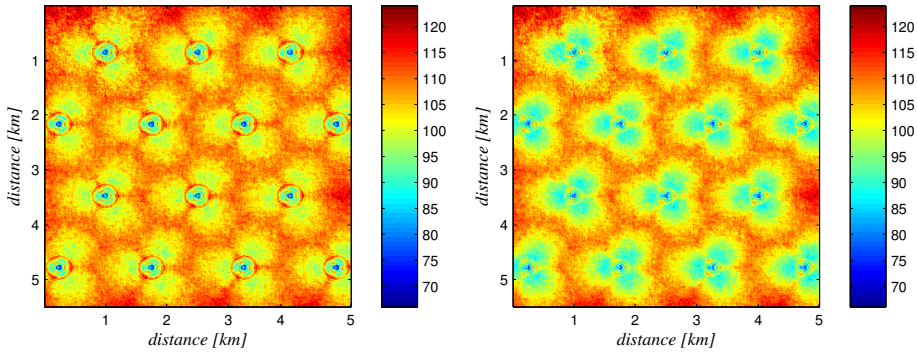

(a) Downtilt 0º (b) Downtilt 3º

Figure B.1: Minimum attenuation level in synthetic layout.

Table B.1: Simulation parameters in the synthetic scenario.

Node-B	Maximum TX power	43 dBm
	Noise power	−104 dBm
	CPICH power	30 dBm
UE	Maximum TX power	21 dBm
	Noise power	−100 dBm
Minimum required CPICH E_c/I_0		−18 dB
Maximum number of cells in AS		3
Addition window		3 dB

ure B.2 shows the horizontal and vertical cuts on the left and the interpolated 3D diagram on the right (logarithmic representationt) when downtilt angle is equal to 0º. Because of the importance of the impact of first and second nulls of radiation, the bottom subfigure contains the attenuation with respect to the maximum gain for the first degrees of the vertical plane, in particular they are at 7º and 14º respectively.

Table B.1 shows other important parameters regarding Node-B and UEs.

When the contrary is not indicated, UEs are uniformly scattered, otherwise, the process to generate heterogeneous distributions is the same as the one used to compute shadowing losses, a bidimensional filtering process described in [FLC03], where correlation distances define the final size of areas with more or less density of UEs.

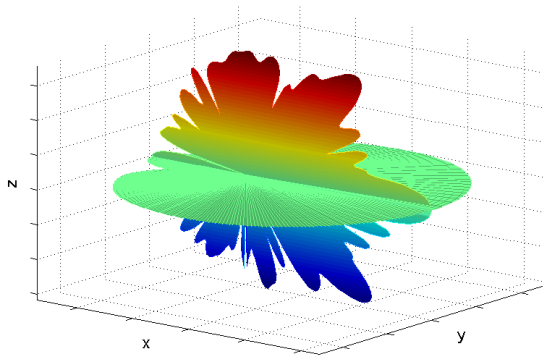

(a) Horizontal and vertical cuts

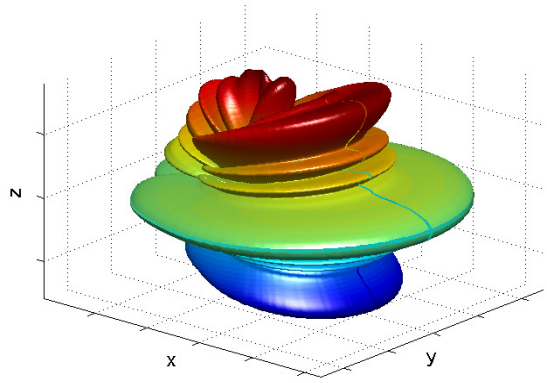

(b) Interpolated 3D diagram

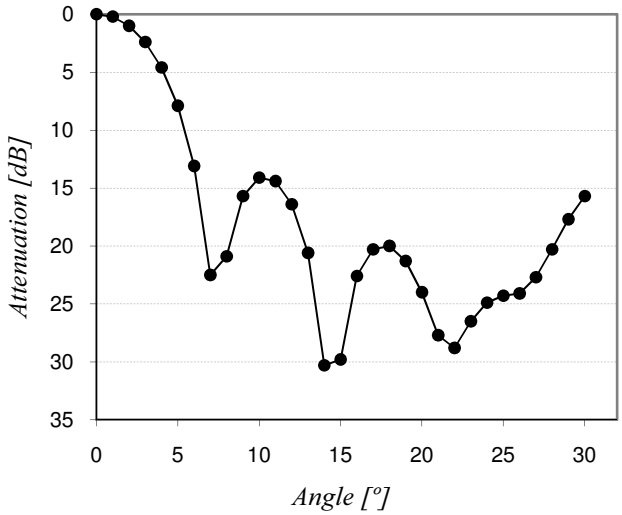

(c) Attenuation with respect to maximum gain in first degrees of vertical plane

Figure B.2: Radiation pattern when downtilt is 0°.

Table B.2: Features of services.

Type of Service		UL E_b/N_0 [dB]	DL E_b/N_0 [dB]	Max DL power [dBm]
Voice	12.2 kbps	2.9	4.4	21
	12.2 kbps (50 km/h)	5.5	7	21
Data	64 kbps	1	2.5	30
	144 kbps	0.4	2.3	30
	384 kbps	0.6	2.4	30

Concerning services, 5 different types have been considered and their main features are contained in Table B.2. More details on the selection of this values can be found in document [ORGL03] which contains a description of the UTRA FDD link level simulator used to generate the link level lookup tables that have been used in this thesis. These are the same as those used in the synthetic scenario of the MORANS (Mobile Radio Access Network Reference Scenarios) initiative [VB03; VBC+04]. This activity is framed within the COST 273 Action and aimed at providing common system simulation environments so that research results and proposals from different researchers were comparable.

When dynamic simulations are run over this scenario, unless the contrary is indicated, users move at 3km/h, with a direction which is corrected with a probability of 0.4 by an angle between -45 and +45 deg.

B.2 Realistic Scenario by Using 2G Measurements

Development of 3G networks will happen within a very competitive and mature 2G environment and it is expected that operators will use their existing infrastructure by means of co-sitting 3G with existing 2G sites to reduce cost and overheads during site acquisition and maintenance.

Taking this into account, a different approach based on real data from a GSM network operating in the 1800 MHz band was developed and used to scatter users around the network and to assign to them realistic propagation losses. Measurement reports performed by mobile terminals were recorded and processed in order to build a database containing realistic propagation conditions. It is important to note that indoor traffic (typically hardly represented) will be implicitly included in the simulations. This database was also used to derive realistic traffic distributions. Thus, both realistic propagation data and realistic traffic distributions where used to feed the UMTS simulator in order to obtain reliable statistics.

It must be acknowledged that these data was provided by Telefonica Moviles within a collaboration project out the context of the current thesis. Also the processing and preparation of this data to be used by the simulator was jointly done with Ph.D. Ferran Adelantado Freixer.

As it was previously mentioned, the first step consisted in the construction of a database with real GSM propagation measurements. The record of this data was made for a long enough period of time, and for all the BS in the scenario. During a call, GSM terminals report the measured received level from the serving cell and up to 6 neighboring cells with a periodicity of 480ms. Knowing BS transmitted powers, a path loss vector can be calculated directly: $[L_1(t), \ldots, L_n(t)]$ being $L_i(t)$ the attenuation from the i-th BS to the mobile at a certain time. Each row of the database will contain the values of a vector ordered from the lowest to the highest attenuation level.

Not only is the database providing a realistic propagation model, it is also indirectly giving information about realistic traffic distributions. If S_i is defined as the radioelectrical region (we are dealing directly with path loss, not with geographical distances) where the i-th BS is best received in terms of CPICH RSCP, S_{ij} represents the sub-region in which the j-th BS is the second best and so on, then, the probability $P(S_i)$ that a mobile is in the area S_i, can be estimated by simply counting how many of the total number of measurement reports (database rows) have $L_i(t)$ in the first position. Similarly $P(S_{ij})$, $P(S_{ijk})$, etc. can be easily estimated. As a consequence, with the help of these probabilities, the simulator tool is able to scatter the users in the scenario according to real traffic distribution, as it is illustrated in Figure B.3. Once the sub-region has been assigned, a propagation vector is randomly chosen from the database among those corresponding to the given sub-region.

The scenario is composed of 13 base stations and Table B.3 shows, as an example, the first level of probabilities $P(S_i)$ which reflects the unbalance in terms of load of the different cells.

Geographical information about the bases is not provided, moreover the reports are not consecutive in time. As a consequence, the main drawback of this scenario is that, with the available data, it is not possible to perform dynamic simulations.

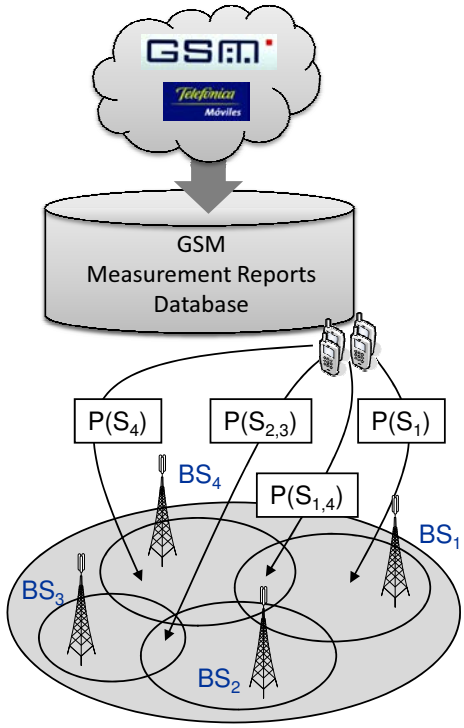

Figure B.3: Procedure to scatter UEs around the network.

Table B.3: First level probabilities $P(S_i)$ derived from measurements.

BSIC BSCH	$P(S_i)$
8 30	19.99
8 38	9.79
8 52	2.39
14 28	0.91
8 33	20.63
847	5.77
8 55	12.28
13 35	9.36
10 62	7.19
13 26	4.36
12 27	2.04
12 53	2.47
8 51	2.92

B.3 Simulation Platform

A very flexible system level simulation tool has been created during the development of this Ph.D. thesis. Some of its more important features are summarized next:

- Three types of simulation:
  1. Standard Montecarlo test: Static simulations in which a significant amount of uncorrelated snapshots are run to obtain statistics.
  2. Dynamic: Apart from statistics during the observation time, a file is recorded with all the states of UEs. An extra software package in Matlab has been programmed to process these records and observe the evolution of different parameters visually: UEs without coverage, non-admitted, degraded, admitted but inactive, connection with BSs, etc. all this for HSDPA and Rel'99 UEs. There is also the option to generate a movie file.
  3. Maximum Capacity: The program increases or decreases the number of UEs in the scenario to find the maximum capacity according to a certain condition and following an intelligent algorithm. Three criteria are

currently available:

(a) A certain number of BSs (usually 1) have $x\%$ (usually $x = 5$) of UEs in degraded mode in the UL.

(b) Idem but evaluating the DL.

(c) A certain number of BSs (usually 1) have reached its maximum power. In all three cases it is possible to inhibit any base from the condition.

- Radio Resource Management:
  - Power Control: A macroscopic approach composed of a coarse plus a fine analysis is executed. This allows finding UL and DL powers by solving a linear equations system with as many equations as BSs in the system, consequently its resolution is very fast. This equation system is able to realistically consider the existence of repeaters according to the mathematical analysis in Chapter 6. Therefore, the effect of interference generated by signal replicas and the finite nature of the search window of Rake receivers are considered.
  - SHO: UEs in SHO are considered as follows: if UE k has $\varepsilon(k)$ BSs in its AS, it is initially characterized as $\varepsilon(k)$ independent UEs, each one connected to a different BS. Obviously, this indirectly implies a higher number of connections in the network and a more hostile scenario in terms of interference. That is why power control is solved twice. Firstly, a coarse adjust is done, with all virtual connections. Subsequently, once the optimum connection is chosen and the others are eliminated, a refined one gives the final solution. For very loaded scenarios it is likely that the proposed solution is not valid (e.g. negative powers are obtained) in those cases the algorithm commutes to a classical iterative one. If the simulation is dynamic, the first iteration considers the transmission power in the previous frame, so convergence criterion is quickly achieved. The BS that requires less power from the UE may not be the same as the best BS in the AS, which is selected according to the E_c/I_0 levels measured on the CPICH.
  - Admission Control: considers a maximum load factor threshold and OVSF codes occupation (or just one of them). The OVSF code tree is assumed to be perfectly managed and appropriately updated to optimize its occupation, more details can be found in Chapter 8, Section 8.5.1.
  - HSDPA Scheduling: it can be chosen between RR and PF, further details on these algorithms can be found in Appendix C. Multiuser scheduling per TTI is supported. The policy to manage this situation was explained in Chapter 8, Section 8.5.1. Scheduling is simulated in a natural way in dynamic simulations, on the other hand, if the simulation is static, each snapshot is run dynamically for 100 ms so that at least 50 TTI are considered. Given this, final throughput values take into account the effect of the scheduler.

  - HSDPA power allocation: The simulator can be configured to allocate a fixed amount of power or to use the power left by Rel'99 channels until reaching the maximum power minus a margin, which can obviously be zero. Regarding HS-SCCHs, Rel'5 specifications do not stipulate power controlling these channels and this decision is left to the infrastructure vendors. Simulations consider that these channels are power controlled.

- Compatible scenarios. Propagation losses can be loaded in ASCII, raw binary or raster format (SunRaster type). There is no restriction in the number of sectors per Node-B. Georeferentiation of the different propagation layers is fully supported without restrictions on their individual size or position with respect to the others. This way, scenarios from the MORANS initiative are compatible in a natural way. This activity was framed within the COST 273 Action and aimed at providing common system simulation environments so that research results and proposals from different researchers are comparable. In this context, several results derived from Chapter 3 were also simulated and rechecked in the MORANS realistic scenario of Turin [GLR05],[GLFR05].

  Another existent option is introducing all the features of each BS (coordinates, type of antenna, maximum power, pilot, tilt, azimuth, etc.) and let the simulator find the corresponding propagation losses. Typical propagation models are programmed (as previously indicated the COST231-Hata model is used in the synthetic scenario of this dissertation), although this is easily updateable. Three algorithms to model shadowing are also available with different degrees of realism and considering shadowing correlation among BSs:

  1. The first one just adds an independent log-normal component without any relationship among limiting pixels.
  2. The second one considers correlation among pixels in one direction.
  3. Finally, in the third one, the bidimensional correlation is realistically considered following the work in [FLC03].

  For the synthetic case, BSs are located automatically if the user provides the geometric radius that will determine the distance among sites and the dimensions of the area to evaluate.

As it has been shown along this dissertation, UEs can be scattered with any distribution when a file with the probability per pixel is provided. There can be as much distributions as type of services.

Regarding repeaters, they can be simulated in two ways:

1. Integrated in the main scenario.

2. In parallel subscenarios without radioelectrical relation with the main one. This is useful to simulate isolated repeaters as for examples in tunnels, but maintaining all effects in the donor cell in the main scenario.

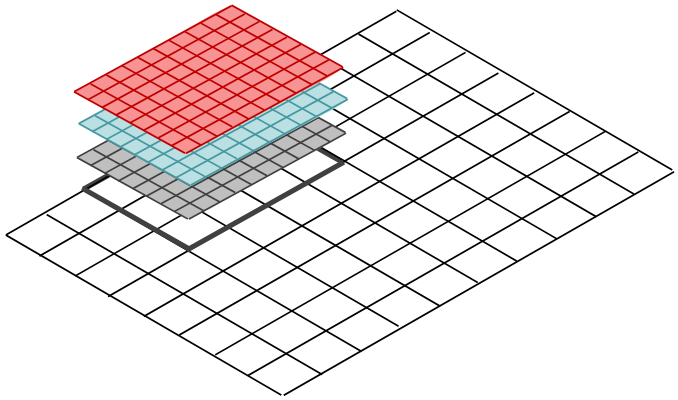

Figure B.4: Indoor areas generation with the use of micropixels.

Indoor areas can also be included provided that external files with attenuation levels are available. This is done by overlapping over the main scenario, a set of pixels with a greater resolution as it is plotted in Figure B.4. Since scenarios are always considered in three dimensions, just assigning different z coordinates to each indoor area, buildings with several floors can be easily generated. This is particularly useful to simulate femtocell deployments or BS hotels configurations.

Finally, it is not needed to mention that all static and dynamic *Automatic Planning* strategies proposed along this dissertation are also implemented.

Appendix C

Considerations on Scheduling Strategies in HSDPA

The basic operation of the HSDPA packet scheduler can be defined as the selection of the user to be served in every TTI. It decides the distribution of radio resources constrained by the satisfaction of individual QoS attributes. Indeed, the TTI reduction from 10 ms in UMTS Rel'99 to 2 ms in Rel'5 (HSDPA)allows the packet scheduler to better exploit the varying channel conditions of different users.

A good design of a scheduling algorithm should take into account not only the maximization of the system throughput, but also being fair to users. That is, scheduling algorithms should balance the trade-off between maximizing throughput and fairness. Several scheduling policies have been proposed in the literature, however a complete evaluation of them and improvement proposals are out of the objectives of the current dissertation. In the context of HSDPA systems, the three basic scheduling algorithms are RR, Maximum Carrier-to-Interference and PF. From them, a wide variety of options exist adapting the basics behind each one to improve particular aspects, [HT06; Ame03; AMHN07].

- **Round Robin (RR)** is considered the basic scheduling reference. It is a channel independent algorithm in which HSDPA users are served with an equal probability in a cyclic ordering. Consequently, two clear advantages arise, first, its implementation simplicity, and second, fairness among users in the cell. The algorithm is fair in the sense of equally distributing the transmission times but this causes different individual throughputs, in detriment of those far from the Node-B. These users require more power to achieve a certain E_b and measure a higher N_0, so, their average rates will be lower when compared with the nearest ones.
- **Maximum Carrier-to-Interference-Ratio scheduler (Max-CIR)** maximizes cell throughput by always serving those users with a higher CIR, that is, those users reporting a higher CQI. As a consequence, unless the cell is very

small, resources are monopolized by a subset of users and those far from the Node-B will hardly be served. Max-CIR and the next approach are channel-aware schedulers, also known as opportunistic algorithms because they exploit the time-variant nature of the radio channel to increase the cell throughput.

- **Proportional Fair (PF)** represents an intermediate point between the two approaches. This algorithm provides an attractive trade-off between average cell throughput and user fairness. Users are served according to their relative channel quality. In particular, the ith user priority $\pi_i(t)$ is given by the quotient of its instantaneous data rate $R_{b,i}(t)$ and average throughput $\overline{R}_{b,i}(t)$:

$$\pi_i(t) = \frac{R_{b,i}(t)}{\overline{R}_{b,i}(t)} \tag{C.1}$$

The traditional method to average the user throughput is the quotient between the amount of successfully transmitted data $\tau_i(t)$ during the user's lifetime Δt_i and that period of time:

$$\overline{R}_{b,i}(t) = \frac{\tau_i(t)}{\Delta t_i} \tag{C.2}$$

This value is usually exponentially smoothed along time and found in a TTI basis. In particular, $\overline{R}_{b,i}$ is updated recursively according to Equation (C.3), which shows the expression to find the user throughput at TTI n:

$$\overline{R}_{b,i}[n] = \begin{cases} (1-\alpha)\,\overline{R}_{b,i}[n-1] + \alpha R_{b,i}[n] & \text{if user } i \text{ is served} \\ (1-\alpha)\,\overline{R}_{b,i}[n-1] & \text{otherwise} \end{cases} \tag{C.3}$$

Where α is a weighting forgetting factor, or similarly, α^{-1} is the averaging period of the smoothing filter measured in TTIs. Depending on the value of α, PF performance tends to RR ($\alpha = 1$) or to Max-CIR ($\alpha = 0$). For intermediate values the performance is something in between. In the context of HSDPA networks, a fairly complete study of standard PF with different parametrization along with comparisons with PF variants can be found in [FN06].

A growing tendency in the literature is posing the problem as an optimization one, but not measuring performance in terms of generic and network-centric indicators, but rather evaluating to which extent the network satisfies each service requirements. In this sense the idea of users *utility* is exploited, see for example [HH07] for a specific HSDPA study case and [SC04] for generic CDMA networks. This is not a novel concept for other types of networks and it was firstly proposed in [Kel97]. It is considered that associated with each user i, there is an utility function U_i representing its satisfaction. From this, the scheduler should select those packets so that the sum of utility functions

for all users is maximized at any given TTI:

$$\begin{array}{rc} \text{Maximize} & \sum_{i=1}^{N} U_i\left(\overline{R}_{b,i}\right) \\ \text{Subject to} & \sum_{i=1}^{N} \overline{R}_{b,i} < R_{ch} \\ \text{and} & \overline{R}_{b,i} \geq 0 \end{array} \tag{C.4}$$

Where R_{ch} is the maximum channel rate and N is the number of UEs in the cell.

This summation constitutes the objective function and, in Equation (C.4), only depends on the mean throughput, however other constraints such as delay could also be included. Under certain circumstances, [HH07], the problem can be solved through the Lagrange method, however since the channel is time varying and so it is the optimal solution, a gradient search method is usually used, [Hos02]. Hence, the priority of each user is given by:

$$\pi_i\left(t\right) = R_{b,i}\left(n\right) \cdot \frac{\partial U_i\left(\overline{R}_{b,i}\left(n\right)\right)}{\partial \overline{R}_{b,i}\left(n\right)} \tag{C.5}$$

For example, in the particular case of elastic data traffic (as most of the internet traffic is and which implies that the transmitter application can handle temporary rate fluctuations), it is admitted that users perceived QoS is a concave function of the mean throughput [JMK+01] well approximated by the logarithm function [EL03]. Intuitively, this means that perceived QoS increases with the mean throughput but just marginally when the user is already correctly served. On the other hand, once the throughput is reduced below a certain level, the satisfaction drops dramatically. Given this, and after solving the optimization problem in Equation (C.4), the scheduling algorithm that maximizes the summation utilities is precisely PF.

With PF, on the average, equal time is assigned to each user but with the particularity that they are scheduled when they have good channel conditions and thus their instantaneous data rate exceeds the average. On the other hand, one of the criticisms that is usually made about PF is the lack of minimum guaranteed QoS parameters. Under the utility approach viewpoint, this can be seen in the fact that PF maximizes an objective function only dependent on the mean throughput.

- **Policies considering QoS differentiations** constitute the fourth group of schedulers. Traditional opportunistic strategies exploit multi-user diversity considering fairness as a constraint, which is mainly efficient for best effort services. However the need for strict QoS support for other services such as streaming, gaming or VoIP is growing. This is indeed the advantage of this fourth group of schedulers, which are QoS-aware driven.

  They often are modifications to the basic PF algorithm aiming at meeting traffic delay constraints, guarantee minimum rates and so on [GYC+07]. The study in [BRC06] deals with VoIP over HSDPA and, even though PF provides bad results for the VoIP service (because of its unawareness of the delay), the

schedulers that obtained better results are some sort of modified PF. Also, the authors in [YZY07] propose an enhanced PF algorithm that takes into account the specific delay requirements of different sensitive data services. Finally, some authors propose the joint use of several utility functions of different types of services [AWL06]. A comparison of the utility functions and its partial derivatives for RR, max-CIR, PF and a set of this fourth group of schedulers can be found in [HT06].

Given the previous paragraphs, it is evident that the variety of scheduling strategies is huge, although PF (and its variations) arises as one of the most interesting options.

Bibliography

[3GPa] *RP-050248. Removal of DSCH (FDD Mode)*, 3GPP Report. [Online]. Available: http://www.3gpp.org/

[3GPb] *TR 25.808 (Release 6) - FDD Enhanced Uplink; Physical Layer Aspects*, 3GPP Technical Report. [Online]. Available: http://www.3gpp.org/

[3GPc] *TR 25.855 (Release 5) - HSDPA; Overall UTRAN Description*, 3GPP Technical Report. [Online]. Available: http://www.3gpp.org/

[3GPd] *TR 25.956 (Release 4) - UTRA Repeaters Planning Guidelines and System Analysis*, 3GPP Technical Report. [Online]. Available: http://www.3gpp.org/

[3GPe] *TR 25.999 (Release 7) - High Speed Packet Access (HSPA) Evolution; Frequency Division Duplex (FDD)*, 3GPP Technical Report. [Online]. Available: http://www.3gpp.org/

[3GPf] *TR 32.8xy (Release 8). Technical Specification Group Services and System Aspects; Telecommunication Management; Study on Self-Healing of SON*, 3GPP Technical Report (draft). [Online]. Available: http://www.3gpp.org/

[3GPg] *TR 36.902 (Release 8). Technical Specification Group TSG RAN Evolved Universal Terrestrial Radio Access Network (E-UTRAN); Self-Configuring and Self-Optimizing Network Use Cases and Solutions*, 3GPP Technical Report. [Online]. Available: http://www.3gpp.org/

[3GPh] *TS 25.133 (Release 5) - Requirement for Support of Radio Resource Management (FDD)*, 3GPP Technical Specification. [Online]. Available: http://www.3gpp.org/

[3GPi] *TS 25.211 (Release 5) - Physical Channels and mapping of Transport Channels onto Physical Channels*, 3GPP Technical Specification. [Online]. Available: http://www.3gpp.org/

[3GPj] *TS 25.214 (Release 5) - Physical Layer Procedures (FDD)*, 3GPP Technical Specification. [Online]. Available: http://www.3gpp.org/

[3GPk] *TS 25.215 (Release 4) - Physical layer; Measurements (FDD)*, 3GPP Technical Specification. [Online]. Available: http://www.3gpp.org/

[3GPl] *TS 25.306 (Release 6). UE Radio Access Capabilities*, 3GPP Technical Specification. [Online]. Available: http://www.3gpp.org/

[3GPm] *TS 25.331 (Release 4). Radio Resource Control (RRC) Protocol Specification*, 3GPP Technical Specification. [Online]. Available: http://www.3gpp.org/

[3GPn] *TS 25.433 (Release 5). UTRAN Iub interface Node B Application Part (NBAP) Signalling*, 3GPP Technical Specification. [Online]. Available: http://www.3gpp.org/

[3GPo] *TS 25.460 (Release 7) - UTRAN Iuant Interface: General Aspects and Principles*, 3GPP Technical Specification. [Online]. Available: http://www.3gpp.org/

[3GPp] *TS 25.942 (Release 4) - RF System Scenarios*, 3GPP Technical Specification. [Online]. Available: http://www.3gpp.org/

[3GPq] *TS 32.403 (Release 4) - Telecommunication management; Performance Management (PM); Performance measurements - UMTS and combined UMTS/GSM*, 3GPP Technical Specification. [Online]. Available: http://www.3gpp.org/

[ACM01] E. Amaldi, A. Capone, and F. Malucelli, "Optimizing Base Station Siting in UMTS Networks," in *Proc. of IEEE Vehicular Technology Conference Spring (VTC 2001 Spring)*, Rhodes (Greece), May 6–9, 2001.

[ACMS03] E. Amaldi, A. Capone, F. Malucelli, and F. Signori, "Optimization models and Algorithms for Downlink UMTS Radio Planning," in *Proc. of IEEE Wireless Communications and Networking Conference WCNC 2003)*, New Orleans (USA), Mar. 16–20, 2003.

[AGLC05] L. Alonso, M. García-Lozano, and F. Casadevall, "Feasibility Condition for the Uplink of a CDMA Multiservice Mobile Communications System with Repeaters," *IEEE Communications Letters*, vol. 9, no. 5, pp. 408–410, May 2005.

[Ahm02] A. Ahmad, "A CDMA Network Architecture Using Optimized Sectoring," *IEEE Transactions on Vehicular Technology*, vol. 51, no. 3, pp. 816–827, May 2002.

[AHNPM01] R. Akl, M. Hegde, M. Naraghi-Pour, and P. Min, "Multicell CDMA Network Design," *IEEE Transactions on Vehicular Technology*, vol. 50, no. 3, pp. 711–722, 2001.

[AJLD+04] R. Abou-Jaoude, J. Luo, M. Dillinger, E. Mohyeldin, and E. Schulz, "Network Controlled Adaptive Antenna Tilting in Multi-Band UMTS FDD," in *Proc. of IEEE International Symposium on Personal, Indoor and Mobile Radio Communications (PIMRC 2004)*, Barcelona (Spain), Sep. 5–8, 2004.

[AK89] E. Aarts and J. Korst, *Simulated Annealing and Boltzmann Machines*, 1st ed. Chicester, UK: John Wiley & Sons, 1989.

[Ame03] P. Ameigeiras, "Packet Scheduling and Quality of Service in HSDPA," Ph.D. dissertation, Institute of Electronic Systems, Aalborg University, Aalborg, Denmark, Oct. 2003.

[AMHN07] B. Al-Manthari, H. Hassanein, and N. Nasser, "Packet Scheduling in 3.5G High-Speed Downlink Packet Access Networks: Breadth and Depth," *IEEE Network*, vol. 21, no. 1, pp. 41–46, Jan. 2007.

[ARO] AROMA (Advanced Resource management solutions for future all IP heterOgeneous Mobile rAdio environments) IST Project (IST-027567), 6th Framework Program of the European Community. [Online]. Available: http://www.aroma-ist.upc.edu/

[AWL06] A. Aguiar, A. Wolisz, and H. Lederer, "Utility-based Packet Scheduler for Wireless Communications," in *Proc. of IEEE Workshop on Wireless Local Networks (WLN 2006)*, Tampa (USA), Nov. 14–17, 2006.

[BBD+05] S. Borst, A. Buvaneswari, L. Drabeck, M. Flanagan, J. Graybeal, G. Hampel, M. Haner, W. MacDonald, P. Polakos, G. Rittenhouse, I. Saniee, A. Weiss, and P. Whiting, "Dynamic Optimization in Future Cellular Networks," *Bell Labs Technical Journal*, vol. 10, no. 2, pp. 99–119, 2005.

[BHHPSS06] L. Bih-Hwang, C. Hsin-Pei, and H. Su-Shun, "Study on Traffic Shedding for Soft-Handoff Using MC-CDMA in Wireless ATM Networks," *IEICE Transactions on Communications*, vol. E89-B, no. 1, pp. 76–87, Jan. 2006.

[BK99] D. Beckmann and U. Killat, "Frequency Planning with Respect to Interference Minimization in Cellular Radio Networks," COST 259, Vienna (Austria), Tech. Rep. available as TD(99)032, Apr. 1999.

[BNI+06] J. Borkowski, J. Niemelä, T. Isolato, P. Lähdekorpi, and J. Lempiäinen, "Utilization of an Indoor DAS for Repeater Deployment in WCDMA," in *Proc. of IEEE Vehicular Technology Conference Fall (VTC 2006 Spring)*, Melbourne (Australia), May 7–10, 2006.

[BNL05] J. Borkowski, J. Niemelä, and J. Lempiäinen, "Applicability of Repeaters for Hotspots in UMTS," in *Proc. of 14th IST Mobile and*

Wireless Communications Summit, Dresden (Germany), Jun. 19–22, 2005.

[BRC06] A. R. Braga, E. B. Rodrigues, and F. R. P. Cavalcanti, "Novel Scheduling Algorithms Aiming for QoS Guarantees for VoIP over HSDPA," in *Proc. of International Telecommunications Symposium (ITS 2006)*, Fortaleza (Brasil), Sep. 3–6, 2006.

[Bun99] S. Bundy, "Antenna Donwtilt Effects on CDMA Cell-site Capacity," in *Proc. of IEEE Radio and Wireless Conference (RAWCON 1999)*, Denver (USA), Aug. 1–4, 1999.

[Cal06] Calcev, G. and Dillon, M, "Antenna Tilt Control in CDMA Networks," in *Proc. of 2nd Annual International Workshop on Wireless Internet (WICON 2006)*, Boston (USA), Aug. 2–5, 2006.

[CBG+06] C. Chevallier, C. Brunner, A. Garavaglia, K. P. Murray, and K. R. Baker, *WCDMA (UMTS) Deployment Handbook: Planning and Optimization Aspects*, 1st ed. Chicester, UK: John Wiley & Sons, 2006.

[CCB01] W. Choi, Y. Cho, and T. Ban, "Automatic On-Off Switching Repeater for DS/CDMA Reverse Link Capacity Improvement," *IEEE Communications Letters*, vol. 5, no. 4, pp. 138–141, Apr. 2001.

[Ce06] L. Correia (ed.), *Mobile Broadband Multimedia Networks. Techniques Models and Tools for 4G*, 1st ed. London, UK: Elsevier (Academic Press), 2006, section entitled: Base Station Parameter Configuration.

[Coe01] C. Coello, "A Short Tutorial on Evolutionary Multiobjective Optimization," *Lecture Notes in Computer Science*, vol. 1993, pp. 21–40, Jan. 2001.

[COPR05] C. Commander, C. Oliveira, P. Pardalos, and M. Resende, "A Greedy Randomized Algorithm for Cooperative Communication in Ad Hoc Networks," in *Proc. of International Conference on Cooperative Control and Optimization*, Gainesville (USA), Jan. 22–25, 2005.

[COS] COST Action 273 Website. Towards Mobile Broadband Multimedia Networks. [Online]. Available: http://www.lx.it.pt/cost273/

[DAKR93] M. Duque-Antón, D. Kunz, and B. Rüber, "Channel Assignment for Cellular Radio Using Simulated Annealing," *IEEE Transactions on Vehicular Technology*, vol. 42, no. 1, pp. 14–21, Feb. 1993.

[DBC03] L. Du, J. Bigham, and L. Cuthbert, "Towards Intelligent Geographic Load Balancing for Mobile Cellular Networks," *IEEE Transactions on Systems Man and Cybernetics Part C. Applications and Reviews*, vol. 33, no. 4, pp. 480–491, Nov. 2003.

[DBC05] ——, "Geographic Load Balancing for WCDMA Mobile Networks Using a Bubble Oscillation Algorithm," in *Proc. of IEEE Wireless Communications and Networking Conference WCNC 2005)*, New Orleans (USA), Mar. 13–17, 2005.

[DC99] E. Damoso and L. M. Correia, "COST 231 Final Report - Digital Mobile Radio: Evolution Towards Future Generation Systems," COST Secretariat, Brussels (Belgium), Tech. Rep., 1999.

[Dor92] M. Dorigo, "Optimization, Learning and Natural Algorithms," Ph.D. dissertation, Politecnico di Milano, Milano, Italy, 1992, in Italian.

[DU92] P. Davies and Z. Urey, "Subcarrier Multiplexing in Optical Communications Networks," *IEEE Electronics and Communications Journal*, vol. 4, no. 2, pp. 65–72, Apr. 1992.

[EFF+03] A. Eisenblätter, A. Fügenschuh, E. R. Fledderus, H.-F. Geerdes, B. Heideck, D. Junglas, T. Koch, T. Kürner, and A. Martin, "Mathematical methods for automatic optimization of UMTS radio networks," MOMENTUM EU IST program project(IST-2000-28088), Tech. Rep. available as Deliberable D4.3, 2003. [Online]. Available: http://momentum.zib.de/

[EL03] N. Enderlé and X. Lagrange, "User Satisfaction Models and Scheduling Algorithms for Packet-Switched Services in UMTS," in *Proc. of IEEE Vehicular Technology Conference Spring (VTC 2003 Spring)*, Jeju (Korea), Apr. 22–25, 2003.

[FLC03] R. Fraile, O. Lázaro, and N. Cardona, "Two Dimensional Shadowing Model," COST 273, Prague (Czech Rep.), Tech. Rep. available as TD(03)171, Sep. 24–26, 2003.

[FN02] J. Flanagan and T. Novosad, "WCDMA Network Cost Function Minimization for Soft Handover Optimization with Variable User Load," in *Proc. of IEEE Vehicular Technology Conference Fall (VTC 2002 Fall)*, Vancouver (Canada), Sep. 24–28, 2002.

[FN06] F. Feller and M. C. Necker, "Comparison of Opportunistic Scheduling Algorithms for HSDPA Networks," in *Proc. of 12th EUNICE Open European Summer School (EUNICE 2006)*, Stuttgart (Germany), Sep. 18–20, 2006.

[For02] Forkel, I. and Kemper, A. and Pabst, R. and Hermans, R., "The Effect of Electrical and Mechanical Antenna Down-tilting in UMTS Networks," in *Proc. of International Conference on 3G Mobile Communication Technologies*, London (UK), May 8–10, 2002.

[FR89] T. Feo and M. Resende, "A probabilistic heuristic for a computationally difficult set covering problem," *Operations Research Letters*, vol. 8, no. 2, pp. 67–71, Apr. 1989.

[GAN] GANDALF (Monitoring and self-tuning of RRM parameters in a multi-system network) EUREKA-CELTIC Project (P-ID-CP2-014). [Online]. Available: http://www.celtic-gandalf.org/

[Gat05] P. Gattei, "WCDMA Radio Network Initial Tuning. Ericsson Experience," Ericsson, Bologna (Italy), Tech. Rep., 2005.

[GBD01] A. Girard, S. B., and L. Dadjo, "A Tabu Search Algorithm for Access Network Design," *Annals of Operations Research*, vol. 106, no. 1–4, pp. 229–262, Sep. 2001.

[GC04] E. Gago and L. Cucala, "Radio on Fibre Systems for Practical 2G and 3G Deployment," COST 273, Athens (Greece), Tech. Rep. available as TD(04)001, Jan. 26–28, 2004.

[GJCT03a] A. Gerdenitsch, S. Jackl, Y. Chong, and M. Toeltsch, "An Adaptive Algorithm for Capacity Optimization in UMTS FDD Networks," COST 273, Prague (Czech Rep.), Tech. Rep. available as TD(03)162, Sep. 24–26, 2003.

[GJCT03b] ——, "Optimization of CPICH Power and Antenna Tilt in UMTS FDD Networks," COST 273, Paris (France), Tech. Rep. available as TD(03)101, May 21–23, 2003.

[GJT04] A. Gerdenitsch, S. Jackl, and M. Toeltsch, "The Use of Genetic Algorithms for Capacity Optimization in UMTS FDD Networks," COST 273, Athens (Greece), Tech. Rep. available as TD(04)012, Jan. 26–28, 2004.

[GLAC+06] M. García-Lozano, L. Alonso, F. Casadevall, S. Ruiz, and L. Correia, "On the Impact of Repeaters Deployment on WCDMA Networks Planning," in *Proc. of IEEE Vehicular Technology Conference Fall (VTC 2006 Spring)*, Melbourne (Australia), May 7–10, 2006.

[GLAC+07] ——, "Enhanced Analysis of WCDMA Networks with Repeaters Deployment," *IEEE Transactions on Wireless Communications*, vol. 6, no. 9, pp. 3429–3439, Sep. 2007.

[GLACR05a] M. García-Lozano, L. Alonso, F. Casadevall, and S. Ruiz, "Capacity and Coverage Tradeoff in WCDMA Environments with Repeaters Deployment," in *Proc. of International Symposium on Wireless Personal Multimedia Communications (WPMC 2005)*, Aalborg (Denmark), Sep. 18–22, 2005.

[GLACR05b] ——, "Impact of Repeaters Deployment on UMTS Admission Control," COST 273, Lisbon (Portugal), Tech. Rep. available as TD(05)117, Sep. 10–11, 2005.

[GLACR07] ——, "Capacity and Coverage Tradeoff in WCDMA Environments with Repeaters Deployment," *Wireless Personal Communications Journal*, vol. 40, no. 2, pp. 329–342, Feb. 2007.

[GLFR05] M. García-Lozano, P. Falavigna, and S. Ruiz, "Detailed UL/DL Analysis of MORANS Torino Scenario under Different Traffic Behaviour," COST 273, Bologna (Italy), Tech. Rep. available as TD(05)022, Jan. 19–21, 2005.

[Glo86] F. Glover, "Future Paths for Integer Programming and Links to Artificial Intelligence," *Computers and Operations Research*, vol. 13, no. 5, pp. 533–549, 1986.

[GLR04] M. García-Lozano and S. Ruiz, "Effects of Downtilting on RRM Parameters," in *Proc. of IEEE International Symposium on Personal, Indoor and Mobile Radio Communications (PIMRC 2004)*, Barcelona (Spain), Sep. 5–8, 2004.

[GLR05] ——, "Effects of Donwtilt on the MORANS Real World Scenario of Turin," COST 273, Lisbon (Portugal), Tech. Rep. available as TD(05)111, Sep. 10–11, 2005.

[GLR08] ——, "Study on the Automated Tuning of HSDPA Code Allocation," COST 2100, Wroclaw (Poland), Tech. Rep. available as TD(08)410, Feb. 06–08, 2008.

[GLRALOC07] M. García-Lozano, S. Ruiz, A. Andújar-Linares, and N. Oller-Camaute, "Automatic Tuning of Soft Handover Parameters in UMTS Networks," COST 2100, Duisbrug (Germany), Tech. Rep. available as TD(07)344, Sep. 10–12, 2007.

[GLRHO04] M. García-Lozano, S. Ruiz, R. Higuero, and J. Olmos, "UMTS Network Optimisation: Impact of Donwtilted Antennas," COST 273, Athens (Greece), Tech. Rep. available as TD(04)033, Jan. 26–28, 2004.

[GLRO03a] M. García-Lozano, S. Ruiz, and J. Olmos, "CPICH Powers Optimization by means of Simulated Annealing," COST 273, Paris (France), Tech. Rep. available as TD(03)103, May 21–23, 2003.

[GLRO03b] ——, "CPICH Powers Optimization by means of Simulated Annealing in an UTRA-FDD environment," *IEE Electronic Letters*, vol. 39, no. 23, pp. 1676–1677, Nov. 2003.

[GLRO04a] ——, "Optimum Cell Balancing for UMTS Inhomogeneous Traffic Distribution," in *Proc. of International Symposium on Wireless Personal Multimedia Communications (WPMC 2004)*, Padova (Italy), Sep. 12–15, 2004.

[GLRO04b] ——, "UMTS Optimum Cell Load Balancing for Inhomogeneous Traffic Patterns," in *Proc. of IEEE Vehicular Technology Conference Fall (VTC 2004 Fall)*, Los Angeles (USA), Sep. 26–29, 2004.

[GLRS+03] M. García-Lozano, S. Ruiz, O. Sallent, F. Adelantado, R. Agustí, M. Díaz-Guerra, J. Montero, E. Gago, J. Miranda, and F. Castejón, "Analysing UTRA-FDD Pilot Power and Active Set Configuration in a Real Urban Scenario," in *Proc. of IEEE International Symposium on Personal, Indoor and Mobile Radio Communications (PIMRC 2003)*, Beijing (China), Sep. 7–10, 2003.

[GLSPR+07] M. García-Lozano, O. Sallent, J. Pérez-Romero, S. Ruiz, A. Gomez, and P. d'Orey, "Automated Up- and Downlink Capacity Balancing in WCDMA Networks," in *Proc. of IEEE Vehicular Technology Conference Fall (VTC 2007 Fall)*, Baltimore (USA), Sep. 30/Oct. 1, 2007.

[GLSPRR08] M. García-Lozano, O. Sallent, J. Pérez-Romero, and S. Ruiz, "Performance Improvement of HSDPA/UMTS Networks through Dynamic Code Tuning," in *Proc. of IEEE International Symposium on Personal, Indoor and Mobile Radio Communications (PIMRC 2008)*, Cannes (France), Sep. 15–18, 2008.

[GYC+07] J. S. Gomes, M. Yun, H. Choi, J. Kim, J. Sohn, and H. I. Choi, "Scheduling Algorithms For Policy Driven QoS Support in HSDPA Networks," in *Proc. of IEEE Vehicular Technology Conference Spring (VTC 2007 Spring)*, Dubling (Ireland), Apr. 22–25, 2007.

[Han99] S. Handly, "Congestion Measures in DS-CDMA Networks," *IEEE Transactions on Communications*, vol. 47, no. 3, pp. 426–437, Mar. 1999.

[HH07] A. Haider and R. Harris, "A Novel Proportional Fair Scheduling Algorithm for HSDPA in UMTS Networks," in *Proc. of IEEE International Conference on Wireless Broadband and Ultra Wideband Communications (AusWireless 2007)*, Sydney (Australia), Aug. 27–30, 2007.

[Hol75] J. Holland, *Adaptation in Natural and Artificial Systems*, 1st ed. Cambridge, USA: MIT Press, 1975.

[Hos02] Hossein, P. A., "QoS Control for WCDMA High Speed Packet Data," in *Proc. of 4th International Workshop on Mobile and Wireless Communications Network*, Stockholm (Sweden), Sep. 9–11, 2002.

[HPVL03] A. Höglund, J. Pöllönen, K. Valkealahti, and J. Lahio, "Quality-based Auto-tuning of Cell Uplink Load Level Targets in WCDMA," in *Proc. of IEEE Vehicular Technology Conference Fall (VTC 2003 Fall)*, Jeju (Korea), Apr. 22–25, 2003.

[HSG00] J. Harmatos, . Sentéis, and I. Gódor, "Planning of Tree-Topology UMTS Terrestrial Access Networks," in *Proc. of IEEE International Symposium on Personal, Indoor and Mobile Radio Communications (PIMRC 2000)*, London (England), Sep. 18–21, 2000.

[HT02] H. Holma and A. Toskala, *WCDMA for UMTS Radio Access for Third Generation Mobile Communications*, 2nd ed. Chicester, UK: John Wiley & Sons, 2002.

[HT06] ——, *HSDPA / HSUPA for UMTS*, 1st ed. Chicester, UK: John Wiley & Sons, 2006.

[Hur02] S. Hurley, "Planning Effective Cellular Mobile Radio Networks," *IEEE Transactions on Vehicular Technology*, vol. 51, no. 2, pp. 243–253, Mar. 2002.

[HV02] A. Höglund and K. Valkealahti, "Quality-based Tuning of Cell Downlink Load Target and Link Power Maxima in WCDMA," in *Proc. of IEEE Vehicular Technology Conference Fall (VTC 2002 Fall)*, Vancouver (Canada), Sep. 24–28, 2002.

[JCP+00] K. Jeong, J. Cheong, T. Park, T. Kim, and S. Park, "Performance Analysis of DS-CDMA Reverse Link with Fiber-Optics Repeaters," in *Proc. of IEEE Vehicular Technology Conference Spring (VTC 2000 Spring)*, Tokyo (Japan), May 15–18, 2000.

[JJ99] D. Jeong and W. Jeon, "CDMA/TDD System for Wireless Multimedia Services with Traffic Unbalance Between Uplink and Downlink," *IEEE Journal on Selected Areas in Communications*, vol. 17, no. 5, pp. 939–946, May 1999.

[JMK+01] Z. Jiang, H. Mason, B. J. Kim, N. K. Shankaranarayanan, and P. Henry, "A Subjective Survey of User Experience for Data Applications for Future Cellular Wireless Networks," in *Proc. of IEEE Symposium on Applications and the Internet (SAINT 2001)*, San Diego, (USA), Jan. 8–12, 2001.

[Kat] Kathrein Website. [Online]. Available: http://www.kathrein.de/

[KC05] V. Kumar and E. Cole, "An ant colony optimization model for wireless ad-hoc network autoconfiguration," in *Proc. of IEEE International Conference on Systems, Man and Cybernetics*, Big Island (USA), Oct. 10–12, 2005.

[KCL99] D. Kim, Y. Chang, and J. Lee, "Pilot Power Control and Service Coverage Support in CDMA Mobile Systems," in *Proc. of IEEE Vehicular Technology Conference Spring (VTC 1999 Spring)*, Houston (USA), May 16–20, 1999.

[Kel97] F. Kelly, "Charging and Rate Control for Elastic Traffic," *European Transactions on Telecommunications*, vol. 8, no. 1, pp. 33–37, Jan. 1997.

[KFN02] I. Kocsis, L. Farkas, and L. Nagy, "3G Base Station Positioning Using Simulated Annealing," in *Proc. of IEEE International Symposium on Personal, Indoor and Mobile Radio Communications (PIMRC 2002)*, Lisboa (Portugal), Sep. 15–18, 2002.

[KGV83] S. Kirkpatrick, C. Gelatt, and M. Vecchi, "Optimization by simulated annealing," *Science*, vol. 220, no. 4598, pp. 671–680, May 1983.

[KJ00] D. Kim and D. Jeong, "Capacity Unbalance Between Uplink and Donwlink in Spectrally Overlaid Narrow-Band and Wide-Band CDMA Mobile Systems," *IEEE Transactions on Vehicular Technology*, vol. 49, no. 4, pp. 1086–1093, Jul. 2000.

[KLKW00] D. Kim, D. Lee, H. Kim, and K. Whang, "Capacity Analysis of Macro/Microcellular CDMA with Power Ratio Control and Tilted Antenna," *IEEE Transactions on Vehicular Technology*, vol. 49, no. 1, pp. 34–42, Jan. 2000.

[Kre06] R. Kreher, *UMTS Performance Measurement. A Practical Guide to KPIs for the UTRAN Environment*, 1st ed. Chicester, UK: John Wiley & Sons, 2006.

[KU02] M. Kamenetsky and M. Unbehaun, "Coverage Planning for Outdoor Wireless LAN Systems," in *Proc. of IEEE International Zurich Seminar on Broadband Communications*, Zurich (Switzerland), Feb. 19–21, 2002.

[LBAN07] F. Luna, C. Blum, E. Alba, and A. Nebro, "ACO vs EAs for solving a real-world frequency assignment problem in GSM networks," in *Proc. of Genetic And Evolutionary Computation Conference (GECCO 2007)*, London (UK), Jul. 7–11, 2007.

[LBSR99] R. Love, K. Beshir, D. Shaeffer, and N. R.S., "A Pilot Optimization Technique for CDMA Cellular Systems," in *Proc. of IEEE Vehicular Technology Conference Spring (VTC 1999 Fall)*, Amsterdam (The Netherlands), Sep. 19–22, 1999.

[LCH05] B. Lee, H. Chen, and S. Huang, "A Traffic Shedding Algorithm for Soft-Handoff in MC-CDMA Systems," in *Proc. of IEEE International Conference on Parallel and Distributed Systems (ICPADS 2005)*, Fukuoka (Japan), Jul. 20–25, 2005.

[LCPD06] B. Lannoo, D. Colle, M. Pickavet, and P. Demeester, "Comparison of Two Optical Switching Architectures to Provide a Broadband Connection to Train Passengers," in *Proc. of Optical Fiber Communications Conference and the National Fiber Optic Engineers Conference (OFC/NFOEC 2006)*, Anaheim, (USA), Mar. 5–10, 2006.

[LCPD07] ——, "Radio-over-Fiber-Based Solution to Provide Broadband Internet Access to Train Passengers," *IEEE Communications Magazine*, vol. 45, no. 2, pp. 56–62, Feb. 2007.

[LFYG05] J. Li, C. Fan, D. Yand, and J. Gu, "UMTS Soft Handover Algorithm with Adaptive Thresholds for Load Balancing," in *Proc. of*

IEEE Vehicular Technology Conference Fall (VTC 2005 Fall), Dallas (USA), Sep. 25–28, 2005.

[LL00] W. Lee and D. Lee, "The Impact of Repeaters on CDMA System Performance," in *Proc. of IEEE Vehicular Technology Conference Spring (VTC 2000 Spring)*, Tokyo (Japan), May 15–18, 2000.

[LOP03] S. Lim, S. Oh, and J. Park, "A New Adaptive Sectorization Method to Use Maximum Capacity of Base Station in Wireless Communications," *Lecture Notes in Computer Science*, vol. 2524, pp. 15–22, Jan. 2003.

[LPRR00] X. Liu, P. Pardalos, S. Rajasekaran, and M. Resende, "A GRASP for Frequency Assignment in Mobile Radio Networks," *Mobile Networks and Computing. DIMACS Series on Discrete Mathematics and Theoretical Computer Science)*, vol. 52, pp. 195–201, 2000.

[LSWA00] J. Laiho-Steffens, A. Wacker, and P. Aikio, "The Impact of the Radio Network Planning and Site Configuration on the WCDMA Network Capacity and Quality of Service," in *Proc. of IEEE Vehicular Technology Conference Spring (VTC 2000 Spring)*, Tokyo (Japan), May 15–18, 2000.

[LWN06] J. Laiho, A. Wacker, and T. Novosad, *Radio Network Planning and Optimisation for UMTS*, 2nd ed. Chicester, UK: John Wiley & Sons, 2006.

[LYLC05] C. Liao, F. Yu, V. Leung, and C. Chang, "Reinforcement-learning-based self-organisation for cell configuration in multimedia mobile networks," *European Transactions on Telecommunications*, vol. 16, no. 5, pp. 385–397, Sep. 2005.

[LZY05] J. Li, J. Zhang, and D. Yang, "Improved Pilot Power Adjustment for Load Balancing in the CDMA System," in *Proc. of International Conference on Wireless Communications, Networking and Mobile Computing (WCNM 2005)*, Wuhan (China), Sep. 23–23, 2005.

[Mac79] H. MacDonald, "The Cellular Concept," *Bell Systems Technical Journal*, vol. 58, no. 1, pp. 15–42, 1979.

[MG04] S. Menon and S. Gupta, "Assigning Cells to Swithces in Cellular Netowrks by Incorporating a Pricing Mechanism into Simulated Annealing," *IEEE Transactions on Systems Man and Cybernetics Part B. Cybernetics*, vol. 34, no. 1, pp. 558–565, Feb. 2004.

[MGWK03] N. Mehta, L. Greenstein, T. Willis, and Z. Kostic, "Analysis and Results for the Orthogonality Factor in WCDMA Downlinks," *IEEE Transactions on Wireless Communications*, vol. 2, no. 6, pp. 1138–1149, Nov. 2003.

[MH01] L. Mendo and J. Hernando, "On Dimension Reduction for the Power Control Problem," *IEEE Transactions on Communications*, vol. 49, no. 2, pp. 243–248, Feb. 2001.

[MMG05] N. Mehta, A. Molisch, and L. Greenstein, "Orthogonality Factor in WCDMA Downlinks in Urban Macrocellular Environments," in *Proc. of IEEE Global Telecommunications Conference (GLOBECOM 2005)*, St. Louis (USA), Nov. 28/Dec. 2, 2005.

[MON] MONOTAS (Mobile Network Optimisation Through Advanced Simulation) Program of the Department of Trade and Industry's Technology Programme in UK. [Online]. Available: http://www.macltd.com/monotas/

[MRRT53] N. Metropolis, A. Rosenbluth, A. Rosenbluth, and E. Teller, "Equations of State Calculations by Fast Computing Machines," *Journal of Chemical Physics*, vol. 21, no. 6, pp. 1087–1092, 1953.

[MSS07] A. Mäder, D. Staehle, and M. Spahn, "Impact of HSDPA Radio Resource Allocation Schemes on the System Performance of UMTS," in *Proc. of IEEE Vehicular Technology Conference Fall (VTC 2007 Fall)*, Baltimore (USA), Sep. 30/Oct. 1, 2007.

[MVC03] K. Maksuriwong, V. Varavithya, and N. Chaiyaratana, "Wireless LAN Access Point Placement Using a Multi-Objective Genetic Algorithm," in *Proc. of IEEE International Conference on Systems, Man and Cybernetics (SMC 2003)*, Kyoto (Japan), Oct. 5–8, 2003.

[NDA06] M. Nawrocki, M. Dohler, and A. Aghvami, *Understanding UMTS Radio Network - Modelling, Planning and Automated Optimisation*, 1st ed. Chicester, UK: John Wiley & Sons, 2006.

[NDF04] T. Nguyen, P. Dassanayake, and M. Faulkner, "Use of Adaptive Sectorisation for Capacity Enhancement in CDMA Cellular Systems with Non-Uniform Traffic," *Wireless Personal Communications*, vol. 28, no. 2, pp. 107–120, Jan. 2004.

[NIL05] J. Niemelä, T. Isotalo, and J. Lempiäinen, "Optimum Antenna Downtilt Angles for Macrocellular WCDMA Network," *EURASIP Journal on Wireless Communications and Networking*, vol. 5, no. 5, pp. 816–827, Oct. 2005.

[NL04] J. Niemelä and J. Lempiäinen, "Impact of mechanical antenna downtilt on performance of WCDMA cellular network," in *Proc. of IEEE Vehicular Technology Conference Spring (VTC 2004 Spring)*, Milan (Italy), May 17–19, 2004.

[NLBL05] J. Niemelä, P. Lähdekorpi, J. Borkowski, and J. Lempiäinen, "Assessment of Repeaters for WCDMA UL and DL Performance in Capacity-limited Environment," in *Proc. of 14th IST Mobile and*

Wireless Communications Summit, Dresden (Germany), Jun. 19–22, 2005.

[ORGL03] J. Olmos, S. Ruiz, and M. García-Lozano, "Description of UTRA FDD Link Level Simulator. Description of UTRA FDD Link Level Lookup Tables (MORANS)." COST 273, Paris (France), Tech. Rep. available as TD(03)095, May 21–23, 2003.

[PBS04] M. Pettersen, L. Braten, and A. Spilling, "Automatic antenna tilt control for capacity enhancement in UMTS FDD," in *Proc. of IEEE Vehicular Technology Conference Fall (VTC 2004 Fall)*, Los Angeles (USA), Sep. 26–29, 2004.

[PDGA04] J. Picard, H. Dubreil, F. Garabedian, and Z. Altman, "Dynamic Control of UMTS Networks by Load Target Tuning," in *Proc. of IEEE Vehicular Technology Conference Spring (VTC 2004 Spring)*, Milan (Italy), May 17–19, 2004.

[PJ03] S. Panthong and S. Jantarang, "3G Mobile Wireless Routing Optimization by Genetic Algorithm," in *Proc. of IEEE Canadian Conference on Electrical and Computer Engineering (CCECE 2003)*, Montréal (Canada), May 4–7, 2003.

[PRO05] M. Patwary, P. Rapajic, and I. Oppermann, "Capacity and Coverage Increase with Repeaters in UMTS Urban Cellular Mobile Communication Environment," *IEEE Transactions on Communications*, vol. 53, no. 10, pp. 1620–1624, Oct. 2005.

[PUAL97] W. Park, H. Um, J. Ahn, and S. Lee, "Performance Analysis on Traffic Load Shedding Schemes for Mobile Communication System," in *Proc. of IEEE International Conference on Universal Personal Communications Record (ICUPC 1997)*, San Diego (USA), Oct. 12–16, 1997.

[QP08] A. Quintero and S. Pierre, "On the Design of Large-Scale UMTS Mobile Networks Using Hybrid Genetic Algorithms," *IEEE Transactions on Vehicular Technology*, 2008, accepted for future publication.

[RE04] M. Rahman and P. Ernstrom, "Repeaters for Hotspot Capacity in DS-CDMA Networks," *IEEE Transactions on Vehicular Technology*, vol. 53, no. 3, pp. 626–633, May 2004.

[Ris07] P. Risavy, "The Evolution of Rel-7 to Rel-8 – HSPA and SAE/LTE," 3G Americas, Brussels (Belgium), Tech. Rep., 2007.

[RSA+03] S. Ruiz, O. Sallent, R. Agustí, M. García-Lozano, F. Adelantado, M. Díaz-Guerra, J. Montero, E. Gago, and J. Miranda, "3G Planning by Using 2G Measurements," COST 273, Barcelona (Spain), Tech. Rep. available as TD(03)073, Jan. 15–17, 2003.

[RSW06] P. Rathinavelu, G. Schapeler, and A. Weber, "UMTS Coverage and Capacity Enhancement Using Repeaters and Remote RF Heads," in *Proc. of International Conference on Advanced Information Networking and Applications (AINA 2006)*, Stuttgart (Germany), Sep. 18–20, 2006.

[SC04] S. Shen and C. Chang, "A Utility-based Scheduling Algorithm with Differentiated QoS Provisioning for Multimedia CDMA Cellular Networks," in *Proc. of IEEE Vehicular Technology Conference Spring (VTC 2004 Spring)*, Milan (Italy), May 17–19, 2004.

[SGH03] Y. Sun, F. Gunnarsson, and K. Hiltunen, "CPICH Power Settings in Irregular WCDMA Macro Cellular Networks," in *Proc. of IEEE International Symposium on Personal, Indoor and Mobile Radio Communications (PIMRC 2003)*, Beijing (China), Sep. 1176–1180, 2003.

[SM07] J. Shapira and S. Miller, *CDMA Radio with Repeaters*, 1st ed. New York, USA: Springer, 2007.

[SNBH00] A. Spilling, A. Nix, M. Beach, and T. Harrold, "Self-Organization in Future Mobile Communications," *Electronics and Communication Engineering Journal*, vol. 12, no. 3, pp. 133–147, Jun. 2000.

[SOC] SOCRATES (Self-Optimisation and self-ConfiguRATion in wirelEss networkS) IST Project, 7th Framework Program of the European Community. [Online]. Available: http://www.fp7-socrates.org/

[Spa03] J. Spall, *Introduction to Stochastic Search and Optimization*, 1st ed. Hoboken, USA: John Wiley & Sons, 2003.

[SRH01] D. Smith, T. R.K., and S. Hurley, "Frequency Assignment with Complex Co-site Constraints," *IEEE Transactions on Electromagnetic Compatibility*, vol. 43, no. 2, pp. 210–218, May 2001.

[SSSMBC04] S. Salcedo-Sanz, R. Santiago-Mozos, and C. Bousoño-Calzón, "A Hybrid Hopfiled Network-Simulated Annealing Approach for Frequency Assignment in Satellite Communications Systems," *IEEE Transactions on Systems Man and Cybernetics Part B. Cybernetics*, vol. 34, no. 2, pp. 1108–1116, Apr. 2004.

[SVY07] I. Siomina, P. Värbrand, and D. Yuan, "Pilot Power Optimization and Coverage Control in WCDMA Networks," *Omega. Special Issue on Telecommunications Applications*, vol. 35, no. 6, pp. 683–696, Dec. 2007.

[SY01] C. Saraydar and A. Yener, "Adaptive Cell Sectorization for CDMA Systems," *IEEE Journal on Selected Areas in Communications*, vol. 19, no. 6, pp. 1041–1051, Jun. 2001.

[SY04] I. Siomina and D. Yuan, "Pilot Power Management in WCDMA Networks: Coverage Control with respect to Traffic Distribution," in *Proc. of the 7th ACM International Symposium on Modeling, Analysis and Simulation of Wireless and Mobile Systems (MSWiM 2004)*, Venice (Italy), Oct. 4–6, 2004.

[Tay03] C. Taylor, "Remote RF is Becoming a Mainstream Solution," Celerica, Tech. Rep., Jun. 2003. [Online]. Available: www.celerica.com

[TE06] G. Thrasivoulos and D. Esmael, "HSDPA Network Dimensioning Challenges and Key Performance Parameters," *Bechtel Telecommunications Technical Journal (BTTJ)*, vol. 4, no. 2, pp. 77–82, Jun. 2006.

[TWLK07] P. Tapia, D. Wellington, J. Liu, and Y. Karimli, "Practical Considerations of HSDPA Performance," in *Proc. of IEEE Vehicular Technology Conference Fall (VTC 2007 Fall)*, Baltimore (USA), Sep. 30/Oct. 1, 2007.

[TYC05] K. Thng, B. Yeo, and Y. Chew, "Performance Study on the Effects of Cell-Breathing in WCDMA," in *Proc. of IEEE International Symposium on Wireless Communications Systems (ISWCS 2005)*, Sienna (Italy), Sep. 5–7, 2005.

[VB03] R. Verdone and H. Buehler, "MORANS White Paper," COST 273, Barcelona (Spain), Tech. Rep. available as TD(03)057, Jan. 15–17, 2003.

[VB07] S. Vangipuram and S. Bhashyam, "Multiuser Scheduling and Power Sharing for CDMA Packet Data Systems," in *Proc. of National Conference on Communications (NCC 2007)*, Kanpur (India), Jan. 26–28, 2007.

[VBC+04] R. Verdone, H. Buehler, N. Cardona, A. Munna, R. Patelli, S. Ruiz, P. Grazioso, A. Zanella, A. Eisenblätter, and H. Geerdes, "MORANS White Paper - Update," COST 273, Athens (Greece), Tech. Rep. available as TD(04)062, Jan. 26–28, 2004.

[VHPH02a] K. Valkealahti, A. Höglund, J. Parkkinen, and A. Hamalainen, "WCDMA Common Pilot Power Control for Load and Coverage Balancing," in *Proc. of IEEE International Symposium on Personal, Indoor and Mobile Radio Communications (PIMRC 2002)*, Lisboa (Portugal), Sep. 15–18, 2002.

[VHPH02b] ——, "WCDMA Common Pilot Power Control with Cost Function Minimization," in *Proc. of IEEE Vehicular Technology Conference Fall (VTC 2002 Fall)*, Vancouver (Canada), Sep. 24–28, 2002.

[VY03] P. Värbrand and D. Yuan, "A Mathematical Programming Approach for Pilot Power Optimization in WCDMA Networks," in *Proc. of Australian Telecommunications, Networks and Applications Conference (ATNAC 2003)*, Melbourne (Australia), Dec. 8–10, 2003.

[WB01] H. Willerbrand and G. B.S., "Fiber Optics without Fiber," *IEEE Spectrum*, vol. 38, no. 8, pp. 41–45, Aug. 2001.

[WBJN06] J. Wu, J. Bigham, P. Jiang, and J. Neophytou, "Tilting and Beamshaping for Traffic Load Balancing in WCDMA Network," in *Proc. of 9th European Conference on Wireless Technology (ECWT 2006)*, Manchester (UK), Sep. 10–12, 2006.

[WC01] W. Wsewolod and L. Cucala, "Sistemas de Distribución para UMTS," *Comunicaciones de Telefonica I+D*, no. 21, pp. 57–70, Jun. 2001.

[WCW98] J. Wu, J. Chung, and C. Wen, "Hot-spot Traffic Relief with a Tilted Antenna in CDMA Cellular Networks," *IEEE Transactions on Vehicular Technology*, vol. 47, no. 1, pp. 1–9, Feb. 1998.

[Wer92] P. Werbos, "Neurocontrol and Fuzzy Logic: Connections and Design," *International Journal of Approximate Reasoning*, vol. 6, no. 2, pp. 185–219, Feb. 1992.

[WQDT01] H. Wu, C. Qiao, S. De, and O. Tonguz, "Integrated Cellular and Ad Hoc Relaying Systems: iCAR," *IEEE Journal on Selected Areas in Communications*, vol. 19, no. 10, pp. 2105–2115, Oct. 2001.

[WRH04] R. Whitaker, L. Raisanen, and S. Hurley, "A Model for Conflict Resolution Between Coverage and Cost in Cellular Wireless Networks," in *Proc. of IEEE Hawaii International Conference on System Sciences (HICSS 2004)*, Big Island (USA), Jan. 5–8, 2004.

[WSK02] A. Wacker, K. Sipilä, and A. Kuurne, "Automated and Remotely Optimization of Antenna Subsystem Based on Radio Network Performance," in *Proc. of International Symposium on Wireless Personal Multimedia Communications (WPMC 2002)*, Honolulu (USA), Oct. 27–30, 2002.

[WW02] S. Wong and I. Wassell, "Channel Allocation for Broadband Fixed Wireless Access," in *Proc. of International Symposium on Wireless Personal Multimedia Communications (WPMC 2002)*, Honolulu (USA), Oct. 27–30, 2002.

[WWW+04] D. Wake, M. Webster, G. Wimpenny, K. Beacham, and L. Crawford, "Radio over Fiber for Mobile Communications," in *Proc. of IEEE International Topical Meeting on Microwave Photonics Conference (MWP 2004)*, Ogunquit (USA), Oct. 4–6, 2004.

[XCW00] Y. Xiao, Chen, and Y. Wang, "A Near Optimal Call Admission Control with Genetic Algorithm for Multimedia Services in Wireless/Mobile Networks," in *Proc. of IEEE National Aerospace and Electronics Conference (NAECON 2000)*, Dayton (USA), Oct. 10–12, 2000.

[YCC06] J. Yao, D. Chong, and Y. Chew, "Capacity Balancing Between the Reverse and Forward Links in Multiservice CDMA Cellular Networks with Cross-Layer Design," *IEEE Transactions on Vehicular Technology*, vol. 55, no. 4, pp. 1397–1411, Jul. 2006.

[YGNT00] X. Yang, S. Ghaheri-Niri, and R. Tafazolli, "Enhanced Soft Handover Algorithms for UMTS System," in *Proc. of IEEE Vehicular Technology Conference Fall (VTC 2000 Fall)*, Boston (USA), Sep. 24–28, 2000.

[YZY07] Z. Yong, X. Zhang, and D. Yang, "QoS Based Proportional Fair Scheduling Algorithm for CDMA Forward Links," in *Proc. of IEEE Vehicular Technology Conference Spring (VTC 2007 Spring)*, Dubling (Ireland), Apr. 22–25, 2007.

[ZBNH02] H. Zhu, T. Buot, R. Nagaike, and S. Harmen, "Load Balancing in WCDMA Systems by Adjusting Pilot Power," in *Proc. of International Symposium on Wireless Personal Multimedia Communications (WPMC 2002)*, Honolulu (USA), Oct. 27–30, 2002.

[ZS05] P. Zanier and D. Soldani, "A Simple Approach to HSDPA Dimensioning," in *Proc. of IEEE International Symposium on Personal, Indoor and Mobile Radio Communications (PIMRC 2005)*, Berlin (Germany), Sep. 11–14, 2005.